Resilience of Rapid Transit Networks in the Context of Climate Change

by

Michael Vincent Martello

Bachelor of Science in Civil Engineering
Manhattan College (2018)

Submitted to the Department of Civil and Environmental Engineering
in partial fulfillment of the requirements for the degree of

Master of Science in Civil Engineering

at the

MASSACHUSETTS INSTITUTE OF TECHNOLOGY

May 2020

Author . . . . . .

Department of Civil and Environmental Engineering

May 8, 2020

Certified by. . . . . .

Andrew J. Whittle

Edmund K. Turner Professor of Civil & Environmental Engineering

Thesis Supervisor

Certified by. . . . . .

Frederick P. Salvucci

Senior Lecturer of Transportation Planning and Engineering

Thesis Supervisor

Accepted by . . . . . .

Colette L. Heald

Professor of Civil and Environmental Engineering

Chair, Graduate Committee

Resilience of Rapid Transit Networks in the Context of Climate Change

by

Michael Vincent Martello

Submitted to the Department of Civil and Environmental Engineering
on May 8th, 2020 in partial fulfillment of the
requirements for the degree of Master of Science in Civil Engineering

Abstract

Climate change and projected rises in sea level will pose increasing flood risks to coastal cities and infrastructure. This thesis proposes a general framework of engineering resilience for infrastructure systems in the context of climate change and illustrates its application for the rail rapid transit network in Boston. Within this framework, projected coastal flood events are treated as exogenous factors that inform exposure. Endogenous network characteristics are modeled by mapping at-grade tracks, water ingress points, track elevations, crossover switches, and critical dispatch yards to produce a dual network representation of the system, capturing physical and topological characteristics. Contextual aspects of system performance and resilience are considered through the assignment of weights to links based on passenger flows. Resilience is computed assuming a simple linear model of recovery from a flooding event. Using a suite of projected coastal flooding events from the Boston Harbor Flood Risk Model (BH-FRM, 2015) for three future sea level states, the analysis shows increasing vulnerability of the MBTA rail rapid transit network. Based on these results, we develop an adaptation roadmap to protect the MBTA rail rapid transit system against future coastal flooding. The proposed resilience assessment framework can be readily extended to consider more sophisticated performance models, other climate-related events (e.g., extreme rainfall) and additional normative factors, such as equity in public transit.

Thesis Supervisor: Andrew J. Whittle
Title: Edmund K. Turner Professor of Civil & Environmental Engineering

Thesis Supervisor: Frederick P. Salvucci
Title: Senior Lecturer of Transportation Planning and Engineering

Acknowledgements

I would like to express my gratitude for the guidance, direction, and insight provided by my advisors. At every step and turn of the project, Prof. Andrew Whittle provided an astonishing depth and breadth of knowledge that never failed to surprise me or offer a fresh perspective. His wealth of knowledge and patient guidance throughout this endeavor have not only ensured an efficient and challenging research trajectory, but have also been key ingredients to my growth as a researcher, for which I am grateful. I am also incredibly thankful to have worked under Fred Salvucci, whose depth and breadth of knowledge have been equally impressive, and whose passion for transit has been infectious. Fred's guidance has given me a greater appreciation and understanding of the nuance and socio-political aspects of public infrastructure projects, which I will carry forward through my career.

I would also like to thank Jesse Keenan for his support and willingness to share his knowledge and expertise in climate change, resilience, and adaptation; his input was immeasurably helpful and influential in forming my understanding of these concepts. Balancing the theory, I am also indebted to Hannah Lyons-Galante, who provided both support and invaluable insight into translating theory into practice for the MBTA. I also wish to acknowledge the support of Andrew Brennan, Jen Elise, and the Massachusetts Bay Transportation Authority, which (through Hannah) provided many useful data sets, as well as the financial support that made this research possible.

I wish to express my deepest gratitude to those who have been supportive of me throughout this research. First and foremost, among these individuals are my family, whose emotional support (particularly during the onset of the pandemic) has made this journey an exceptionally smooth one. Second, I would like to thank my MIT colleagues, including but not limited to (and in no particular order) Omar, Patrick, Katya, Rafa, Hao, Bing, Wei, Ignacio, Ivo, Sophia, Michela, Enrique, Karen, Charlotte, Karly, Ruben, John, Cody, Piotr, Brandon, Pepe, Chris, Jeanette, Mark, and the squeaky hinges of Prof. Whittle's office door. Similarly, I am thankful to friends outside of MIT, including but not limited to Alan, Brother Rob, Matt, Evan, Ben, Savio, Nicole, and Chesney who have also been supportive, lending their ears to my endless discussion of work and offering their own insights.

Table of Contents

List of Figures

List of Tables

Chapter 1: Introduction

Ever since coastal communities have existed, the ocean has threatened to engulf them. Throughout history, the sea has offered the prospects of its fruit, trade, and conquest, yet also its raw and destructive power. It has made nations great yet has also brought them to its knees. Venice rose by the sea, its dominance established and secured for centuries by its maritime prowess. It has also been drowned by it, bringing the ruin of crops, famine, pestilence, as well as the destruction of wealth, spurring large-scale flood protection projects dating back to at least the 13th century (Crouzet-Pavan, 2002) efforts that are still ongoing today. The sea and its presence are often taken for granted, considered static, and fully demarcated from the land. Yet this is not the case; the sea is an abstract construct, whose true manifestation is not bounded by a line on a map (Cunha, 2018). It is ever changing, by virtue of the tides and floods, which occur in timescales readily observable by man, or through the imperceptibly slow yet constant sea level fluctuations throughout geologic time. The sea moves, breathes, gives life, provides for man, yet also threatens his creations.

Man now threatens the seas, and in turn, they threaten his creations to an even greater degree. Over the past several decades, the scientific community has established that anthropogenic climate change is a real phenomenon (NASEM, 2016), whose impacts have already been measured and are projected to become increasingly acute over the next several decades. Principal among these impacts is sea level rise, a phenomenon that is readily observable. NOAA tide gauge records show that sea level has already risen by over a foot in New York Harbor (since 1900; NOAA, 2019b). If the trend of the previous century is to continue, a conservative assumption neglecting the latest projections and decades of advance in climate science (NOAA, 2017), sea level rise will pose a significant threat to coastal communities and urban centers by the end of the 21st century.

While there is some uncertainty in the attribution of existing sea level changes to anthropogenic causes (as climate change skeptics point out) the existing trend itself is nonetheless alarming and urges action. If

current sea level trends are indicative of the future rate of sea level rise, there is a well-founded cause for alarm and immediate action. In particular, sea level rise (SLR) along the Northeast seaboard of the United states, has been well documented and is projected to continue (Kirshen et al., 2008), further exacerbated by the ongoing process of glacial isostatic adjustment in the region (Engelhart et al., 2009). For coastal cities in this region, SLR poses a significant existential threat, placing areas of high economic productivity in ever increasing risk from coastal flooding associated with storm surges. Given the economic significance of coastal cities in the Northeast United States, recovery from coastal flood events will be a high priority, as demonstrated in the response following Superstorm Sandy in 2011 wherein $50 billion in federal aid was spent in support of rapid recovery and a restoration of economic activities (HSRTF, 2013). Sandy also highlighted the critical role that restoration of transportation systems plays in the recovery of urban communities. Hurricane Sandy flooded 8 of the NYCT's tunnels, completely submerged 2 subway stations in lower Manhattan, severely flooding 8 additional stations, damaged 6 rail terminals and maintenance yards, and washed out a significant portion of the A train line, inflicting a total of $3.3 billion in direct damages to subway infrastructure (FHWA, 2017). The damage resulted in the suspension of subway for three full days after the storm, with restoration of service not completed for over 200 days after the storm (Chan & Schofer, 2016).

Sandy was not the first major storm to strike in the Northeast, nor will it be the last. As NYC painfully learned firsthand, existing rapid transit systems are even more vulnerable to flooding than the neighborhoods they serve. These transit systems contain critical assets that are often located below existing mean sea level (principally tunnel infrastructure), within current floodplains (such as coastal rail yards, bus garages, or revenue track), or within areas expected to be exposed to flood risk as sea level rise progresses. Transit agencies across the US are growing more cognizant of these risks and are recognizing the need for proactive solutions to operational challenges posed by climate change (Miao et al. 2018). More specifically, transit agencies, including the NYC MTA, LA Metro, and the Massachusetts Bay Transportation Authority (MBTA) are actively working towards improving the resilience of their transit systems in the face of climate

change (NASEM, 2017). But what is resilience - and what does it really mean in the context of an urban transit system?

The principal goal of this research is to answer this question, specifically for the MBTA's rail rapid transit network in Greater Boston. Chapter 2 begins by investigating climate change and its local implications in Boston. Chapter 3 presents a comprehensive survey of the existing literature on the concept of resilience. A thorough examination of these concepts across a variety of academic disciplines shows the polysemic nature of this concept (beyond the immediate context of both climate change and urban transit networks). This survey briefly describes the analytical methods that have been proposed to study and quantify the resilience of transit networks, placing them in the broader context of resilience literature. Chapter 4 proposes a new theoretical framework for defining and quantifying the resilience of urban transit networks under single perturbations. This definition is aligned with existing IPCC (Field et al., 2014) definitions. In chapter 5 the theoretical framework is applied to analyze and understand the resilience of the MBTA's rail rapid transit network. Chapter 6 discusses the response of the raid transit network to projected events, outlines a potential adaptation roadmap through 2070, and explores the advantages and limitations of the assessment presented. Finally, the implications of this work will be discussed, along with potential future research directions within the fields of climate science, climate adaptation, and transportation systems.

Chapter 2: Climate Change and its Local Implications in Boston

Climate change is a real and well-documented phenomenon (NASEM, 2016). In today's political climate, it is unfortunate that such a factual statement is so contentious. Yet regardless of political orientation, the fact remains that sea level does not remain constant. As climate change skeptics point out, the earth's climate, and by extension its mean temperature and mean sea level have fluctuated naturally over geologic time. This has been well-established for decades (Kenney, 1964), though this fact neither contradicts nor negates current scientific consensus and copious evidence attributing recent changes in mean temperature and sea level to anthropogenic factors. While there are some who refuse to accept scientific consensus,[1] there is no doubt that tide gauges records across the globe show a clear trend in sea level rise (SLR) over the past century (NOAA, 2019b). Should the historic trend continue at the same rate (a best case scenario which ignores climate models and their associated uncertainty) rising sea levels, particularly along the Northeastern seaboard of the United States will result in increasingly severe flood risks (Kirshen et al., 2008) and will require action. Restated, even under the most optimistic emissions scenarios (in which carbon emissions are dramatically reduced) SLR will continue to impose increasingly severe flood risks. Mitigation alone cannot remediate the effects of climate change; adaptation, particularly in heavily urbanized coastal environments, is also necessary.

Coastal flooding in the heavily urbanized Northeastern U.S. poses significant economic risks. Hurricane Sandy, which made landfall as a tropical storm in 2012, resulted in $88 billion in direct damages, a value comparable to the $100 billion in direct damage caused by the much stronger (category 4) Hurricane Katrina in 2005 (Ayyub, 2019). The dense coastal development and lack of substantive flood protection in the Northeastern US[2] makes it particularly vulnerable to coastal flood risks, as Hurricane Sandy

[1] A subset of politically motivated individuals refuse to accept scientific consensus on climate change, as they believe that the academic establishment is purposefully defrauding the public by pushing a self-enriching climate change agenda (Morano, 2018).

[2] Coastal flood barriers were constructed in New Bedford, MA and Stamford, CT by the USACE in the 1960s, though these efforts only provide protection for a very small fraction of the Northeastern US coastline (Mooyaart et al.,2014).

demonstrated. Yet as sea levels rise, these risks will grow more severe. This chapter investigates these increasing coastal flood risks, first at the scale of the Northeastern US, focusing in on Greater Boston, and finally investigating a historic case study of the MBTA's Blue Line.

2.1: Climate Change and the US Northeastern Seaboard

The Northeastern seaboard of the United States is prone to increasingly frequent flooding, high tides, and king tides. Boston experienced a record 22 days of high tide flooding in 2017 (Sweet et al., 2018), while 2018 saw record-setting coastal floods (two 1-100 year flood events) in January and March of that year (NOAA, 2019a). The highest tides and subsequently the worst floods along the Northeastern seaboard, are more likely to occur in the winter months (December-February) as this corresponds with both the highest astronomical tides and extratropical winter storms blowing in from the Atlantic, commonly referred to as Nor'easters (Sweet et al., 2018). Projected future increase in frequency of flooding can be attributed primarily to two factors: more intense storms and local changes in mean sea level (the latter of which likely has greater local implications) both of which will be briefly outlined below.

2.1.1: Changes in Storm Intensity

Cyclones originating in the Atlantic and tracking westerly, whether tropical or extratropical in origin, pose the greatest coastal flood risk to the Northeast seaboard. In the Greater Boston area, extratropical cyclones originating in the Northern Atlantic, commonly referred to as Nor'easters, generally pose a slightly greater flood risk than tropical cyclones, as they affect Greater Boston with greater frequency. As climate change progresses, it is unclear whether the frequency of these storms will change. While climate models for the Northeast US predict an increase in extreme precipitation events in the 21st century, as a result of increased presence of water vapor and other factors, they do not agree on changes in the expected frequency or intensity of Nor'easters (Pfhal et al., 2017). Further, the prediction of Nor'easter trends is also complicated by the natural variability of the El-Nino Southern Oscillation cycle (ENSO; Colle et al., 2015). However, even though the prediction of a trend in Nor'easter frequency lies beyond the cusp of current

climate science, at their current rate of occurrence, they are a significant and principal source of coastal flood hazard in the Northeastern US.

Tropical cyclones/hurricanes are better understood and projected to decrease in frequency in the Northeastern US. Those hurricanes that do occur are expected to become more intense (Knutson et al., 2010). Such an increase in intensity are intuitive from a thermodynamic perspective, as tropical storms typically derive their energy from the warm waters of the Equatorial Atlantic, which will slowly become warmer over time, as both atmospheric and sea temperatures rise. However, tropical storms are complex, and are influenced by more than simple thermodynamics. Therefore, the retrospective attribution of the intensity of a given tropical storm to anthropogenic climate change is not straightforward, in part due to the natural variability in intensity of tropical cyclones. Geologic records have shown intense periods of Atlantic hurricane activity in the 1200s, 1400s, and late 1800s (Knutson et al., 2010). The presence of these periods, whose origins are still largely unknown, prevent the simple attribution of increased intensity to temperature increases. Even if the intensity of tropical and extratropical storms remains constant or uninfluenced by anthropogenic factors, the impact of these events will grow increasingly severe as SLR progresses.

2.1.2: Changes in Mean Sea Level

Although global mean sea level has risen by 0.17 meters in the 20th century (Knutson et al., 2010), sea level rise is somewhat unintuitively, a very local phenomenon, that is affected by resource extraction, recent geological history, ocean temperature, and total ocean volume. In Venice, Italy for example, the extraction of water from a non-replenishable aquifer for industrial use in the 20th century caused a measurable subsidence of the Venetian lagoon with recent settlement rates as rapid as 4 mm/yr (Bock et al., 2012), thereby exacerbating the impacts (magnitude and frequency) of the recurring *acqua alta* events. Existing depositional environments, such as that of the Mississippi Delta in Louisiana, wherein the rapid and significant deposition of sediment causes land subsidence, can also result in exacerbated rates of SLR (Yuill et al., 2009).

More relevant to the city of Boston, the geologic past of the Wisconsin glaciation (approx. 20,000 years bp) and its effects along the Northeastern seaboard still affect rates of SLR. The geologic process, known as glacial isostatic adjustment (GIA), in which a region experiences long-term vertical motion of land, causes land subsidence in areas beyond the periphery of glacial extents, as the proglacial forebulge beyond the ice sheet margin collapses (Karegar et al., 2016). Figure 1 summarizes rates of land subsidence along the northeastern seaboard that have been attributed in part to GIA. Specifically in Boston, the rate of land subsidence attributed to this phenomenon has been on the order of 0.8 millimeters per year (Zervas et al., 2013). While the variation in sea level rise along the coast of the United States is an intriguing phenomenon worthy of attention, its investigation lies beyond the scope of this work; thus further discussion of SLR will focus exclusively on the Greater Boston area.

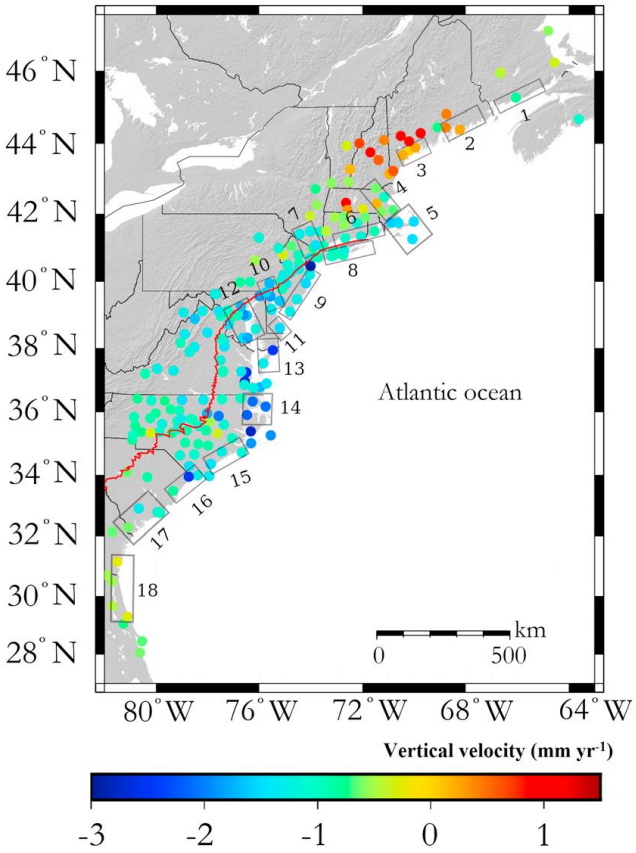

Figure 1: Map of the Eastern seaboard of the United States and measured levels of glacial isostatic adjustment (GIA) as presented in Karegar et al. (2016). Note that blue and green denote subsidence.

2.2: Sea Level Rise in Greater Boston

The National Oceanographic and Atmospheric Administration (NOAA) currently monitors and maintains coastal and riverine tide gauges stationed throughout the United States. In Greater Boston, one such tide gauge station, located in the Fort Point Channel of Boston Harbor, has been continuously monitored since 1921. Based on the data collected and the linear trend line fitted to the mean sea level measurements published by NOAA, from 1921 to 2019, Boston has experienced 11 inches (i.e., 0.28 m or 2.85mm/yr) of mean SLR. This trend can be readily observed in the data shown in Figure 2.

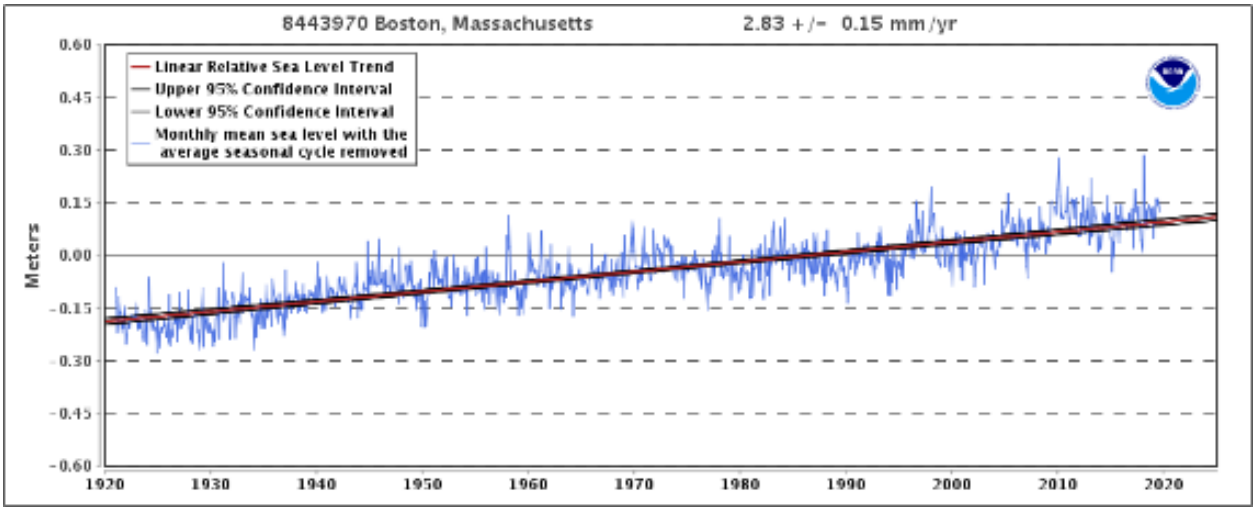

Figure 2: Historic tide gauge measurements in the Boston Harbor (NOAA, 2019a).

While the linear trendline shown describes historic trends, the latest climate science projects an acceleration in the rate of sea level rise along with global mean temperature. The USGCRP (2017) and Moss et al. (2010), expect the global mean temperature to increase through 2100 under the business-as-usual Representative Concentration Pathway, RCP8.5 scenario (in which no mitigation actions are taken), as shown in Figure 3. Under more optimistic RCP2.6 and RCP4.5[3] scenarios, global mean temperatures are

[3] The RCP2.6 and RCP4.5 scenarios assume successful efforts to curtail global emissions, with peak atmospheric CO2 levels at 450 ppm and 550 ppm respectively (USGCRP, 2017). The RCP2.6 scenario also assumes implementation of policies that result in net-negative carbon emissions before the end of the century.

expected to increase at a reduced rate and plateau by 2050 for the RCP2.6 scenario. Locally in Boston, such increases in temperature will not only increase the frequency and duration of heat waves (City of Boston, 2016a), a serious problem worthy of separate study and attention, but will also affect local SLR.

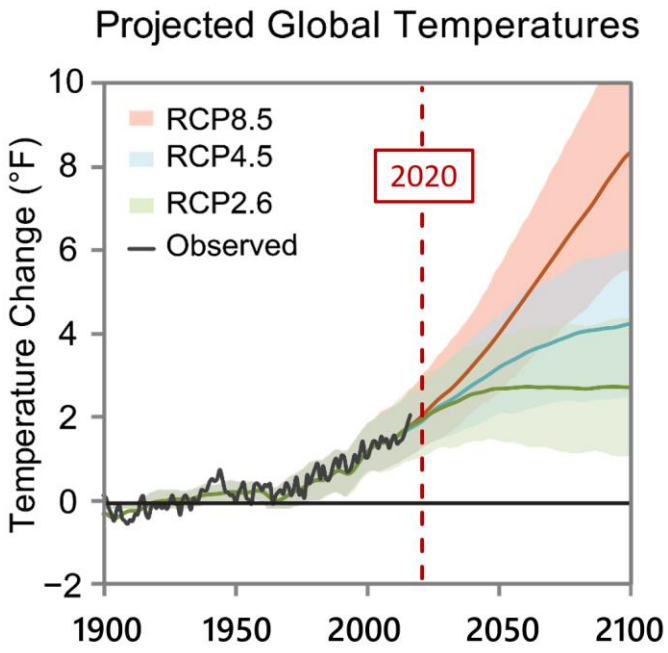

Figure 3: Measured and projected global temperature changes based on RCP scenarios (USGCRP, 2017).

Figure 4 below summarizes the current predictions of sea level in Boston Harbor reported by the US Army Corps of Engineers (USACE, 2019). Under the most optimistic scenario, RCP2.6, the rate of mean SLR, shown in blue, will be comparable to that which has been observed thus far in the 20th century. Yet, the expected SLR under the more likely scenarios, RCP4.5 and RCP8.5 shown in green and red respectively, will yield larger increases in mean sea level by the end of the century. Under the RCP8.5 scenario, on which most local SLR analysis is based, nearly 1.5 meters of additional SLR is projected between the time of writing and the end of this century (USACE, 2019).

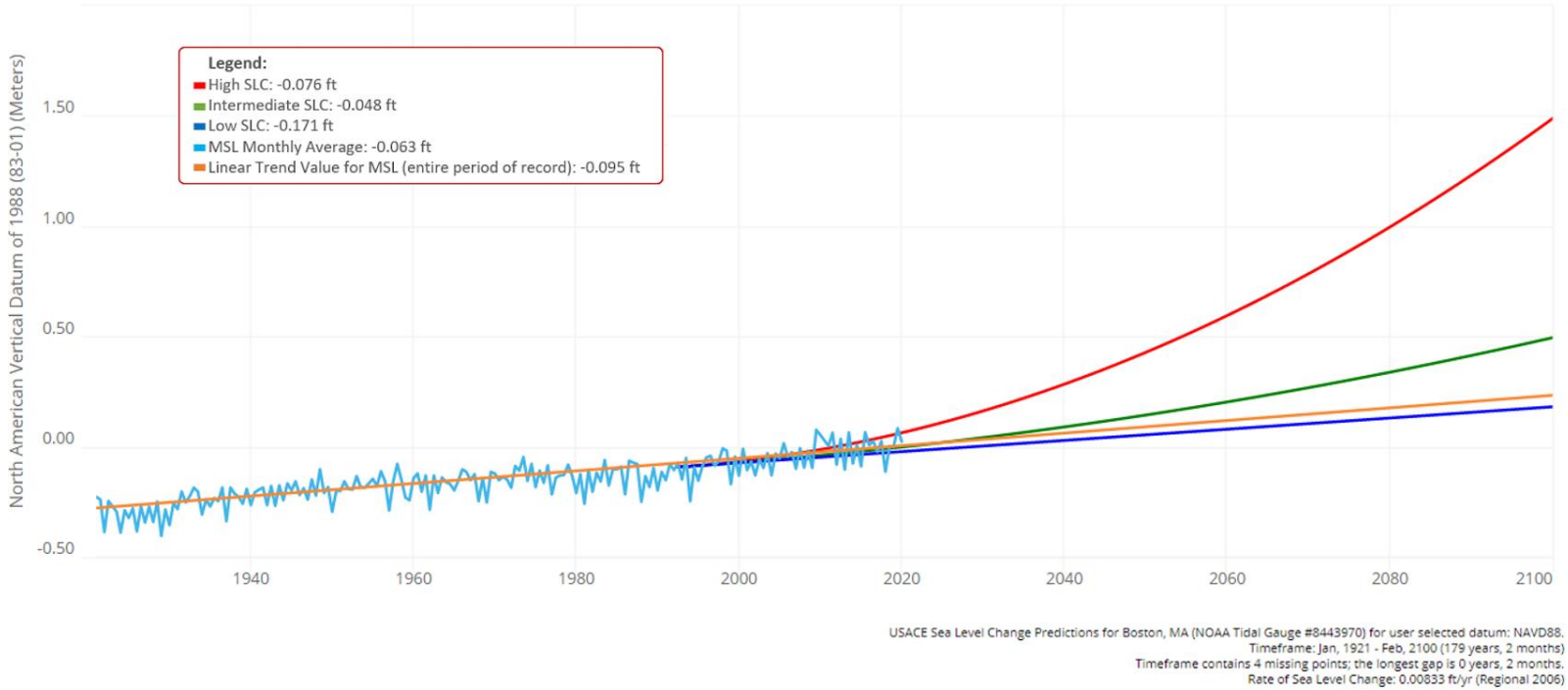

Figure 4: Historic MSL trends from 1921 to present and projected SLR for Boston Harbor through 2100 (USACE, 2019). Low SLR projection approximately corresponds to the RCP2.6 scenario. High SLR projection approximately corresponds to the RCP8.5 scenario.

Cognizant of the potential threat posed by an RCP8.5 SLR scenario, local municipalities and government agencies in the Greater Boston area have proactively undertaken a large number of studies investigating the effects for this SLR scenario. The City of Boston, through its Climate Ready Boston initiative (2016a; 2016b; 2017; 2018), the City of Cambridge (2015; 2017), and MIT (Strzepek, 2018) have all recently conducted climate change vulnerability studies. The first vulnerability assessment conducted by the City of Cambridge (2015) and the ongoing Boston Water and Sewer Commission (BWSC) vulnerability assessment (which has yet to be released to the public; Sullivan, 2019) also consider projected changes in precipitation-based flood vulnerability. Most notable among the local reports is a 2015 study performed for MassDOT to model flood risk of the Central Artery Tunnel (CA/T; Bosma et al., 2015). This study, which produced the Boston Harbor Flood Risk Model (BH-FRM), provides a series of coastal flood risk maps for Greater Boston through the end of the 21st century. These coastal flood risk maps have proven useful (beyond the original scope) and are highly relevant to this work making their description worthy of the attention given in the next section.

2.3: The Boston Harbor Flood Risk Model

What follows is a brief review of the science and techniques underpinning the Boston Harbor Flood Risk Model (BH-FRM) that was released to the public in June, 2015. Unless otherwise cited, the information that follows in this section derives directly from Bosma et al. (2015). The output of the BH-FRM created for this report was utilized extensively to assess the coastal flood risk, vulnerability, and resilience of the MBTA's rapid transit system. Therefore, considerable effort was taken to understand the model and its inherent limitations.

Although it was commissioned to focus on the CA/T system (in Downtown Boston and South Boston neighborhoods) the extent of the BH-FRM study area roughly coincides with the reach of the MBTA's rail rapid transit system. The hazards mapped by the BH-FRM exclusively reflect the anticipated coastal flood risk, as no precipitation or drainage-based flood modeling was incorporated into the analysis.

2.3.1: Sea Level Rise Scenarios Considered

The model considers local sea level rise based on the fourth assessment report (AR4) scenario SLR conditions given in the NOAA Technical Report OAR CPO-1 (Parris et al., 2012). The AR4 scenario predates but roughly corresponds to the RCP 8.5 scenario and reflects "business-as-usual," in which economic growth is projected to increase and there are no substantive attempts to curtail CO2 emissions. Figure 5 shows the sea level rise values used in the BH-FRM compared to estimates based on RCP scenarios, as well as those being used in the Massachusetts Coastal Flood Risk Model (MC-FRM; development ongoing at the time of writing).

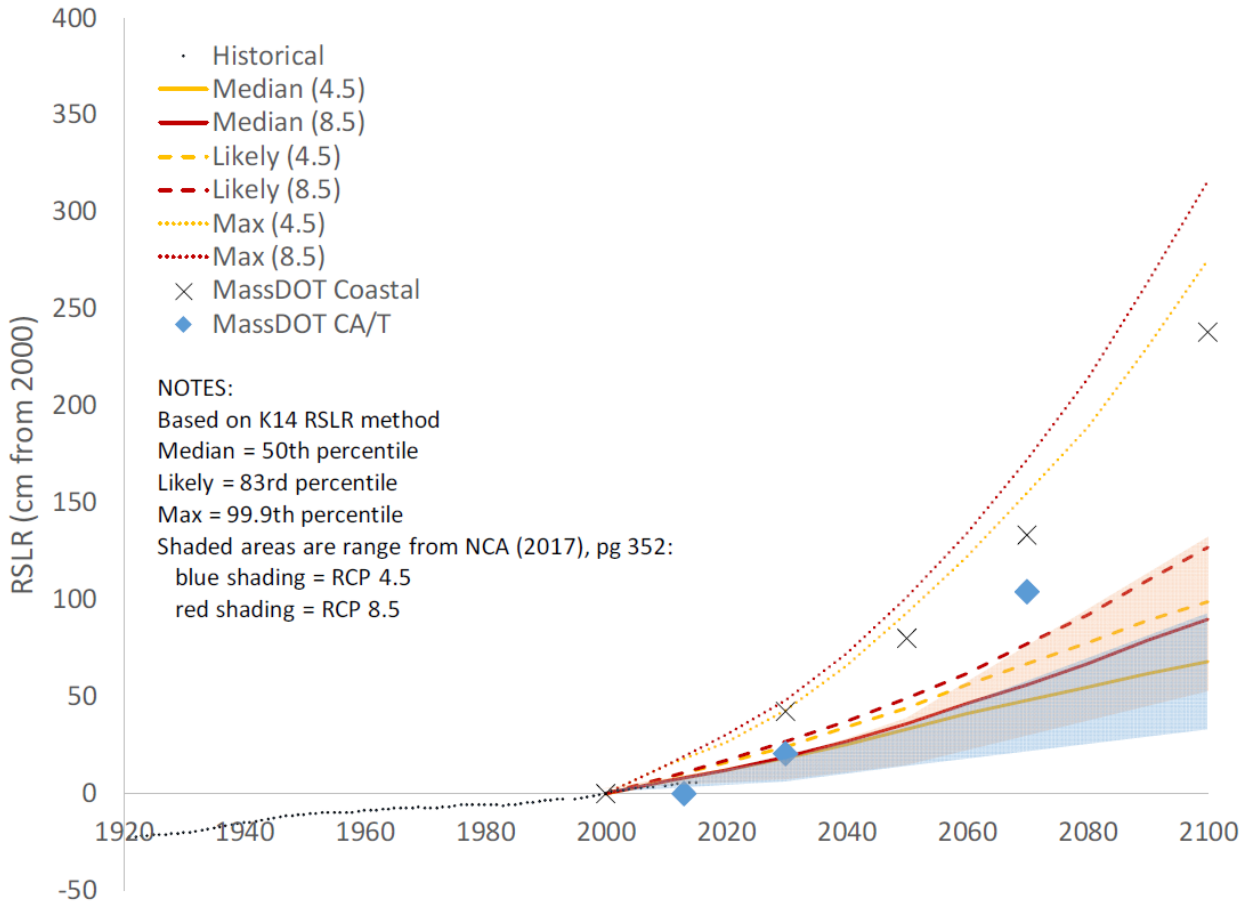

Figure 5: Relative sea level rise projections used in the BH-FRM compared to RCP projections (Miller, 2019).

2.3.2: Simulation of Coastal Flooding

The BH-FRM used a suite of 40,000 synthetic tropical storms and 213 extratropical storms as inputs into the model. The synthetic tropical storms were simulated over a region spanning from the Gulf Coast to Newfoundland; 20,000 of these storms were simulated under 20th century climate conditions, while the remaining were simulated under projected 21st century climate conditions. The suite of tropical storms was generated via statistical processes and historical data sets. Extratropical storms were simulated based on the historical data of the 213 extratropical storm events that impacted Greater Boston in the 20th century. Each storm, tropical or extratropical, was assigned an annual probability of occurrence, which allowed for the eventual determination of coastal flood exceedance probabilities (CFEP).

Using these storms, the model simulates water levels throughout Boston Harbor, accounting for the effects of wind shear, tides, dams, riverine flows, waves, and sea level rise. The model relies on two simulation programs: i) ADCIRC (**AD**vanced **CIRC**ulation Model; Luettich et al., 1992), and ii) SWAN (**S**imulating **W**ave **A**ction **N**earshore; Delft University of Technology, 2020) coupled together to determine the inundation of coastal regions associated with a given storm event. For each time step, ADCIRC is used to model the incremental effects of wind shear, tides, dams, and riverine flows on water levels in the harbor. These results are then passed directly to SWAN, which simulates the incremental effect of nearshore waves generated by a given storm. By passing model information directly between ADCIRC and SWAN, the interaction of tides and storm waves are captured.

Both components of the model rely on a grid mesh at two scales to define water depths and bathymetric parameters. Figure 6 shows the high resolution grid mesh in the proximity of South Boston. This high resolution grid was unstructured and utilized a spacing that ranged from 5 meters to 30 meters. Therefore, the spatial resolution of the BH-FRM is at best 5 meters. The vertical resolution of the terrain model, dependent upon the resolution of the LiDAR topographic data used to model the terrain, is 10 centimeters or less.

Figure 6: Boston Harbor Flood Risk Model (BH-FRM) high resolution mesh grid in Downtown Boston, South Boston, East Boston, and Inner Boston Harbor (Bosma et al., 2015).

Using this coupled hydrodynamic model, each input storm was simulated as it progressed through Boston Harbor in 0.5 second increments. According to Bosma (personal communication, September 18th, 2019) for each time step, if the model projects water will flow into a new grid node and reach a depth of 5 centimeters or greater, it will inundate the terrain; the node is then considered wet and included in the next set of hydrodynamic calculations. For each storm, the maximum water surface elevation and water depth for all nodes within the model are recorded in a partial duration series (PDS) in which all flood events per node are recorded. Aggregating the data from all simulations, these PDS were sorted from low to high flood height, and were assigned an exceedance probability, Q, reflecting the rank of a given flood height within

the sample. This distribution was converted into an annual maximum exceedance series, which reflects the probability of inundation in a given year. This was ultimately used to create a cumulative distribution function (CDF) for the probability of flooding under both event types (tropical and extratropical), from which the distribution of annual coastal flood risks was ultimately determined. In this manner, the flood maps produced by the BH-FRM reflect the probabilistic average of inundation under simulated coastal flood events.

2.3.3: Model Calibration and Observed Discrepancies

The BH-FRM was initially calibrated using a "typical storm," and a simulated Blizzard of 1978. The model was validated using a simulation of the Perfect Storm of 1991, for which the root mean square error (RMSE) was 0.84 inches at the Boston Harbor tide gauge. Figure 7 shows a sample of the model validation results at Narragansett Bay, Rhode Island.

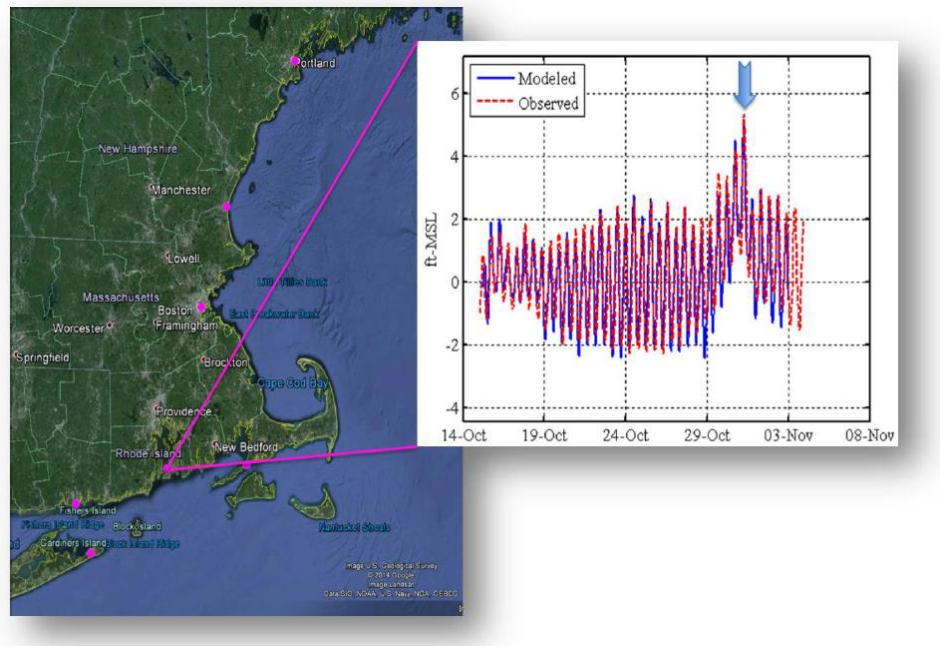

Figure 7: Model validation results for the Perfect Storm of 1991. Narragansett Bay, Rhode Island. (Bosma et al., 2015).

As mentioned previously, the spatial resolution of the BH-FRM is at best 5 meters (16.4 feet). Because of this resolution, some flood pathways that would arise in reality are not shown in the BH-FRM, whilst

other areas may be shown to flood, but would not likely be flooded. For example, Figure 8 compares the BH-FRM 2030 floodplain for the 1% coastal flood exceedance probability (CFEP) event (the projected 1-100 year event) with the FEMA 500 year floodplain (FEMA, 2017). As shown in Figure 8, areas such as the South Boston Bypass Road are not expected to flood according to the BH-FRM but are inundated based on the FEMA 500 year floodplain. In contrast, the bridge abutment on the Orange Line near Wellington Yard is expected to flood according to the BH-FRM when it is not inundated based on the FEMA 500 year floodplain. The spatial resolution of the BH-FRM limits its accuracy; it is important to acknowledge and understand this limiting aspect of the data set prior to its use in analysis.

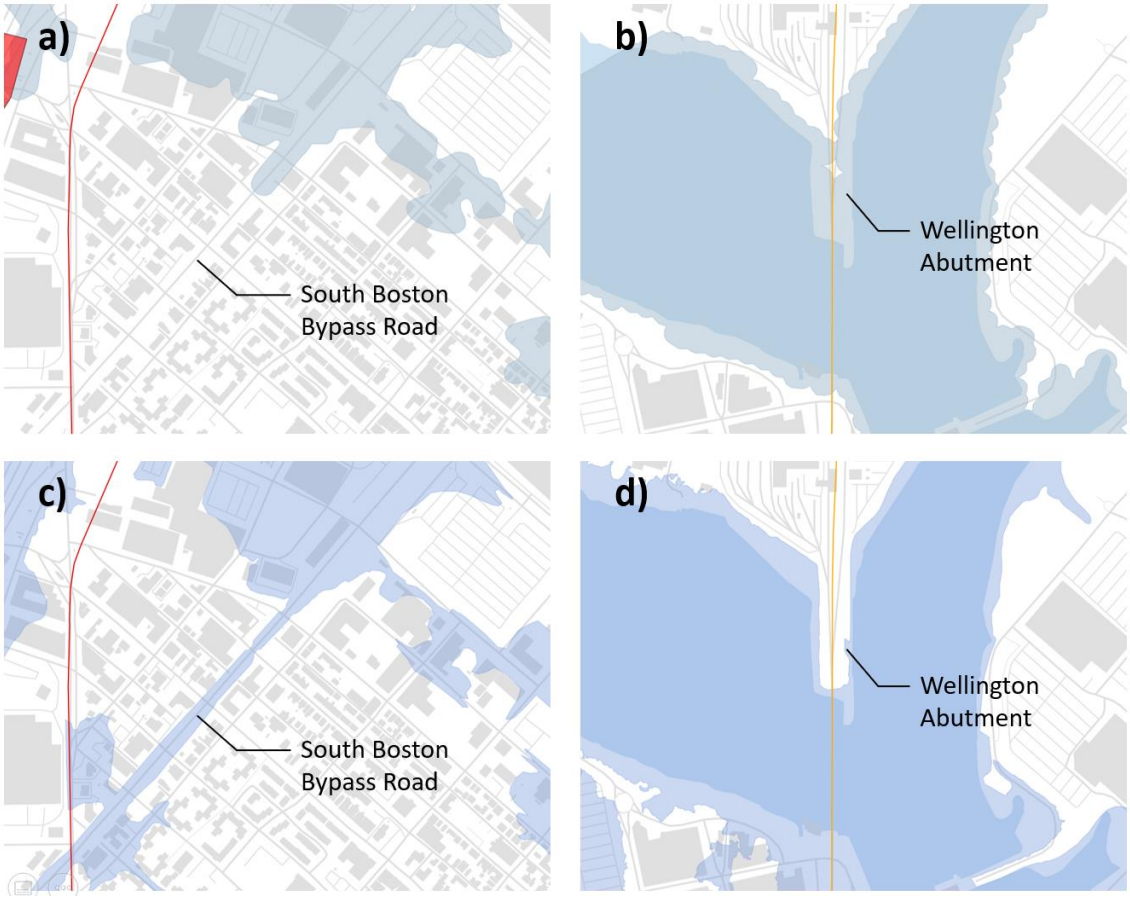

Figure 8: Discrepancies between the BH-FRM 2030 1% CFEP (a, b) and the FEMA 1-500 year floodplain (c, d). A flood path along the South Boston Bypass Road not captured by the BH-FRM (left). An area of inundation along the Orange Line ROW in Wellington shown in the BH-FRM that is not congruent with historic FEMA data (right).

However, despite the inherent limitations of this data, in the absence of alternative risk projections, they still have the potential to provide useful insights for analysis, planning, and design guidance, particularly when considering the impacts to infrastructure assets that are expected to remain serviceable through the end of this century. Considering risks for long-term infrastructure projects is crucial to their continued and lasting service, as will be explored by way of a retrospective case study in the next section.

2.4: The Blue Line: A Historical Case Study

The Blue Line today is the rapid transit line most vulnerable to flooding. Yet 120 years ago, it was neither a rapid transit line nor nearly as vulnerable as it is today. The right of way that currently comprises the majority of MBTA's Blue Line was initially a portion of the Boston, Revere Beach, and Lynn (BRB&L) Railroad. The BRB&L Railroad was chartered in 1874 and first served passengers in 1875 (for a fare of just 20 cents) and served local commuters until 1940 ("Ask the Globe", 2000). The BRB&L ferried passengers from Boston's North End to a rail terminus in East Boston, which ran train service on a narrow-gauge track north to Revere, Winthrop, and Lynn (Leonard, 2011). Shown in , the rail terminus in East Boston bypassed Jeffries Point by means of railway tunnels, since abandoned, running parallel to the Bremen Rail Yard (now Bremen Park) past the local airport, later to become Logan Airport, making its first stop at Wood Island along the east Boston Shore, as noted in the route schematic in Figure 10. The BRB&L Railroad ran to Wonderland and beyond, following close to the Revere and Lynn coastlines, until reaching its northern terminus at Lynn.

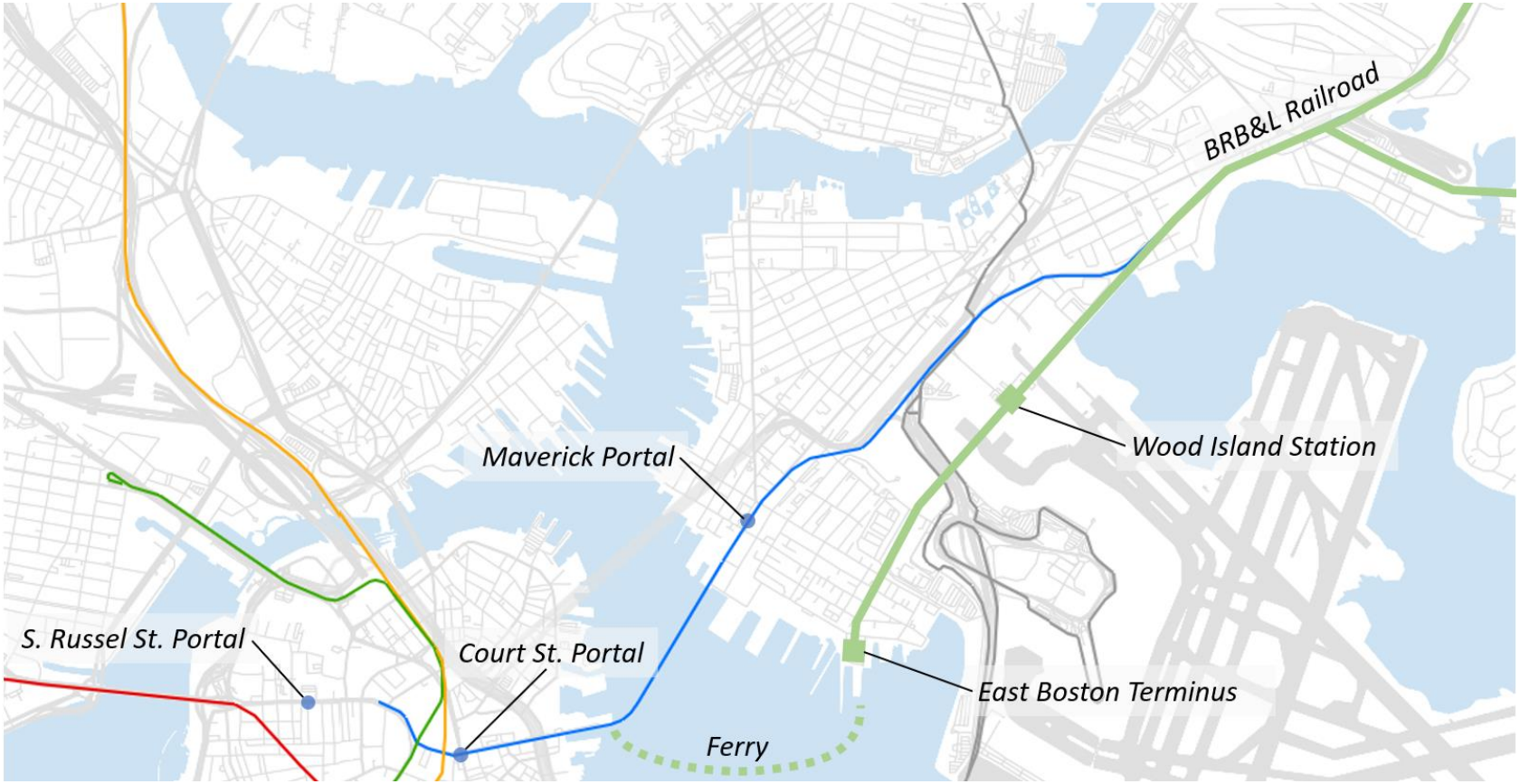

Figure 9: Historic locations on the Blue Line, and right of way of the Boston, Revere Beach and Lynn (BRB&L) Railroad in East Boston. Location of ferry terminus in Downton Boston is approximate. After Bromley & Bromley (1922).

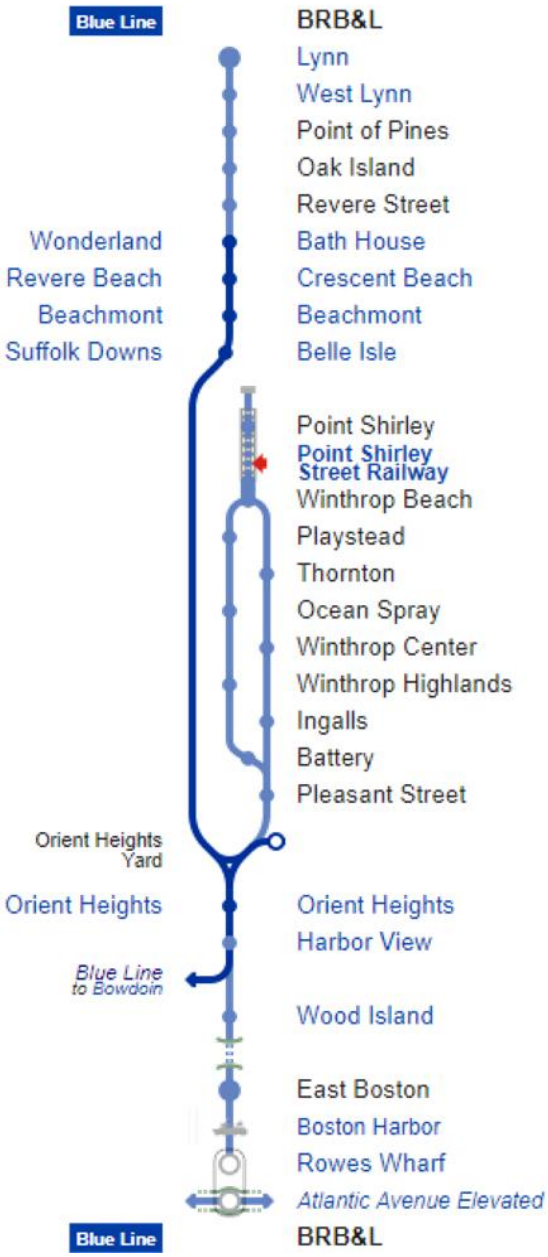

Figure 10: Schematic of the BRB&L Railroad, with a comparison to today's MBTA Blue Line (Wikipedia, 2019).

Prior to the completion of the East Boston Tunnel in 1904, the BRB&L ferry, among other ferry services, was the only means by which commuters could cross Boston Harbor from East Boston to

Downtown. The East Boston Tunnel, the first under-harbor crossing, originally connecting Court Street and Maverick Square, allowed for streetcar service to East Boston and Chelsea (Belcher, 2019). In 1916, the tunnel was extended past Bowdoin via a portal at South Russel Street, a precursor to the mythic "Red-Blue Line Connector," providing continuous streetcar service from Cambridge all the way to East Boston (Belcher, 2019). While this portal would later be closed in 1924 to allow high-platform train service in the tunnel, its conversion from streetcar service would eventually allow for the utilization of the BRB&L right-of-way for rapid transit service in 1952 (Belcher, 2019).

Much like today, both components of what is now the Blue Line, the railway line from Downtown to East Boston, and the BRB&L Railroad were critical pieces of the region's transportation infrastructure. However, unlike today, it is highly probable that they existed outside the 1-100 year floodplain at the time of construction. Based on NOAA (2019a) data, from 1920, the year from which historic tide gauge records have been continuously kept for Boston Harbor, mean sea level rose approximately 0.23 m by the year 2000. By virtue of this knowledge alone, one can deduce that the coastal flood risk in Greater Boston in 1920 was on the whole less severe than in 2000. This assertion is corroborated by the 1-100 year extreme water levels published by NOAA (2019a) shown in Figure 11 below. In 1920, the 1-100 year storm surge was approximately 0.23 m lower than in the year 2000.

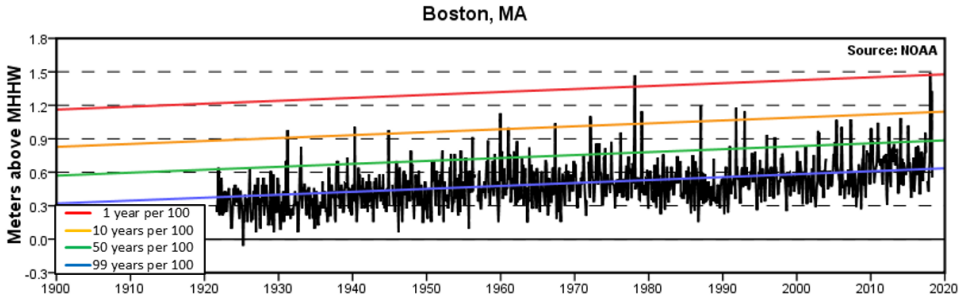

Figure 11: Historic extreme water levels in Boston Harbor (NOAA, 2019a).

Further, should one be so inclined to attempt to estimate the extent of this 1-100 year floodplain in 1920, a rough approximation can be found via the BH-FRM. Under the BH-FRM 2030 assumptions, 0.21

m of SLR, relative to the year 2000, are expected. Comparing the year 2000 1-100 year coastal flood (Figure 12a) with the floods projected under 2030 conditions (assuming +0.21m of SLR), in East Boston, a 1-20 year storm (Figure 12b) comes the closest to approximating the 1-100 year storm with no SLR, as shown in Figure 12.

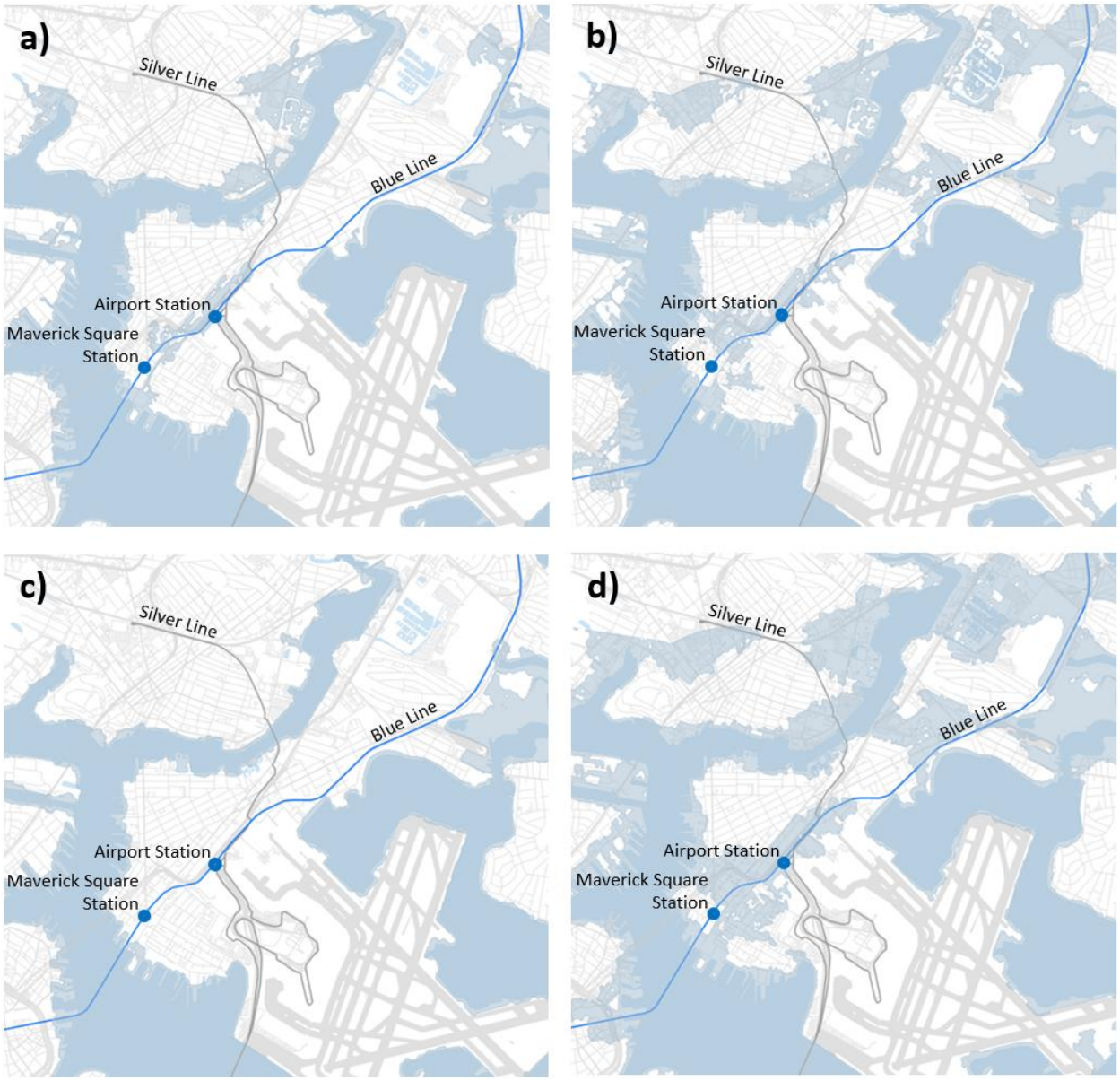

Figure 12: Comparison of the BH-FRM a) 1-100 year coastal flood under 2000 sea level conditions, b) 1-20 year flood with +0.21 m SLR, c) 1-20 year flood under 2000 sea level conditions, d) 1-100 year flood with +0.21 m SLR.

By a rough first-order deduction, one can then extrapolate that the 1-20 year storm under 2000 sea level conditions (Figure 12c) approximates the 1-100 year coastal flood risk in 1920. Short of running the BH-FRM with period correct bathymetric data and a 9 inch lower sea level, or finding a flood map of the area constructed during that time period (of which no record was found by the author), this provides the best means of approximating the 1-100 year flood risk in the Boston area circa 1920. Observing this flood layer at both Maverick Station and elsewhere along the Blue Line, one can surmise flood risks were markedly less severe a century ago, as illustrated in Figure 12c and in greater detail in Figure 13.

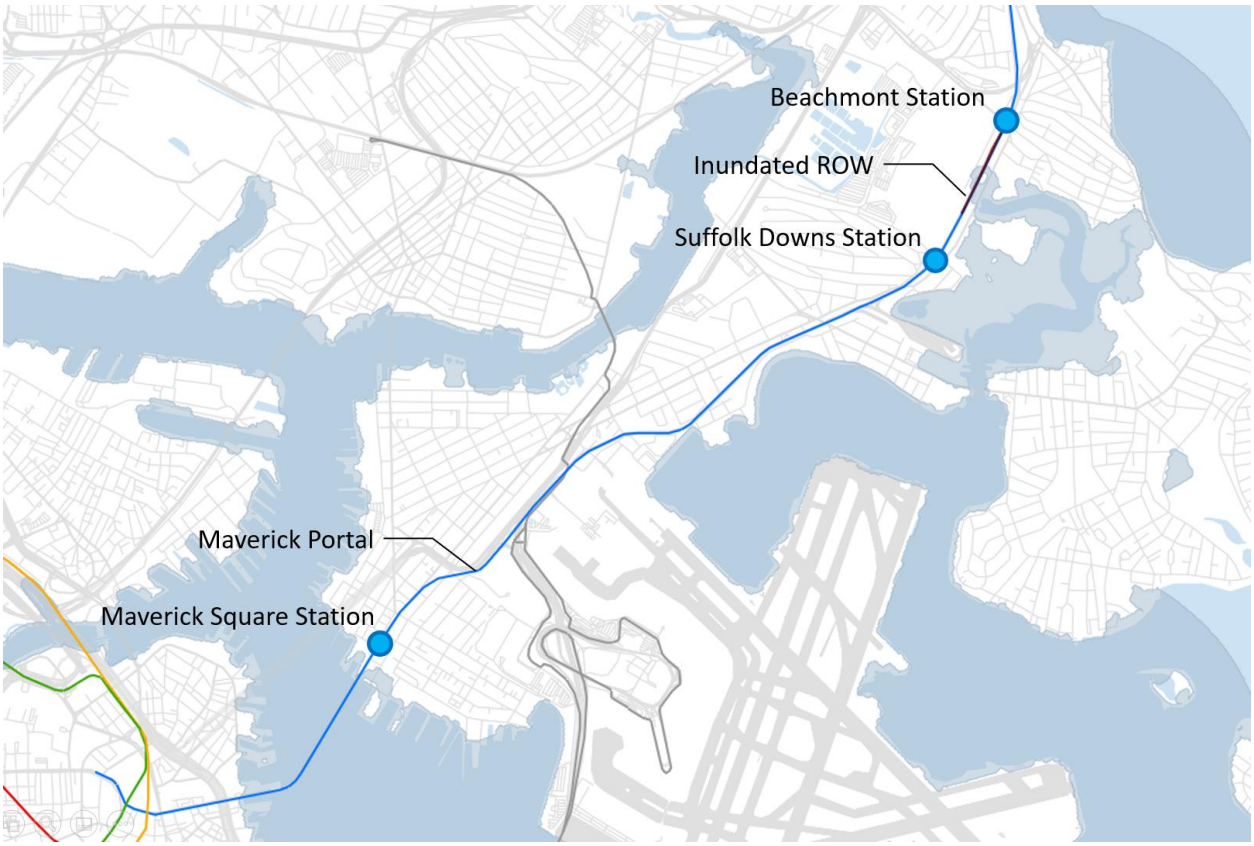

Figure 13: Estimate of the 1-100 year floodplain in East Boston, circa 1920.

Notably, Maverick Square Station, and the flood pathway that exposes Maverick portal and Airport Station are not inundated in the model. Only a small stretch of the ROW between Suffolk Downs Station and Beachmont Station is shown as inundated, with the remaining sections of the Blue Line remaining unexposed to coastal flooding.

Yet, such a geospatial comparison is ultimately imperfect. Bostonians have had a long, complicated (and contentious) history of land reclamation in the harbor, dating back to the Ordinance of 1641-1647, which in stark contrast to the legal precedent of the time, granted coastal property owners rights to the line of low tide (Rawson, 2010). Land reclamation has continuously altered the bounds of the shoreline in Boston for centuries, and much has changed in East Boston since 1920, including the shoreline and bathymetry on which the BH-FRM is based. In fact, one merely needs to consult an atlas to observe this. As shown in Figure 14 below, the shoreline north of what is today Logan Airport in East Boston was drastically different in 1920; a portion of track northeast of what is today Wood Island Station was open water 100 years ago. Ultimately, the conditions shown in Figure 13 above do not provide a definitive measure of historic flood risk, but rather convey a rough sketch of what they may have been.

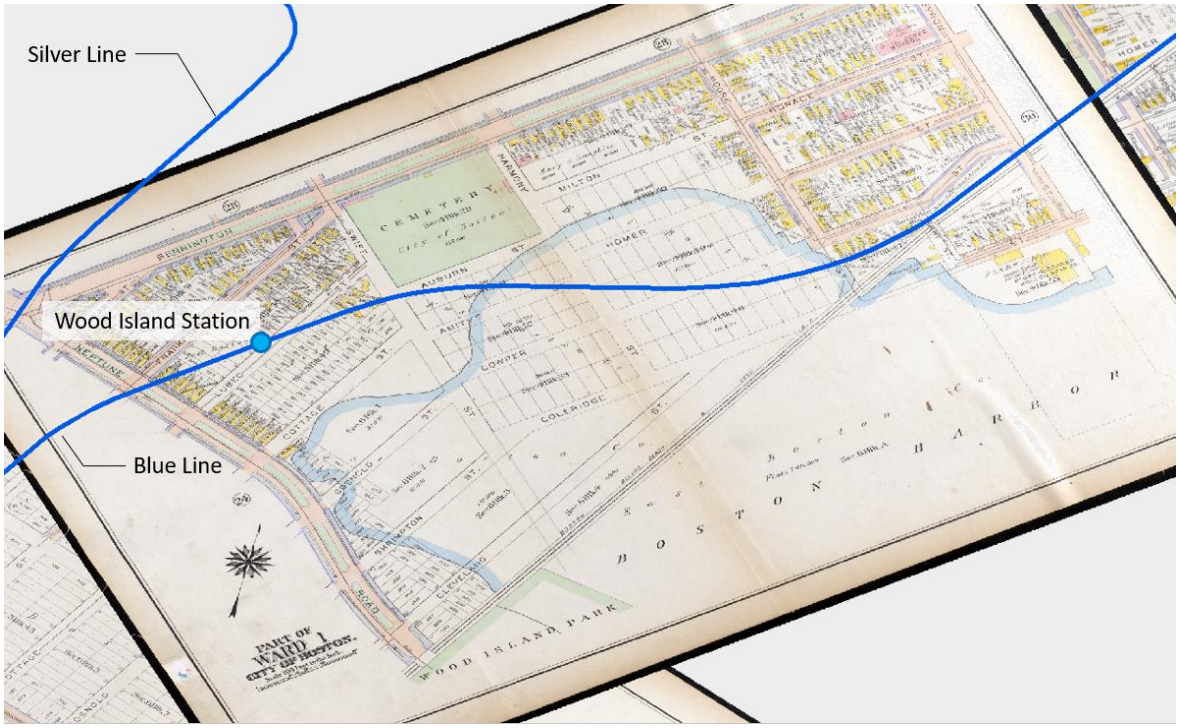

Figure 14: Overlay of the existing MBTA system on the East Boston shoreline, as documented circa 1920 (Bromley & Bromley, 1922).

Despite the rough nature of the retrospective analysis relied upon to visualize the increased flood risk on the Blue Line, the evidence presented, namely historic records and analysis by NOAA (2019a) do in fact

point towards a considerably lower flood risk in East Boston. Considering that flood maps were not drawn in the early 20th century, short of a rigorous re-formulation of the BH-FRM, the sketches above provide the best available insight into historic flood risks.

Despite the probable lack of consideration of coastal flood risk during the design of either the East Boston Tunnel at the turn of the century, or the BRB&L Railroad in the 1870s, it is clear that, by virtue of the changes in sea level, they were more resilient to coastal floods a century ago than they are today. Through this case study, one can surmise that climate change and sea level rise are already impacting Greater Boston, the MBTA, and most specifically, the Blue Line.

These changes were not sudden or extreme but were rather imperceptible and slow increments of environmental change, the sum total of which has proven to be a noticeable and tangible increase in risk. As Hill (2016) notes, the recognition of the need for resilience under the threat of a small and compounding stress is obfuscated by the difficulty of recognizing these incremental changes and properly attributing them to climate change. Yet through advances in climate science and local modeling, such as the BH-FRM, the threat posed by these incremental changes is becoming increasingly well-defined and quantified, thereby allowing for assessment of risk and vulnerability by stakeholders. In the following chapters, a further investigation into the current and future flood risks for one such local stakeholder, the MBTA, is performed, considering the entirety of the MBTA system.

Chapter 3. Theories of Resilience

3.1: Resilience: A Word with Many Meanings

The term resilience, like many other words extant in a living language, has taken on several varied meanings across a diverse range of contexts since its introduction into the English language (ca. 1630). Deriving from the Latin verb, "resiliere" which literally means "to bounce back," resilience in common usage refers to the ability of an entity to return to its initial conditions after it is disturbed (Hosseini et al., 2016). Originally also used to denote the retraction of agreement in a legal context during the 16th century, the term was eventually co-opted by engineering science in the 18th century to describe the behavior and response of materials to cycles of loading (Alexander, 2013). The term also gained prevalence in the field of psychology, wherein it is used as a character trait attributed to individuals capable of overcoming significant adversity and demonstrated a consistent ability to return to a stable mental state (Alexander, 2013; Jay, 2017).

Resilience as a concept has gained increasing prominence in various fields, including ecology, engineering, the social sciences, and climate science, serving as a boundary object between fields (Brand & Jax, 2007; Olsson et al., 2015). While the proliferation of the concept has united disparate fields and sparked interdisciplinary research, the concept has become polysemic: Sharifi (2017) notes that its propagation has led to a diversifying set of definitions, each of which may be sensible in its own context but has ultimately led to the dissolution of substantive and operationalizable meaning when absent of context. Thus, to properly engage in discussion of resilience within an academic setting, its mention must be prefaced by the context within which it is to be invoked (Davidson et al., 2016). Such distinctions are crucial, as notions of resilience developed for separate contexts can surficially contradict and paradigmatically conflict with one another.

Definitions of resilience cited within literature are nuanced and can vary greatly. Through a lens of subjectivity, definitions can be classified on a spectrum of varying degrees of normativity and notions of

equilibrium. The term "normative" as it is being used here is defined as "the prescribing of norms" (Merriam-Webster, 2019) when attempting to characterize and classify the aspects and behaviors of a given complex system. This process of prescribing norms requires the rendering of a judgement and is inherently subjective, as will be discussed later in this chapter. Keenan (2019) illustrates the concept of resilience across a range of academic disciplines, the definition of which can vary considerably dependent on the discipline-specific context.

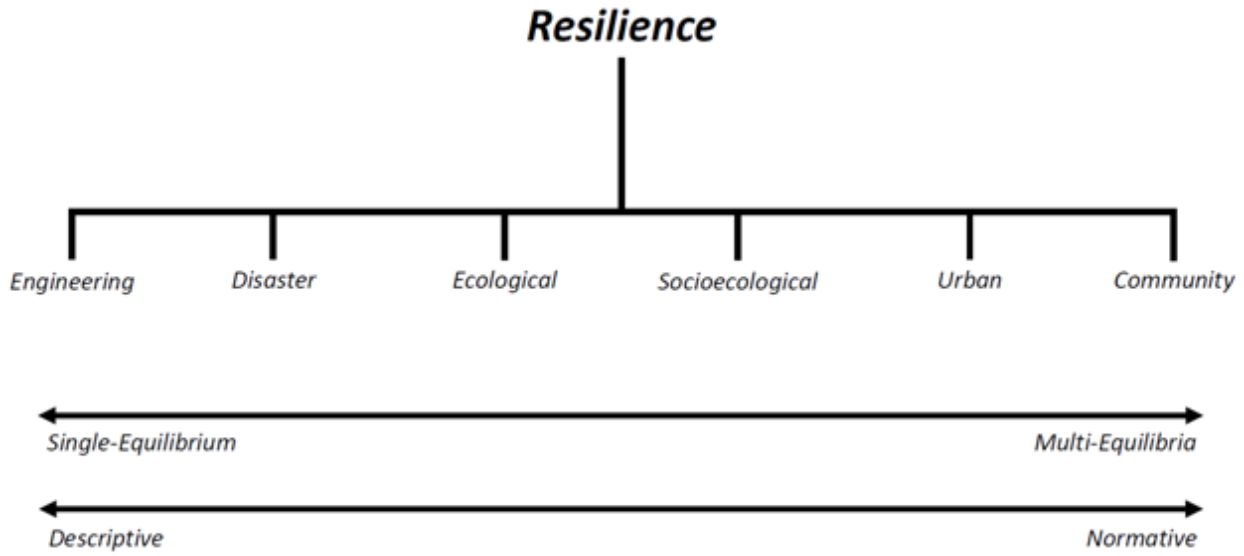

Figure 15: Topology of resilience definitions across fields of study, after Keenan (2019).

Viewing resilience through this lens, definitions found within literature are manifest along a spectrum of equilibrium states and normativity characteristics. In the context of engineered or closed systems, definitions tend to presuppose a single-equilibrium system which possesses as an assembly of components arranged to achieve a predefined system state. In other words, engineered systems have intentionality (Park et al. 2013). By extension, within such systems, notions of resilience are predicated on a predefined value judgement regarding the desired system state and are therefore, of a purely descriptive nature, lacking the need for judgement and by extension normativity.

In contrast, systems that are perceived to be more open and indeterminate, such as socio-ecological systems, can achieve (and maintain) multiple equilibria. In such systems, processes can manifest without intentionality. In order to define resilience in such a system, processes and outputs must be interpreted, requiring value judgements, such as which actions or system states are desirable, thereby implying resilience is of a normative nature (Nelson, 2011). That is, within such systems, description of system processes and responses to perturbation are ultimately dependent upon value judgements and relation of outcomes to predefined cultural, organizational, or ideological norms.

The plethora of resilience definitions that are distinct to and recognized as valid within domain-specific contexts does not detract from the usefulness of the concept (Brand & Jax 2007). However, this does not imply that *any* definition of resilience is valid. A definition must be logically coherent, aligned with general consensus, and properly invoke key concepts accepted within its field of applicability.

3.2: Climate Change Resilience

In the broader context of climate change, any definition of resilience should be in alignment with the definition set forth by the Intergovernmental Panel on Climate Change, hereafter referred to as the IPCC (Field et al. 2014, pp.1772):

"[Resilience is] the capacity of social, economic, and environmental systems to cope with a hazardous event or trend or disturbance, responding or reorganizing in ways that maintain their essential function, identity, and structure, while also maintaining the capacity for adaptation, learning, and transformation."

While many quite reasonably consider resilience to be an inherent property of the system, agnostic to and independent of a hazardous event (Linkov & Trump, 2019), conceptions of resilience divorced from a portfolio of risks are too abstract to have practical relevance in a planning context. Thus, resilience in the context of climate change is partially informed by the hazardous events impacting the system, the structure and intrinsic characteristics of the system, and the system's capacity to adapt. Rayner (2010) highlights that the IPCC (2007) further formalized these relations and defined resilience as a function of vulnerability and

adaptive capacity, where vulnerability is a function of the exposure level for the hazard of interest, how sensitive a system or its components are to the specific hazard, and the relevant adaptive capacity inherent in the system. Combining the above stated definition of resilience (IPCC, 2014) and that of vulnerability (IPCC, 2007) the ontological relation shown in Figure 16 below can be deduced, in which resilience is a function of vulnerability and adaptive capacity.

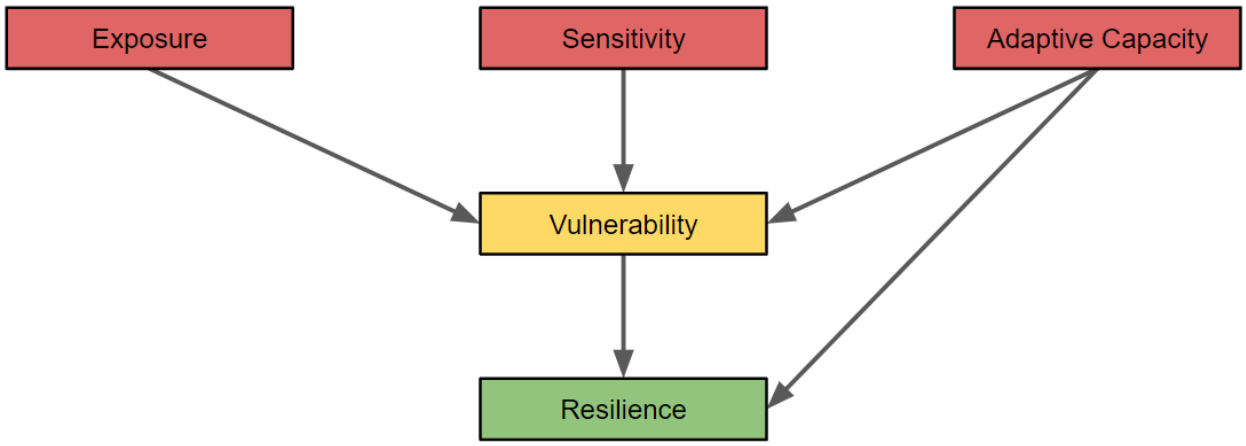

Figure 16: An ontological relationship between components of resilience.

Admittedly, such a definition of resilience is ambiguous and abstract, but can serve as a frame onto which further detail, distinction, and nuance can be applied. What follows is a brief survey of these details and nuances ascribed to the concept of resilience as it has been defined within several relevant academic disciplines, with emphasis placed on concepts with the most potential for transferability to the context of urban transit networks. While the focus may appear overly broad, understanding the current state of resilience literature provides a strong base from which a sensible and credible engineering resilience definition can be constructed. Resilience definitions in the context of ecological systems, urban areas, communities, engineered systems, and transportation networks will be reviewed with an emphasis placed on relevant quantification frameworks.

3.3: Ecological Resilience

Many trace current conceptions of resilience, as well as its application to complex systems to the seminal work by Holling (1973). In the context of ecology, Holling (1973) defines resilience as the ability of an ecological system to maintain its state functions given a perturbation, irrespective of the persistence of a single component of the ecosystem. For example, an ecosystem may still be resilient in the face of a drought even if a given plant species is decimated, assuming that another species takes its place or assumes its functional role. This implies that resilience of a component of the system is not required to achieve resilience of the entire system.

In order to adequately acknowledge and describe this multiscale aspect of ecological resilience, the concept of panarchy, has become pervasive and paradigmatic (Gunderson & Holling, 2002). Panarchy offers a concise way to conceptualize the complexities of dynamic systems within and across scales of space and time, as shown in an example ecological system in Figure 17 below (Allen et al., 2014). At each scale, interactions and feedback between other adjacent elements or other scales are described as an adaptive cycle, in which a system experiences phases of growth, conservation, release, and reorganization (Allen et al., 2014). For those unfamiliar with applying the concept of panarchy in a temporal domain, an imaginative hypothetical example is offered in appendix A to further illustrate the concept.

Through a lens of panarchy, the adaptive actions of an individual or component support or undermine the resilience of a localized portion of the system, which then in turn supports or undermines a slightly larger portion of the system, recursively interacting with incrementally larger portions of the system, until the global effect of adaptive efforts are observed at the level of the entire system. Extending this logic in a temporal domain, adaptive efforts in incrementally small time horizons support or undermine the resilience of the system in larger time horizons. Consequently, such temporal distinctions imply that actions supporting resilience in the short-term may not necessarily support system resilience in the long term. This implication is crucial and will be discussed in further detail in a later chapter.

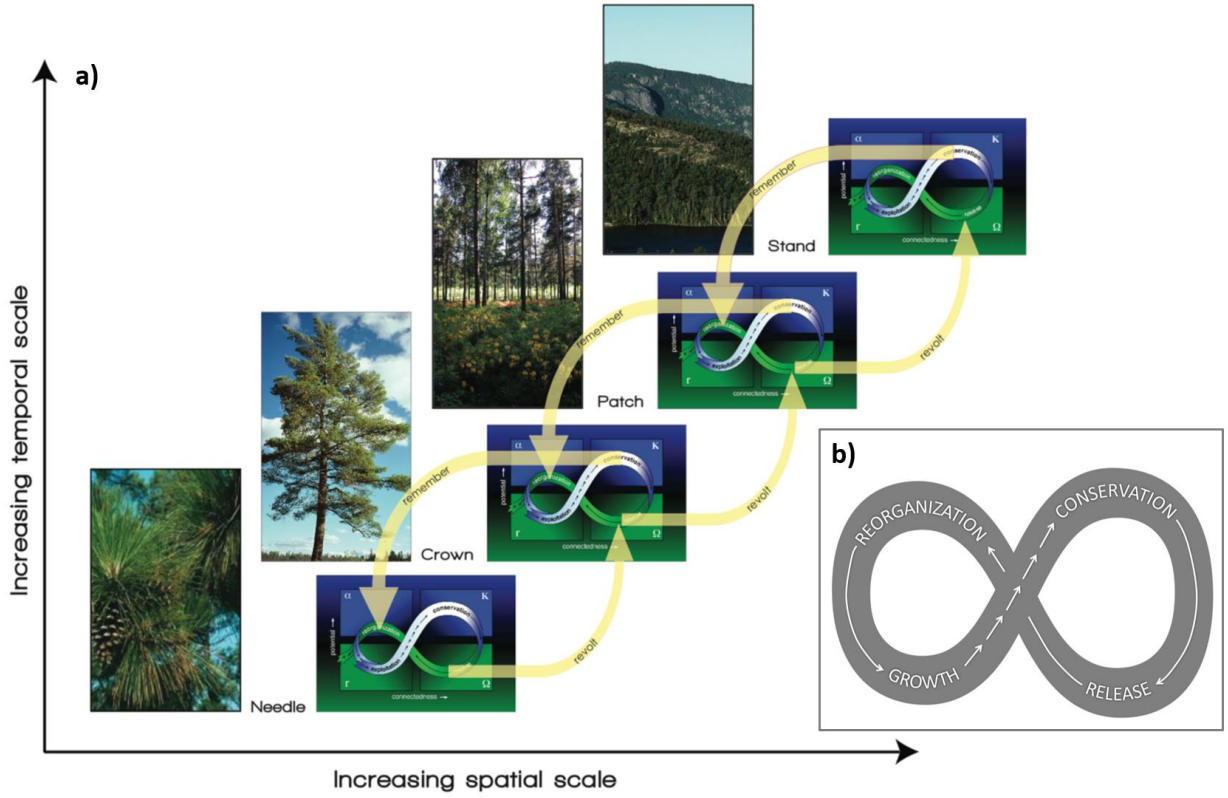

Figure 17: a) An example of panarchy, demonstrating the relations and nested cross-scale interactions extant in a pine forest (Allen et al., 2014); b) The adaptive cycle, after Gunderson & Holling (2002).

Another important aspect of resilience theory in ecological and socio-ecological contexts is the notion of multiple equilibria. According to Gunderson (2000) resilience can also describe the response of a system in which a perturbation causes sufficient instability as to catalyze a regime change, after which a new equilibrium will prevail. This rather abstract concept can be visualized through a ball and cup heuristic, as seen in Figure 18. Once these new regime changes are catalyzed, or the ball moves past a peak into a new valley, new equilibria are reached through adaptive cycles (Davidson et al., 2016). These adaptive cycles can be considered panarchic in nature (i.e. nested across scales) and ultimately act to shift the system towards equilibrium, or in the ball and cup heuristic, towards the local minimum of the new valley.

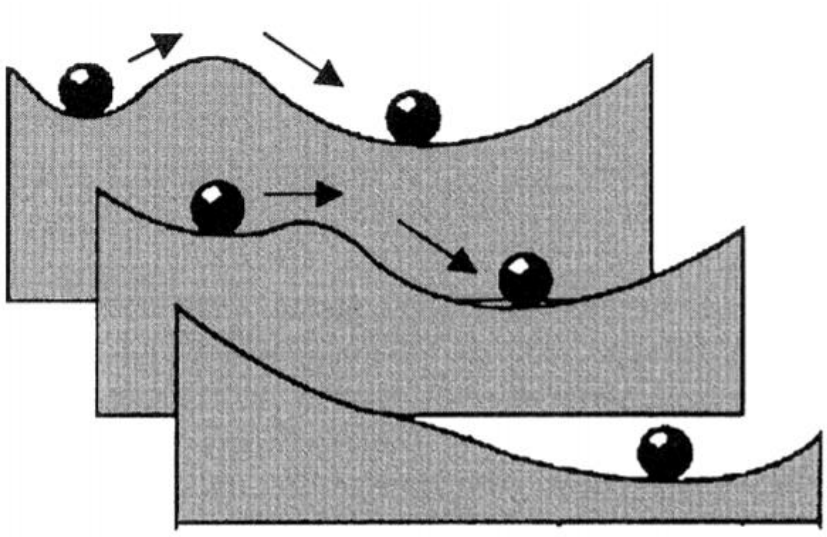

Figure 18: Ball and cup heuristic visualizing the concept of multiple system equilibria (Gunderson, 2000).

Ecological resilience offers two distinct contributions to broader resilience theory: panarchy and allowance for multiple system equilibria. First, panarchy provides a formal framework for recursively describing complex systems, whilst recognizing the cross scale and multi-temporal nature of system dynamics, response, and resilience. Second, through acknowledging the potential for multiple stable system states, resilience becomes less descriptive, and allows for the inclusion of regime changes within a resilience paradigm. These aspects of ecological resilience are borrowed heavily in subsequent urban resilience and community resilience definitions, as will be outlined next.

3.4: Urban Resilience

The notion or urban resilience extends that of ecological resilience into anthropocentric contexts. Whilst closely aligned with community resilience, urban resilience definitions focus at a larger and more ambiguous scale, generally do not place emphasis on the localized needs of individuals or collections thereof (i.e., communities), and has not garnered as much attention as community resilience. Urban

resilience can provide a lens with which one can begin to observe the response of a cohesive urban fabric to perturbations. Meerow et al. (2016) define urban resilience as:

"the ability of an urban system-and all its constituent socio-ecological and socio-technical networks across temporal and spatial scales-to maintain or rapidly return to desired functions in the face of a disturbance, to adapt to change, and to quickly transform systems that limit current or future adaptive capacity" (Meerow et al. 2016, pp. 39)

The above definition recognizes the panarchic nature of complex systems and provides sufficient latitude as to allow for equilibrium changes, whilst recognizing the subsequent potential for maladaptation across scales.

Meerow et al. (2016) also note that other existing urban resilience definitions, which are single-equilibrium in nature, and are predicated on the notion that the original system state is in fact a desirable one, can lead to maladaptive outcomes. Under such single equilibrium definitions, any changes to the system, arising during perturbation or recovery, even if perceived as beneficial, are deemed non-resilient (Davidson et al., 2016). Thus, urban resilience underscores the recognition of multiple possible equilibrium states, and the normativity associated with identifying the potential existence of a more favorable equilibrium state.

Several additional authors, including Nelson (2011) and Davis (2012) recognize the tacit subjectivity inherent in single equilibrium definitions, wherein a subjective value judgement is applied, assuming that a return to the prior system state is in fact desirable. Davis (2012) underscores this by viewing complex urban systems from the perspective of social inequity, arguing that resilience, when it acts to support systemic injustice and marginalization, is maladaptive in the long-term. Social equity considerations force the question, "resilience for whom?" and underscore the complexity and ethics of intervening in a complex socio-ecological or socio-technical system. Yet, addressing such inequities via a top-down process

introduces additional assumptions, assumptions which community resilience frameworks aim to circumvent.

3.5: Community Resilience

Community resilience, perhaps surficially, diverges from urban resilience in name only and appears to promote resilience at a smaller scale. The notion of community resilience has roots in civil engineering and earthquake recovery (Bruneau et al., 2003) and has gained significant traction, both in the academic community and in policy (FEMA, 2016). As with urban resilience, community resilience requires the prioritization of system functions. However, under community resilience frameworks, these judgements are to be made collectively and democratically by the community or stakeholders. Prominent in the context of civil engineering, the *NIST Community Resilience Guide* recognizes these normative aspects of community resilience by advocating the collective formulation of resilience goals and objectives by each individual community (NIST, 2015). The NIST (2015) advocates for a participatory process through which a community can collectively determine priorities, set desired levels of protection or adaptive capacity, and actionable goals, constituting a community resilience plan specific to the community.

While the process outlined by NIST (2015) is undoubtedly thorough, it serves more as a management framework for local policy makers and decision makers, rather than as a lens through which one can understand what constitutes community resilience. It is clear that such frameworks are event driven and risk dependent, as they direct communities to identify natural and anthropogenic disasters, the risks they pose, as well as the interdependencies extant within the built environment that complicate these risks (NIST, 2015). By considering these events in conjunction with system interdependencies, community stakeholders are encouraged to take a systems approach to resilience planning. Such an approach is driven by notions like panarchy, wherein an understanding of a system's interaction with its subcomponents and subsystems is crucial to understanding system response, and negative feedback loops (Linkov & Trump, 2019). Multi-level systems approaches to community resilience have also been studied and presented through the lens of panarchy (Hill, 2016; Berkes & Ross, 2016).

These approaches, while academically rigorous, can obfuscate intuitive, time independent notions of system dependency that are most critical when planning at the community level. NIST (2015) points out (without referencing the concept of panarchy) an external dependency occurs when a system or a constituent component requires the functionality of another ancillary system in order to maintain its core functionality. Failure of the ancillary system can cause a cascading failure, in which the adjacent system or a constituent subsystem also fails. An intuitive example of an external dependency is the dependence of a transit system on the power grid. Should the power grid fail in a key location providing power to a substation, then a large portion of the transit system may become inoperable, as noted by Sela et al. (2017) and illustrated in Figure 19. Identification of system dependencies is imperative for understanding the impacts of given perturbations or stressors. Improving community resilience is predicated upon such an understanding of system interdependencies.

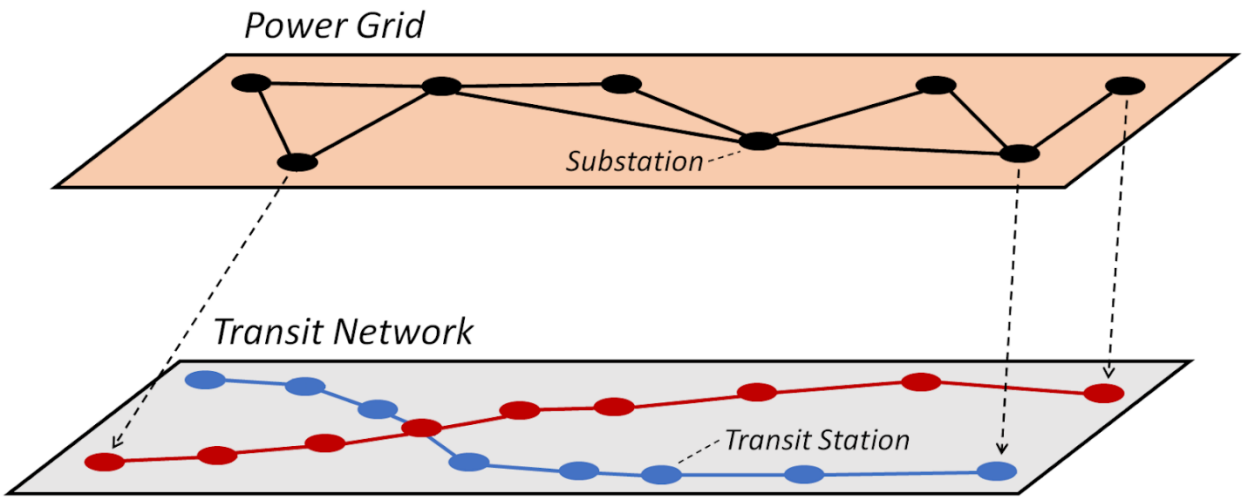

Figure 19: Illustration of the dependency of a transit network to the power grid.

When considering the resilience of a community longitudinally through time, the concept of panarchy can also aide in understanding resilience at varying temporal scales. Actions that may increase resilience from the perspective of a shorter time horizon may decrease resilience when viewed from the perspective

of a longer time horizon. For example, a beach nourishment project may improve shoreline resilience for a coastal community in the short term, but if it erodes faster than anticipated, the cost of the project could be greater than the benefit of protection it provided over its lifespan. In such a scenario, the project cost more than doing nothing, thereby making the project maladaptive. By deferring action or by choosing actions that are maladaptive at longer time horizons, the burdens of climate change and the cost of adaptation can be deferred to future generations, to their detriment (Hill, 2016).

When a community formulates a resilience plan, decisions must be made to prioritize the systems or regions that receive priority during recovery efforts. When planning and prioritizing recovery measures, an implicit question arises, "resilience for whom? And when?" (Berkes & Ross, 2016). Such questions bring to mind both the spatial and temporal aspects of resilience and considerations of priority. Graham et al. (2016) note that prioritization of recovery may be inequitable, thereby turning resilience and adaptation into privileged goods. This was exemplified in New York City's recovery efforts after Hurricane Sandy, wherein isolated and low-income communities were disproportionately neglected during post-event recovery efforts (Byrum, 2019; Graham et al., 2016). Far Rockaway, a relatively isolated low-income neighborhood, served by the A train subway service, was inoperable for over 200 days after Hurricane Sandy (Chan & Schofer, 2016). This section of track represented a very small portion of the New York City subway system, and its lack of network centrality allowed decision makers to decrease the priority of its restoration. For residents of Far Rockaway, the lack of restoration prolonged the adverse mobility impacts of Hurricane Sandy, and significantly decreased their connectivity to the rest of New York City. Such spatial isolation, coupled with a low prioritization of recovery, greatly impacted the ability of the Far Rockaway community to recover from the disaster, decreasing the resilience of the community (Graham et al., 2016).

It is clear that the Far Rockaway community shouldered a disproportionately large burden compared to other areas of New York City. As Hill (2016) notes, resilience also forces into question the ethics of the spatial prioritization of recovery efforts and who will shoulder the burden of climate change. Pre-existing

urban development dynamics and civic infrastructure can greatly affect the ability of low-income areas to rebound from a disaster. In other words, community resilience and adaptation are at risk of becoming "privileged goods" bringing in questions of distributional equity (Graham et al., 2016). Questions of distributional equity are inherently subjective, political, context dependent, and difficult to quantify or address. However, acknowledgement of inequity and the spatial distribution of relative importance within a community is an important step in determining the objectives and goals outlined in support of community resilience.

3.6: Engineering Resilience

There are competing views of resilience in the context of engineered systems. Some authors view resilience as an intrinsic characteristic of a system, one which lies beyond the context or risk (Linkov & Trump, 2019). Others view resilience as an emergent property of a system, one that is inherently context and risk dependent. Through this lens, resilience is an outcome, arising from a recursive process of sensing, anticipation, learning and adaptation (Park et al., 2013).While these two definitions appear paradigmatically opposed, they are not wholly incompatible perspectives. Intrinsic definitions of resilience, those which are agnostic to risk, define system behavior at an additional level of abstraction compared to emergent definitions, characterizing system response irrespective of perturbations. Emergent definitions instead focus on a singular risk or a subset of risks, providing further context and salience for decision makers.

Many authors choose to characterize engineering resilience using the "4R's" of resilience (Bruneau et al., 2003; ASCE & Ayyub, 2018; Laboy & Fannon, 2016):

- Robustness: The ability to withstand a given level of stress or demand without suffering degradation or loss of functionality.
- Redundancy: The degree to which constituent components are substitutable in the event of disruption such that the system can satisfy its intended functionality.

- Resourcefulness: The ability to identify problems and allocate available resources to maintain functionality under a pre-established hierarchy of priorities.
- Rapidity: The rate at which functionality is restored in the event of a disruption.

These components of resilience include organizational and managerial decisions and actions taken in response to perturbations, in addition to the response of the system's physical assets. However, these more intangible aspects of resilience are harder to model and quantify, as will be observed in the following section.

3.6.1: Existing Quantitative Frameworks

In the context of engineered systems, many definitions of resilience rely upon a quantitative framework that describes the response of a single-equilibrium system to a single known perturbation (Henry & Ramirez-Marquez, 2012; Franchin & Cavalieri, 2015; Chan & Schofer, 2016; Li et al., 2017; Zhang et al., 2018). Such metrics incorporate the risk associated with an event into the measure of resilience, implying resilience is not solely an inherent property of the system, but also depends upon the specific risk considered in design (Linkov & Trump, 2019). While these definitions may conflate risk and resilience to some degree (when determining the resilience of a system to a given class of risks), this event-dependence is a sensible exercise as a component of design intent. However, single perturbation events cannot be isolated and assessed outside the context of a full portfolio of risks and prevailing uncertainties.

Existing resilience frameworks are also time-dependent and aim to describe system performance through pre-disruption, disruption (response and recovery), and post-disruption phases, shown in Figure 20. Most existing frameworks rely on a first order linear representation of system recovery and define resilience using a "resilience triangle" approach (Ayyub, 2014), shown in Figure 21. The resilience triangle is a measure of performance loss over the response and recovery periods relative to a predefined level of service. In contrast, resilience is the normalized area under the system performance curve over the period

from t_0 to t_1, representing the performance maintained over the same period (Franchin & Cavalieri, 2015; Zhang, et al., 2018; Saadat et al., 2019).

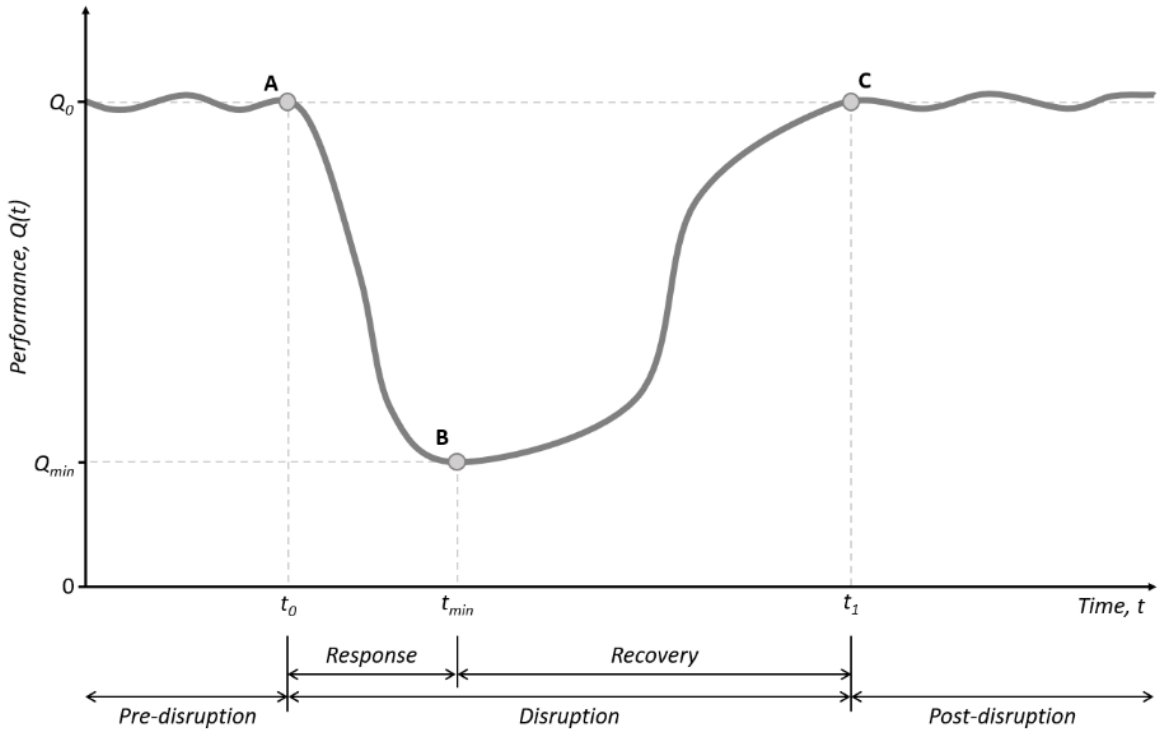

Figure 20: Generalized conception of system performance to exogeneous perturbation, after Wan et al. (2018).

Defining resilience as a function of system performance loss, Franchin & Cavalieri (2015), Zhang et al. (2018), and Saadat et al. (2019) expand on the resilience triangle definition to define resilience as a normalized area under the system performance curve for the length of the recovery period, which can be mathematically represented as the following:

$$R = \frac{\int_{t_0}^{t_1} Q(t)dt}{(t_1 - t_0)Q_0} \tag{3.1}$$

Quantifying resilience in this manner is possible, assuming that system performance is conscientiously defined and modeled or approximated adequately.

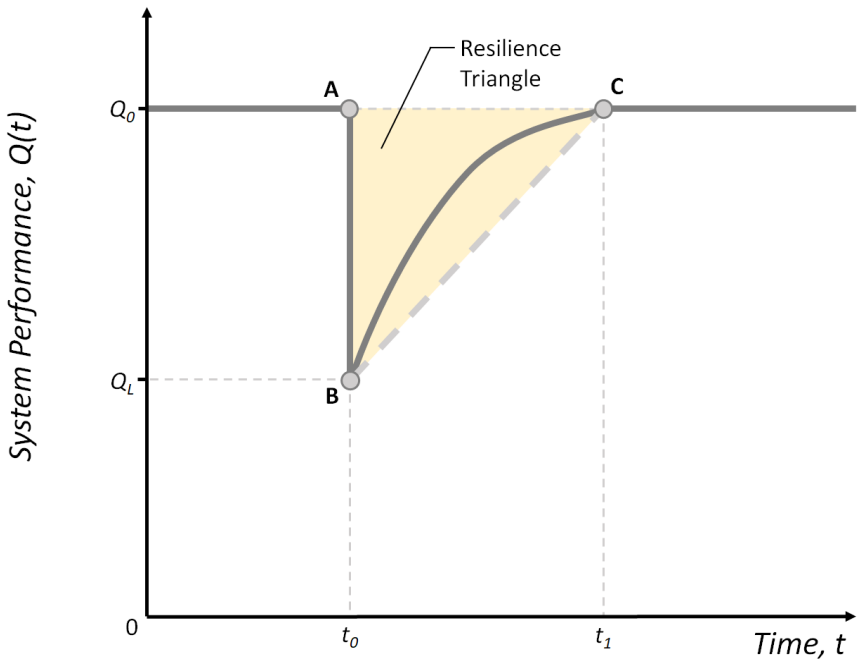

Figure 21: The resilience triangle, defined as the approximate area of performance loss from the start of a perturbation event at time t_0 to the point of full recovery at t_1, is highlighted in yellow.

3.6.2: Measures of Transit Network Performance

Existing assessment methods focusing on transportation and transit networks primarily emphasize the endogenous aspects of resilience, and provide system performance measures via graph theoretic representations of a network (Saadat et al., 2019; Zhang et al., 2018; Li et al., 2017; Xing et al., 2017; Existing assessment methods focusing on transportation and transit networks primarily emphasize the endogenous aspects of resilience, and provide system performance measures via graph theoretic representations (Testa et al., 2015; Li et al., 2017; Xing et al., 2017; Zhang et al., 2018; Saadat et al., 2019). These assessment methods focus on connectivity of the network consisting of undirected links with various system performance measures that are usually related to network efficiency (Testa et al., 2015; Xing et al., 2017; Zhang et al., 2018; Saadat et al., 2019). Network efficiency (E_G) in the context of graph theory, first outlined by Latora & Marchiori (2001), describes the connectivity of a network by assessing the length of

the shortest path between all node combinations in a network, and can be mathematically expressed as the following:

$$E_G = \frac{1}{N(N-1)} \sum_{i \neq j} d_{ij} \quad 2)$$

Wherein N denotes the number of nodes in the network, and d_{ij} is the shortest path length between nodes i and j.

In less formal parlance, efficiency provides a measure of overall system connectivity. Network efficiency provides a measure of the topological redundancy of a network but neglects the physical, socio-technical, and temporal characteristics of the system. With the notable exception of Xing et al. (2017), most existing quantitative metrics do not consider the relative importance of links in the system. More broadly, the context in which systems of interest operates and perturbations occur are neglected in existing resilience metrics, thereby minimizing their relevance to stakeholders and decision-makers.

Understanding asset criticality and the relative importance of system components to core functionality is a key step in determining the risks posed to infrastructure systems (Dowds & Aultman-Hall, 2015). With the exception of Xing et al. (2017) the network-based metrics surveyed did not attempt to describe the relative importance of links in the system. In the context of describing network vulnerabilities, Dall'Asta et al. (2006) proposed weighting links within a network by the inverse of link capacity. When using shortest path lengths as a measure of system performance or relative importance, weighting links in this manner assigns higher capacity links more priority, as they become shorter and therefore more valuable in the context of shortest path assignment. Xing et al. (2017) similarly assign weight to network links on the basis of the inverse of bi-directional passenger flow on a given link. Through assigning relative importance to links, the impacts of perturbations and restoration strategies on passenger flows through the system can be better characterized.

Post-perturbation restoration strategies and their long-term performance implications have also been investigated by several authors. Sela et al. (2017) investigated post-perturbation recovery strategy,

comparing strategies that prioritized various graph theoretic measures of node importance against restoration of random nodes. Other authors, notably ASCE & Ayyub (2018), also challenged the assumption of a return to pre-perturbation performance levels, as well as a constant level of baseline system performance (ASCE & Ayyub, 2018; Ayyub, 2014). Figure 22 illustrates the performance of a degrading system over time (due to aging, etc.). ASCE & Ayyub (2018) note how systems can fail in a variety of ways (f_1, f_2, f_3; Figure 22), yet can also be restored to various levels of performance (r_1 – r_6; Figure 22). Considering aging effects and varying levels of post-perturbation restoration adds another layer of temporal complexity to definitions of resilience.

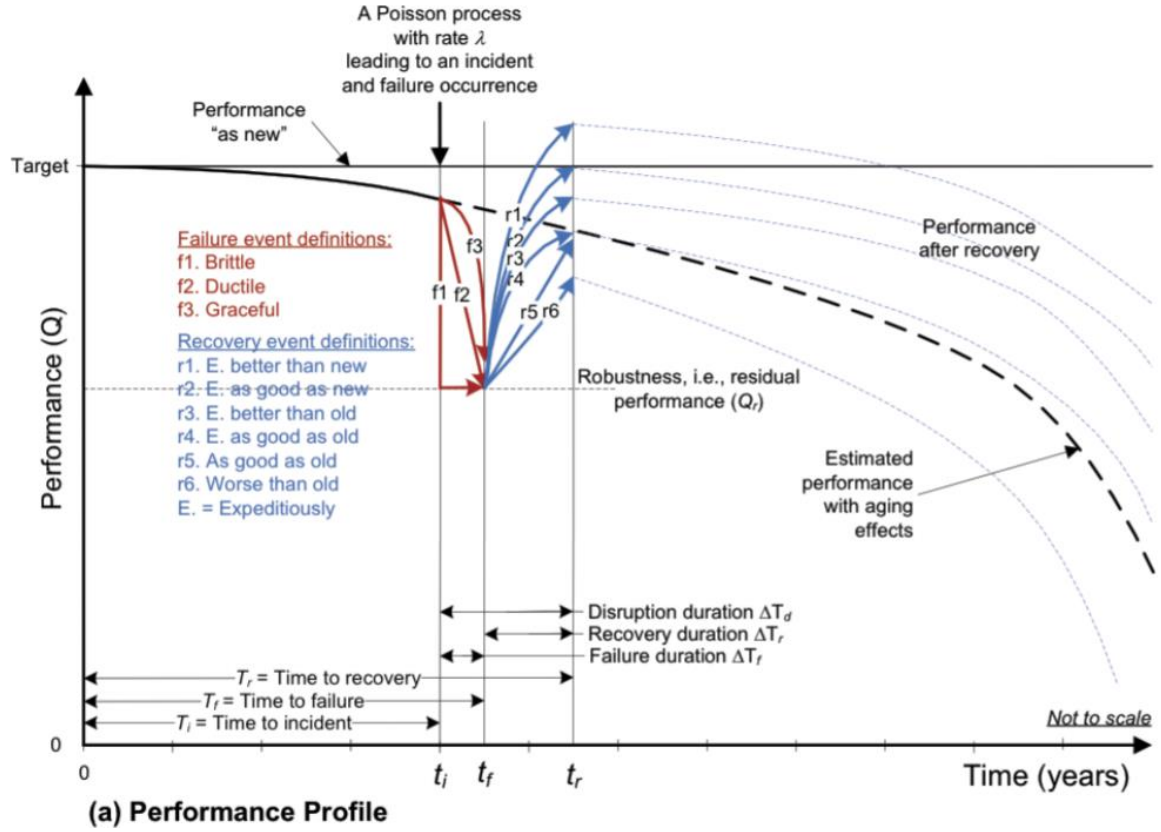

Figure 22: Hypothetical resilience curve depicting brittle, ductile, and graceful failures, which can transition into recovery events of varying levels of restoration. Note that long term performance decreases with time due to presumed aging effects. (ASCE & Ayyub, 2018).

The engineering resilience metrics and analysis frameworks reviewed largely exclude relevant contextual details that are important for understanding the relative importance of different components in the system and the time-dependent nuances of system performance and recovery. In the following chapter, a coherent and robust framework for climate change resilience in the context of engineered systems and transit will be formulated, in which relevant contextual details will not be excluded.

Chapter 4. Analysis Methodology and Framework

4.1: Theoretical Approach

A common thread of the resilience definitions surveyed in Chapter 3 is the attempt to characterize system response to external stimuli. These external stimuli, which are the set of all possible perturbation scenarios (under a threat agnostic definition) or a subset of potential perturbation scenarios (under a risk-specific definition) place stress on a system of interest, prompting a perturbation dependent response. Therefore, any definition or measure of resilience reflects not only the endogenous components of the system, but also the exogenous factors that inform the degree to which the system is exposed and how it will respond. In the case of threat agnostic definitions in which measures of resilience consider the entire set of perturbation scenarios, the resulting measure is an intrinsic system property, describing the average behavior under all possible scenarios. While rigorous, such a definition is abstracted to such a degree that it lies outside the realm of relevance in the context of traditional capital investment planning within transit agencies. Thus, the definition adopted in this work is event dependent and, in part, characterized by exogenous factors, thereby allowing decision makers to evaluate system response under a perturbation of interest, such as a design event of prescribed magnitude.

Measures of resilience for any engineered system rely on the synthesis of analysis boundaries, as well as the characterization of the context within which the system operates. It can be argued that any definition of resilience for decision making, should appropriately acknowledge these contextual aspects and relate these to the other exogenous and endogenous components of resilience. Here we adopt the following definition of engineering resilience in the context of managed infrastructure systems:

Resilience is the endogenous capacity of a system to cope with a predefined exogenous perturbation, responding or reorganizing in ways that maintains its perceived essential function, identity, and structure, while also maintaining the capacity for adaptation and transformation.

Figure 23 shows the interrelationships of the exogeneous exposure factors associated with climate change, the endogenous system parameters most often associated with engineering resilience, and the normative context (e.g., passenger service priorities for urban transit) in which the system operates.

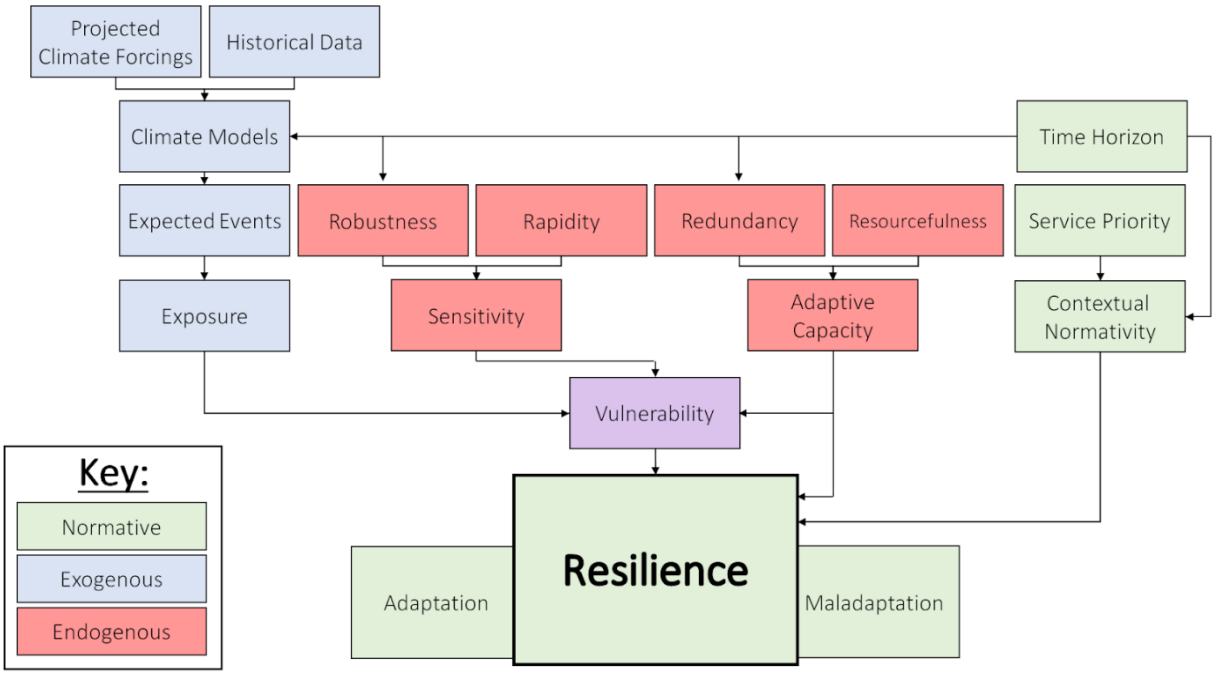

Figure 23: Topology of engineering resilience in the context of managed infrastructure systems.

This approach is consistent with previous definitions where resilience is reciprocally informed by the vulnerability of the system and its managed adaptive capacity (IPCC, 2007). Vulnerability is a function of endogenous system characteristics (sensitivity and adaptive capacity), as well as exogenous components that inform exposure. Commonly accepted characteristics of engineering resilience, namely robustness, rapidity, redundancy and resourcefulness (Bruneau et al., 2013) are incorporated into resilience as components of system sensitivity and adaptive capacity.

Sensitivity measures how well the system can withstand a class of exposures and is dependent upon the ability of the system to remain minimally unaffected by an exposure (i.e. robustness) and how quickly it regains lost performance after exposure (i.e., rapidity). Adaptive capacity, describing how the system may reorient during the recovery period, is dependent upon the inherent topology of the network (i.e.,

redundancy), as well as changes in passenger behavior, and the temporary deployment of available resources by the operating transit agency (i.e., resourcefulness). Exposure in the context of climate change is informed by projected climate forcings and historical data, which inform climate models that ultimately provide expected events and projected risks for a given region.

Defining a core system functionality and assigning perceived value of system components based on this core functionality serves as a key component of describing the socio-temporal context in which the system operates. In addition to those components outlined by the IPCC and existing literature, we include contextual normativity to better characterize core functionality. The inclusion of relative service priority for individual links within the network, and the planning horizon of interest are necessary to provide meaningful context to descriptions of system performance, and by extension resilience. These components ultimately rely on either value-based judgements or implicit biases of the modeler (transportation agency, etc.) and are crucial to placing system performance in the proper spatial and temporal context to support decision-making. For example, the time horizon of interest will influence the robustness and redundancy of a system, as both are subject to change over time as constituent parts degrade due to lack of maintenance (Ayyub, 2015). These could also result in removal of system links from service, altering system redundancy. In contrast, robustness and redundancy can be improved via planning and capital improvement projects.

Resilience is closely related to and shadowed by adaptation and maladaptation. Each of these three concepts have the potential to be characterized and quantified within a range of possibilities, yet they are also subject to uncertainty. The perception of each concept is ultimately dependent on the actor orientation and time horizon from which system performance is viewed. Hence, they are truly normative, and ultimately allow only for a partial characterization of each concept. Under certain circumstances, resilience priorities may be maladaptive, as unforeseen adverse path dependencies may result (Brown, 2011; Pelling et al., 2015; Fisichelli et al., 2016). For instance, the expected value of average annual loss reduction for a particular resilience measure may be less than the amortized long-term capital and operating liabilities. Transit agencies and planners should be cognizant of the potential for such path dependencies and adverse

outcomes, even when actions are performed in the name of resilience. Of the assessment frameworks surveyed within existing literature, none adequately addressed these nuances of resilience in the context of climate change, in particular the exogenous and normative aspects, or the uncertainty associated with resilience and adaptive actions.

4.2: Assessment Framework

Based on the generalized theory of resilience outlined above, an assessment framework for the resilience of rapid transit networks in the context of climate change (with specific focus on coastal flood risks) is proposed and shown in Figure 24.

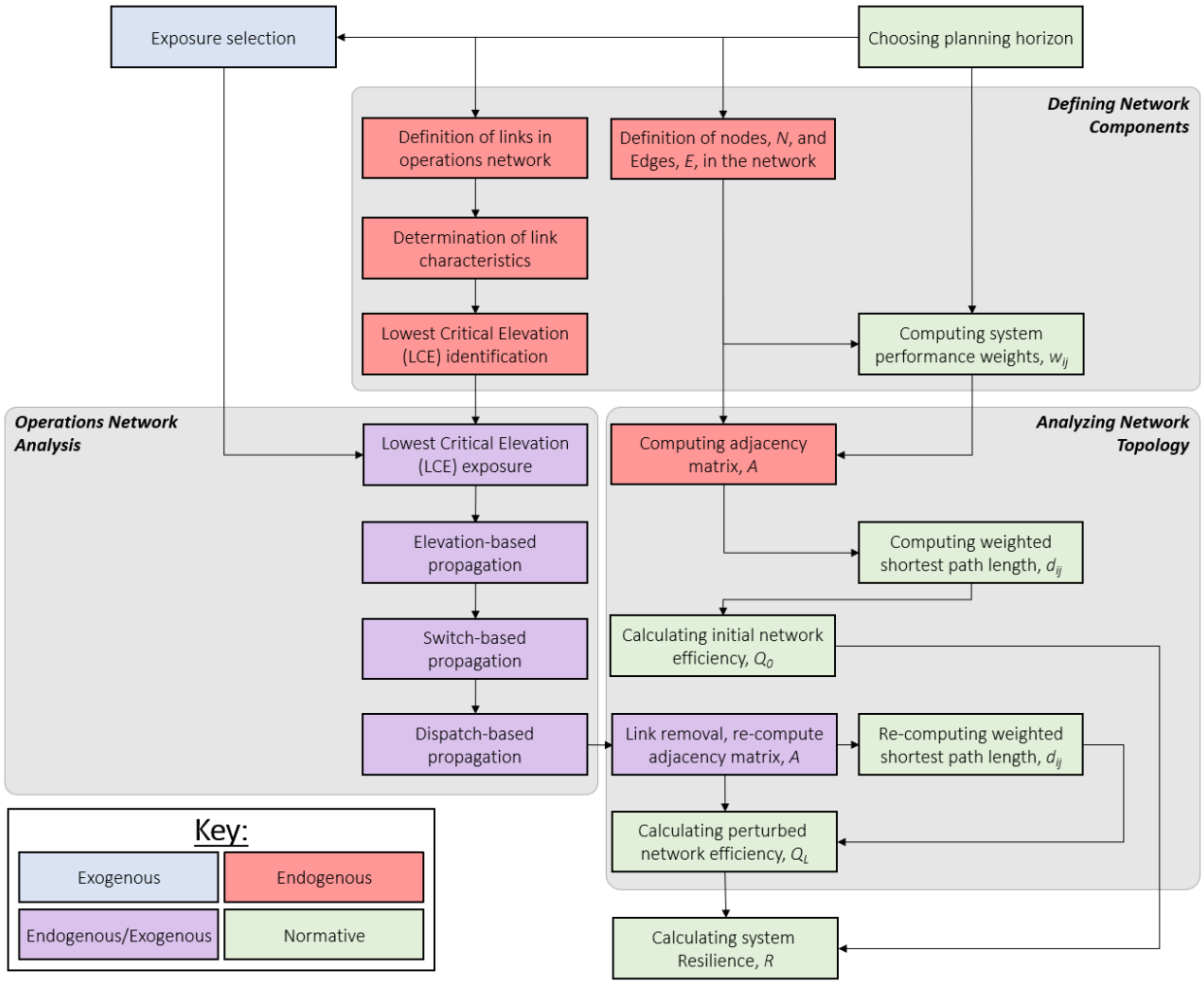

Figure 24: Proposed framework for calculating rapid transit system resilience.

Under this analysis framework, the time horizon of interest must first be specified, as it informs all subsequent aspects of analysis. The choice of time horizon should be informed by available risk projections, capital improvement planning criteria, and the design life of a given asset or asset of interest (as applicable). The selection of a time horizon should be in alignment with a transit agency's existing design and planning criteria (should such criteria already exist). Once a time horizon (and asset(s) of interest) is determined, an exposure scenario, whose intensity is dependent upon the risks projected for a given time horizon, can be selected. Generally, the exposure scenario of interest would be the agency's design flood event (e.g. 1-500 year flood).

The choice of time horizon interacts with the endogenous characteristics and topology of the system, as both are subject to change over time. However, unless information pertaining to these future changes is readily available, future deviations from present conditions cannot be captured. This increases the epistemic uncertainty present in the model constructed for analysis, particularly when considering scenarios further into the future. Despite this potential for increasing uncertainty over longer time horizons, existing system conditions are the most reasonable basis on which to assess future exposure, particularly in the context of capital project planning. Therefore, existing endogenous characteristics of the system, namely the known/current lowest critical elevations (LCE's) in the system (i.e. where water can enter or directly flood a portion of the system), track elevations, switch locations, train dispatch locations, and network topology should be characterized.

After the network topology is modeled, relative system performance weights, which will be detailed in a subsequent section, can be assigned to each undirected link in the network. Next, similar to existing graph theoretic frameworks, such as that outlined by Saadat et al. (2019), from the network topology, an adjacency matrix, the characteristic path length between each station-station combination in the network, and the efficiency of the network are assessed.

Using the additional endogenous characteristics outlined above, the response of the system to the exposure scenario selected can be approximated. Unlike other assessment frameworks, which only consider

endogenous characteristics described by a graph theoretic model, a more comprehensive model of the system, incorporating additional aspects of the system captures the robustness and redundancy of the system to a greater degree. However, even with this additional endogenous information, the assessment framework and system model outlined is incomplete. The framework does not attempt to characterize the recovery actions that can be taken by the transit agency, and therefore neglects the rapidity and resourcefulness of the transit network.

4.3: Resilience Framework Applied to Rail Rapid Transit Network in Boston

The remaining sections of this chapter will detail the creation of a model of the MBTA's rapid transit network and the evaluation of each step of the framework outlined above. The model and assessment framework were coded into CRaVAT transit (Climate Resilience and Vulnerability Assessment Tool for transit), a web-based resilience assessment tool using HTML, CSS, and JavaScript for use by decision makers at the MBTA.

4.3.1: Planning Horizon

The choice of planning horizon is subject to change, depending on the context in which a resilience analysis is performed. The resilience assessment tool allows the user the flexibility to choose an exposure scenario reflective of the time horizon for which they are planning. For instance, if a planner is deciding on whether to add flood protection to a critical piece of infrastructure that will temporarily be placed in a flood zone, they may choose a shorter time horizon. This time horizon would be characterized by a different portfolio of risks than if a planner were attempting to design a comprehensive flood protection system for the Blue Line. For the purposes of the recommendations laid out in the subsequent chapter, we treat 2100 (+80 years) as a long-term planning horizon, such that a cohesive adaptation roadmap for the MBTA system can be proposed.

4.3.2: Exposure Selection

Chapter 2 has shown the potential impacts of climate change in the Greater Boston area, specifically sea level rise and the associated increase in coastal flood risk. Our current state of knowledge is encapsulated in the BH-FRM (Bosma et al., 2015). For each of the 3 coastal flood exceedance probability (CFEP) raster layers produced by the BH-FRM, 9 separate exposure events were extracted using the 'Reclassify' and 'Raster to Polygon' tools in ArcMap 10.6. Across 3 SLR conditions, a total of 27 coastal flood exposure scenarios were prepared for analysis, shown in Table 1.

Table 1: Coastal flood exceedance probability (CFEP) scenarios considered in resilience analysis.

Sea Level Rise from 2000 [m]	**Coastal Flood Exceedance Probability (CFEP)**								
+0	100%	50%	25%	10%	5%	2%	1%	0.2%	0.1%
+0.21	100%	50%	25%	10%	5%	2%	1%	0.2%	0.1%
+1.04	100%	50%	25%	10%	5%	2%	1%	0.2%	0.1%

The sea level rise conditions assessed in the BH-FRM are indicative of a worst-case outcome, in which the high AR4 scenario (Parris et al., 2012) was fully realized, with an additional +0.21 m of SLR by 2030 and +1.04 m of SLR expected by 2070 (relative to year 2000 mean sea level; Bosma et al., 2015). Consideration of the full suite of exposure scenarios provides the greatest understanding of climate change related coastal flood risks, at which point in the future portions of the system are vulnerable, and the probability that a given portion of the system will be affected.

4.3.3: System Performance and Acknowledgement of Normativity

While transit networks possess design intentionality and are closed engineered systems, they exist in the context of and interact with a broader socio-economic system, as their primary objective and core function is to transport people. Previous definitions of resilience, namely those which rely on unweighted links to represent a transit network (Saadat et al., 2019; Zhang et al., 2018; Li et al., 2017; Testa et al.,

2015), are inadequate to describe this core functionality. System performance measures should reflect the intended core functionality of the system and incorporate service to passengers.

The relative priority assigned to each link in the system should reflect the quantity and characteristics of the passengers served by each link. In this way, the criticality of links and associated assets can be evaluated, providing decision makers with a more complete understanding of system components and how to prioritize resilience and adaptation efforts (Dowds & Aultman-Hall 2015). Dall'Asta et al. (2006) proposed weighting links within a network by the inverse of link capacity (i.e., higher capacity links became shorter and more valuable in the context of shortest path assignment). Xing et al. (2017) assign weight to network links on the basis of the inverse of bi-directional passenger flow on a given link. Building off these previous works, a relative system performance weight, based on a normalized passenger flow is proposed:

$$w_{ij} = \frac{q_{max}}{q_{ij}} \tag{4.1}$$

The relative system performance weight for the link between stations i and j, w_{ij}, is the ratio between the largest bi-directional passenger flow in the system, q_{max}, and the bi-directional passenger flow for the link of interest, q_{ij}. Similar to the capacity-based weighting proposed by Xing et al. (2017), this weight prioritizes links with larger passenger flows, and places less priority on less frequently travelled links.

This system performance weighting was applied to the MBTA network, using the average weekday passenger flows for September to December 2017, obtained from ODX (Origin-Destination Matrix) data collected by and processed for the MBTA (Gordon, 2019). The resulting dataset, queried from automatic fare collection (AFC) records, provides the best available measure of the level of ridership in the system. However, it likely underestimates ridership on the Green Line, where morning peak hour commuters boarding from at-grade stations often avoid paying fares (as they board at the side and rear entrances of the crowded cars). Additionally, the Silver Line, the only bus rapid transit (BRT) line included in the analysis, provides its own data collection challenges. Due to the partially subterranean nature of the Silver Line's route, its automatic vehicle location (AVL) data is inaccurate, rendering fare collection information unreliable (J. Gordon, pers. comm., April 19th, 2019). Further, riders taking the Silver Line from any

terminal at Logan Airport do not need to pay for a fare and are not accounted for in the data. Therefore, instead of relying upon AVL/AFC data, passenger flow on the Silver Line was estimated using ridership estimates provided by the MBTA (2014). The relative system performance weight (Eqn. 4.1) was normalized by the passenger flow from Downtown Crossing to South Station (an average 115,763 passengers per weekday over the stated period). Figure 25 shows the resulting network map, providing an intuitive understanding of the relative importance of each line in the system.

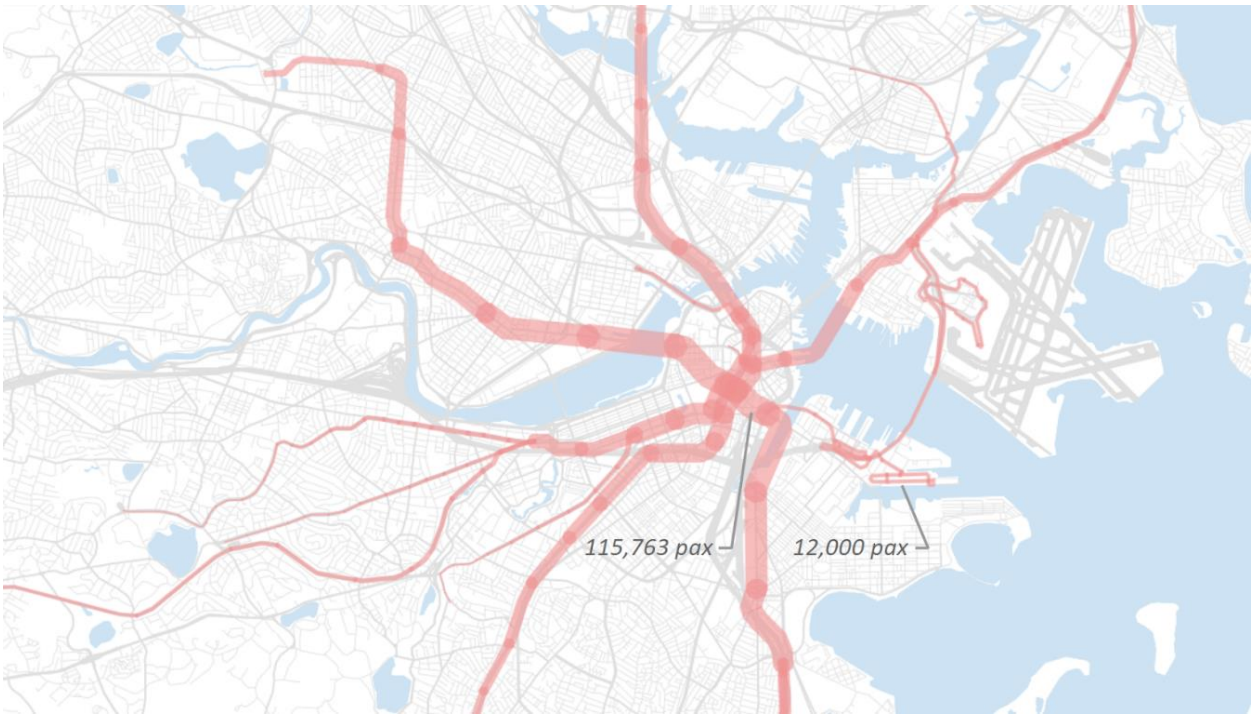

Figure 25: Relative importance of links in the MBTA rapid transit network based upon weekday passenger flows in Fall 2017. The most heavily travelled link, Downtown Crossing to South Station, carried an average of 115,763 passengers per day; Silver Line passenger flows were estimated at 12,000 passengers per day.

Inclusion of ridership levels captures the spatial variations in service priority within the system but does not capture the relative importance of transit service to individual passengers. For more disadvantaged populations with fewer alternate modes of transportation, connection to the transit network (or lack thereof) is more critical (i.e. there is an underlying equity issue). Several authors, such as Ben-Elia and Benenson

(2019) and Song et al. (2018), have investigated the spatial distribution of transit equity based on socioeconomic status, though research in this domain is only just emerging.

Equity considerations in the context of transit are beyond the scope of the current research, though they should not be overlooked. A measure of equity, incorporating the economic concept of diminishing marginal utility and using publicly available census data, can be synthesized with equity weights proposed by Kind et al. (2011). These weights can be spatially distributed across a transit network, with connectivity to predetermined locations prioritized. Such an analysis is clearly worthy of future study.

4.3.4: Network Topology

Similar to Xing et al. (2017), system performance is based on the analysis of a weighted, undirected graph, *G (N,E,W)* in which stations are represented as nodes, $N = \{n_i | \ i = 1,2, \dots, N\}$ and tracks between stations are represented as undirected edges, $E = \{e_{ij} = (v_i, v_j) | \ i, j = 1,2, \dots, N, i \neq j\}$. Weights, $W = \{w_{ij} | \ i, j = 1,2, \dots, N, i \neq j\}$ are assigned to each link in the network as described in equation 4.2. Associated operations graph links, $O = \{o_{ij} | \ i, j = 1,2, \dots, N', i \neq j\}$ are also assigned to each link, thereby coupling the graph theoretic model to an ancillary model which will be detailed in the subsequent section. The topology of the network is characterized by an adjacency matrix, A, in which an entry is defined as the relative performance weight, w_{ij}, if the nodes are connected, or infinity, if the links are unconnected. Mathematically, each adjacency matrix entry is defined as:

$$a_{ij} = \begin{cases} w_{ij} & (v_i, v_j) \in E \\ \infty & (v_i, v_j) \notin E \end{cases} \tag{4.2}$$

With the relative performance weight as defined, an adjacency value of infinity between nodes *i* and *j* represents a connection through which an infinitesimally small number of passengers (asymptotically approaching 0) travel the network between the nodes. This is logically consistent with the relative performance weight definition (Eqn. 4.2). With this weighting, the shortest path between a given pair of links represents the relative importance of the connection in the system, with shorter connections considered

as more important in the network. To provide a system wide measure performance, the network efficiency, E_G, of the network (Latora & Marchiori, 2001) is used:

$$E_G = \frac{1}{N(N-1)} \sum_{i \neq j} d_{ij} \tag{4.3}$$

wherein d_{ij} denotes the shortest weighted path length between any given nodes. With the relative performance weighting as described, the efficiency of the network provides an average measure of the relative importance of station-to-station combinations in the network. When links are removed from the network, losses in connectivity are weighted in proportion to their impact on passenger flows. Defining system performance in this manner captures a passenger-based service priority and the redundancy inherent in the topology of the network.

4.3.5: Operations Network Layer

The network-based model captures topology as it is perceived by passengers but does not represent the operational characteristics of the network. These operational characteristics govern system response and the ability to recover from a perturbation and are therefore crucial to understanding the impacts of a given event on the system. Of primary interest are the locations of track switches (crossovers), at which trains can be turned around within the system. The presence of these crossovers enables partial rail operations along line segments, making their location important when attempting to characterize the partial closure of a given line.

Here we introduce a separate ancillary representation of the MBTA rapid transit network, termed the operations network layer, $O\ (N', L, I^D, E^L, S^w, D^s, A^D)$. In this ancillary system, each rapid transit line is subdivided by the presence (or lack thereof) of a track switch or siding, based off a publicly available map (Vanshnookenraggen, 2017) and track geometry data reported by HNTB (2016a-j). A track switch/crossover (Figure 26a) enables a train to cross from one track to the other, enabling bi-direction

operations. A track siding (Figure 26b) is a short spur of track on which trains can be temporarily staged or stored.[4]

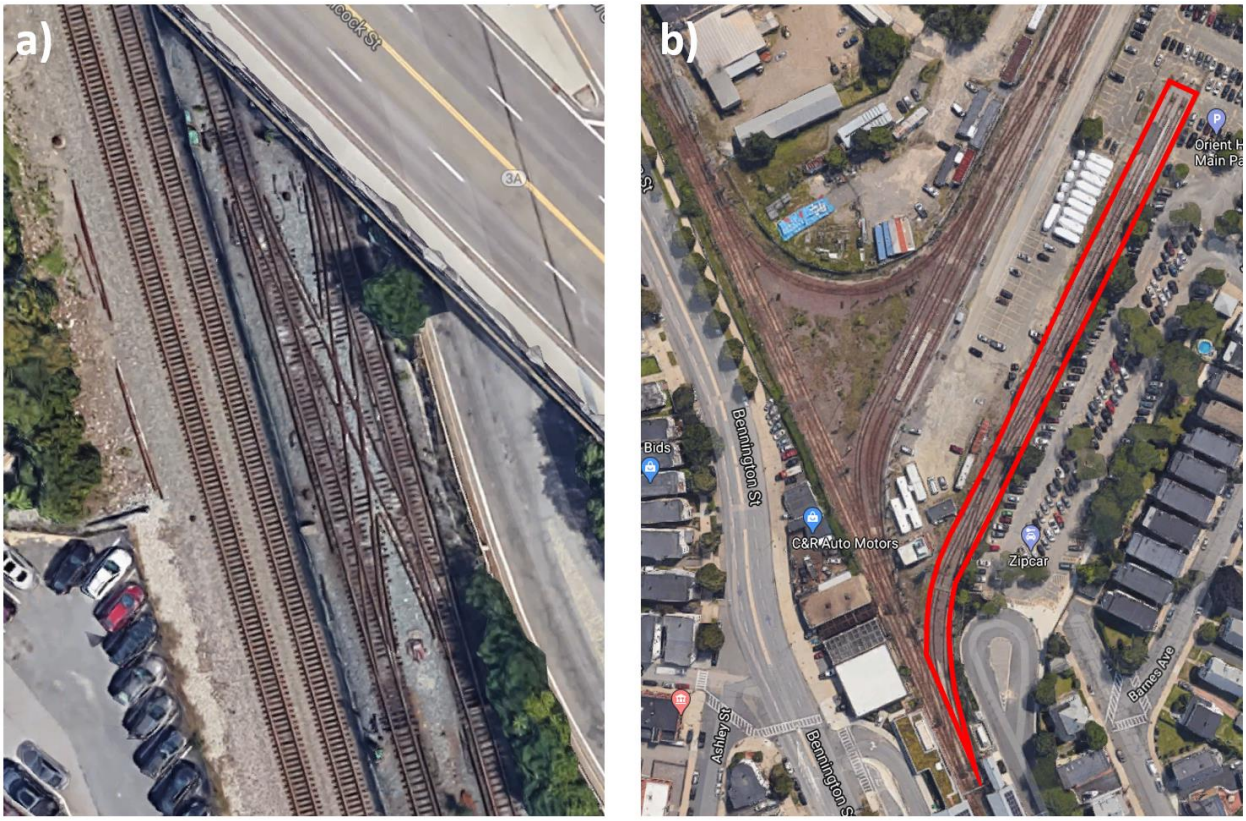

Figure 26: a) An example of a track switch on the Red Line in the proximity of North Quincy Station; b) a track siding on the Blue Line in the proximity of Orient Heights Yard, outlined in red.

In this operations-centric representation of the system, nodes, $N' = \{n'_i | \, i = 1,2, \dots, N'\}$ are not stations, but simply demarcate the ends of each operations segment and carry no additional significance. Links, $L = \{l_{ij} = (v_i, v_j) | \, i, j = 1,2, \dots, L, i \neq j\}$ denote different operation segments and are described by several attributes. The operations network layer was constructed using ArcMAP 10.6 and the ArcGIS JavaScript API.

[4] Alternatively, the operations network can be divided based on the location of signal blocks within the system, however this information was not readily available for the entire transit network.

Each operations network link, L_{ij}, has an associated link identification number, $I^D = \{i_{ij}^D | \, i, j = 1,2, \dots, N', i \neq j\}$. The operations network links in each rapid transit line are sequentially numbered, starting from the northernmost terminus of each line (with the exception of the Silver Line, which was numbered starting from South Station) as shown in Table 2. For lines that branch, namely the Red and Green Lines, one branch was numbered sequentially, while the remaining branches are numbered sequentially from the branch point towards the distal (outbound) terminus.

Table 2: Operations network layer identification number, I^D , numbering scheme.

Rapid Transit Line	**Section [Station – Station]**	**Numbering Scheme**
Red – Ashmont, Mattapan	Alewife – Mattapan	1-21
Red – Braintree	JFK/UMass – Braintree	22-35
Orange	Oak Grove – Forest Hills	101-118
Green "A", E Branch	Lechmere – Heath Street	201-217
Green "A", D Branch	Hynes - Riverside	217-235
Green – C Branch	Kenmore – Cleveland Circle	236-241
Green – B Branch	Kenmore – Boston College	242-250
Blue	Wonderland - Bowdoin	301-317
Silver	South Station - Chelsea	401-450

Using track alignment data provided by the MBTA (HNTB, 2016a-j), each link is also assigned a critical elevation, $E^L = \{e_{ij}^L | \, i, j = 1,2, \dots, N', i \neq j\}$ expressed in feet relative to the North American Vertical Datum of 1988 (NAVD88). This critical elevation was either the highest, lowest, or average elevation of a given segment, depending on the elevation profile of the segment and those adjacent to it. Figure 27 below shows a sample elevation profile for a section of the Blue Line and the chosen critical elevations corresponding to the operations network links.

Additional characteristics of each link, namely the presence of a switch, the presence of a dispatch location, and non-sequential adjacent links were also incorporated into the model. The presence or absence of a switch, $S^W = \{s_{ij}^W \mid i,j = 1,2,\dots,N', i \neq j\}$ is denoted by a binary flag:

$$s_{ij}^w = \begin{cases} 1 & if\ present \\ 0 & if\ absent \end{cases} \tag{4.4}$$

Similarly, the presence or absence of a dispatch location, $D^S = \{d_{ij}^S \mid i,j = 1,2,\dots,N', i \neq j\}$ is also binary:

$$d_{ij}^s = \begin{cases} 1 & if\ present \\ 0 & if\ absent \end{cases} \tag{4.5}$$

Dispatch locations were assigned to operations network links which provided connection to a MBTA rail yard, siding from which trains are regularly dispatched (H. Lyons-Galante, pers. comm., Nov. 8th, 2019), and the terminus or each line.

Lastly, adjacent links that are not along the same transit line are also characterized. These are locations at which transit lines run: 1) in parallel (such as the Orange and Green Lines at North Station); 2) fork (such as where the C and D branches of the Green Line diverge); or 3) intersect (such as where the Red Line passes over the Orange Line at Downtown Crossing).

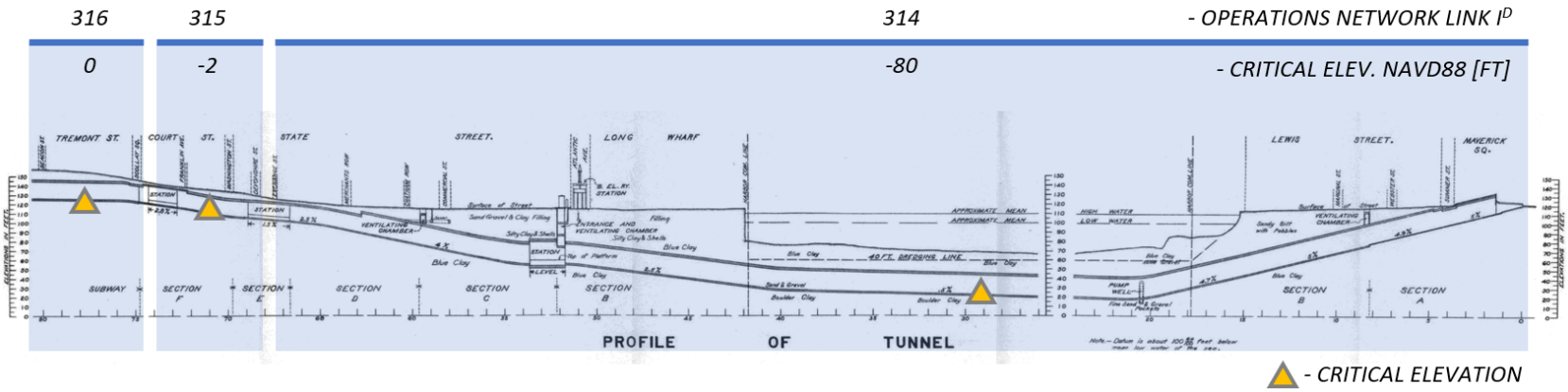

Figure 27: Elevation profile of the Blue Line from State Street to Boston Harbor (Boston Transit Commission, 1895). The associated operations network links, and their corresponding critical elevations are shown in relation to the tunnel profile.

For a given link l_{ij}, should such an adjacent link, $A^D = \{a^D_{kl} | \, k, l = 1,2, \ldots, N', k \neq l\}$ exist:

$$a^D_{ij} = i^D_{kl} \tag{4.6}$$

$$a^D_{kl} = i^D_{ij}$$

Else, if no adjacent link exists for a given operations network link:

$$a^D_{ij} = 0 \tag{4.7}$$

In this manner, the endogenous characteristics of the transit system relevant to performance are characterized. Each edge in the graph theoretic representation of the system, G, was associated with a concurrent operations graph link. For edges in *G* that were concurrent with several links in *O*, the link without a switch or the link with the lowest elevation was associated with the edge in *G*. The operations graph was used to determine the extent of impact posed by a given exposure scenario.

4.3.6: Lowest Critical Elevations (LCE's)

To approximate the system's robustness under a portfolio of risks associated with coastal flooding or extreme precipitation-based flooding, a set of lowest critical elevations (LCE's) are flagged and identified for the MBTA's rapid transit network. These LCE's are points at which the transit system is at grade, or ingress points where water could conceivably enter the system, such as subway ventilation grates on sidewalks, or station entrances.

After consultation with the MBTA and a survey of available documents, it was clear that the locations of flood ingress points, or LCE's, were not previously well-documented or stored in a central location. To determine potential flood ingress locations, the Author performed a methodical Google Maps (n.d.) based survey of the MBTA rail rapid transit system. Using Google's satellite imagery, the alignment of each rapid transit line was inspected, looking for subway ventilation shafts, station entrances, portals, or at-grade sections of track. Possible LCE's were verified using Google's street view, as well as in person inspections (Blue Line from Aquarium Station to State Street). Once identified, each LCE was assigned to the

appropriate operations network link. Coordinates of LCE's were initially transcribed directly into a GeoJSON file, which was later converted into two shapefiles (one containing point features, the other containing polygon features) using ArcMap. These shapefiles were then converted into ArcGIS Online feature layers for use with the ArcGIS API for JavaScript. Figure 28 below shows a sample LCE identification along a section of the Silver Line's alignment in South Boston.

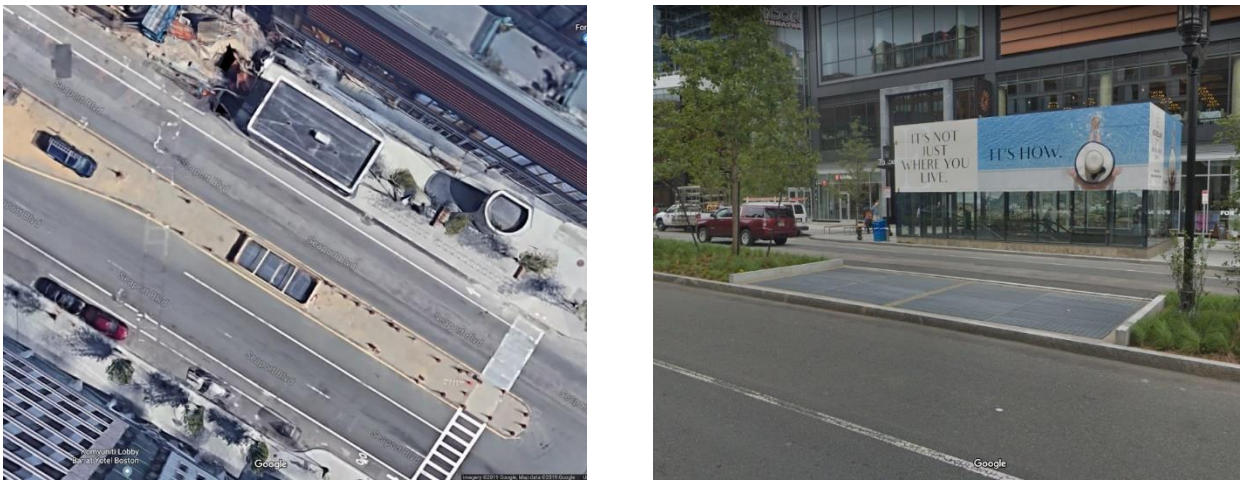

Figure 28: Identification of an LCE using Google Maps along the Silver Line in South Boston (Google Maps, n.d.).

A total of 247 LCE's were identified for the MBTA system; 164 LCE points and 83 LCE polygon features. A subset of these LCE's, shown in black, can be seen in Figure 29 below. For a complete list of LCE's see Appendix C.

With a complete set of LCE's, the impact of each of the 27 coastal flood exposure scenarios can be characterized by performing a simple geospatial intersection between the LCE layers and the flood extent layer using a custom function written for the ArcGIS JavaScript API. For each flooded LCE, the associated operations graph link is considered flooded and flagged for further analysis, which will be subsequently detailed.

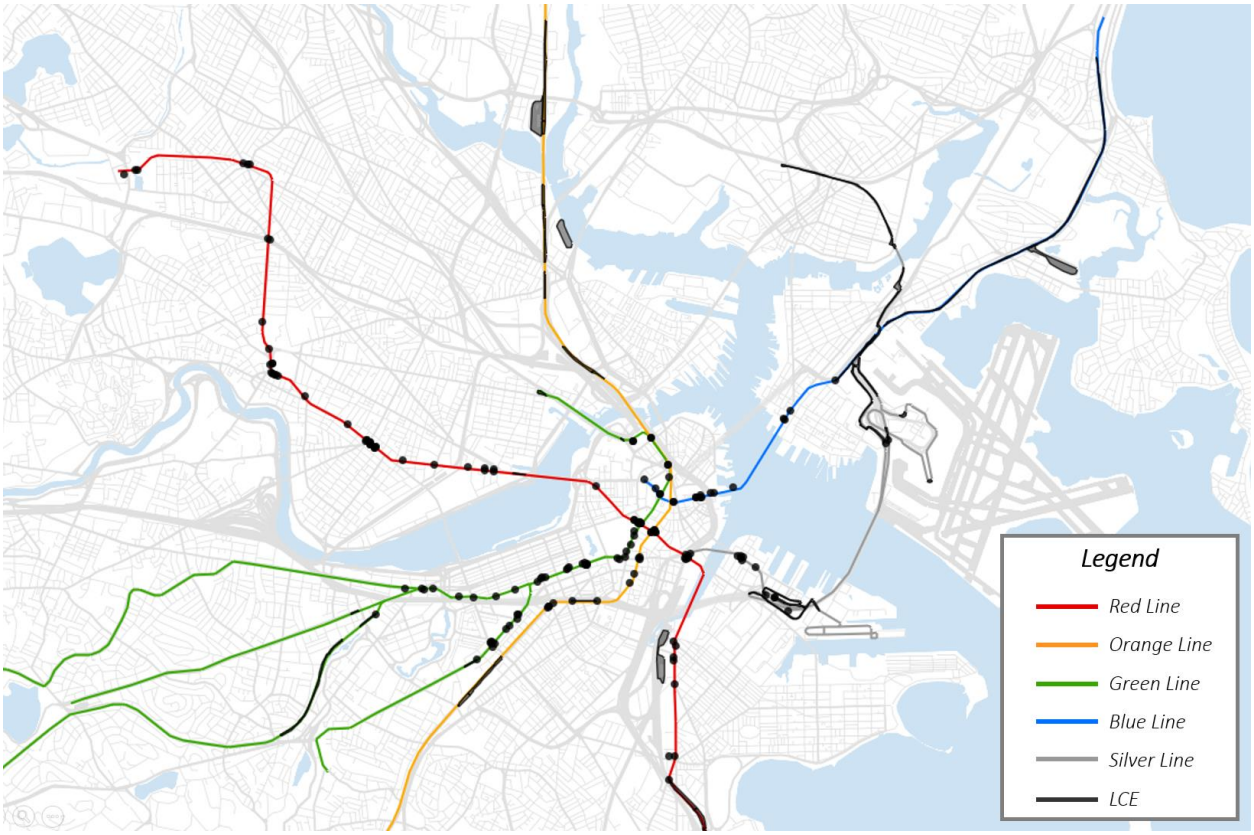

Figure 29: Lowest Critical Elevations (LCE's), shown in black, for the MBTA's rapid transit lines. LCE's represent locations at which tracks are at grade, or surface water could enter into the system.

4.3.7: Operations Network Analysis

For each of the operations network links flagged through the LCE analysis, further analysis using elevation, switch, and dispatch location is performed to determine the extent of system functionality affected. First, track elevation data is used to determine the direction and extent of water flow in the system, under a worst-case assumption of a large inflow of water. Each flagged link is input into a recursive algorithm, comparing its critical track elevation to that of its neighboring and adjacent links. If a neighboring or adjacent link has a lower critical elevation, then it is also considered flooded, as shown in Figure 30. The links neighboring or adjacent to the “newly flooded” link are then be checked for a lower critical elevation amongst its neighbors or adjacent links, recursively repeating until a link is found with no adjacent or interconnected links with a lower critical elevation. Further details, such as the location and

degree of criticality of assets along a given link, as well as the degree of flooding are ignored, due to a lack of availability of asset management data and estimates of flow rates and inundation duration at flood ingress points.

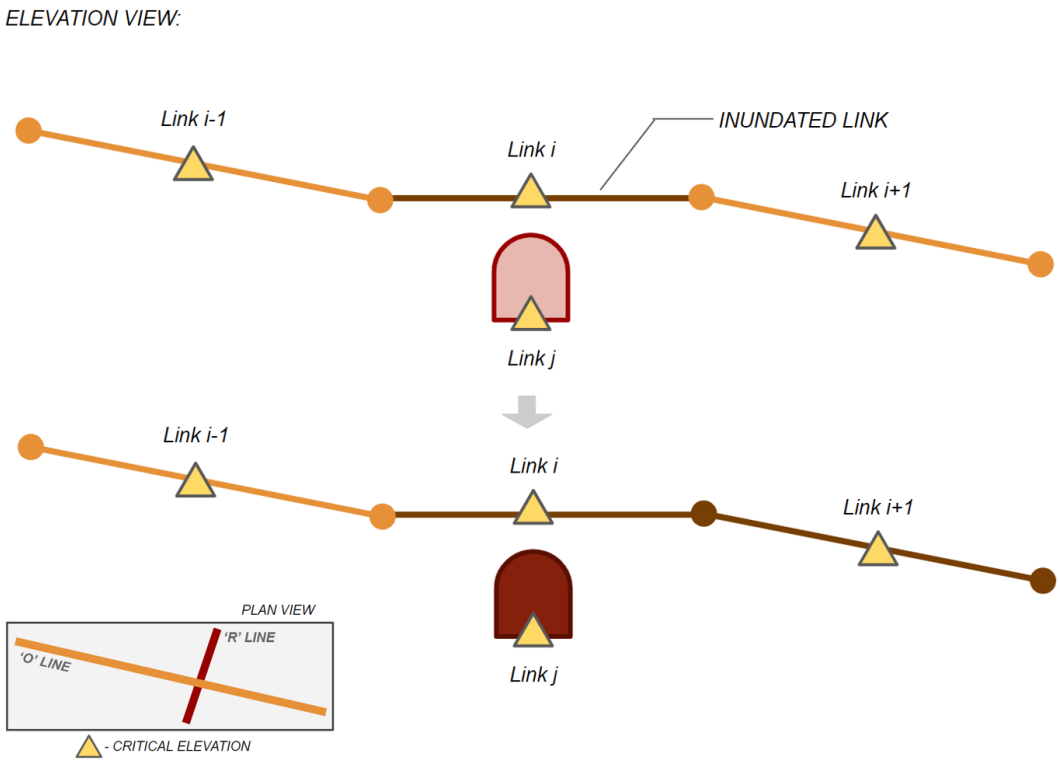

Figure 30: Illustration of the elevation based operations network link loss propagation.

Next, the remaining segments of each transit line are assessed, ensuring that plausibly operable segments are bounded by switch locations. Under typical operating procedures, for a train to "turn around" it must be able to switch over to the parallel track. In the model, it is assumed that trains must be able to turn around at the terminus of the line. In the special case of the Silver Line, which is a bus rapid transit (BRT) line, it is assumed that a bus can turn around on any operations network link. Should a given operations link with no switch present neighbor a link flagged as inoperable, the link would also be flagged as inoperable, as illustrated in Figure 31.

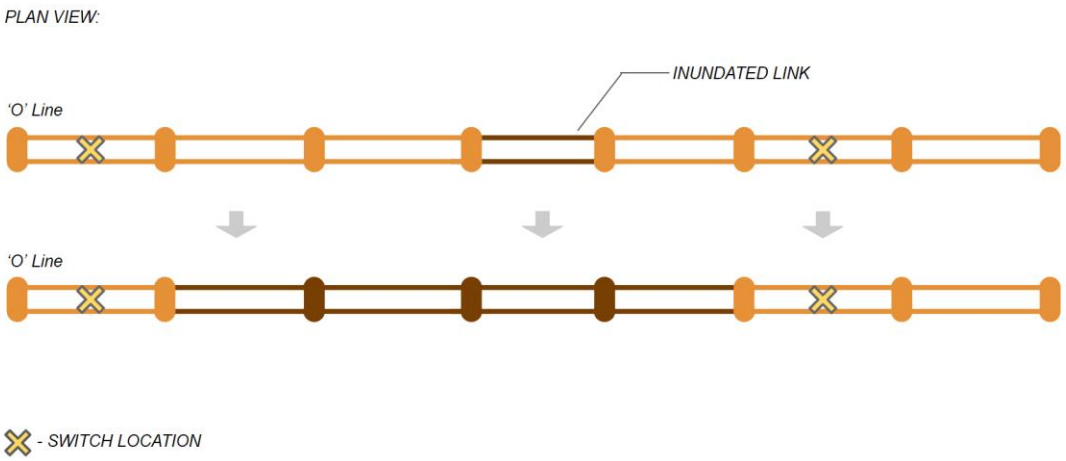

Figure 31: Illustration of the switched based operations network link loss propagation.

Lastly, each plausibly operable segment within the operations network is checked for a dispatch location (a yard or track siding from which revenue vehicles are regularly dispatched under normal operations). Should a plausibly operable segment not contain a dispatch location, it is assumed that no trains could be present to operate on the segment; any such segments are then removed from the operations graph. An illustration of the dispatch based link loss propagation is shown in Figure 32.

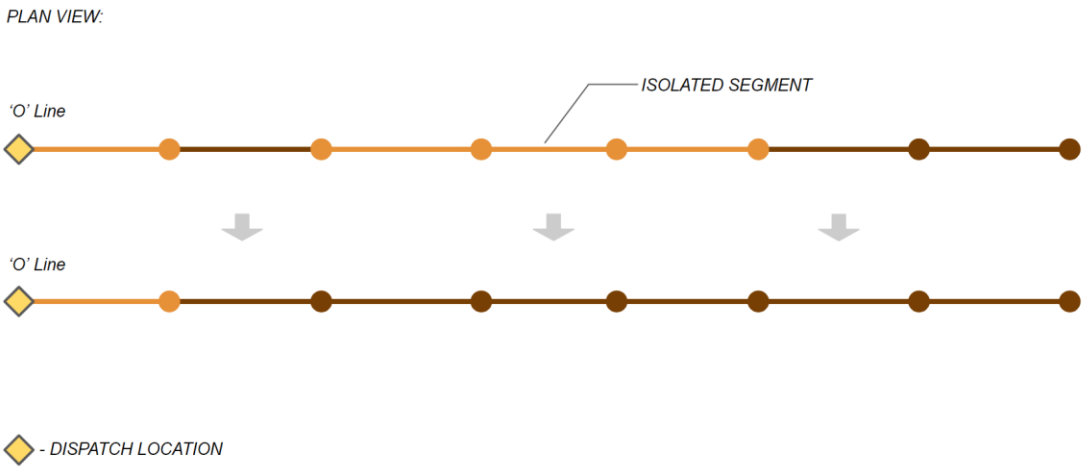

Figure 32: Illustration of the dispatch based operations network link loss propagation.

After completing the analysis of the operations network, operations graph links are removed; corresponding revenue track graph links are also removed, thereby constructing a worst-case perturbed

system topology. An example perturbed system topology is shown in Figure 33. With this perturbed system, the shortest path length between each station-to-station combination is re-computed, from which the minimum system performance (network efficiency), Q_L can be computed.

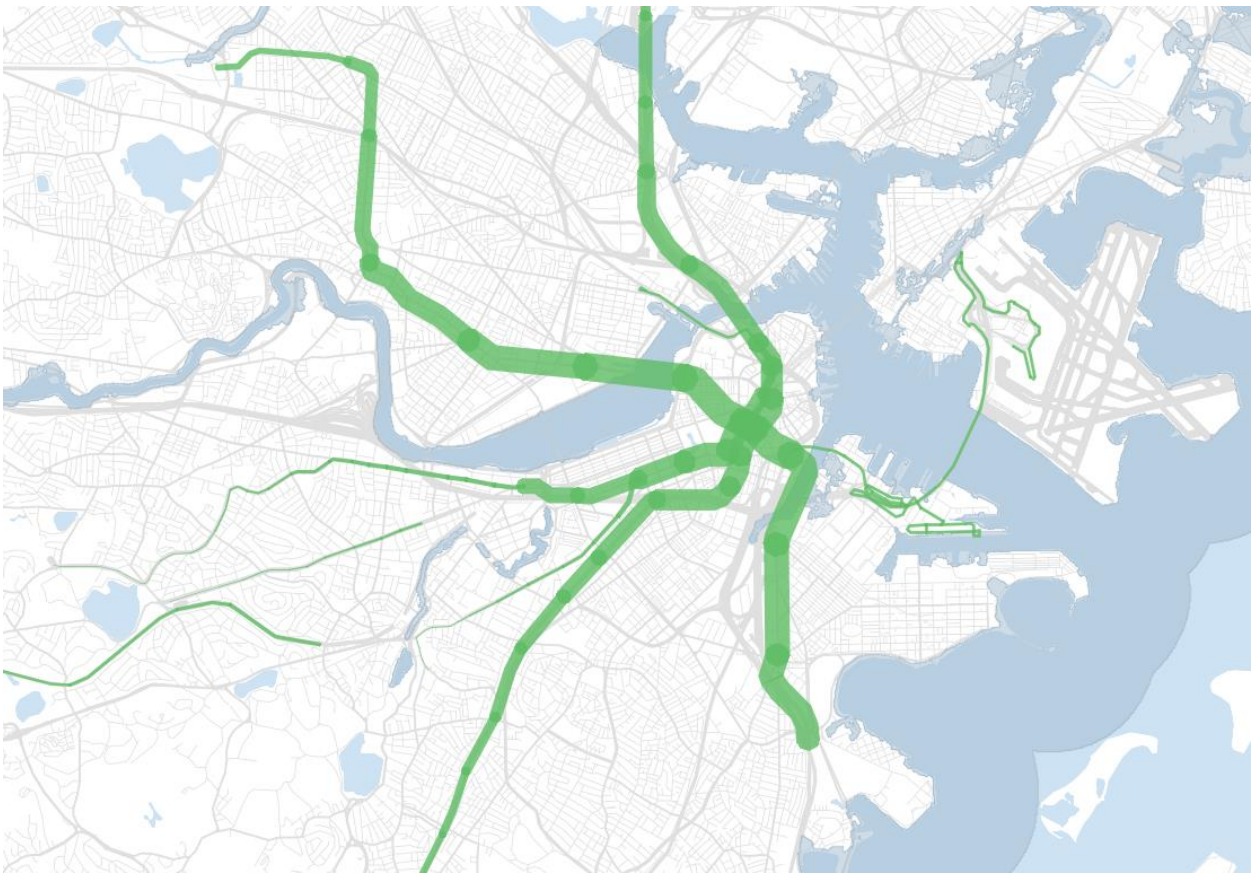

Figure 33: An example of perturbed system topology under the projected 1-100 year event in 2013 from the Boston Harbor Flood Risk Model (BH-FRM).

4.3.8: Computing System Resilience

In computing the resilience, we assume that system performance will return to pre-disruption levels of service. In practice this implies sufficient and immediate funding is available to support recovery actions (e.g., emergency repairs to restore flooded track sections). While this is not fully representative of options available to decision-makers, it serves as a reasonable initial basis for analysis. In reality, post-disruption

funding could be limited or delayed, such that full recovery is contingent on financial resources (from the capital budget, or through the issuance of resilience bonds; Kennan, 2018a). The details behind such financing are beyond the scope of this work. Similarly, post-perturbation recovery levels may also reflect performance reductions consistent with accelerated deterioration of capital assets directly or indirectly stressed by the flooding event (Kurth et al., 2019).

Here we assume that system performance recovery occurs linearly over time, as shown in Figure 34. This neglects details of the rapidity and resourcefulness of the system, but has been shown to be a reasonable approximation under minor perturbations (Chan & Schofer, 2016). Resilience can be calculated as a normalized area under the system performance curve:

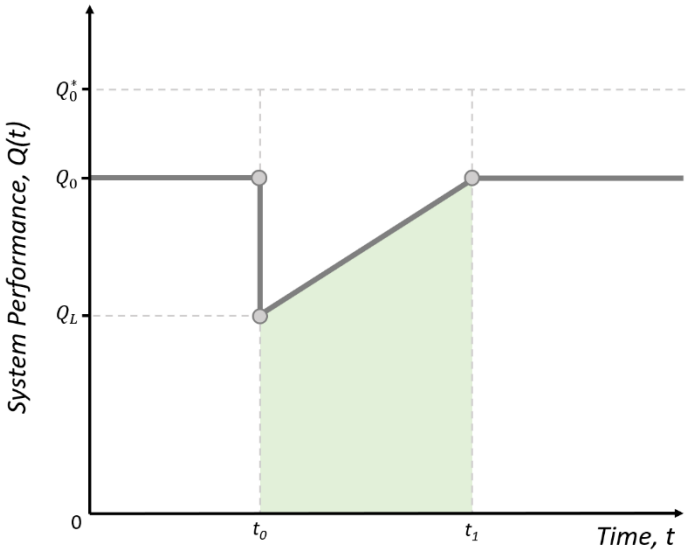

Figure 34: Assumed system performance curve for determination of system resilience.

With the assumptions of linearity established above, resilience can be calculated as a normalized area under the system performance curve, and takes the following form:

$$R = \frac{Q_0 + Q_L}{2Q_0^*} \tag{4.4}$$

where Q_L is the minimum system performance associated with the given perturbation, Q_0 the baseline system performance described above, and Q_0^* the system performance level against which response is measured. Characterizing resilience in this fashion does not consider time, neglecting the associated dimensionality of system response and the duration of perturbation impacts.

This definition is independent of the recovery time, and hence, neglects the associated dimensionality of system response and the duration of perturbation impacts. In lieu of such spatial and temporal simplifying assumptions, a more comprehensive assessment method should be developed. This method would consider more complex interactions between the transit network at a given level of exposure; including specific recovery actions, the rate at which they occur, and more detailed asset information that would allow for a more realistic representation of system performance. For example, specific recovery actions, such as providing bridging bus services over affected rail links, would allow for a nonlinear recovery curve, requiring a more general definition of resilience (Saadat et al., 2019; Zhang et al., 2018; Franchin & Cavalieri, 2015):

$$R = \frac{\int_{t_0}^{t_1} Q(t)dt}{(t_1 - t_0)Q_0} \tag{4.5}$$

Simulation of these processes better recognizes the time dependence of resilience, as well as the endogenous system characteristics that are typically neglected in analyses. Although the additional information may not be readily available, it may be estimated through scenario planning exercises within a transit agency. A case study of the recovery actions taken by the MBTA during the winter of 2015 was investigated and is detailed in Appendix E to illustrate how interventions affected service restoration.

4.3.9: Calculating Connectivity Loss

Through discussion with stakeholders at the MBTA, it became clear that quantification of resilience in the manner described above was too abstract for applications such as capital project planning. In order to provide a practical metric with a more substantive physical significance, the connectivity loss metric was

conceived. Mathematically and with respect to system performance, connectivity loss, C_L (identical to the systemwide vulnerability metric described by Saadat et al., 2019 was included in CRaVAT transit):

$$C_L = \frac{Q_0^* - Q_L}{Q_0^*} \tag{4.6}$$

where Q_0^* denotes the baseline system performance and Q_L denotes the perturbed system performance, as shown in Figure 34. In contrast to the resilience metric (Eqn. 4.4), which measures the normalized degree of performance sustained over a perturbation period, connectivity loss measures the relative decrease in system performance under the peak extent of a given perturbation.

With system performance defined as the efficiency of the network weighted by normalized passenger flows, connectivity loss provides a measure of systemwide functionality loss weighted by passenger flows. Thus, when a given link is removed from the network, all new shortest station-station paths reliant upon the link are affected, thereby lowering system performance in proportion to the relative significance of each station-to-station combination affected. In other words, since links are weighted by proportion of passenger trips, connectivity loss measures the relative proportion of systemwide trips affected by the perturbation. Framing systemwide rapid transit vulnerability from this passenger-oriented perspective provides additional context and meaning to the analysis such that it may be readily grasped by transportation professionals.

Connectivity loss also provides a meaningful basis on which to assess the relative importance of individual links in the system. A separate connectivity loss analysis was also performed, assessing the systemwide effect of flooding at each location found to be vulnerable under the three 1-100 year coastal flood exposure events. For each vulnerable location, the corresponding operations network link was flagged for removal, after which the operations network analysis outlined above was performed to determine the extent of the transit system affected, and by extension the minimum system performance, Q_L, from which the associated connectivity loss, C_L, was calculated. Vulnerable locations were ranked based on the scenario under which they became vulnerable, and the degree of connectivity loss incurred by the system when they

were exposed. The results of this ranking process, which will be detailed in the following chapter, directly inform the recommendations for an adaptation roadmap.

5. Results

Boston's rail rapid transit system, colloquially known as "the T", consists of 5 separate lines, and is operated and maintained by the MBTA. The above resilience assessment framework was applied for the MBTA system under various (n=27) coastal flooding exposure scenarios projected by the Boston Harbor Flood Risk Model (Bosma, et al., 2015). A selection (n=9) of coastal flood scenarios of varying annual coastal flood exceedance probability (CFEP; 100%, 50%, 25%, 10%, 5%, 2%, 1%, 0.2%, 0.1%)[5] were assessed for 3 SLR conditions relative to local sea level in the year 2000:

1) +0 m in 2013
2) +0.21 m in 2030
3) +1.04 m expected in 2070

This chapter summarizes the results of these assessments; a complete set of results, generated via the CRaVAT transit program, can be found in Appendix B. These results were used to compile a list of critical locations projected to be exposed to coastal flooding by the end of the 21st century; these locations are summarized in this chapter and are discussed in further detail in Appendix D. Lastly, model validation and limitations are also outlined.

5.1: Pre-Perturbation System Performance

System resilience is predicated on the return to a pre-perturbation system performance level, Q_0. As SLR increases, this pre-perturbation performance level will decrease. Assuming that no adaptive actions are taken, portions of the system will eventually be below mean sea level, or flooded at high tide, thereby reducing daily system performance as defined. To reflect this, the 1-1 year coastal flood event (100% CFEP) was taken to approximate average high tide conditions and by extension, the pre-perturbation system performance, Q_0. Figure 35 shows the decrease in baseline system performance estimated by the model for

[5] A 1% CFEP is equivalent to a 1 in 100 year event. Similarly, a 5% CFEP is equivalent to a 1 in 20 year event.

the SLR scenarios outlined previously, and an interpolated degradation curve through 2080 due to the stress imposed on the system by SLR.

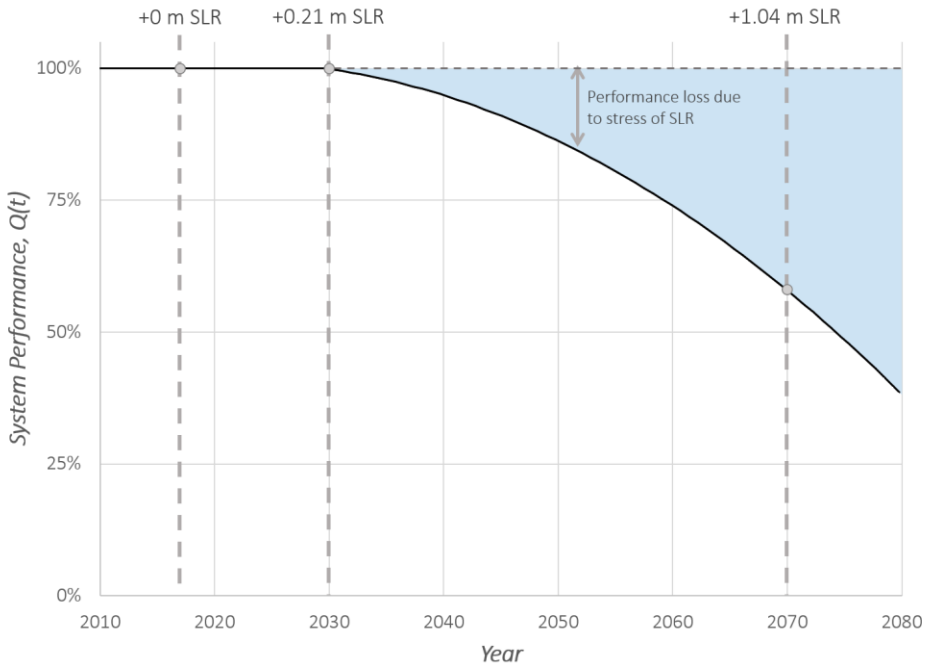

Figure 35: Projected MBTA rapid transit system performance degradation through end of century arising from sea level rise (SLR).

Under conditions projected with +0.21 m of SLR, the system is unaffected, but on the cusp of performance loss, as the emergency egress east of Aquarium Station on the Blue Line is potentially subject to surface inundation in the model. However, the emergency egress pavilion sits approximately 0.3 m (1 ft) above the surrounding wharf, already has some degree of flood protection, and can also be easily protected from inundation by simple flood protection measures, some of which the MBTA is actively considering (Weston & Sampson, 2019). Thus, it is assumed that baseline system performance in 2030 would not be adversely impacted by high tide flooding.

In contrast, under +1.04 m of SLR, shown in Figure 36 below, inundation of Long Wharf is much more severe, causing flooding of the Aquarium Station head house, as well as all the Aquarium Station entrances

on State Street. Further inundation along the Blue Line, including at the Maverick Portal, Airport Station, tracks adjacent to Suffolk Downs and leading to Wonderland Station, and tracks in the Orient Heights Yard. Such inundation would render daily Blue Line service an impossibility. Severe inundation in South Boston and at Airport Station would make the majority of the Silver Line impassable, with the potential to inundate Red Line tracks at South Station, which though an overly conservative assumption, is included in the model. Further inundation on the Red Line in the proximity of and including the entirety of North Quincy Station would also severely impact Red Line service. The resulting baseline system performance level, just 58% of the performance expected under sunny day conditions in 2013, underscores the severity of climate change induced stress that existing urban systems will be exposed to by end-of-century. This increase in stress would also serve to exacerbate and accelerate the effects of infrastructure degradation, further decreasing system performance over time, as outlined by Ayyub (2015).

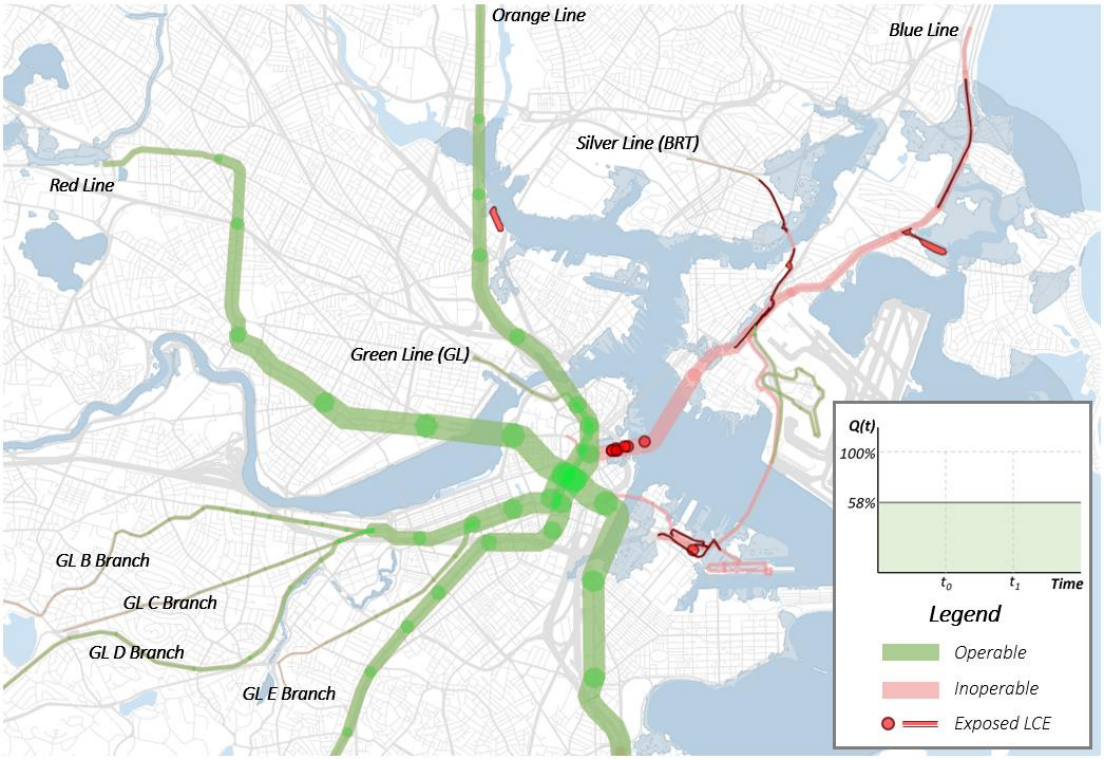

Figure 36: Extent of inundation present at high tide (100% CFEP) under projected 2070 conditions, with +1.04 m SLR. Baseline system performance is 58%.

5.2: Minimum System Performance

In the analysis framework outlined, the minimum system performance, though an intermediate output of the model, provides a concise characterization of the systemwide vulnerability, and is critical to calculating the resilience of the network in each scenario. Rather than reporting the minimum system performance, Q_L, a normalized minimum system performance, $Q_{L\,norm}$, is instead reported, computed as follows:

$$Q_{L\,norm} = \frac{Q_L}{Q_0^*} \tag{5.1}$$

where the baseline system performance, Q_0^*, was taken to be the system performance under the 2013 1-1 year coastal flood scenario. This baseline system performance, representing ridership patterns in 2017, was kept constant for all scenarios and was also used in calculation of system resilience. A constant baseline system performance allows for consistent comparison of vulnerability and resilience across scenarios and time horizons, thereby affording a reasonable basis of comparison for planning purposes. Table 3 provides the normalized minimum system performance under each coastal flood scenario.

Table 3: Normalized minimum system performance, $Q_{L\,norm}$, of the MBTA rapid transit system under projected coastal flooding through the end of century

SLR	Year	100% CFEP	50% CFEP	25% CFEP	10% CFEP	5% CFEP	2% CFEP	1% CFEP	0.2% CFEP	0.1% CFEP
+0 m	2013	100%	100%	100%	75%	61%	61%	57%	44%[T1]	44%
+0.21 m	2030	100%	76%	76%	61%	44%[T1]	37%	37%	37%	37%
+1.04 m	2070	58%	31%	31%	11%[T2]	11%	11%	9%[T3]	5%	5%

(T1-3) – indicate performance thresholds

While system response will be discussed in greater detail later in this chapter through the lens of system resilience, there are a few noteworthy aspects of these results. First, there exists several inundation thresholds, beyond which performance degradation plateaus. The first such threshold, arises due to the

inundation of two individual flood pathways: Ryan Playground in Charlestown, causing flooding of the Orange Line, and the South Boston waterfront, causing flooding of the Silver and Red Lines. These flood pathways arise in the +0 m SLR 0.2% CFEP (1-500 year) scenario and the +0.21 m SLR 5% CFEP (1-20 year) scenario. Thus, the baseline 1-500 year coastal flood is projected to become 25 times more frequent with a SLR of +0.21m.

The second threshold, occurring in the +1.04 m SLR 10% CFEP (1-10 year) scenario arises from another two flood pathways: the Fort Point Channel, which floods the open cut in Downtown Boston, affecting the Back Bay tunnel portals on the Orange Line, and the overtopping of the Amelia Earhart Dam, which floods Alewife Station, thereby eliminating nearly all Red Line connectivity.

Lastly, System performance in the +1.04 m SLR 1% CFEP (1-100 year) scenario (and in more severe scenarios) is less than 10% of system performance is maintained. In other words, under these scenarios, system connectivity is degraded to such a degree that nearly all potential trips in the network are impossible. Notably, under these scenarios, due to its comparatively shallow depth and inland route, the Green Line remains largely unaffected. Though as one subway line does not make a transit system, neither does the minimum system performance define system behavior or response.

5.3: Rapid Transit System Resilience Under Coastal Flood Exposure and SLR

In contrast to the normalized minimum system performance, system resilience better characterizes the impacts of climate change, that is the added daily stress and resultant increase in severity of shocks imposed by SLR. Using the baseline system performance values outlined in Figure 35, system resilience was calculated under each of the above coastal flood exposure scenarios, providing a more detailed characterization of system response over time as shown in Table 4. It is worth noting that these scenarios ignore events that may be coupled to coastal flooding, such as simultaneous precipitation-based flooding, or heavy snowfall.

Table 4: Concise summary of MBTA rapid transit system resilience under coastal flooding projected through the end of century

SLR	Year	100% CFEP	50% CFEP	25% CFEP	10% CFEP	5% CFEP	2% CFEP	1% CFEP	0.2% CFEP	0.1% CFEP
+0 m	2013	100%	100%	100%	88%	81%	81%	78%	72%	72%
+0.21 m	2030	100%	88%	88%	81%	72%	69%	69%	69%	68%
+1.04 m	2070	58%	45%	45%	35%	34%	34%	33%	31%	31%

Aside from the threshold exposure levels noted earlier in the context of the minimum system performance, the tabulated results do not provide additional insight into system response. However, when scenarios of constant probability (CFEP) are plotted versus SLR, Figure 37, the impacts of more statistically probable flood events show some striking features.

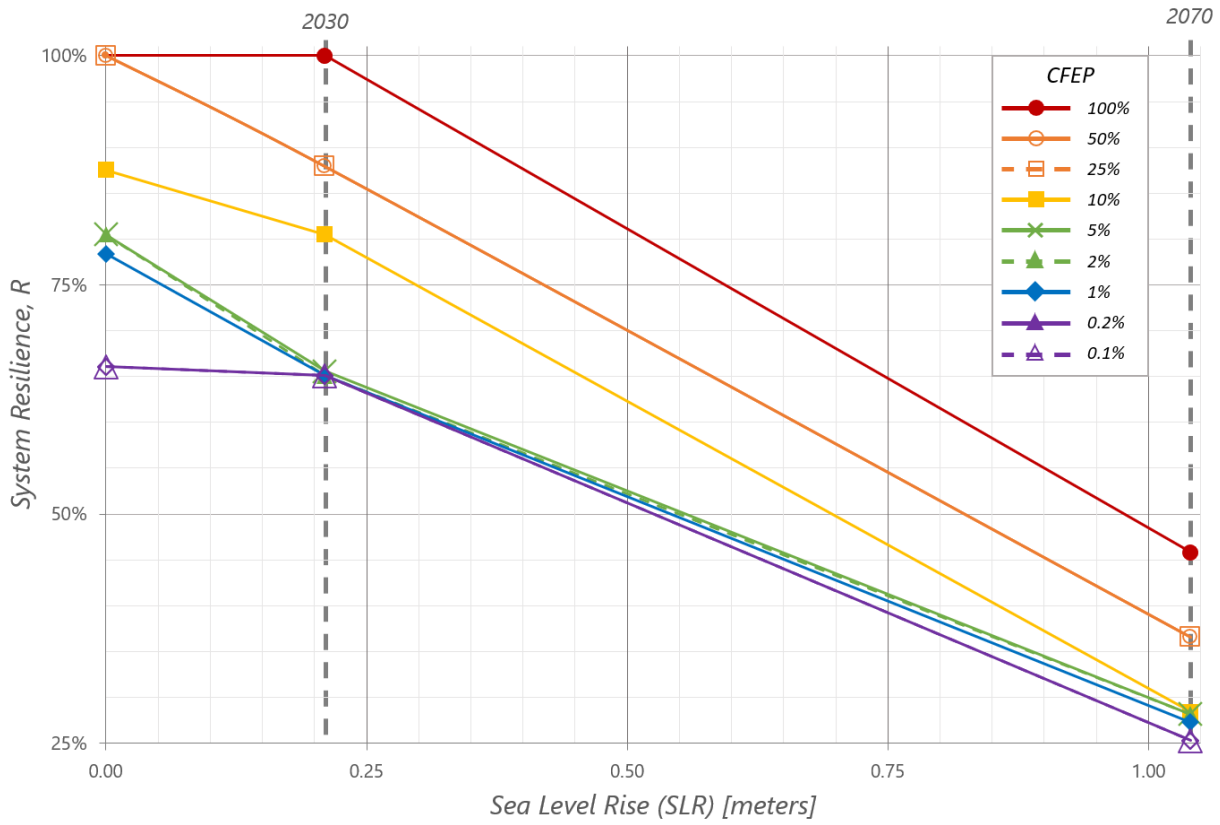

Figure 37: MBTA rapid transit system resilience against coastal flood exposure and sea level rise (SLR).

As SLR increases, the resilience of the MBTA rail rapid transit system to coastal flood events decreases considerably. System resilience under the 1-20 year event (5% CFEP) with +0.21 m of SLR (Figure 38), is similar to system resilience under the 1-1000 year (0.1% CFEP) event with no SLR under 2013 conditions. Further, resilience under the 1-10 year (10% CFEP) event with +0.21 m of SLR, which is probabilistically expected to occur between 2030-2040, is comparable to that under the 1-50 year (2% CFEP) event without SLR. With sea level conditions projected for 2070, the system is less resilient during a 1-1 year (100% CFEP) event than during a 1-1000 year (0.1% CFEP) event under 2013 sea level conditions.

Under +0.21 m of SLR, Blue and Silver Lines are projected to be impacted by coastal flooding with much greater frequency (Figure 37). Despite the heightened risk of severe flooding to these lines, assuming flood events do not cause extensive damage to the system, daily transit system operation likely will not be perceptibly impacted by climate change.

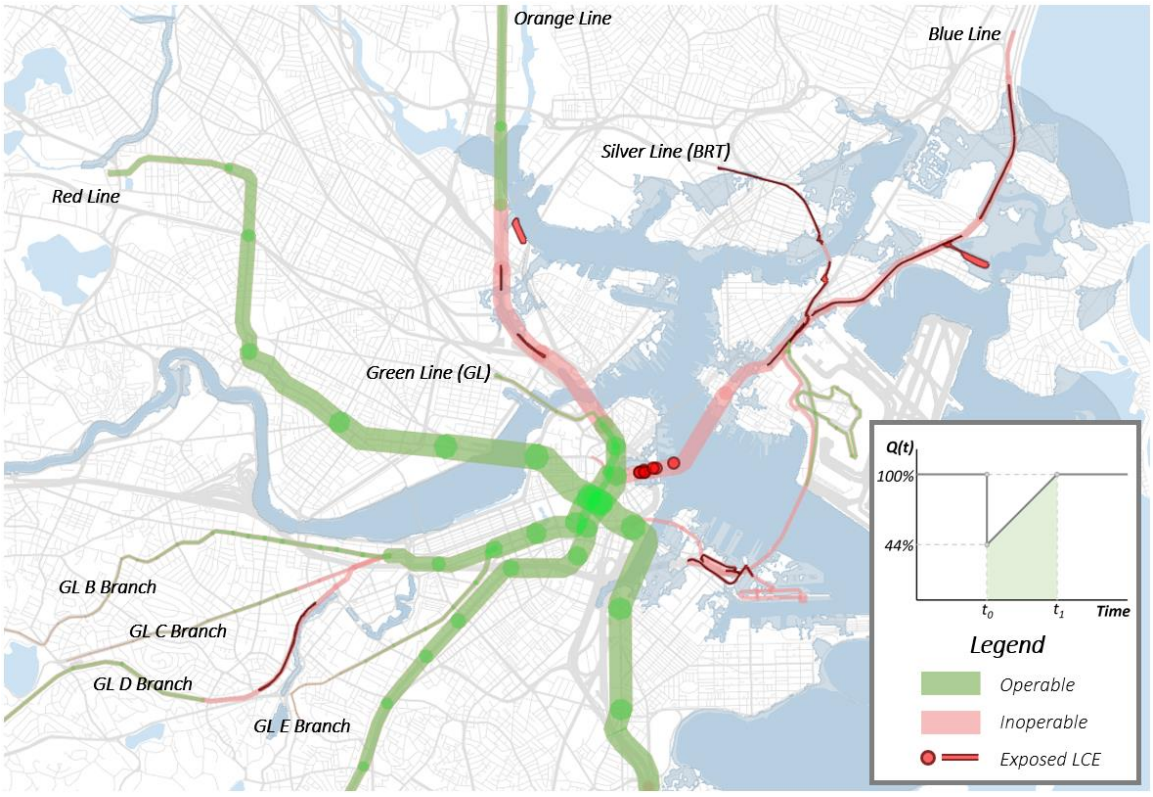

Figure 38: Extent of inundation and approximated effects of the 1-20 year coastal flood event with 2030 sea level (+0.21 m of SLR) on the MBTA system. System resilience is 72%.

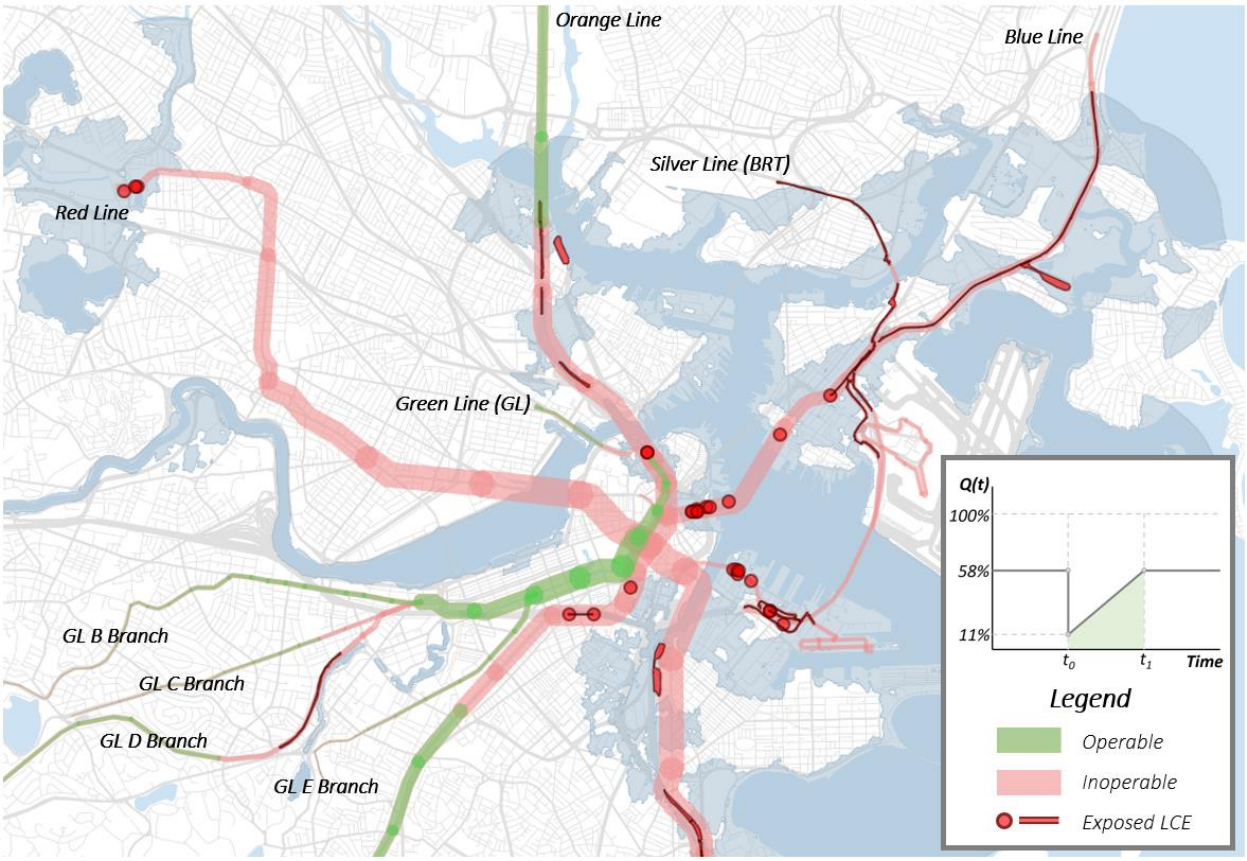

Figure 39: Extent of inundation and approximated effects of the 1-10 year coastal flood event with 2070 sea level (+1.04 m of SLR) on the MBTA system. System resilience is 35%.

Extensive flooding, eliminating service on nearly the entire system, expect for portions of the Orange Line and the majority of the Green Line, would not only inconvenience customers, but would also prove catastrophic to assets critical to operation. Yet, if such an event occurs as the result of a Nor'easter (such as the January 2018 winter storm) the impact on the Green Line and the remaining portions of the Orange Line due to snow accumulation could further decrease the minimum system performance, and by extension the system resilience under such an event. Further, while not considered within the model, one can speculate that as a time independent measure of system resilience decreases, the time required for system recovery greatly increases. Such flood events, were they to occur under present system and asset conditions, are an

existential threat to the MBTA. For a complete set of more comprehensive results, see Appendix B, in which the detailed model outputs for each scenario is shown.

5.4: Projected Design Events with SLR

As outlined above, the model was used to predict a worst-case system performance under a suite of coastal flood exposure events. However, for the purposes of design and planning, the system response under a pre-determined design event is of primary concern. While the design event used for a given project is partially dependent upon the expected lifespan of the assets (being installed or improved) for larger projects and for the entire system, a design event of high severity with a long return period is sensible. When designing against flood risk in the US, a return period of 100 years is typical (ASCE, 2015) and corresponds to Type A or Type V FEMA flood zone (both of which have a 1% annual chance of inundation based on historical data; FEMA, 2019). As flood risks are expected to increase and therefore diverge from the historic record (and by extension FEMA flood zones) ensuring adequate protection against a true 1-100 year storm will require asset managers to exceed existing code requirements in the short-term and design to the projected long-term risks expected with SLR. The remainder of this section details the expected system response under these projected design events under the two SLR regimes presented in the BH-FRM. Locations that are vulnerable under these scenarios are highlighted in more detail in the subsequent section.

5.4.1: Projected 1-100 year Event in 2030 (+8.2 in of SLR)

Figure 40 shows inundation projected for a 1-100 year (1% CFEP) event for sea level conditions projected for 2030 (+0.21 m of SLR). The entirety of the Blue and Silver Lines, as well as a significant portion of the Red Line, and a portion of the Orange Line are inundated. Of particular importance on the Red Line are the projected flooding of the main rail yard, Cabot Yard, and the right-of-way at JFK/UMass station. Orient Heights Yard on the Blue Line is completely inundated under this exposure scenario. Recovery from such an event would likely take longer than the January 2018 winter storm, as inundation

to rail yards implies damage of rolling stock and critical maintenance equipment (Botros et al., 2019). System resilience under this scenario is 65%.

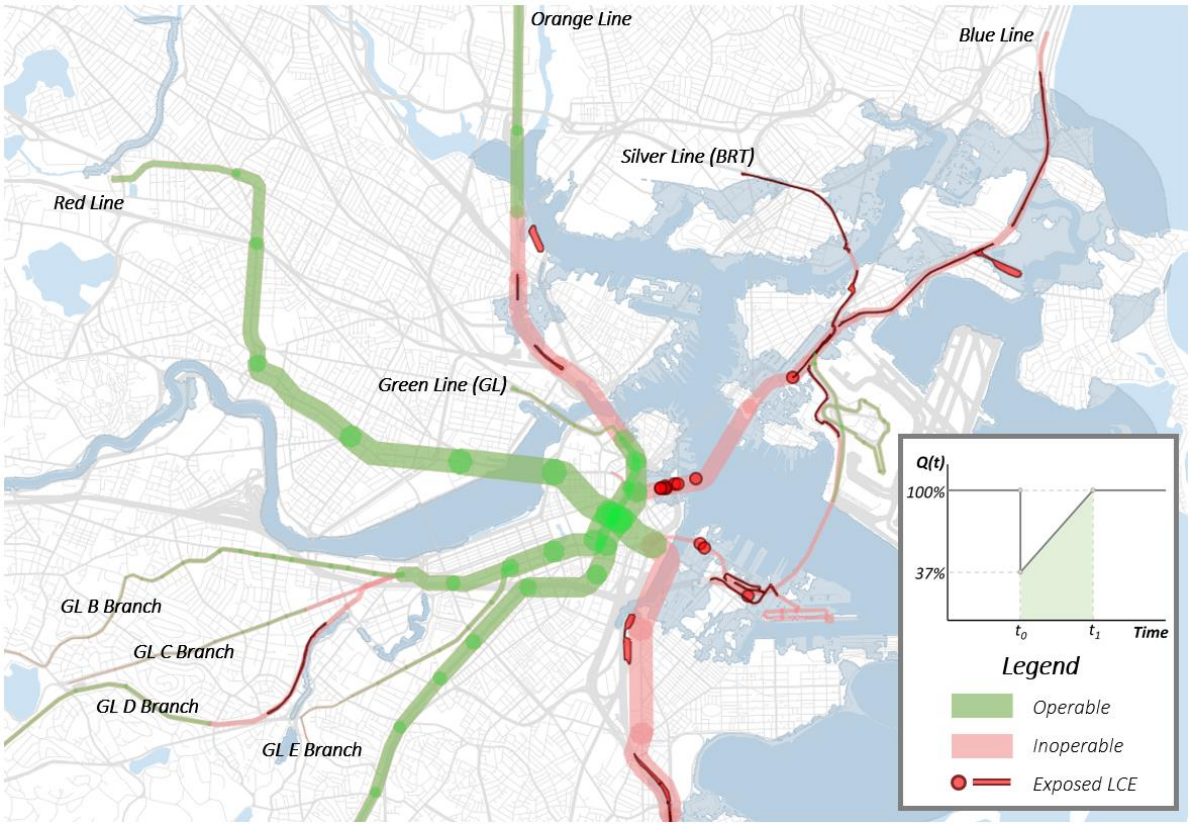

Figure 40: Extent of inundation and approximated effects of the 1-100 year coastal flood event projected for 2030 (+0.21 meters of SLR) on the MBTA system. System resilience is 69%.

This design scenario has the same impacts on system resilience as much larger storms (1-500 year and 1-1000 year) under the baseline SLR regime, shown in Figure 37. It also coincides with the current FEMA 1-500 year flood map (FEMA, 2017) which the MBTA currently uses to assess the vulnerability of projects to climate change and severe weather when evaluating capital improvement projects (MBTA, 2019). Therefore, current MBTA project evaluation practices already take into consideration the exposure and vulnerabilities present under this design scenario. For a more detailed comparison of the BH-FRM scenarios and the current FEMA 1-500 year floodplain, see Appendix C.

5.4.1: Projected 1-100 year Event in 2070 (+41 in of SLR)

Figure 41 shows the impact of the reference design storm (1-100 year; 1% CFEP) for sea level conditions projected for 2070 (+1.04 m of SLR).

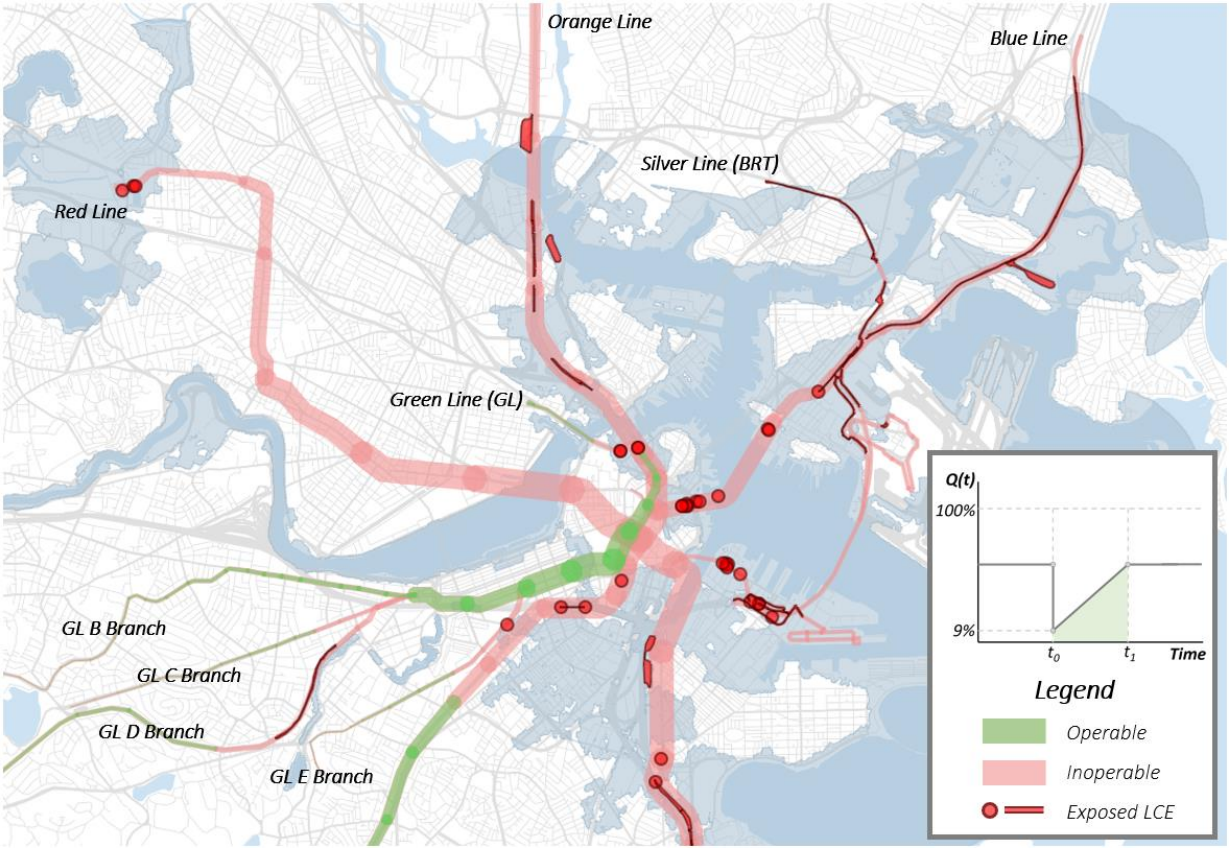

Figure 41: Extent of inundation and approximated effects of the 1-100 year coastal flood event projected for 2070 (+1.04 meters of SLR) on the MBTA system. System resilience is 33%.

The entirety of the Blue and Silver Lines, as well as a nearly the all of the Red Line, a large portion of the Orange Line, and a portion of the Green Line are impacted by coastal inundation. The projected flooding of Orient Heights Yard, Cabot Yard, and the tracks at JFK/UMass station are much more severe, with flooding from the portal south of Andrew Station likely reaching South Station. Based on interviews with MBTA personnel, full recovery from such an inundation scenario on the Blue Line, would take up to one

year (Botros et al., 2019). System resilience under this scenario is 33%, implying that the minimum system performance, $Q_L = 9\%$. The recovery challenges of such a scenario, would be immense, complex, and call into question the current model of linear recovery.

5.5: Ranking of Critical Locations

Despite the MBTA's use of the current FEMA 1-500 year floodplain for capital improvement project evaluation, significant portions of their transit system are currently not protected against present 1-100 year coastal flood conditions. The rail rapid transit system is currently exposed to significant levels of coastal flood risk which will continue to grow as climate change and SLR progress. This section outlines the locations vulnerable to coastal flood risk under the 1-100 year event in current conditions, and under the 1-100 year events outlined in the previous section. Locations exposed were ranked based on the time horizon in which they are expected to become exposed under 1-100 year conditions, as well as by the connectivity loss associated with their inundation.

5.5.1: Urgent Locations

Portions of the rapid transit system that are exposed under the current 1-100 year coastal flood scenario were classified as urgent locations. Except for the Mattapan Trolley line, these locations, are exclusively along the Blue Line, shown in Figure 42 and summarized in Table 5. Under this scenario, the Blue line will lose all service capacity. Locations closer to Downtown Boston, due to their proportionally higher volume of passengers, are more important to system connectivity, and their removal results in a higher connectivity loss, making them a higher priority than stations further north along the Blue Line.

Table 5: Summary of Urgent Locations (based on coastal flood vulnerability) in the MBTA rapid transit system.

Rank	Line	Location	1-100 year Event Exposure			Connectivity Loss, C_L
			+0m SLR	+0.21m SLR	+1.04m SLR	
1	Blue	Aquarium Station	Yes	Yes	Yes	11%
2	Blue	Orient Heights Yard	No	Yes	Yes	18%
3	Blue	Maverick Station and Portal	Yes	Yes	Yes	12%
4	Blue	Airport Station	Yes	Yes	Yes	11%
5	Blue	Wood Island - Orient Heights	Yes	Yes	Yes	8%
6	Blue	Suffolk Downs - Beachmont	Yes	Yes	Yes	5%
7	Blue	Beachmont - Wonderland	Yes	Yes	Yes	3%
8	Red	Mattapan Trolley	Yes	Yes	Yes	<1%

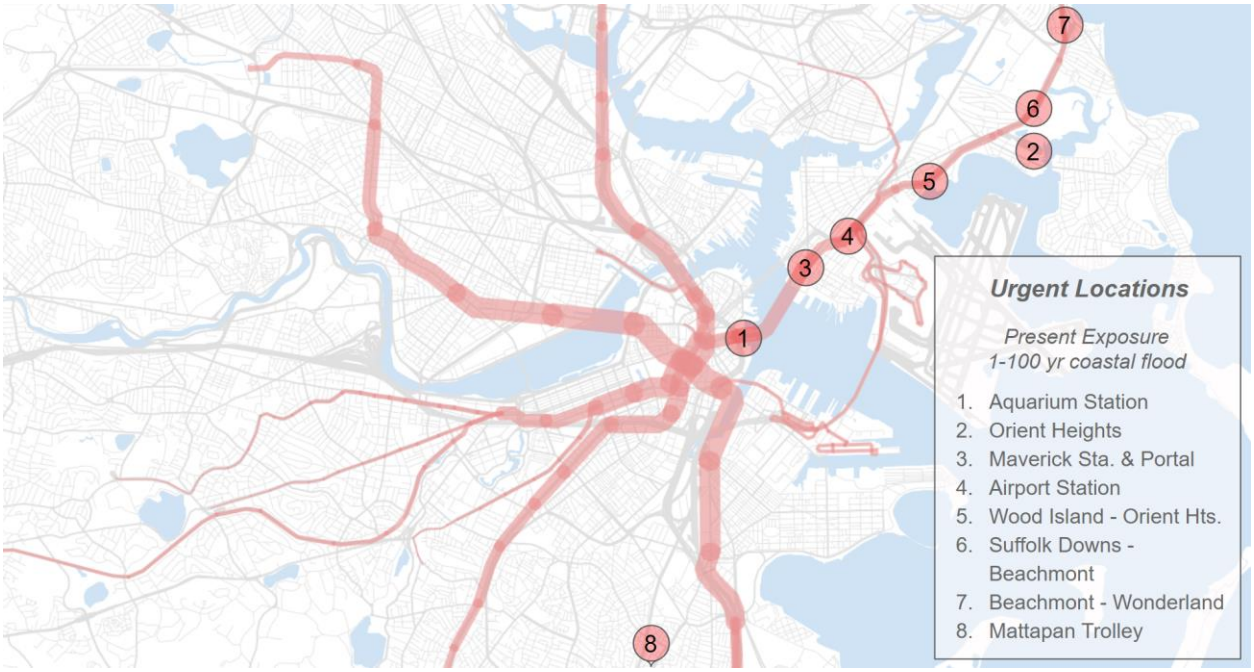

Figure 42: Locations in the MBTA rapid transit system currently exposed during a 1-100 year coastal flood event. These events, categorized as urgent, were ranked by the connectivity loss associated with their inundation under current and future sea level rise (SLR) regimes. See Appendix B for flood extents.

Aquarium Station is considered the most urgent location, due in part to the severity of inundation for all 1-100 year exposure scenarios, and its observed exposure to flooding. Inundation of the Orient Heights Yard would result in a larger outage, but inundation under the current 1-100 year flood is marginal. The Orient Heights Yard is subject to more substantial inundation under the 2030 and 2070 1-100 year flood scenarios (0.3m and 1.07m of inundation respectively). Under either scenario, critical maintenance equipment and rolling stock could be damaged, with more severe impacts under the 2070 1-100 year scenario. Further, considering the low-lying nature of the Blue Line, moving rolling stock from Orient Heights Yard is not a viable long-term adaptive action, as only a small section of track in the proximity of Beachmont Station is safe from flood risks as SLR progresses. For a more detailed analysis of the impact of inundation at each of these locations, see Appendix C.

5.5.2: High Priority Locations

Portions of the rail rapid transit system that are exposed under the projected 2030 1-100 year coastal flood scenario (with +0.21 m SLR) are classified as high priority locations, along with a select scenario that is exposed only under 2070 conditions. These locations, shown in Figure 43, are located along the Red, Orange, and Silver Lines. While these locations are less likely to be flooded than those in the "urgent" category, the loss in connectivity arising from inundation is more severe for several of these locations, compared to the losses incurred by the complete removal of the Blue Line.

Table 6 summarizes these locations, their exposure under each 1-100 year flood scenario assessed, and the connectivity loss associated with its inundation. Of highest priority is the exposure of Cabot Yard, where the majority of Red Line trains are housed when not in use. Should Cabot Yard be flooded and the majority of rolling stock be damaged, in a worst case scenario, the entirety of the Red Line could be removed from service, affecting 45% of system connectivity. The MBTA has plans for a complete upgrade of Cabot Yard and the procurement of new Red Line rolling stock within the next 5 years (in its current CIP, FY 2020-2024) at a total budgeted cost of $409M (MassDOT, 2019). The projected vulnerability of Cabot Yard,

coupled with the planned investment, underscore the importance of adaptation projects that would protect this location.

Similarly, the inundation of Alewife Station, projected to occur as a result of coastal flooding by 2070 (and currently vulnerable to precipitation-based flooding; City of Cambridge, 2015) could severely impact the Red Line, particularly if both Cabot Yard and Alewife Yard are inaccessible. Coastal inundation of Alewife station would arise from the flanking of the Amelia Earhart Dam on the Mystic River; avoiding such inundation would require the fortification or replacement of the dam.

Courthouse Station, for which the MBTA has already budgeted $18.5M in the current CIP to address station leaks (MassDOT, 2019) is projected to be exposed by 2030, with more severe inundation by 2070. Should this station be exposed to flooding, in a worst-case scenario, the Red Line, by means of South Station could also be affected. The probability of such a flood propagation is rather uncertain, as data pertaining to the elevation of the Silver Line tunnel beneath the Fort Point Channel was not available. Additional locations, which are vulnerable as a result of SLR are JFK/UMass Station, North Quincy Station, and Sullivan Square would also severely impact system connectivity. An adaptation project proposed by the City of Boston (2017) as part of its Climate Ready Boston initiative has the potential to eliminate the vulnerability on the Orange Line at Sullivan Square, should it be completed. For further detailed analysis of the impact of inundation at each of these locations, see Appendix C.

Table 6: Summary of High Priority Locations (based on coastal flood vulnerability) in the MBTA rapid transit system.

Rank	Line	Location	1-100 year Event Exposure			Connectivity Loss, C_L
			+0m SLR	+0.21m SLR	+1.04m SLR	
9	Red	Cabot Yard	No	Yes	Yes	21%-45%
10	Silver	Courthouse Station	No	Yes	Yes	30%*
11	Red	JFK/Umass - Andrew Station	No	Yes	Yes	21%
12	Red	North Quincy Station	No	Yes	Yes	11%
13	Orange	Sullivan Square to Community College Station	No	Yes	Yes	10%
14	Red	Alewife Station and Yard	No	Yes	Yes	6%
15	Silver	Ted Williams Tunnel	No	Yes	Yes	3%
16	Silver	Airport to Chelsea Station	No	Yes	Yes	3%

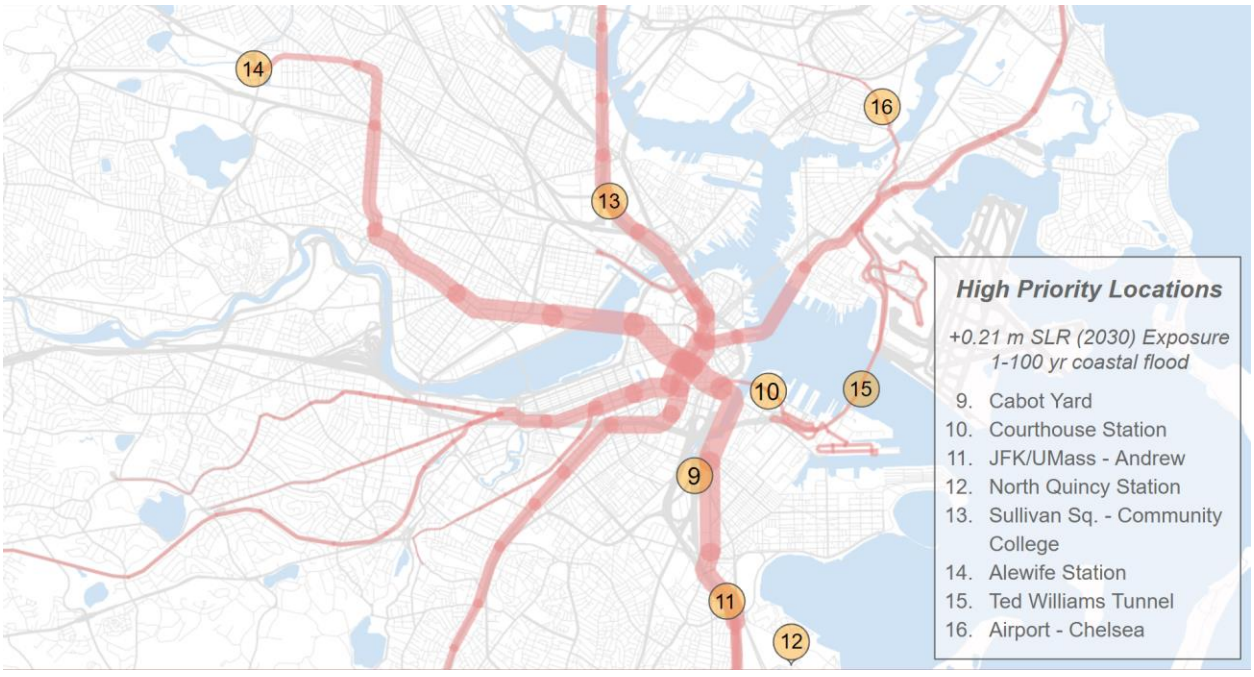

Figure 43: Locations in the MBTA rapid transit system exposed during a 1-100 year coastal flood event with expected sea level rise (SLR) in 2030. These events, categorized as high priority, were ranked by the connectivity loss associated with their inundation under the future SLR regimes.

5.5.3: Priority Locations

Portions of the rail rapid transit system that are exposed under the projected 2070 1-100 year coastal flood scenario (with +1.04 m SLR) are classified as priority locations. These locations, shown in Figure 44, are located along the Red and Orange Lines. The majority of these locations would result in severe connectivity losses, as they comprise central locations that serve a large number of passengers. Table 7 summarizes these locations, their exposure under each 1-100 year flood scenario, and the connectivity loss associated with inundation. North Station, which carries substantial commuter rail traffic in addition to the Orange and Green Lines, could result in 33% of system connectivity loss, should both the Orange and Green Lines be inundated. A similar impact on the system could also arise from the inundation of Wellington Yard, though the extents of the BH-FRM data available only characterized flood exposure for a portion of the yard. Further south on the Orange Line, the Tufts Medical Center Station and the portals at Back Bay are also exposed, which could also result in extensive damage to commuter rail assets. Additionally, flooding of the Orange Line portal at Community College Station would greatly impact system connectivity.

Lastly, the Red Line portal south of Andrew Station was also projected to be inundated with several feet of water. Should this occur, the Red Line would likely be subject to inundation as far north as South Station. For a more detailed analysis of the impact of inundation at each of these locations, see Appendix C.

Table 7: Summary of High Priority Locations (based on coastal flood vulnerability) in the MBTA rapid transit system.

Rank	Line	Location	1-100 year Exposure			Connectivity Loss, C_L
			+0m SLR	+0.21m SLR	+1.04m SLR	
17	Orange/Green	North Station	No	No	Yes	33%
18	Orange	Wellington Yard	No	No	Yes	8%-33%
19	Orange	Tufts Medical Center Station	No	No	Yes	25%
20	Red	Andrew Station	No	No	Yes	20%
21	Orange	Back Bay Tunnel Portals	No	No	Yes	17%
22	Red	Tenean Maintenance Yard	No	No	Yes	13%
23	Orange	Community College Portal	No	No	Yes	10%

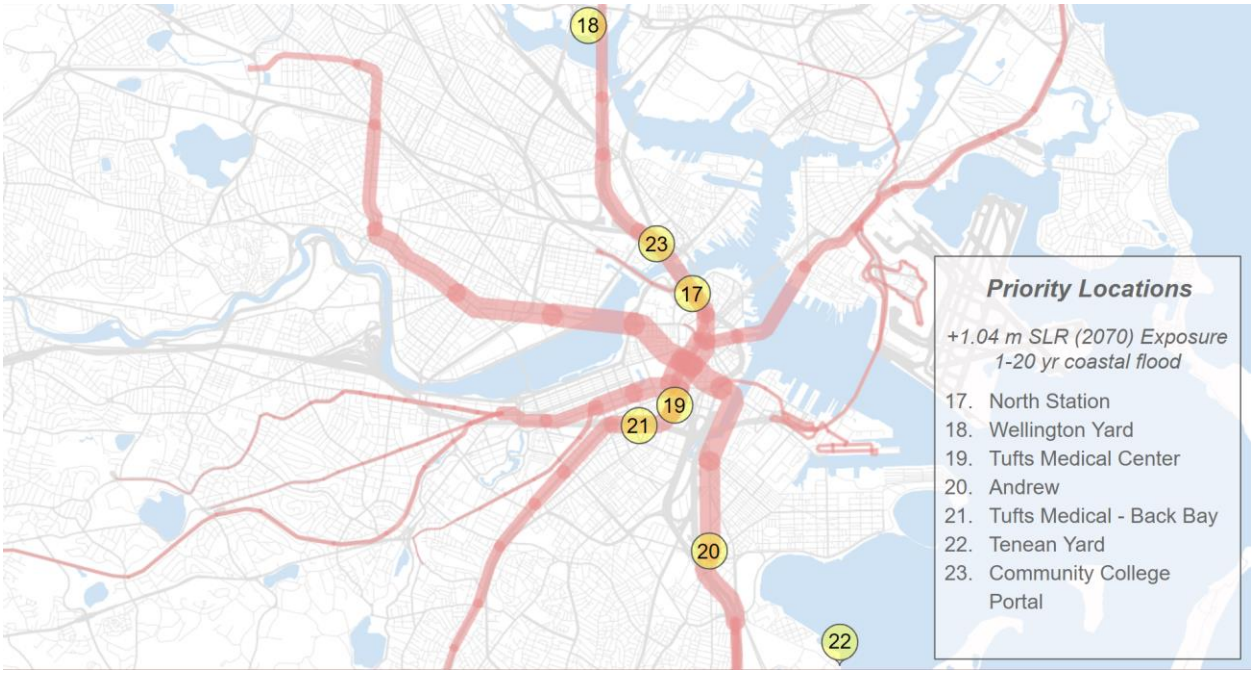

Figure 44: Locations in the MBTA rapid transit system exposed during a 1-20 year coastal flood event with expected sea level rise (SLR) in 2070. These events, categorized as priority, were ranked by the connectivity loss associated with their inundation under the future SLR regimes.

5.5.4: Recognized Locations

Two additional locations that are exposed under the projected 2070 1-100 year coastal flood scenario (with +1.04 m SLR) are classified as recognized locations. These locations, shown in Figure 45, are projected to have a minimal coastal flood vulnerability; both locations are on the Green Line. Prudential Center Station, located along the E branch of the Green Line, is projected to flood (though to a lesser degree than most other locations exposed under the same flood scenario). The Fenway Portal and Longwood Station are expected to flood under all scenarios, though are only expected to experience minor flooding. Further, an ongoing project to install flood gates at the Fenway Portal is expected to mitigate this flood vulnerability (MassDOT, 2019).

Table 8 summarizes these locations, their exposure under each 1-100 year flood scenario assessed, and the connectivity loss associated with its inundation. For a more detailed analysis of the impact of inundation at each of these locations, see Appendix C.

Table 8: Summary of High Priority Locations (based on coastal flood vulnerability) in the MBTA rapid transit system.

Rank	Line	Location	1-100 year Exposure			Connectivity Loss, C_L
			+0m SLR	+0.21m SLR	+1.04m SLR	
24	Green	Prudential Center Station	No	No	Yes	7%
25	Green	Fenway Portal, Longwood Station	Yes	Yes	Yes	13%-33%

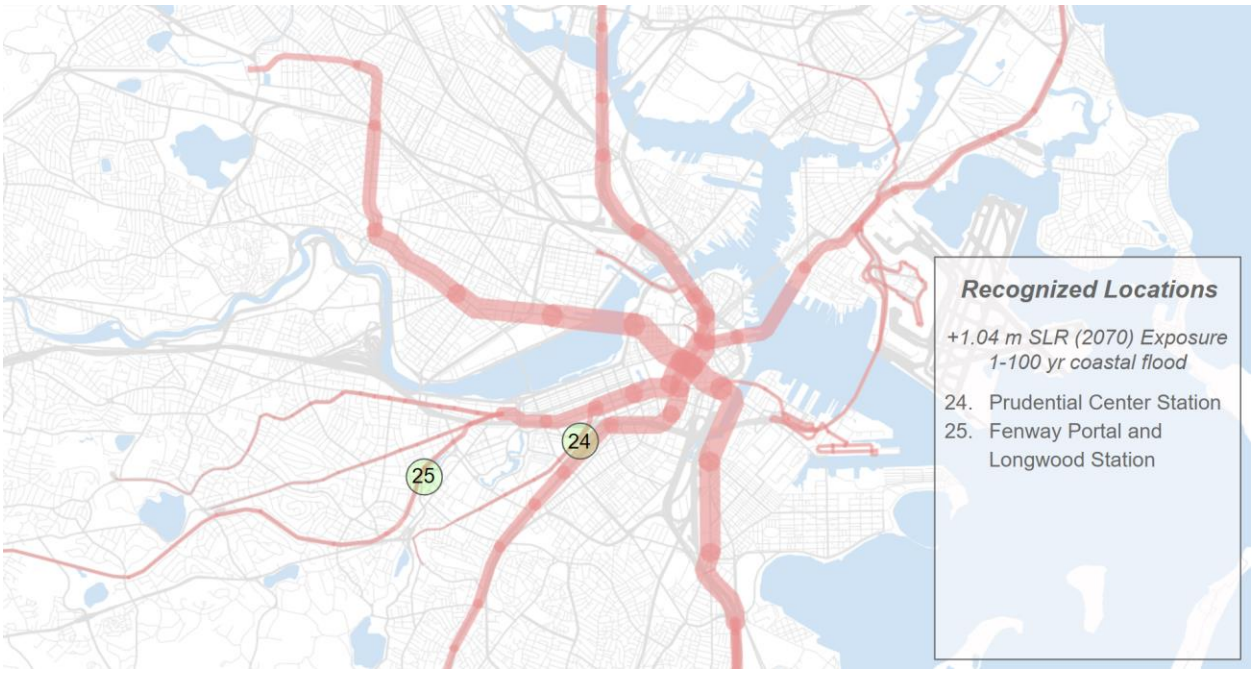

Figure 45: Locations in the MBTA rapid transit system exposed during a 1-100 year coastal flood event with expected sea level rise (SLR) in 2070. These events, categorized as recognized, were ranked by the connectivity loss associated with their inundation under the future SLR regimes.

5.6: Model Validation and Limitations

All models which serve to approximate real processes, fail to capture certain aspects and nuances of physical reality; the model created and detailed above is no exception. What follows is an attempt to enumerate the limitations of the model arising from its various assumptions and approximations. First, an attempt at model validation is outlined, followed by a more general discussion of sources of inaccuracy and uncertainty.

5.6.1: The Nor'easter of January 4th, 2018

Fortunately for the residents of Greater Boston, flood events that impact the rapid transit system are infrequent. Yet for the purposes of model validation, this leaves few scenarios from which comparisons can be drawn. What follows is a comparison between the service impacts that occurred as a result of the coastal flooding during a Nor'easter on January 4th, 2018 and the BH-FRM 1-100 year event under 2013 conditions.

On January 4th, 2018 a significant Nor'easter arrived with high tide, causing record flooding in Greater Boston, with the Boston Harbor tide gauge reaching a record level of 1.45 m above mean higher high water (MHHW) or El. 2.94 m NAVD88 (NOAA, 2019a). According to extreme water level trends published by NOAA (2019a) this was a 1-100 year event at the time of occurrence. Areas of South Boston, Long Wharf, East Boston, and Revere were inundated as a result. Based on information available, the approximate extents of flooding observed in South Boston were comparable to estimates from the BH-FRM, as shown in Figure 46.

Similarly, at Aquarium Station, flooding was limited to Long Wharf and the Aquarium Station headhouse, as shown in below in Figure 47. This was also consistent with the BH-FRM. Flooding was also reported along the tracks east of Suffolk Downs (MBTA, 2018a), but none in the proximity of the Maverick Portal or Airport Station. Based on the BH-FRM, under the 2013 SLR regime shown in Figure 48, Maverick Portal and Airport Station are expected to be inundated by means of a narrow flood pathway in East Boston, yet it would appear that this flooding did not occur or was mitigated in some fashion. Additional flooding was also projected for small portion of the Silver Line route in Chelsea, the Red Line in the proximity to North Quincy Station, and the Green Line near Longwood Station. The author has not been able to find any reports of inundation at these locations affecting transit service. This divergence from the expected service impacts are likely the result of discrepancies in the BH-FRM flood extents, rather than the model as constructed.

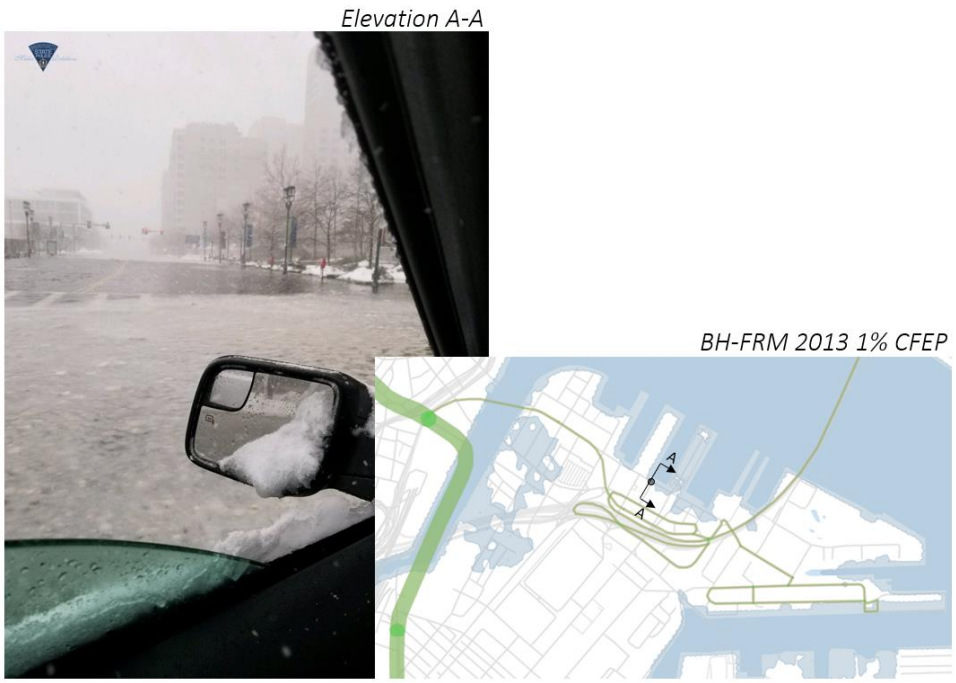

Figure 46: View southeast down Seaport Blvd. from a patrol car at the intersection of Seaport Lane and Seaport Blvd. during the January 4th, 2018 Nor'easter (Mass State Police, 2018).

Figure 47: View northeast down Long Wharf during the January 4th, 2018 Nor'easter; the Aquarium Station headhouse was inundated at the time of the photo (MBTA, 2018b).

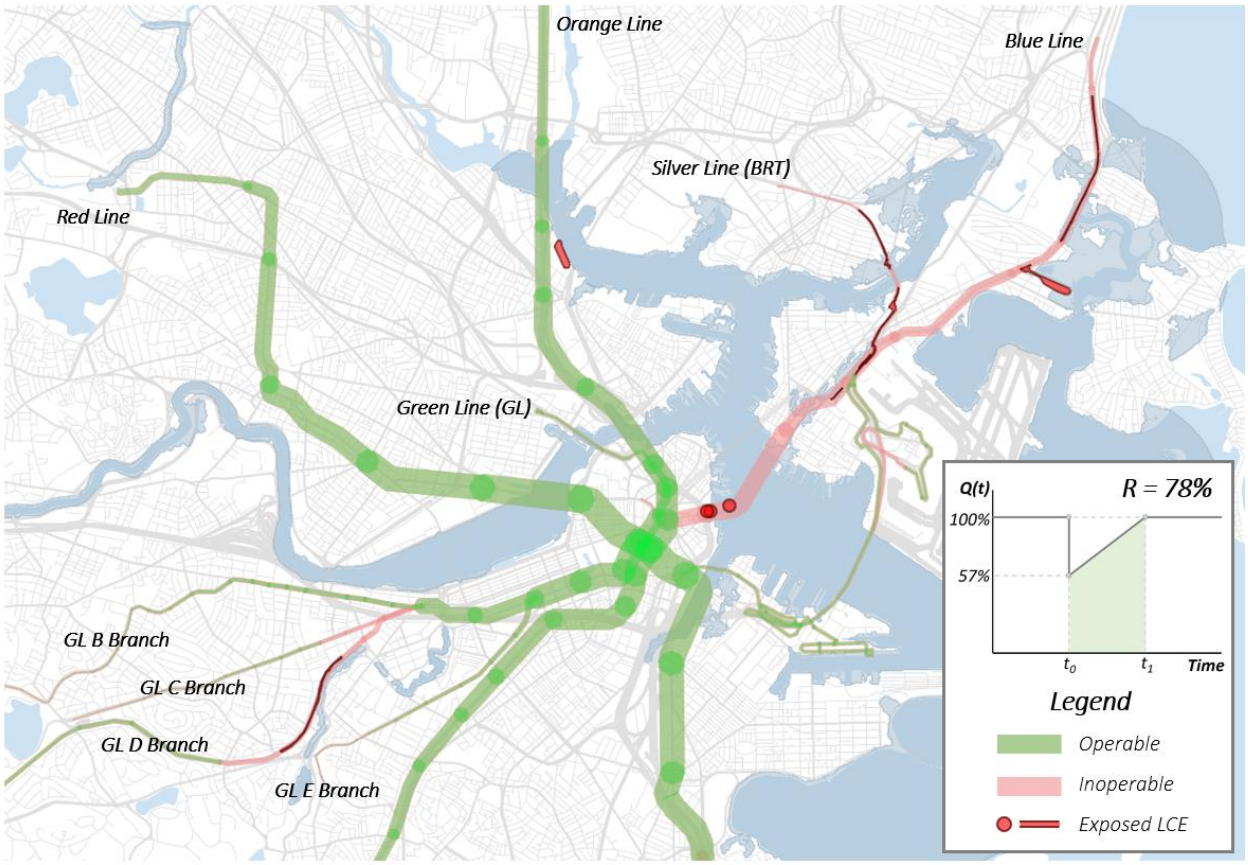

Figure 48: Extent of inundation and approximated effects of the 1-100 year coastal flood event with 2013 (+0 m of SLR) sea level on the MBTA system. System resilience is 78%.

In contrast to observations (from the January 2018 storm) the BH-FRM 1-100 year scenario (+0 m of SLR) predicts flood impacts along the entirety of the Blue Line. The service announcements on January 4th mention only a closure of Aquarium Station and the suspension of service from Orient Heights to Wonderland. For the purposes of the model, the bypassing of Aquarium Station is not equivalent to the removal of the associated link. Thus, the connectivity loss arising from the coastal flooding during the January 2018 storm was only 5%, while that predicted based on the BH-FRM event is 43%. This discrepancy partly arises from a key assumption of the model which assumes that inundation of Aquarium Station adversely affects train operations on the Blue Line. Yet the lack of flooding in the Blue Line tunnel is partially due to the resourceful mitigation efforts enacted during the storm, such as the temporary barrier

construction at the station entrance and the action of tunnel pumps (Weston & Sampson, 2019), which were not assumed to occur in the model. Future work detailing the effects of partial inundation at LCE's and the resourcefulness/adaptive capacity of the system would improve the accuracy of the model under such circumstances.

5.6.2: Limitations

In addition to the inaccuracies arising from the BH-FRM data, there are several other shortcomings of the model presented that limit its predictive accuracy. Mentioned previously the model assumes immediate inundation of tracks and removal from service when an associated LCE is exposed. Also implicit in the model is the assumption that peak inundation lasts only through a single tide cycle (i.e., the system is only at the minimum performance level for a short period). This may not be the case, as inundated tunnels will likely require additional pumping capacity, and may remain inundated for extended periods. Both assumptions approximate system response, but may not be indicative of system behavior in every part of the system in every scenario.

Another notable limitation pertaining to flood propagation (within the network) is the discretization of the operations network links for purposes of elevation-based propagation. The links were divided principally on the basis of the locations and presence of switches on the system, and hence each link in the operations network can be over several hundred meters but is characterized by only one critical elevation. The model could be further improved by creating a separate network for elevation-based propagation, discretizing the system into shorter links of more consistent length such that the extent of flooding along a given line could be better characterized.

The current model does not consider any adaptive capacity of the system. This includes actions taken to limit water inflow, such as placement of sandbags, closing of flood barriers, or drainage provided by pumps throughout the system. Other resourceful actions that could be taken by the transit agency, including the bypassing of flooded stations, providing bus service to reduce the passenger impact of rapid transit

system closure, or providing service with alternative rolling stock are not considered and limit the predictive accuracy of the model.

Similarly, the resourcefulness of passengers is not accounted for either, through dynamic re-routing of passengers to remain in the system (and avoid affected links) or through their actions to take ancillary transit, such as buses or commuter rail trains. This lack of bus or commuter rail service within the model also inhibits its capacity to quantify the extent to which bus or rail assets are vulnerable or how resilient the entire public transit network is to climate change. The model also lacks characterization or inclusion of additional ancillary systems, such as the power grid or signal system. Loss of portions of these systems would affect transit system operations, and by extension vulnerability and resilience.

The current model also assumes a static system performance measure is adequate for purposes of planning and decision making. While ODX data represents the best available representation of relative ridership, it can only provide ridership retrospectively. For projects with longer time horizons, ridership projections could be utilized to consider changes in total or relative ridership through time. Such changes will occur, causing the true relative performance weights assigned within the model to increasingly misrepresent the relative passenger flows through the network. Ridership projections, as well as planned service expansions (such as the Green Line extension into Somerville) are typically considered when planning capital projects, though are not yet included in the model.

Also important for capital planning, and neglected in the model, are estimates costs of damage to the system. In its current state of development, the model lacks the ability to financially quantify the benefits of resilience or costs of exposure and damage. This limits the ability of planners to use this tool for cost benefit analyses. It should be noted that the requisite asset information was not available from the MBTA at the time of this research.

While this research attempts to characterize resilience of the MBTA's rail rapid transit network to climate change, only coastal flood exposure arising from SLR and storm surge exposures were considered.

This was primarily due to a lack of geospatial data for other climate change related exposures. Flooding risks from extreme precipitation events haven been reported for the City of Cambridge (2015), but no data is yet available for the City of Boston at the time of writing (a recent BWSC study has yet to be released to the public; Sullivan, 2019). Additionally, there are no snow or extreme heat data sets considered in the analysis. Further research to characterize these risks would be beneficial to Greater Boston in general, but would also prove beneficial for the MBTA, as the resilience of the system to these types of exposures could also be characterized.

Despite these limitations, the model as constructed can still effectively serve the function of providing a measure of system resilience under worst-case performance scenarios, which can still prove useful for planners when attempting to evaluate the criticality of ingress points and the vulnerability of transit assets.

6. Discussion

The analysis performed in the previous section is predicated upon estimates of future sea level rise and climatic conditions. In the case of the BH-FRM, these regimes were meant to represent the worst-case, highest SLR regime presented by Parris et al. (2012). While a given SLR regime in practice has been conflated with the year it is nominally meant to represent, the degree of SLR presented is a moderately conservative estimate of future conditions (compared to the full range of the business-as-usual projections; RCP 8.5) and is subject to uncertainty. While a measurable relative SLR has occurred from 2000 to 2010 for example, climate projections can at best define a probabilistic range of future relative SLR. Thus, there is a probability of both a higher and lower SLR regime for each of the years projected, though the actual probability distribution is dependent upon assumptions relating to global climate forcings (i.e. RCP 2.6, RCP 8.5, AR4, etc.) used in the analysis. This uncertainty inherent in climate models and projected SLR should be acknowledged in analysis to some degree, rather than rigidly associating each SLR value with the year it is prescribed to represent.

If the projections outlined by the Boston Harbor Flood Risk Model accurately represent sea level by end of century, a greater than 50% probability (Miller, 2019), then climate change poses an existential threat to the MBTA's rail rapid transit system by 2070. While the coastal flood vulnerabilities in near-term SLR scenarios are less severe, they are more urgent given their temporal proximity and emphasize the need for adaptation. Quantitative resilience analyses are simply the first step towards the creation and successful implementation of adaptation efforts.

This chapter will further outline a general adaptation roadmap for the MBTA, accounting for and considering projects already proposed in the Greater Boston area that would provide benefits to the rapid transit system. Relevant short-term adaptation strategies proposed by others for the MBTA, as well as general long-term adaptation strategies will be briefly elucidated, though these options are not meant to be either a definitive or exhaustive set of solutions. Lastly, several key aspects of the resilience assessment

framework presented are contrasted with other existing frameworks in the literature, highlighting the nuances of engineering resilience in the context of climate change.

6.1: Characteristic Response of the MBTA Rapid Transit System to Coastal Flood Risk

The lowest lying areas of the MBTA rapid transit network (nearly the entire Blue Line) which are naturally the first to flood, are projected to be subject to the most severe inundation as SLR progresses. Such areas of the system will likely require a multi-phase adaptation approach, in which adaptive efforts in the short-term will likely differ from long-term adaptive efforts. These areas will likely require the greatest degree of triage and may require retreat and relocation of facilities if flooding becomes too frequent or the risk too severe. Further, as SLR increases, events of the same frequency can lead to more extensive flooding through new flood pathways. For example, the flood pathway at Ryan Playground and Schrafft's City Center in Charlestown (Figure 49) under the +0.21 m SLR regime creates a new vulnerability on the Orange Line which was not expected to flood under the baseline sea level regime.

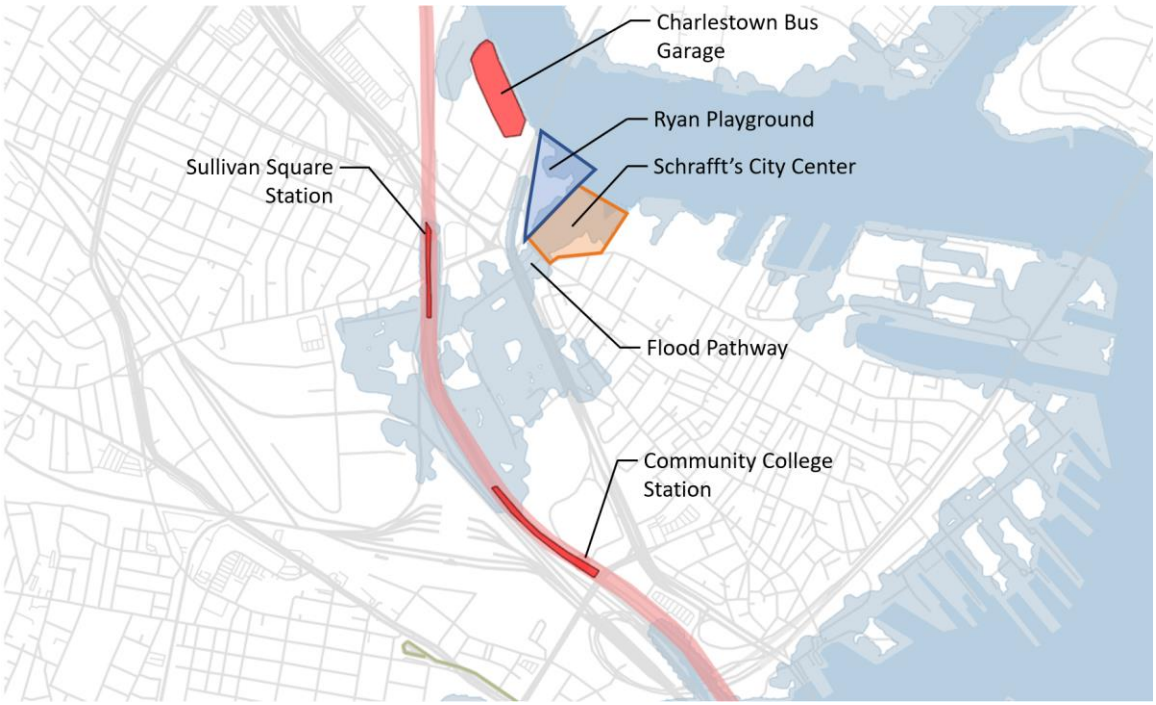

Figure 49: Flood pathway at Ryan Playground and Schrafft's City Center in Charlestown under the projected 1-100 year coastal flood event with +0.21 m SLR.

These additional vulnerabilities create tipping points within the system as new flood pathways expose new portions of the system. Each threshold corresponds to a marked change in overall system connectivity, as can be observed in the change in system response between the +0 m SLR 1% CFEP event and the +0.21 m SLR 1% CFEP event (78% and 69% resilience respectively; Table 4). After these thresholds are surpassed, for events of decreasing probability in a given SLR regime, system resilience does not degrade significantly further. For example, in the +0.21 m SLR regime, system resilience under the 5% CFEP event is close to that of the more infrequent events (approximately 70%; Table 4). The protection of flood pathways that contribute to such thresholds should be given priority when planning adaptation projects, as will be discussed in the following section.

6.2: Proposed Adaptation Roadmap

A total of 25 locations on the MBTA system are projected to lie within the 1-100 year flood plain by end-of-century. These locations, which were ranked based on: 1) the SLR regime in which they become exposed (see Figures 42-45) and 2) the degree of connectivity loss arising from their exposure. These locations require varying degrees of triage from the MBTA and some may only require indirect intervention. Figure 50 presents these locations, ranked and color coded by priority.

Table 9 further details these locations and provides recommended protection deadlines for each flood vulnerability, assuming the SLR rates presented in the BH-FRM. In conjunction with these recommended protection deadlines, a proposed adaptation roadmap is presented in Figure 51, which further details the proposed chronology of action at these locations. Locations which would be protected by projects presented by the Climate Read Boston initiative are denoted with an asterisk (*) and locations at which projects are planned in the MBTA 2020-2024 Capital Improvement Plan (CIP) are marked with a subscript (^{C}).

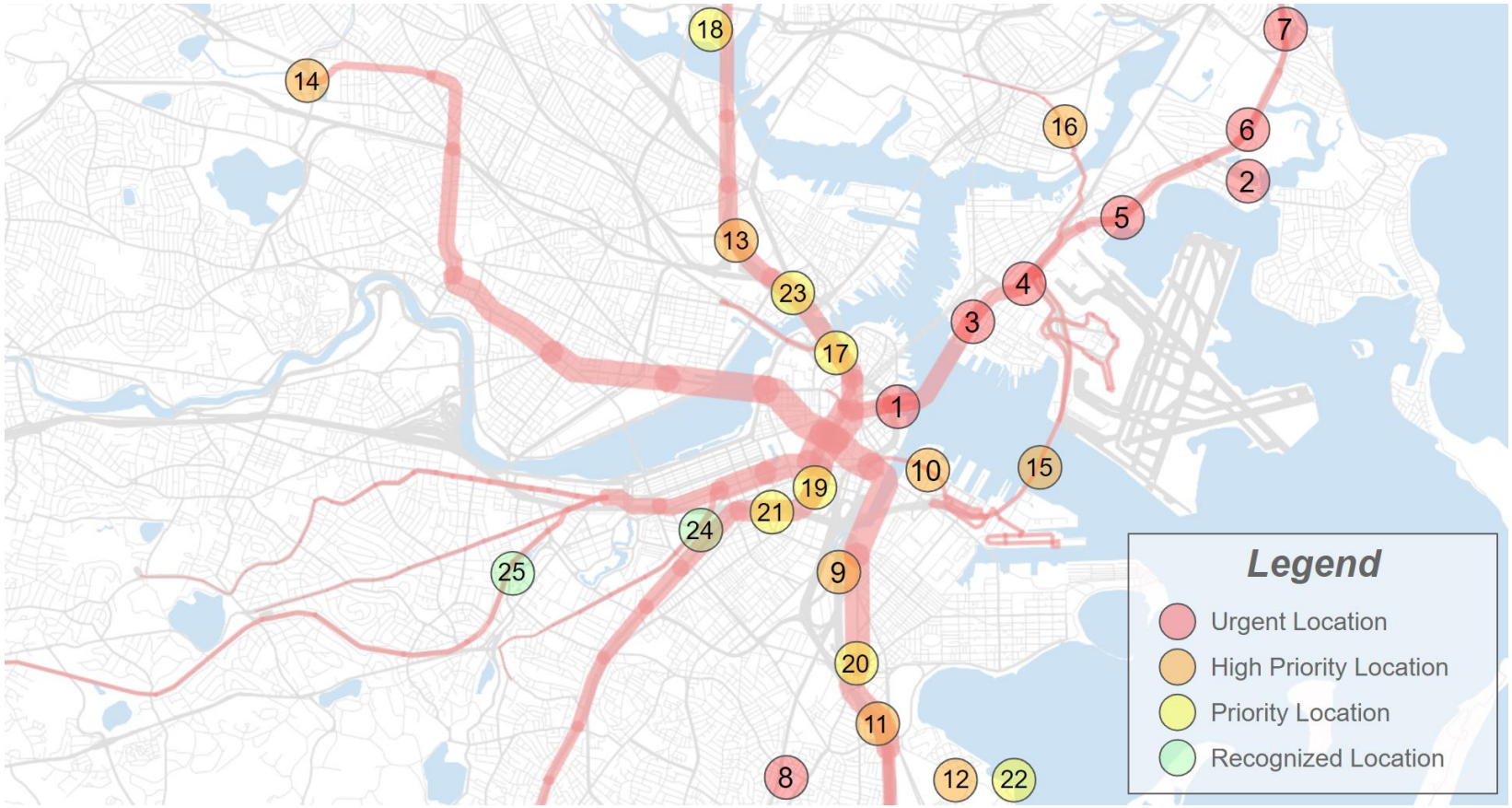

Figure 50: Summary of rapid transit network locations vulnerable to coastal flooding by end-of-century.

Table 9: Summary of MBTA rapid transit network locations vulnerable to coastal flooding by end-of-century and recommended protection deadlines, based on BH-FRM projections.

Rank	Line	Location	Connectivity Loss, C_L	Protection Deadline
1	Blue	Aquarium Station	11%	2025
2	Blue	Orient Heights Yard	18%	2025
3	Blue	Maverick Station and Portal	12%	2025*
4	Blue	Airport Station	11%	2025*
5	Blue	Wood Island - Orient Heights	8%	2035
6	Blue	Suffolk Downs - Beachmont	5%	2035
7	Blue	Beachmont - Wonderland	3%	2035
8	Red	Mattapan Trolley	<1%	2035
9	Red	Cabot Yard	21%-45%	2025[C]
10	Silver	Courthouse Station	30%	2025[C]
11	Red	JFK/UMass - Andrew Station	21%	2035
12	Red	North Quincy Station	11%	2040
13	Orange	Sullivan Square to Community College Station	10%	2030*
14	Red	Alewife Station and Yard	6%	2040
15	Silver	Ted Williams Tunnel	3%	2050*
16	Silver	Airport to Chelsea Station	3%	2050
17	Orange, Green	North Station	33%	2060
18	Orange	Wellington Yard	8%-33%	2060
19	Orange	Tufts Medical Center Station	25%	2070*
20	Red	Andrew Station	20%	2070
21	Orange	Back Bay Tunnel Portals	17%	2070*
22	Red	Tenean Maintenance Yard	13%	2070
23	Orange	Community College Portal	10%	2050
24	Green	Prudential Center Station	7%	2070*
25	Green	Portal at Kenmore Station	13%-33%	2020

(*) – indicates protection under proposed Climate Ready Boston projects
([C]) – indicates current CIP project that should address climate change resilience

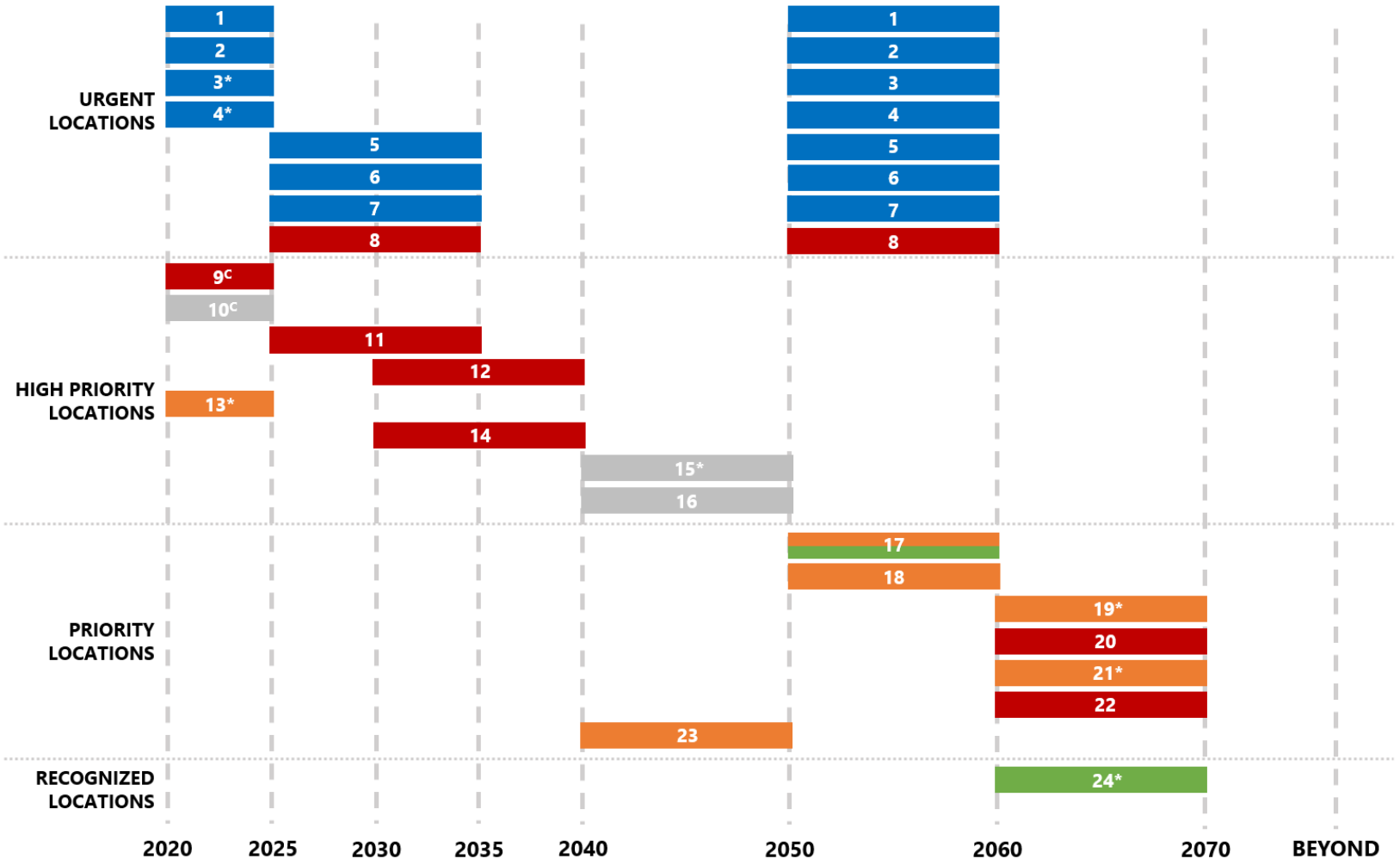

Figure 51: Proposed adaptation roadmap for the MBTA rapid transit network. Projects locations listed are vulnerable to coastal flood risk under projected sea level rise (SLR) by end-of-century. See Figure 50 for locations and Table 9 for location details.

(*) – indicates protection under proposed Climate Ready Boston projects

(^{C}) – indicates current CIP project that should address climate change resilience

Two of the identified locations, Cabot Yard on the Red Line and Courthouse Station on the Silver Line, shown in Figure 52, currently have projects listed in the CIP project portfolio. The Courthouse Station project, initiated to address leaks at the station, is currently budgeted at $18.5M (MassDOT, 2019). It is unclear if this project will attempt to reduce coastal flood risk, though expanding the project's scope to include protection against flood risk under the projected 2030 SLR regime would prove prudent. Similarly, at Cabot Yard, where new rolling stock ($225M) and a complete yard upgrade ($184M) at a cost of $409M are planned over the next 5 years; investment in flood protection measures against projected risk is crucial for protecting the long-term upgrade of these assets.

Both of these locations, as well as 7 others, are addressed formally as recommended projects by the Climate Ready Boston (CRB) initiative (City of Boston, 2017; City of Boston, 2018). At the time of writing, CRB has developed coastal flood protection plans through end-of-century for East Boston, a portion of Charlestown, and South Boston. While it is unclear if these proposed projects have been allocated funding by the city at the time of writing (City of Boston, 2020) the proposed project timelines were incorporated into the adaptation roadmap presented.

CRB currently proposes several projects in East Boston, of which the first phase is projected to be completed by 2025, with additional projects projected to be complete by 2050 (City of Boston, 2017). These projects, shown in Figure 52, would protect Maverick Station, Maverick Portal, and the right of way approaching Airport Station at a cost of $96.7M. An additional set of projects proposed in Charlestown at Ryan Playground and an adjacent private site, shown in Figure 52, would eliminate the flood pathway that exposes the Orange Line in the proximity of Sullivan Square and Community College Stations by 2030 at an estimated cost of $56.1M (City of Boston, 2017).

A more complex project timeline was proposed for South Boston, in which several mid-term and long-term solutions would protect the Silver Line and downtown portions of the Orange Line (Tufts Medical Center Station and the portals at Back Bay) by 2070. Adaptation plans for several other neighborhoods in the city are currently underway, with several solutions presented that would benefit the Red Line at Tenean

Yard, Andrew Station, and JFK/UMass Station (City of Boston, 2019). Each of these projects exist largely outside the domain of the MBTA but would provide the agency significant direct benefits.

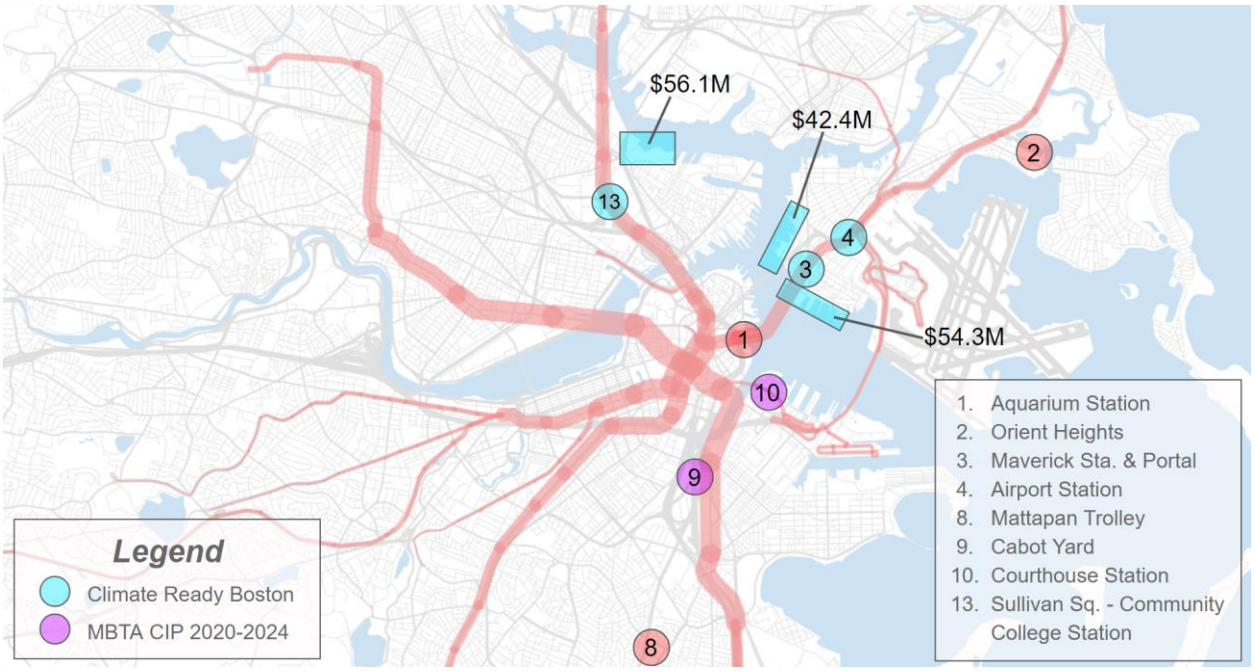

Figure 52: Recommended adaptation projects for 2020-2025, highlighting several locations at which Climate Ready Boston has proposed projects (City of Boston, 2017) which would improve the climate change resilience of the MBTA rapid transit system.

The most cost effective solutions to coastal flood vulnerabilities faced by the MBTA will likely exist outside of the agency's domain. Coordination with and support of the efforts of the City of Boston, other local municipalities, and local government agencies will likely yield more resilient outcomes than hyper-local action focused exclusively on transit asset risk reduction. For example, reduction of coastal flood exposure at Alewife station by end-of-century will likely depend on successful improvements of the Amelia Earhart Dam on the Mystic River, requiring the collaboration of coordination of several local municipalities and government agencies. As risks increase due to climate change, cross-agency cooperation will become an increasingly critical part of engineering resilience into the fabric of the urban environment.

Adaptative actions should also be sufficiently malleable that they allow for further iterative improvements or adaptation as they reach the end of their intended life cycle (or if prevailing risks increase faster than projected). This would also afford planners and decision makers the option to provide protection against only the risks associated with near-term SLR projections, are they are less uncertain than those associated with longer-term projections. Such a strategy is suggested for the Blue Line, where it may be sensible (and more economically feasible) to provide less expensive short-term actions that protect against the risks associated with near-term SLR projections. As such, a secondary set of adaptation projects will be needed for the Blue Line to ensure protection against projected risk by 2070 (Figure 51). This secondary set of adaptations will depend on the protection afforded by the first set of adaptations and may also encompass new approaches, such as the creation of elevated structures as opposed to the use of berms or levees to raise track elevation.

6.3: Potential Adaptation Strategies

In addition to the adaptation efforts proposed by the City of Boston, the MBTA can adapt at a smaller, more localized scale. Localized adaptation efforts focus on individual assets or flood ingress points that can sufficiently reduce risk in the short-term against less frequent exposures (under more severe SLR regimes, more extensive design and permanent protection measures are needed). This section will detail relevant and viable short-term and long-term adaptation strategies the MBTA can deploy to protect Greater Boston's rail rapid transit network. These adaptation strategies focus exclusively on the reduction of system sensitivity to coastal flood exposures, and do not consider projects or recommendations that would improve the adaptive capacity of the system.

6.3.1: Potential Short-Term Adaptation Strategies

Weston & Sampson (2019) detailed several viable adaptation strategies relevant for Aquarium Station and Maverick Station and Portal on the Blue Line. Many of these strategies can easily be extrapolated to

other locations in the system that also require adaptive efforts against coastal flood exposure, as they focus on protection of underground facilities and historic subway tunnels.

These structures themselves can become a source of water ingress through small cracks and fissures. While these defects do not compromise the structural integrity of these tunnels, they do allow for water to flow into the system and can be fixed by injection grouting solutions (Nir, 2018). Grouting and eliminating such leaks can help improve the operational resilience of a station or tunnel segment, as reducing leaks reduces the demand placed on pumps both on a daily basis and during flood events.

In addition to percolation through cracks in foundation elements, water can penetrate via utility connections and manholes that lead to subsurface assets (Weston & Sampson, 2019), as well as through station entrances, ventilation shafts, and tunnel portals. Weston & Sampson (2019) recommend the following adaptive actions to minimize water ingress at vulnerable locations:

i) Installation of watertight manholes or sealing locations at which utilities enter a station.

ii) Preparation for and deployment of temporary flood barriers for station entrances, ventilation shafts, and tunnel portals.

iii) Installation of permanent flood barriers or elevating of ventilation shafts.

iv) Installation of permanent flood gates at tunnel portals, similar to the Kenmore Station portal flood gate under construction at the time of writing (Riley-Gilbert, 2018).

A separate study performed by AECOM (2018) to investigate the vulnerability of Orient Heights Yard recommended the following adaptation strategies:

i) Elevation of critical systems and rolling stock replacement components.

ii) Insure vulnerable equipment that cannot reasonably be elevated (the wheel truing machine in the maintenance garage).

While such strategies are viable for the 2030 scenario, the extent, depth, and frequency of inundation expected under the SLR regime projected for 2070 likely makes such a strategy insufficient in the long-term.

6.3.2: Potential Long-Term Adaptation Strategies

Adaptation efforts thus far presented tacitly presuppose that existing assets will remain in their present configuration, and simply require additional protection against increasing coastal flood exposures. Yet as SLR progresses, the risk at certain locations will likely grow intolerable, despite proposed adaption efforts (i.e., adaptation efforts will grow obsolete over time). If adaptation efforts are well designed, then this obsolescence will occur at the end of their expected life cycles. Yet regardless of when this obsolescence occurs, additional protections, or new adaptation strategies will eventually be required.

In addition to raising elevations of critical assets and increasing the elevations of ventilation shafts and station entrances, more extreme adaptation strategies may be warranted. The Blue Line can serve as a case study for more urgent adaptive efforts. For SLR conditions projected for 2070, daily flooding of the Blue Line will make it inoperable in its present configuration. Should a significant flood event impact the Blue Line, such as a 1-100 year event (with +1.04 m SLR) damage to the line, yard, and rolling stock would impact service for a year or more (Botros et al., 2019). Thus relocation, elevation, or retreat should be considered when planning a long-term adaptation strategy for the Blue Line. Considering the extent, frequency, and impact of coastal flooding on the Blue Line shown in the analysis above, a cohesive long-term adaptation strategy for the Blue Line would prove prudent.

The Blue Line and its corresponding maintenance yard at Orient Heights could be elevated above the existing grade, similar to the number 1 train in New York City, which enters the Bronx on an elevated track above Broadway and has a rail yard and maintenance facility elevated above grade adjacent to the 242nd Street/Van Cortlandt Park terminus. While there are some inherent drawbacks from elevated rail rapid transit lines, such as the increased noise and the potentially polarizing aesthetic, given the projected

frequency and extent of inundation on the Blue Line, such a long-term strategy might be the only viable solution using the existing right of way.

6.4: Planning Horizon and its Implications

As noted in the theoretical frame and the proposed assessment framework, selection of a planning horizon of interest is the first place a planner or transit agency exercises judgement when attempting to determine system resilience to climate change. When attempting to synthesize an adaptation project, the choice of planning horizon is partially dependent upon the desired or expected life cycle of the adaptation itself and those assets which it is meant to protect. As sea level rises and risks increase over time, protection against the design flood expected near the end of useful life is required to ensure adequate protection for the duration of the adaptation project's life cycle. Planning and design should acknowledge this perishable nature of protection when working against coastal flood risk.

Selection of a planning horizon will dictate the degree and length of protection provided by a given adaptation project. This, in turn, informs the time period through which benefits are expected to accrue and ultimately impacts the expected benefit-cost ratio (BCR) of a given adaptation project. Yet beyond the expected life cycle of an adaptation project, its presence may continue to provide some benefits, or may prove costly if it was poorly designed, short-sighted, or performed poorly. Thus, performance of adaptation projects beyond their expected life cycles should be considered in some capacity. A planner should question whether the presence of a given adaptation after the end of useful life promotes further adaptation, or creates a costly path dependency that would make the project maladaptive if viewed from the perspective of a longer planning horizon (see Appendix A for an example).

The calculated BCR also depends on what benefits are considered (e.g. economic benefits accrued by not losing productivity arising from a transit system shutdown), and the discount rate used in the calculation of benefits. Costs of adaptation strategies can be as simple as estimates of project life cycle costs (i.e. for both construction and operations/maintenance for the life of the constructed assets) but can also consider

associated opportunity costs. The benefits of a given adaptation strategy derive largely from the costs avoided from a perturbation event, as adaptation strategies ultimately aim to minimize these costs. When considering either these benefits or any associated project costs, particularly those which are to be amortized over long time horizons, the choice of discount rates greatly affects the BCR. While the United States Office of Management and Budget (OMB) procedure calls for usage of a 3% discount rate (NIBS, 2017), several authors have suggested that such a discount rate for time horizons beyond several decades inadequately portrays both cost and value to later generations (Lee & Ellingwood, 2015). Several countries, including the United Kingdom and France, have allowed for the implementation of variable discount rates (which decrease as expected life increases) for projects spanning several generations (Lee & Ellingwood, 2015). Further, in the context of engineering economics, the real cost of borrowing is frequently used as the discount rate; for government agencies, this is typically far below 3%; for most municipal agencies within the US government, the real cost of borrowing (i.e., interest rate less the inflation rate) is 0.66% (NIBS 2017). Usage of a 0.66% discount rate in lieu of the required 3% rate would better reflect costs of borrowing and also notably inflate BCR. Hence, when considering costs and benefits, the choice of time horizon and discount rate informs the perceptions decision makers have of a project and highlights the criticality of implementing sound long-term adaptation strategies.

The resilience assessment framework presented and implemented provides the preliminary information required to compute a BCR for a project, as the systemwide customer impact can be used to determine economic losses avoided by adaptive efforts, and vulnerable locations can be studied to determine the extent and cost of flood damage expected. Transit agencies and planners should exercise caution and due diligence when considering the costs and benefits of adaptation measures and how to support resilience of the system across and beyond a given planning horizon.

6.5: Assessment Framework Considerations

Aside from use in comparative analysis between exposure scenarios, a single-perturbation resilience metric provides limited information to planners and decision makers. Despite the intrinsic limitations, the

existing literature is quite fixated in presenting resilience through such a lens. It is more useful to consider the nuances of system performance under exposure, namely the locations found to be vulnerable and the system-wide impacts arising from the loss of such vulnerable locations. These locations are not links or nodes in a graph (theoretical representation of the network) but rather physical locations. They are part of the physical and social reality of the urban environment in which they are embedded. Analyses of transit system resilience should reflect this contextual reality, as well as the physical realities of rapid transit operation and exposure-specific vulnerability.

6.5.1: Context and Normative Aspects of Resilience

While resilience can be considered an inherent property of a system rather than an emergent one, the inherent resilience of a system must be determined via a threat agnostic analysis (Linkov & Trump, 2019). Such threat agnostic analyses by definition divorces the concept from a portfolio of risks, placing it outside the context of specific types of risks, thereby making the concept too abstract to have practical relevance in a planning context. In contrast, viewing resilience as an emergent system property (i.e. describing the degree of core functionality maintained for the duration of a single perturbation) can highlight individual vulnerabilities and provide decision makers with actionable areas of improvement.

This is predicated on the definition of core functionality, which existing resilience assessment frameworks overlook. In the context of transit networks, this core functionality is the transport of passengers, which should be reflected in the performance metric chosen to define system response, and by extension resilience. By assigning weights to a graph theoretic representation of a transit network, the relative importance of individual links in system can be characterized. Inclusion of such a weighting is crucial for properly characterizing the impact of service disruption that arises from a perturbation, as certain links in a system may be crucial from a passenger-centric perspective. While graph theoretic models are a sensible means of representing a transit network, a disproportionate emphasis is placed on their mathematical intricacies, overlooking contextual aspects of system performance. Sensible resilience metrics should relate a system of interest to the context in which it exists (i.e., passenger demand patterns;

relation to the socio-economic system) else the resulting metric will lack substantive meaning for decision makers.

6.5.2: System Characterization

Further, while other assessment frameworks such as Xing et al. (2017) and Saadat et al. (2019) provide a more mathematically rigorous analysis of the inherent topological redundancy of a system, they lack a mechanism to consider the exposure-specific robustness of a system. With the exception of Adjetey-Bahun et al. (2016), existing assessment frameworks neglect the physical realities of transit systems, thereby rendering such analyses unrealistic and of little value for planners attempting to improve their engineering resilience. Without such a mechanism, system interdependencies and cascading failures cannot be captured, which are crucial to assessing the resilience of interconnected systems (Linkov & Trump, 2019; Adjetey-Bahun et al., 2016; NIST, 2015). The proposed assessment framework presented allows for such a characterization through the operations network, which can be further connected to and modeled in conjunction with any number of ancillary systems, such as signal and power delivery systems.

Yet the assessment framework proposed and the resulting model of a transit system are not without limitations. Assumptions pertaining to lowest critical elevation exposure, flood propagation, and linear recovery though reasonable under certain conditions, may not always hold. Further, assessing the resilience of only the rail rapid transit network does not reflect all transit assets that would be exposed, nor does it reflect the adaptive capacity afforded to passengers by other modes of transportation. Like most other assessment frameworks in literature, adaptive capacity, which includes actions such as bus bridging for inundated subway routes, placement of temporary barriers, or movement of rolling stock, was not (though should be) included in the analysis. Ultimately, assessments of resilience undertaken without modelling adaptive capacity of the system are partial vulnerability assessments, as they only characterize system sensitivity to given exposures. This exclusion of adaptive capacity, along with the exclusion of other ancillary systems in analysis is the result of a lack of available system information or formalized recovery

procedures. Inclusion of such information would allow for a more accurate representation of system response under perturbation.

7. Conclusions and Future Work

7.1: Summary

This thesis presents a coherent definition of engineering resilience applicable to managed transportation and infrastructure systems facing climate change related risks. From this definition, an assessment framework specific to rail rapid transit systems was formulated and applied to assess the resilience of the MBTA's rail rapid transit system to climate change. A model of the rail rapid transit system was created using the assessment framework, incorporating endogenous network characteristics (i.e., network topology, lowest critical elevations, track geometry, and dispatch locations), exogenous aspects of resilience (i.e., a suite of projected coastal flood events based on climate and storm surge modeling; Bosma et al., 2015), and normative components of resilience (i.e., relative service priority based on passenger flows and choice of planning horizons). System performance was defined as the weighted efficiency of the network, from which resilience was computed assuming linear system recovery to pre-perturbation levels of performance. Resilience of the system was computed for a suite of 27 coastal flood scenarios across 3 SLR regimes to determine the projected impact of climate change through 2070 on the MBTA rail rapid transit system.

Using the model resulting from the framework above, twenty five locations within the rapid transit system will be vulnerable to coastal flood inundation by the end of the century, with the inundation of some locations causing larger degrees of system-wide connectivity loss than others. Locations that are exposed earlier in the century, which principally lie along the Blue Line, will likely require two phases of adaptive action in the 21st century, should they be protected against a 1-100 year return period design level storm. A proposed adaptation roadmap to 2070 is provided, along with a list of several adaptation strategies proposed that can be implemented.

7.2 Conclusions

The definition and theoretical frame of engineering resilience proposed incorporates these exogenous, endogenous, and normative aspects of resilience, all of which are crucial for understanding the emergent

properties of a system. Through inclusion of these aspects of resilience, the assessment framework proposed and implemented can capture the physical realities of transit operation, complex system interdependencies, exposure specific sensitivity, and the impact of service outages from a passenger-focused perspective. The final output of the assessment framework, a resilience metric describing the percentage of service provided throughout the perturbation, is useful for comparative analyses between individual perturbations and between sea level rise regimes. However, identification of vulnerable locations, an intermediate result of the model, will likely prove more useful for purposes of planning and decision making.

Climate change and sea level rise will pose an existential threat to the MBTA rapid transit system by the end of the 21st century. This increased risk greatly degrades system resilience over time as events of constant frequency grow more intense. The results highlight the vulnerability of the MBTA's current rail rapid transit system to future SLR as new flood pathways inundate critical links and rail yards in the system. By presenting system performance from a passenger-oriented perspective, this analysis provides useful insights into the severity of future flood events and can assist in prioritizing adaptation strategies.

The results also show adaptation strategies proposed to date fail to acknowledge the large-scale strategies that will be necessary to ensure the resilience of the system. Most critically, the resilience assessment results show that only a terminus-to-terminus Blue Line adaptation strategy will ensure its resilience in the long-term. Lastly, proposals by other agencies (i.e., Climate Ready Boston, City of Cambridge) which would provide protection to MBTA assets demonstrate that partnership with other municipalities will likely be the most effective and economical approach the MBTA can take to reduce its vulnerability and increasing its resilience to climate change related risks.

7.3: Recommendations

Future work could further expand the assessment framework proposed to include aspects of adaptive capacity. This can include:

1) Actions a transit agency can take to reduce damage at vulnerable locations.

2) Dynamic passenger re-routing through the perturbed system.

3) Movement of rolling stock during a perturbation event.

4) Provisions of temporary service during the recovery period.

Characterizing the capacity of the system to perform adaptive actions would allow for the evaluation and optimization of recovery plans given resource constraints. Additional expansion of the assessment framework to include bus and commuter rail would further allow for modeling of adaptive capacity and would also prove useful to determine the resilience of the entire public transport network.

Dependent upon available data sets, the model could be expanded to assess the impacts of additional climate stressors, such as extreme precipitation events, extreme heat, and extreme snowfall. Alternatively, expansion of the model to estimate the depth of inundation experienced and the arising damage would help decision makers to estimate the total time of disruption and to estimate the total direct cost to the system caused by inundation.

Additional economic analyses can be incorporated to estimate the externalized costs associated with transit service impact, which could be used to conduct a more extensive cost-benefit analysis. Further work characterizing the equity implications of climate change-related service disruption could also be pursued by the further refinement of the system performance weighting to consider passenger travel time, level of service, and dependence on transit. For longer-term scenarios, it may also be sensible to adjust these performance weights based on projected ridership growth, as well as consider expected ridership on future expansions of the network.

The theoretical frame of engineering resilience presented can also be used and applied in the context of other managed infrastructure systems (e.g. water supply network, wastewater network, road networks, electric grids, gas distribution networks, airline networks). Of particular pertinence to climate change related risks would be the application of this frame to construct an assessment framework to determine the resilience of coastal flood protection systems. Given that flood risk affects the entire fabric of a coastal

urban environment, characterization of coastal flood protection system resilience would prove useful in their design and life cycle management.

References

Adjetey-Bahun, K., Birregah, B., Châtelet, E., and & Planchet, J. L. (2016). A model to quantify the resilience of mass railway transportation systems. *Reliability Engineering & System Safety, 153*(1), 1-14.

AECOM. (2018). *Massachusetts Bay Transportation Authority: Orient Heights Maintenance and Storage Facilities Current and Future Vulnerabilities to Climate Stressors.* Boston, MA.

Alexander, D.E. (2013). Resilience and disaster risk reduction: An etymological journey. *Natural Hazards and Earth Systems Sciences, Vol. 13*, 2707-2716.

Allen, C. R., Angeler, D. G., Garmestani, A. S., Gunderson, L. H., & Holling, C. S. (2014). Panarchy: theory and application. *Ecosystems, 17*(4), 578–589. https://doi.org/10.1007/s10021-013-9744-2

American Society of Civil Engineers (Ed.). (2015). *Flood resistant design and construction*. American Society of Civil Engineers.

American Society of Civil Engineers (ASCE), & Ayyub, B. M. (Eds.). (2018). *Climate-resilient infrastructure: Adaptive design and risk management.* Reston, Virginia: American Society of Civil Engineers.

Ask the Globe. (2000, May 20) *The Boston Globe.* Retrieved from: https://global.factiva.com/ha/default.aspx?ftx=Narrow%20Gauge%20to%20Boston:%20A%20Nostalgic%20Window%20on%20the%20Boston,%20Revere%20Beach%20&%20Lynn%20Railroad#./!?&_suid=157486717738305155711127849945

Ayyub, B.M. (2014). Systems resilience for multihazard environments: Definitions, metrics, and valuation for decision making. *Risk Analysis*, 34(2), 340-355.

Ayyub, B. M. (2015). Practical resilience metrics for planning, design, and decision making. *ASCE-ASME Journal of Risk and Uncertainty in Engineering Systems, Part A: Civil Engineering, 1*(3), 04015008.

Ayyub, B. M. (May, 2019). *Practical Resilience Measures for Coastal Infrastructure Features.* USACE. Retrieved from https://apps.dtic.mil/dtic/tr/fulltext/u2/1073955.pdf

Belcher, J. (2019). *Changes to Transit Service in the MBTA District: 1964-2019.* Retrieved from: http://www.transithistory.org/roster/MBTARouteHistory.pdf

Ben-Elia, E., & Benenson, I. (2019). A spatially-explicit method for analyzing the equity of transit commuters' accessibility. *Transportation Research Part A: Policy and Practice, 120*, 31–42. https://doi.org/10.1016/j.tra.2018.11.017

Berkes, F., & Ross, H. (2016). Panarchy and community resilience: Sustainability science and policy implications. *Environmental Science & Policy, 61*, 185–193. https://doi.org/10.1016/j.envsci.2016.04.004

Bock, Y., Wdowinski, S., Ferretti, A., Novali, F., & Fumagalli, A. (2012). Recent subsidence of the Venice Lagoon from continuous GPS and interferometric synthetic aperture radar. Geochemistry, *Geophysics, Geosystems, 13*(3). https://doi.org/10.1029/2011GC003976

Bosma, K., Douglas, E., Kirshen, P., McArthur, K., Miller, S., Watson, C. (June, 2015). *MassDOT-FHWA Pilot Project Report: Climate Change and Extreme Weather Vulnerability Assessments and Adaptation Options for the Central Artery.* MassDOT.

Boston Transit Commission. (1895). *Annual Report of the Boston Transit Commission, Ninth Annual Report.* Boston, MA: Rockwell and Churchill. Retrieved from: https://archive.org/details/annualreportofbo91903bost

Botros, R., Diaz, N., Rambert, R., and Shah, A. (2019). *Final Memorandum: MBTA Climate Resilience Decision-Making Tool.*

Brand, F. S., & Jax, K. (2007). Focusing on the meaning(s) of resilience: Resilience as a descriptive concept and a boundary object. *Ecology and Society, 12(1),* 23.

Bromley, G.W., and Bromley, W.S. "Atlas of the city of Boston, Charlestown and East Boston." Map. 1922. *Norman B. Leventhal Map & Education Center*, https://collections.leventhalmap.org/search/commonwealth:1257c1410 (accessed December 05, 2019).

Brown, K. (2011). Sustainable adaptation: An oxymoron?. *Climate and Development, 3*(1), 21-31.

Bruneau, M., Chang, S. E., Eguchi, R. T., Lee, G. C., O'Rourke, T. D., Reinhorn, A. M., … von Winterfeldt, D. (2003). A framework to quantitatively assess and enhance the seismic resilience of communities. *Earthquake Spectra, 19*(4), 733–752. https://doi.org/10.1193/1.1623497

Byrum, G. (November, 2019). *Digital Equity and Climate Resilience*. Lecture presented at the Climate Adaptation Forum. EBC New England & UMass Boston. Retrieved from: https://climateadaptationforum.org/wp-content/uploads/2019/10/Click-to-View-the-Presentation-Byrum-November-22-2019.pdf

Chan, R., & Schofer, J. L. (2016). Measuring transportation system resilience: response of rail transit to weather disruptions. *Natural Hazards Review, 17*(1), 05015004.

City of Boston, Green Ribbon Commission, MA Office of Coastal Zone Management, Boston Planning and Development Agency. (2016a). *Climate Ready Boston: Final Report*. Boston, MA: City of Boston.

City of Boston, Green Ribbon Commission, The Boston Research Advisory Group. (2016b). *Climate Change and Sea Level Rise Projections for Boston*. Boston, MA: City of Boston.

City of Boston, MA Office of Coastal Zone Management, Barr Foundation, Green Ribbon Commission. (October, 2017). *Coastal Resilience Solutions for East Boston and Charlestown: Final Report*. Boston, MA: City of Boston.

City of Boston, Barr Foundation, Green Ribbon Commission. (October, 2018). *Coastal Resilience Solutions for South Boston: Final Report*. Boston, MA: City of Boston.

City of Boston. (2019, October). *Climate Ready Dorchester: Design Options Survey*. Retrieved from: https://docs.google.com/forms/d/e/1FAIpQLSfc1-mfWITmhO_gEKYBKw61nG2qAubVsVMYZT87RyV9mnOLNw/viewform

City of Boston. (2020, January). *Preparing for climate change*. Retrieved from: https://www.boston.gov/departments/environment/preparing-climate-change

City of Cambridge. (November, 2015). *Climate Change Vulnerability Assessment: The CCVA Report.* Cambridge, MA: City of Cambridge.

City of Cambridge. (February, 2017). *Climate Change Vulnerability Assessment Part 2: Sea Level Rise and Storm Surge.* Cambridge, MA: City of Cambridge.

Colle, B. A., Booth, J.F., Chang, E.K.M., (2015). A review of historical and future changes of extratropical cyclones and associated impacts along the US East Coast. *Current Climate Change Reports, 1*(3), 125–143, https://doi:10.1007/s40641-015-0013-7

Crouzet-Pavan, E. (2002). *Venice triumphant: The horizons of a myth.* Baltimore: Johns Hopkins University Press.

Cunha, D. da. (2018). *The invention of rivers: Alexander's eye and Ganga's descent* (1st edition). Philadelphia: University of Pennsylvania Press.

Dall'Asta, L., Barrat, A., Barthélemy, M., Vespignani, A. (2006). Vulnerability of weighted networks. *Journal of Statistical Mechanics: Theory and Experiment*, *2006*(04), P04006–P04006. https://doi.org/10.1088/1742-5468/2006/04/P04006

Davidson, J., Jacobson, C., Lyth, A., Dedekorkut-Howes, A., Baldwin, C., Ellison, J., Holbrook, N., Howes, M., Serrao-Neumann, S., Singh-Peterson, L., & Smith, T. (2016). Interrogating resilience: toward a typology to improve its operationalization. *Ecology and Society*, *21*(2), Art 27.

Davis, D. E. (2012). *Urban Resilience in Situations of Chronic Violence*. Cambridge, MA: MIT Center for International Studies.

Delft University of Technology. (2020). *SWAN*. TU Delft Civil Engineering and Geosciences. https://www.tudelft.nl/en/ceg/about-faculty/departments/hydraulic-engineering/sections/environmental-fluid-mechanics/research/swan/

Dowds, J., & Aultman-Hall, L. (2015). Barriers to implementation of climate adaptation frameworks by state departments of transportation. *Transportation Research Record: Journal of the Transportation Research Board, 2532*(1), 21–28. https://doi.org/10.3141/2532-03

Engelhart, S. E., Horton, B. P., Douglas, B. C., Peltier, W. R., & Tornqvist, T. E. (2009). Spatial variability of late Holocene and 20th century sea-level rise along the Atlantic coast of the United States. *Geology, 37*(12), 1115–1118. https://doi.org/10.1130/G30360A.1.

Federal Emergency Management Agency (FEMA). (2016). *Draft Interagency Concept for Community Resilience Indicators and National- level Measures. Mitigation Framework Leadership Group Draft Concept Paper.* Washington, DC: U.S. Department of Homeland Security. Retrieved from https://www.fema.gov/media-library-data/1466085676217-a14e229a461adfa574a5d03041a6297c/FEMA-CRI-Draft-Concept-Paper-508_Jun_2016.pdf

Federal Emergency Management Agency (FEMA). (2017). *MassGIS Data: FEMA National Flood Hazard Layer* [Map]. Massachusetts Bureau of Geographic Information. Retrieved from: https://docs.digital.mass.gov/dataset/massgis-data-fema-national-flood-hazard-layer

Federal Emergency Management Agency (FEMA). (2019, March 18). *Flood Zones*. Retrieved from: https://www.fema.gov/flood-zones

Federal Highway Administration (FHWA). (2017, October). *Post Hurricane Sandy Transportation Resilience Study in New York, New Jersey, and Connecticut*. (Report No. FHWA-HEP-17-097) Washington, DC: FHWA.

Field, C. B., Barros, V. R., & Intergovernmental Panel on Climate Change (Eds.). (2014). *Climate change 2014: impacts, adaptation, and vulnerability: Working Group II contribution to the fifth assessment report of the Intergovernmental Panel on Climate Change.* New York, NY: Cambridge University Press.

Fisichelli, N. A., Schuurman, G. W., & Hoffman, C. H. (2016). Is 'Resilience' maladaptive? Towards an accurate lexicon for climate change adaptation. *Environmental Management, 57*(4), 753-758.

Franchin, P., & Cavalieri, F. (2015). Probabilistic assessment of civil infrastructure resilience to earthquakes: probabilistic assessment of civil infrastructure resilience to earthquakes. *Computer-Aided Civil and Infrastructure Engineering, 30*(7), 583–600.

Google Maps. (n.d.) [Boston, MA]. Retrieved Jan 8, 2020 from: https://www.google.com/maps/@42.3547602,-71.0533024,13z

Gordon, J. (2019, April). "MBTA Rail Rapid Transit Link Flows: Fall 2017." Unpublished raw data.

Graham, L., Debucquoy, W., & Anguelovski, I. (2016). The influence of urban development dynamics on community resilience practice in new york city after superstorm sandy: Experiences from the lower east side and the rockaways. *Global Environmental Change*, *40*, 112–124. https://doi.org/10.1016/j.gloenvcha.2016.07.001

Gunderson, L.H. (2000). Ecological resilience - in theory and application. *Annual Review of Ecology and Systematics*, *31*(2000), pp. 425-439.

Gunderson, L.H., Holling, C.S. (2002) Panarchy: understanding transformations in human and natural systems. Island Press, Washington, DC.

Henry, D., & Emmanuel Ramirez-Marquez, J. (2012). Generic metrics and quantitative approaches for system resilience as a function of time. *Reliability Engineering & System Safety*, *99*, 114–122. https://doi.org/10.1016/j.ress.2011.09.002

Hill, K. (2016). Climate change: Implications for the assumptions, goals and methods of urban environmental planning. *Urban Planning*, *1*(4), 103. https://doi.org/10.17645/up.v1i4.771

HNTB. (2016a). *Draft: MBTA E&M Blue Line Track Chart: Bowdoin - Wonderland*. Boston, MA.

HNTB. (2016b). *Draft: MBTA E&M Green Line Track Chart Beacon Street – 'C' Line: Kenmore – Cleveland Circle*. Boston, MA.

HNTB. (2016c). *Draft: MBTA E&M Green Line Track Chart Central Subway – 'A' Line: Kenmore - Lechmere*. Boston, MA.

HNTB. (2016d). *Draft: MBTA E&M Green Line Track Chart Commonwealth Avenue – 'B' Line: Kenmore – Boston College*. Boston, MA.

HNTB. (2016e). *Draft: MBTA E&M Green Line Track Chart Highland Brach – 'D' Line: Beacon Junction – Riverisde*. Boston, MA.

HNTB. (2016f). *Draft: MBTA E&M Green Line Track Chart Huntington Avenue – 'E' Line: Copley Junction – Heath Street*. Boston, MA.

HNTB. (2016g). *Draft: MBTA E&M Orange Line Track Chart: Forest Hills – Oak Grove*. Boston, MA.

HNTB. (2016h). *Draft: MBTA E&M Red Line Track Chart: Alewife – Braintree*. Boston, MA.

HNTB. (2016i). *Draft: MBTA E&M Red Line Track Chart Ashmont Line: Columbia Junction – Ashmont*. Boston, MA.

HNTB. (2016j). *Draft: MBTA E&M Red Line Track Chart Mattapan High Speed Line: Ashmont – Mattapan*. Boston, MA.

Holling, C. S. (1973). Resilience and stability of ecological systems. *Annual Review of Ecology and Systematics, 4*, 1-23.

Hosseini, S., Barker, K., & Ramirez-Marquez, J. E. (2016). A review of definitions and measures of system resilience. *Reliability Engineering & System Safety, Vol. 145*, 47-61.

Hurricane Sandy Rebuilding Task Force (HSRTF). (2013, August). *Hurricane Sandy Rebuilding Strategy: Stronger Communities, A Resilient Region.* Retrieved February 2nd, 2019, from U.S. Department of Housing and Urban Development website: https://www.hud.gov/sites/documents/HSREBUILDINGSTRATEGY.PDF

Intergovernmental Panel on Climate Change (IPCC). (2007). *Impacts, Adaptation and Vulnerability. Contribution of Working Group II to the Fourth Assessment Report of the Intergovernmental Panel on Climate Change.* Cambridge University Press, Cambridge.

Jay, M. (2017). *Supernormal: The untold story of adversity and resilience* (First edition). New York: Twelve.

Karegar, M. A., T. H. Dixon, S. E. Engelhart. (2016). Subsidence along the Atlantic Coast of North America: Insights from GPS and late Holocene relative sea level data. *Geophys. Res. Lett., 43*, 3126–3133, https://doi:10.1002/2016GL068015

Keenan, J.M. (2018). Types and forms of resilience in local government planning: Who does what? *Environmental Science and Policy, 88*(1), 116-123. doi: 10.1016/j.envsci.2018.06.015

Keenan, J.M. (2019, February). Theories of Resilience. Lecture presented at the Harvard University Graduate School of Design. Harvard University Graduate School of Design.

Kenney, T. C. (1964). Sea-level movements and the geologic histories of the post-glacial marine soils at Boston, Nicolet, Ottawa and Oslo. *Géotechnique, 14*(3), 203–230. https://doi.org/10.1680/geot.1964.14.3.203

Kind, J., Wouter Botzen, W. J., & Aerts, J. C. J. H. (2017). Accounting for risk aversion, income distribution and social welfare in cost-benefit analysis for flood risk management: Accounting for risk aversion, income distribution and social welfare. *Wiley Interdisciplinary Reviews: Climate Change, 8(2), e446.* https://doi.org/10.1002/wcc.446

Kirshen, P., Watson, C., Douglas, E., Gontz, A., Lee, J., & Tian Y. (2008). Coastal flooding in the Northeastern United States due to climate change. *Mitigation & Adaptation Strategies to Global Climate Change, 13,* 437-451. https://doi.org/10.1007/s11027-007-9130-5.

Knutson, T. R., McBride, J. L., Chan, J., Emanuel, K., Holland, G., Landsea, C., Held, I., Kossin, J. P., Srivastava, A. K., & Sugi, M. (2010). Tropical cyclones and climate change. *Nature Geoscience, 3*(3), 157–163. https://doi.org/10.1038/ngeo779

Kurth, M. H., Keenan, J. M., Sasani, M., and Linkov, I. (2019). Defining resilience for the US building industry. *Building Research & Information, 47*(4), 480-492.

Laboy, M., & Fannon, D. (2016). Resilience theory and praxis: A critical framework for architecture. *Enquiry The ARCC Journal for Architectural Research, 13*(1). https://doi.org/10.17831/enq:arcc.v13i2.405

Latora, V., & Marchiori, M. (2001). Efficient behavior of small-world networks. *Physical Review Letters, 87(19).* https://doi.org/10.1103/PhysRevLett.87.198701.

Lee, J.Y, & Ellingwood, B. R. (2015). Ethical discounting for civil infrastructure decisions extending over multiple generations. *Structural Safety, Vol. 57,* 43-52.

Leonard, S. (2011, March 13). Mass. Author takes a trip on an old railroad. *Boston.com*. Retrieved from http://archive.boston.com/news/local/massachusetts/articles/2011/03/13/mass_author_takes_a_trip_on_an_old_railroad/

Li, M., Wang, H., & Wang, H. (2017). Resiliency assessment of urban rail transit networks: a case study of Shanghai Metro. *Intelligent Transportation Systems Conference, IEEE ITSC, & ITSC. Vol. 20,* 620-625.

Linkov, I., & Trump, B. D. (2019). *The science and practice of resilience.* https://doi.org/10.1007/978-3-030-04565-4

Luettich, R.A., Jr. J.J. Westerink, & N.W. Scheffner. (1992). ADCIRC: *An advanced three-dimensional circulation model for shelves, coasts, and estuaries. Technical Report DRP-92-6*. U.S. Army Engineer Research and Development Center, Vicksburg, MS.

Massachusetts Bay Transportation Authority (MBTA). (2014). *Ridership and Service Statistics, Fourteenth Edition*. Boston, MA.

Massachusetts Bay Transportation Authority (MBTA). (2018a, January 4). "Service suspended btwn Wonderland & Orient Heights Stations [Twitter moment]." Retrieved from https://twitter.com/MBTA/status/948992218878103552

Massachusetts Bay Transportation Authority (MBTA). (2018b, January 4). " #MBTA #BlueLine: The Harbor side entrance at Aquarium Station is temporarily closed. [Twitter moment]." Retrieved from https://twitter.com/MBTA/status/948992218878103552

Massachusetts Bay Transportation Authority (MBTA). (2019, February 13). *MBTA FY20-24 Capital Investment Plan: Evaluation Guide*. Boston, MA.

Massachusetts Department of Transportation (MassDOT). (2019). *2020-2024 Capital Investment Plan Update*. Boston, MA. Retrieved from: http://massdot.maps.arcgis.com/apps/MapJournal/index.html?appid=33a118c32b3f47b3b90a769498aa68bd#

Mass State Police. (2018, January 4). " #MAflood View from Seaport Lane #Boston looking east down Seaport Blvd. [Twitter moment]." Retrieved from https://twitter.com/MassStatePolice/status/948982040761917440

Meerow, S., Newell, J. P., & Stults, M. (2016). Defining urban resilience: A review. *Landscape and Urban Planning*, *147*, 38–49. https://doi.org/10.1016/j.landurbplan.2015.11.011

Merriam-Webster (2019). Definition of normative. (n.d.). Retrieved October 27, 2019, from https://www.merriam-webster.com/dictionary/normative

Miao, Q., Feeney, M. K., Zhang, F., Welch, E. W., & Sriraj, P. S. (2018). Through the storm: Transit agency management in response to climate change. *Transportation Research Part D: Transport and Environment*, *Vol. 63,* 421–432. https://doi.org/10.1016/j.trd.2018.06.005.

Miller, S.J. (2019, April). *MassDOT/MBTA Actions contained in the SHMCAP and Coastal Flood Risk Modeling*. Presentation at the MassDOT Transportation Innovation Conference, Worcester, MA. Retrieved from: https://www.umasstransportationcenter.org/Document.asp?DocID=694

Morano, M. (2018). *The politically incorrect guide to climate change*. Washington, DC: Regnery Publishing.

Moss, R. H., Edmonds, J. A., Hibbard, K. A., Manning, M. R., Rose, S. K., van Vuuren, D. P., Carter, T. R., Emori, S., Kainuma, M., Kram, T., Meehl, G. A., Mitchell, J. F. B., Nakicenovic, N., Riahi, K., Smith, S. J., Stouffer, R. J., Thomson, A. M., Weyant, J. P., & Wilbanks, T. J. (2010). The next generation of scenarios for climate change research and assessment. *Nature*, *463*(7282), 747–756. https://doi.org/10.1038/nature08823

Mooyaart, L.F., Jonkman, S.N., de Vries, P.A.L., van der Toorn, A., & van Ledden, M. (2014). Storm surge barrier: Overview and design considerations. *Coastal Engineering Proceedings*, *1*(34), 45. https://doi.org/10.9753/icce.v34.structures.45.

National Academies of Sciences, Engineering, and Medicine (NASEM). (2016). *Attribution of Extreme Weather Events in the Context of Climate Change*. Washington, DC: The National Academies Press. doi: 10.17226/21852.

National Academies of Sciences, Engineering, and Medicine (NASEM). (2017). *Improving the Resilience of Transit Systems Threatened by Natural Disasters, Volume 2: Research Overview*. Washington, DC: The National Academies Press. https://doi.org/10.17226/24974.

National Institute of Building Science (NIBS). (2017). *Natural Hazard Mitigation Saves: 2017 Interim Report*. Washington, DC: Multihazard Mitigation Council, NIBS.

National Institute of Standards and Technology (NIST). (2015). *Community Resilience Planning Guide for Buildings and Infrastructure Systems, Volume II. (NIST SP 1190v2).* National Institute of Standards and Technology. https://doi.org/10.6028/NIST.SP.1190v2

National Oceanic and Atmospheric Administration (NOAA). (2017, January). *Global and regional sea level rise scenarios for the United States. NOAA technical report NOS CO-OPS 083.* Retrieved September 4, 2018, from https://tidesandcurrents.noaa.gov/publications/techrpt83_Global_and_Regional_SLR_Scenarios_for_the_US_final.pdf.

National Oceanic and Atmospheric Administration. (NOAA). (2019a). *Boston, MA - Station ID: 8443970.* Retrieved from: https://tidesandcurrents.noaa.gov/stationhome.html?id=8443970

National Oceanic and Atmospheric Administration (NOAA). (2019b). Relative sea level trend: 8518750 The Battery, New York. NOAA tides & currents. Retrieved October 21, 2019, from https://tidesandcurrents.noaa.gov/sltrends/sltrends_station.shtml?id=8518750

Nelson, D.R. (2011). Adaptation and resilience: Responding to a changing climate. Wiley Interdisciplinary Reviews: *Climate Change, 2*(1), 113-120.

Nir, S. M. (2018, February 12). Water, water everywhere in New York subway. And with it, problems. *The New York Times*. Retrieved from: https://www.nytimes.com/2018/02/12/nyregion/water-nyc-subway.html

Olsson, L., Jerneck, A., Thoren, H., Persson, J., & O'Byrne, D. (2015). Why resilience is unappealing to social science: Theoretical and empirical investigations of the scientific use of resilience. *Science Advances*, *1*(4), e1400217. https://doi.org/10.1126/sciadv.1400217

Park, J., Seager, T. P., Rao, P. S. C., Convertino, M., & Linkov, I. (2013). Integrating risk and resilience approaches to catastrophe management in engineering systems. *Risk Analysis, 33*(3), 356-367.

Parris, A., P. Bromirski, V. Burkett, D. Cayan, M. Culver, J. Hall, R. Horton, K. Knuuti, R. Moss, J. Obeysekera, A. Sallenger, and J. Weiss. (2012). *Global Sea Level Rise Scenarios for the US National Climate Assessment.* NOAA Tech Memo OAR CPO-1. NOAA.

Pelling, M., O'Brien, K., & Matyas, D. (2015). Adaptation and transformation. *Climatic Change*, *133*(1), 113–127. https://doi.org/10.1007/s10584-014-1303-0

Pfahl, S., O'Gorman, P.A., & Fischer, E.M. (2017). Understanding the regional pattern of projected future changes in extreme precipitation. *Nature Climate Change, Vol. 7,* 423-427. https://doi.org/10.1038/NCLIMATE3287.

Rawson, M. (2010). *Eden on the Charles: The making of Boston*. Cambridge, MA: Harvard University Press.

Rayner, R. (2010). Incorporating climate change within asset management In C. Lloyd (Ed.), *Asset Management: Whole-Life Management of Physical Assets* (pp. 161-180). London, United Kingdom: Thomas Telford/ICE Publishing.

Riley-Gilbert, M. (2018, January). *Weather and Climate Resiliency at the MBTA*. Presentation at NCSE 2018 Conference: The Science, Business, and Education of Sustainable Infrastructure, Washington, DC.

Saadat, Y., Ayyub, B. M., Zhang, Y., Zhang, D., & Huang, H. (2019). Resilience of metrorail networks: Quantification with Washington, DC as a case study. *ASCE-ASME J Risk and Uncert in Engrg Sys Part B Mech Engrg, 5*(4), 041011. https://doi.org/10.1115/1.4044038

Sela, L., Bhatia, U., Zhuang, J., & Ganguly, A. (2017). Resilience strategies for interdependent multiscale lifeline infrastructure networks. *Computing in Civil Engineering 2017*, 265–272. https://doi.org/10.1061/9780784480847.033

Sharifi, A. (2016). A Critical Review of Selected Tools for Assessing Community Resilience. *Ecological Indicators, Vol. 69,* 629-647.

Song, Y., Kim, H., Lee, K., & Ahn, K. (2018). Subway network expansion and transit equity: A case study of Gwangju metropolitan area, South Korea. *Transport Policy*, *72*, 148–158.

Strzepek, K., Fant, C., Preston, M., Emanuel, K., Goldberg, B. (March, 2018). *MIT Climate Resilience Planning: Flood Vulnerability Study* (Report 326). MIT Office of Sustainability.

Sweet, W.W., Marcy, D., Dusek, G., Marra, J.J., & Pendleton, M. (June, 2018). *2017 State of U.S. High Tide Flooding with a 2018 Outlook.* Supplement to *State of the Climate: National Overview for May 2018*. NOAA National Centers for Environmental Information. Retrieved from: https://www.ncdc.noaa.gov/monitoring-content/sotc/national/2018/may/2017_State_of_US_High_Tide_Flooding.pdf

Sullivan, J. (November, 2019). *Preparing Boston's Water and Sewer Systems for Future Design Storms*. Lecture presented at the Climate Adaptation Forum. EBC New England & UMass Boston. Retrieved from: https://climateadaptationforum.org/wp-content/uploads/2019/10/Click-to-View-the-Presentation-Sullivan-November-22-2019.pdf

Testa, A. C., Furtado, M. N., & Alipour, A. (2015). Resilience of coastal transportation networks faced with extreme climatic events. *Transportation Research Record: Journal of the Transportation Research Board, 2532(1),* 29–36.

United States Army Corps of Engineers (USACE). (2019). Sea level tracker. Retrieved December 2, 2019, from https://climate.sec.usace.army.mil/slr_app/

United States Global Change Research Program (USGCRP). (2017). Climate Science Special Report. https://science2017.globalchange.gov/. Accessed 3 Dec. 2019.

Vanshnookenraggen. (2017). *Boston MBTA System Track Map* [map]. (ca. 1:22,000.) New York, New York: Vanshnookenraggen. Retrieved from: http://www.vanshnookenraggen.com/_index/2017/08/a-complete-and-geographically-accurate-boston-mbta-subway-track-map/

Wan, C., Yang, Z., Zhang, D., Yan, X., and Fan, S. (2018). Resilience in transportation systems: a systematic review and future directions. *Transport Reviews, 38*(4), 479-498.

Weston & Sampson. (2019). *Flood Resilience Recommendations for Aquarium Station through the Maverick Portal*. Peabody, MA.

Wikipedia. (2019). Template: Boston, Revere Beach and Lynn Railroad. Wikipedia. Retrieved from https://en.wikipedia.org/w/index.php?title=Template:Boston,_Revere_Beach_and_Lynn_Railroad&oldid=911484230

Woodruff, S. C., Meerow, S., Stults, M., & Wilkins, C. (2018). Adaptation to resilience planning: Alternative pathways to prepare for climate change. *Journal of Planning Education and Research*, 0739456X1880105. https://doi.org/10.1177/0739456X18801057

Xing, Y., Lu, J., Chen, S., & Dissanayake, S. (2017). Vulnerability analysis of urban rail transit based on complex network theory: A case study of Shanghai Metro. *Public Transport, 9*(3), 501–525. https://doi.org/10.1007/s12469-017-0170-2

Yuill, B., Lavoie, D., & Reed, D. J. (2009). Understanding subsidence processes in coastal Louisiana. *Journal of Coastal Research, 10054,* 23–36. https://doi.org/10.2112/SI54-012.1

Zervas, C., Gill, S., Sweet, W. (May, 2013). *Estimating Vertical Land Motion from Long-Term Tide Gauge Records* (Technical Report NOS CO-OPS 065). Silver Spring, MD: NOAA.

Zhang, D., Du, F., Huang, H., Zhang, F., Ayyub, B. M., & Beer, M. (2018). Resiliency assessment of urban rail transit networks: Shanghai metro as an example. *Safety Science, Vol. 106*, 230–243.

Appendix A: Frederickstown – A Hypothetical Case Study

Consider a hypothetical coastal community, Frederickstown, depicted in Figure 53 below, faced with significant flood risk in its historic city center. The year is 2020, and the newly elected mayor of Frederickstown, already angling to win re-election in his progressively-minded town, decides to promote a Frederickstown 2070 initiative. The 2070 initiative includes a federally funded project to build a seawall with a design life of 50 years to protect against existing coastal flood risks and improve the resilience of the community. The project is heavily promoted by the mayor's office, is approved, moves quickly through the environmental permitting process, and becomes popular amongst the locals. Four years later in 2024, the mayor is voted out of office by a narrow margin, losing to a pro-business candidate, but the project is well underway.

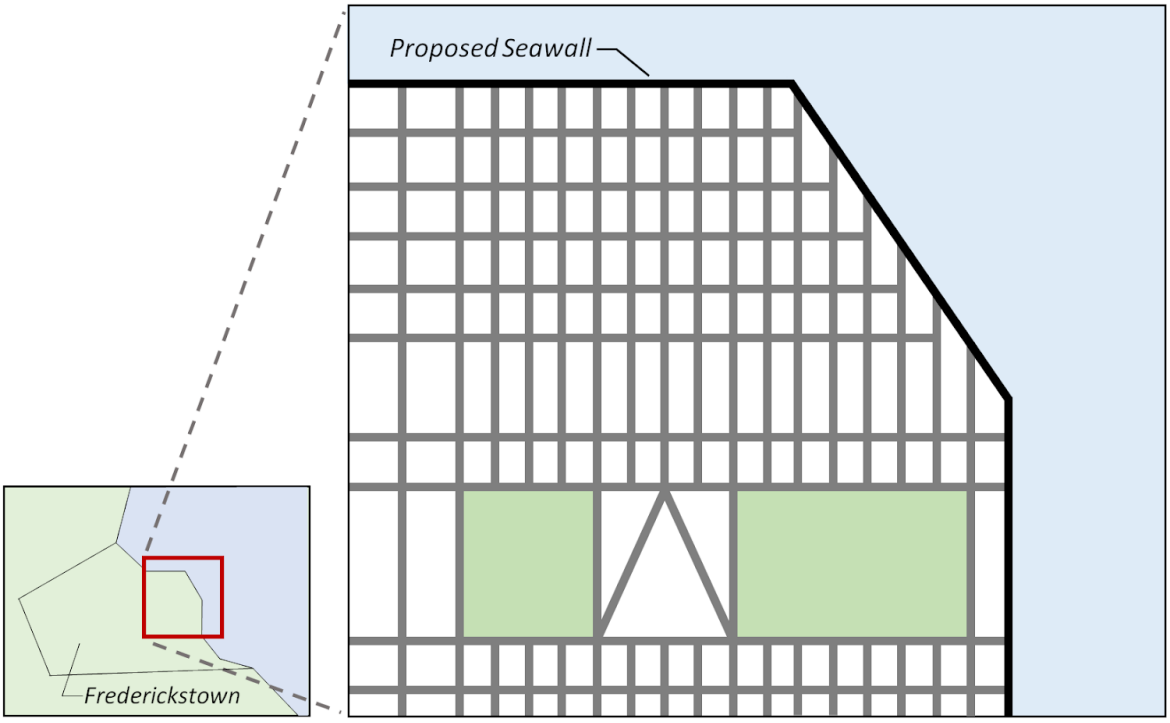

Figure 53: The hypothetical city of Frederickstown and its historic downtown center.

Three years later in 2027, the project is a success, completed ahead of schedule and under budget. Local flood maps, already redrawn to reflect the increased protection provided by the seawall, immediately go into effect. Community resilience to climate change is improved by lowering coastal flood exposure. Lower

insurance rates, coupled with additional tax incentives, provided by the new mayor in an effort to revitalize the historic city center (and his re-election campaign) spur development. Businesses take advantage of the tax incentives, as do real estate developers, who redevelop dozens of city blocks with mixed-use residential buildings. Frederickstown's population grows, as its revitalized downtown draws in college graduates from all over the region. Hoping to win more support, the mayor also convinces the local hospital, a major employer in the community, to develop the last remaining site downtown. A year later in 2028, despite the veritable economic boom in Frederickstown, whose economic growth rate was twice that of the surrounding municipalities, the mayor loses his bid for re-election. But five years later in 2033, true to his campaign promise, a new state-of-the-art hospital is completed downtown. The presence of the sea wall has greatly benefitted the business community in Frederickstown.

Fast forward to May 2100, Frederickstown's downtown area has doubled in population since 2020, its regional GDP has tripled, and its downtown tax revenue has sextupled in the same period; the downtown hospital has grown to become the region's largest. Mean sea level has risen 0.6 meters since the seawall was proposed, and the latest projections estimate another 0.6 meters in the next 20 years alone. Despite the bleak prognosis and exacerbated flood risks, Frederickstown has been comparatively lucky; there have only been three coastal floods that have managed to over-top the well-designed, though degraded seawall. However, the last of which, occurring in January 2099, caused extensive damage to a critical section of the seawall and managed to inundate 80% of the downtown area, causing significant damage to commercial spaces at ground level.

Some of these businesses were insured for just such an event, as their storefronts were within existing FEMA flood zones. However, other local businesses, whose storefronts were outside the FEMA flood zone and were not insured, went bankrupt as a result. Many of these store fronts remained vacant throughout 2099, as landlords were weary of fronting the costs for renovating affected commercial spaces. The business community, recognizing the need for adaptation, lobbies the city of Frederickstown for improved flood protection. The local municipality faces a difficult decision: invest in a new seawall, the funds for which

they do not have readily available or begin the process of a managed retreat. The seawall, and the protection it provided, enticed decades of significant investment downtown, all of which is now at risk.

Wishing to postpone their decision, the local municipality choses to commission a special study to redraw the flood map for downtown, which had not been updated since 2075. The prognosis was not good; under projected sea level conditions in 2120, the entirety of the downtown would be exposed to high tide flooding, even with the wall in place. The seawall had provided the coastal resilience for the time horizon it was designed for to the city, but at a larger time horizon, that is twice its design life, its presence enticed and exposed far more people and assets into greater flood risks than it had originally been designed to protect from. At this longer time scale, its presence could be viewed as maladaptive, as more assets are now placed under more severe flood risks due to its presence and the protection it previously provided.

From this later frame of reference, which considers the Frederickstown community not only from 2020-2070, but several additional generations out (to 2120), the end of the seawall's life cycle is disruptive to the business community, and the greater Frederickstown community, as illustrated through the lens of panarchy in Figure 54.

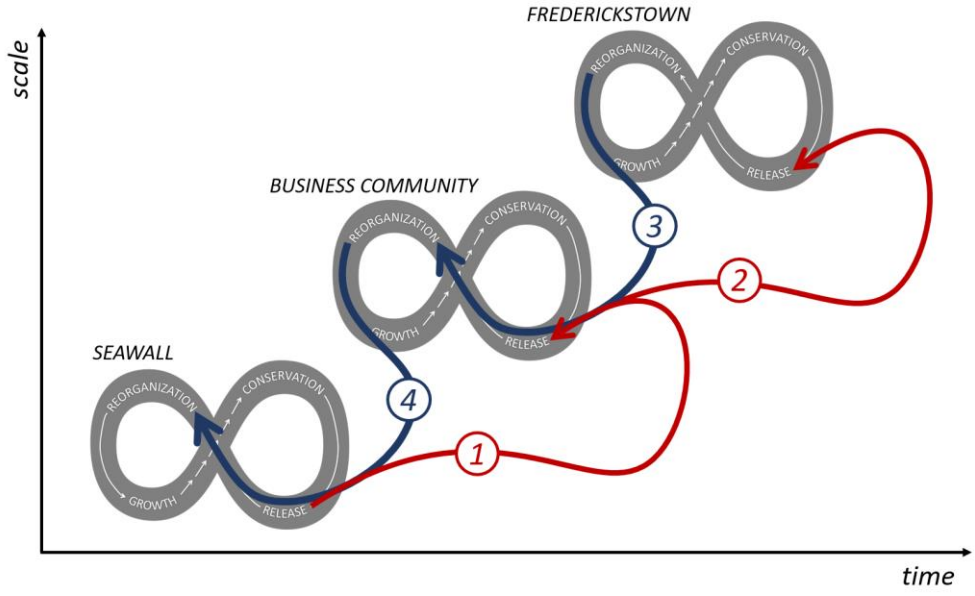

Figure 54: A panarchic representation of the relationship between the nested adaptive cycles described in the Frederickstown example.

In their effort to conserve the existence of a vibrant Frederickstown, in 2020 the community, considering a 50-year planning horizon, reorganized its priorities and targeted growth of the business community downtown (transition 1). At the same time, to ensure later conservation of the business community, they planned a grey infrastructure adaptation project: the seawall (transition 2). Within its design life, the seawall served its purpose, lowering flood risk and improving the coastal resilience of the community.

However, as its life cycle was completed (i.e. after the original planning horizon), its ineffectiveness and failure undermined the conservation of the Frederickstown community. The deterioration of the seawall and the resulting damage to the business community (transition 3) forced businesses into bankruptcy and stalled investment (transition 4), which in turn prompted a release of capital from downtown Frederickstown.

At this critical juncture, Frederickstown can choose to synthesize policy for a managed retreat, which would shift the capital of the business community elsewhere (transition 1) thereby allowing the city to divest from the seawall entirely (transition 2). Alternatively, the Frederickstown community could choose to adapt to the rising seas, prompting businesses to remain downtown (transition 1) and contribute to the planning process for a new seawall (transition 2), thereby informing the reorganization (and also partially funding) of the seawall. Through the lens of panarchy, the case study of Frederickstown[6] highlights the importance of proper asset management and adaptation planning across scales.

[6] While Frederickstown is purely fictional, upon reflection, its situation bears a striking resemblance to a number of coastal cities in the US, most notably Charleston, SC.

Appendix B: MBTA Rapid Transit System Resilience Assessment Model Outputs

+0 m SLR (2013): 1 year Return Period

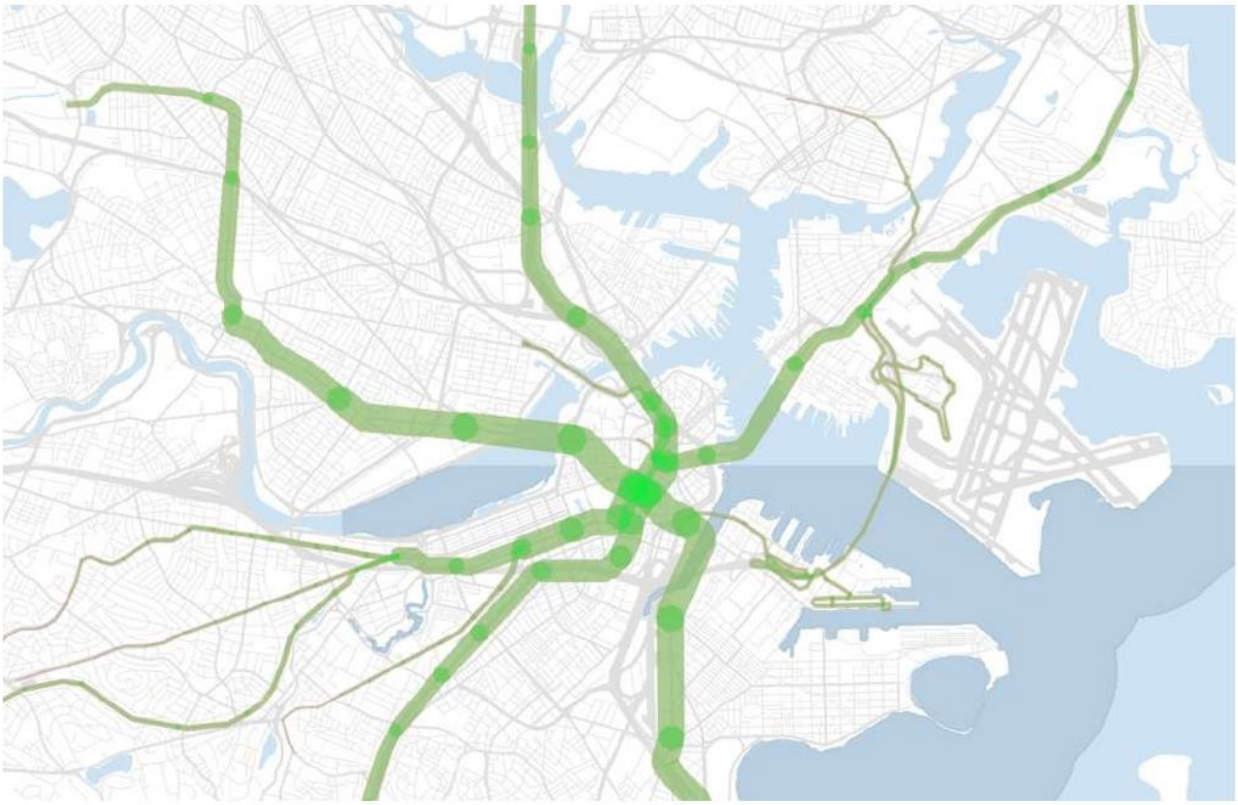

In this scenario, system resilience = 100%.

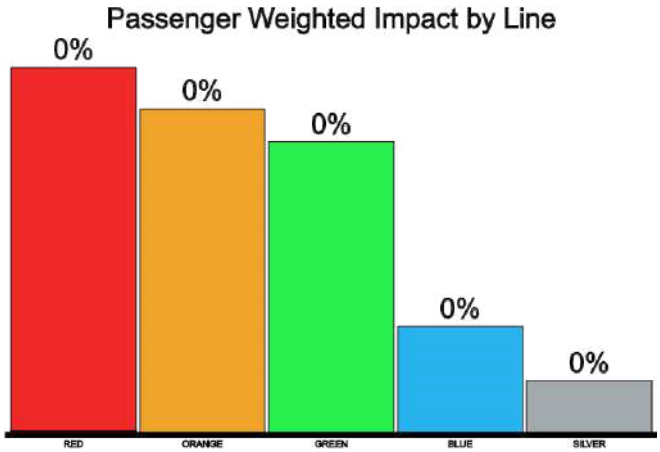

This analysis was performed using CRaVAT transit. The systemwide impacts shown assume that a large volume of water enters the rapid transit system at the relevant lowest critical elevations within the bounds of the coastal flood extents shown. Removal of links is determined by average track elevations, locations of track switches, and train/bus dispatch locations. The analysis assumes no flood mitigation efforts are undertaken and therefore represents a worst-case systemwide impact.

Vulnerable Locations For Selected Coastal Flood Scenario

None

This analysis was performed using CRaVAT transit. The systemwide impacts shown assume that a large volume of water enters the rapid transit system at the relevant lowest critical elevations within the bounds of the coastal flood extents shown. Removal of links is determined by average track elevations, locations of track switches, and train/bus dispatch locations. The analysis assumes no flood mitigation efforts are undertaken and therefore represents a worst-case systemwide impact.

+0 m SLR (2013): 2 year Return Period

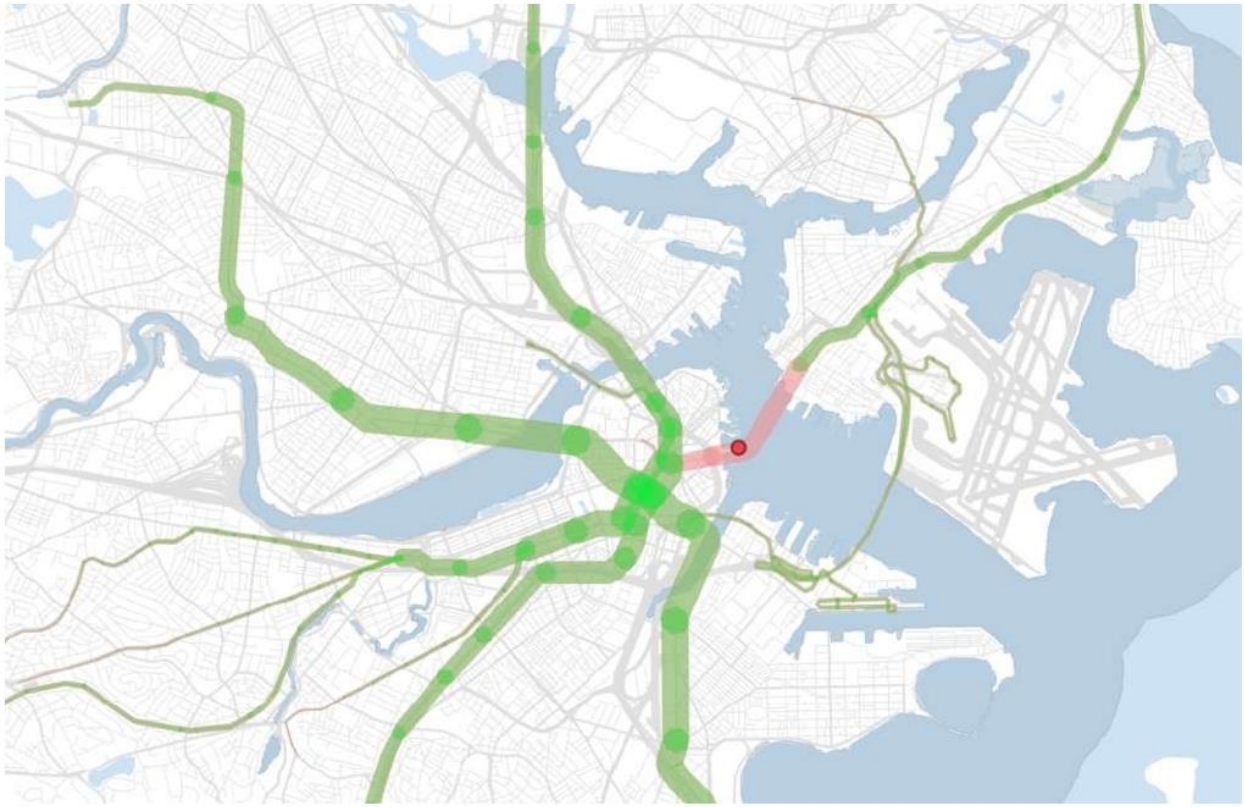

In this scenario, system resilience = 94%.

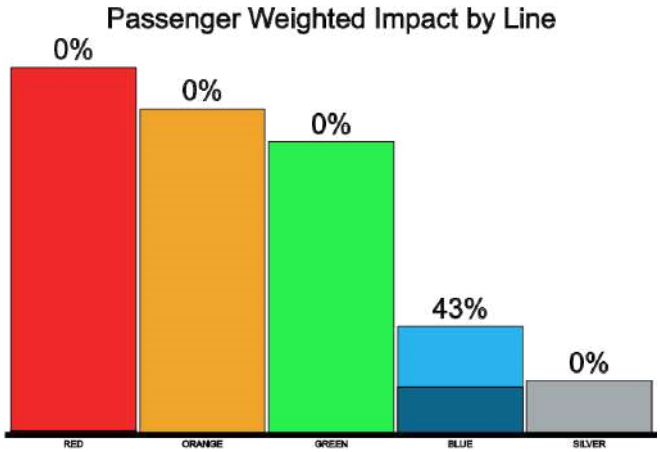

This analysis was performed using CRaVAT transit. The systemwide impacts shown assume that a large volume of water enters the rapid transit system at the relevant lowest critical elevations within the bounds of the coastal flood extents shown. Removal of links is determined by average track elevations, locations of track switches, and train/bus dispatch locations. The analysis assumes no flood mitigation efforts are undertaken and therefore represents a worst-case systemwide impact.

Vulnerable Locations For Selected Coastal Flood Scenario

Blue Line – Aquarium Station Emergency Egress

This analysis was performed using CRaVAT transit. The systemwide impacts shown assume that a large volume of water enters the rapid transit system at the relevant lowest critical elevations within the bounds of the coastal flood extents shown. Removal of links is determined by average track elevations, locations of track switches, and train/bus dispatch locations. The analysis assumes no flood mitigation efforts are undertaken and therefore represents a worst-case systemwide impact.

+0 m SLR (2013): 4 year Return Period

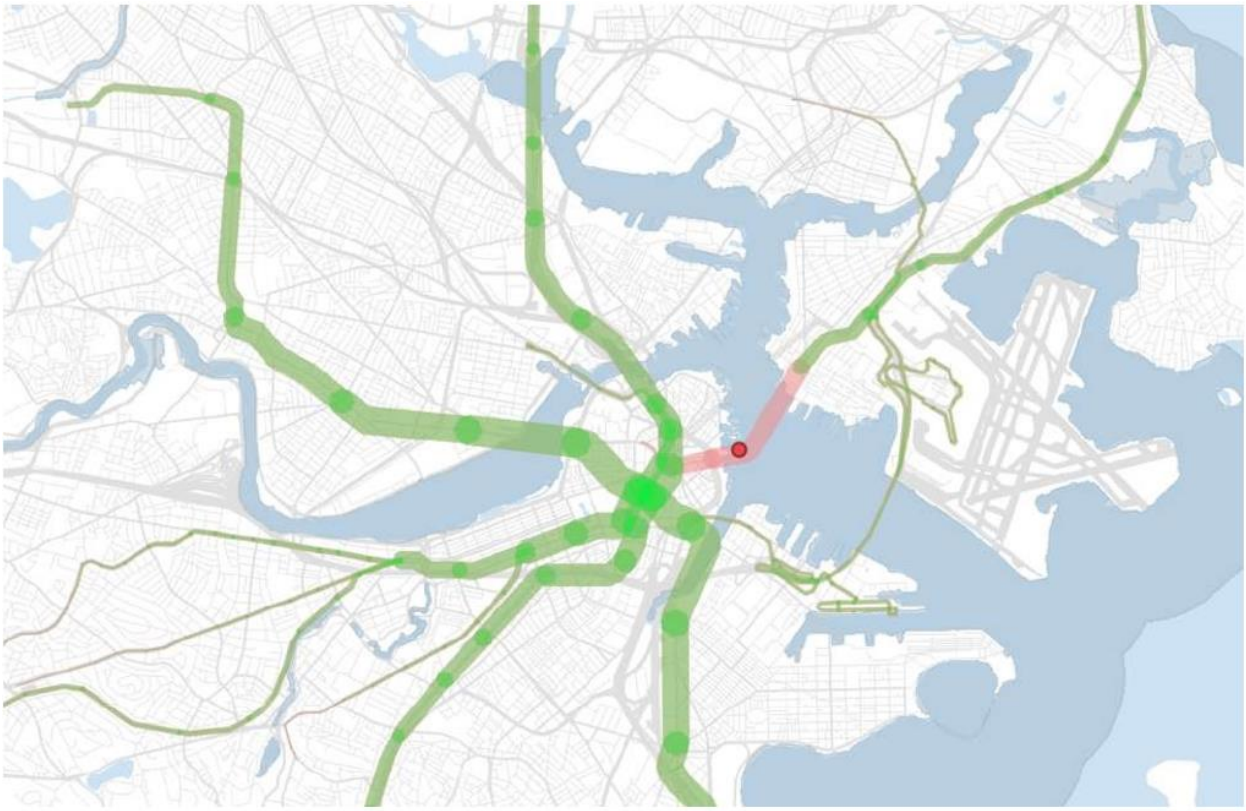

In this scenario, system resilience = 94%.

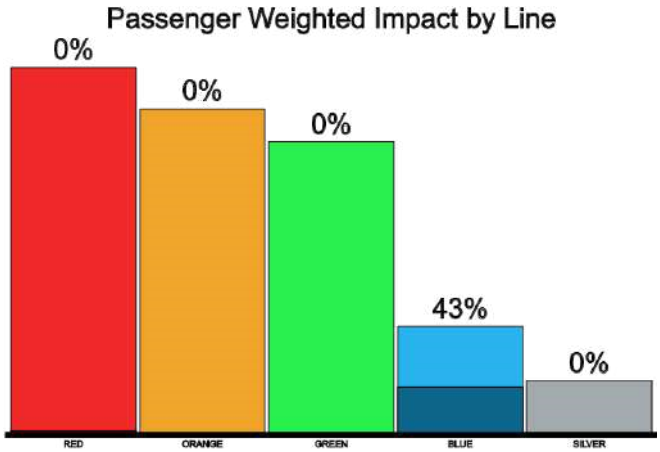

This analysis was performed using CRaVAT transit. The systemwide impacts shown assume that a large volume of water enters the rapid transit system at the relevant lowest critical elevations within the bounds of the coastal flood extents shown. Removal of links is determined by average track elevations, locations of track switches, and train/bus dispatch locations. The analysis assumes no flood mitigation efforts are undertaken and therefore represents a worst-case systemwide impact.

Vulnerable Locations For Selected Coastal Flood Scenario

Blue Line - Aquarium Station Emergency Egress

This analysis was performed using CRaVAT transit. The systemwide impacts shown assume that a large volume of water enters the rapid transit system at the relevant lowest critical elevations within the bounds of the coastal flood extents shown. Removal of links is determined by average track elevations, locations of track switches, and train/bus dispatch locations. The analysis assumes no flood mitigation efforts are undertaken and therefore represents a worst-case systemwide impact.

+0 m SLR (2013): 10 year Return Period

In this scenario, system resilience = 88%.

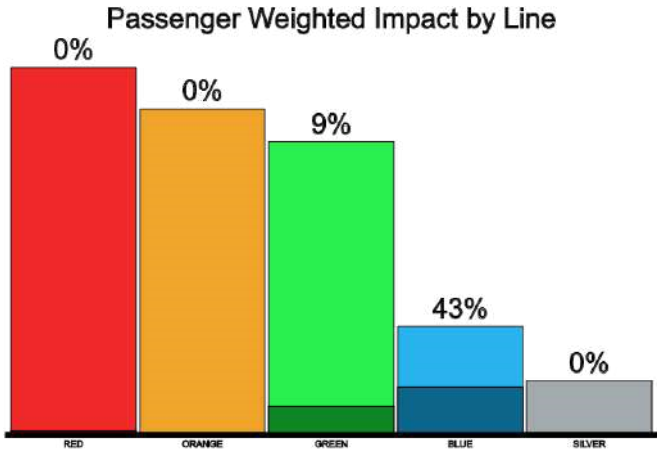

This analysis was performed using CRaVAT transit. The systemwide impacts shown assume that a large volume of water enters the rapid transit system at the relevant lowest critical elevations within the bounds of the coastal flood extents shown. Removal of links is determined by average track elevations, locations of track switches, and train/bus dispatch locations. The analysis assumes no flood mitigation efforts are undertaken and therefore represents a worst-case systemwide impact.

Vulnerable Locations For Selected Coastal Flood Scenario

Blue Line – Aquarium Station Emergency Egress

This analysis was performed using CRaVAT transit. The systemwide impacts shown assume that a large volume of water enters the rapid transit system at the relevant lowest critical elevations within the bounds of the coastal flood extents shown. Removal of links is determined by average track elevations, locations of track switches, and train/bus dispatch locations. The analysis assumes no flood mitigation efforts are undertaken and therefore represents a worst-case systemwide impact.

+0 m SLR (2013): 20 year Return Period

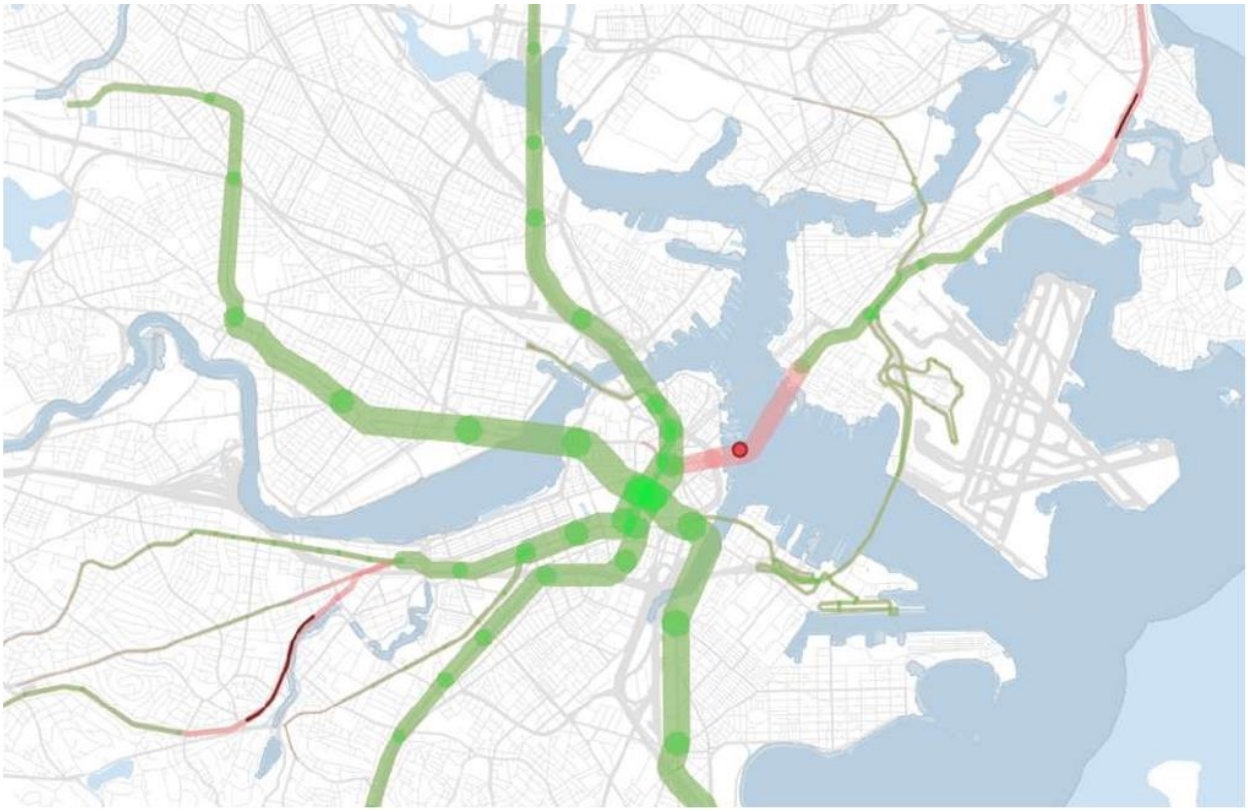

In this scenario, system resilience = 81%.

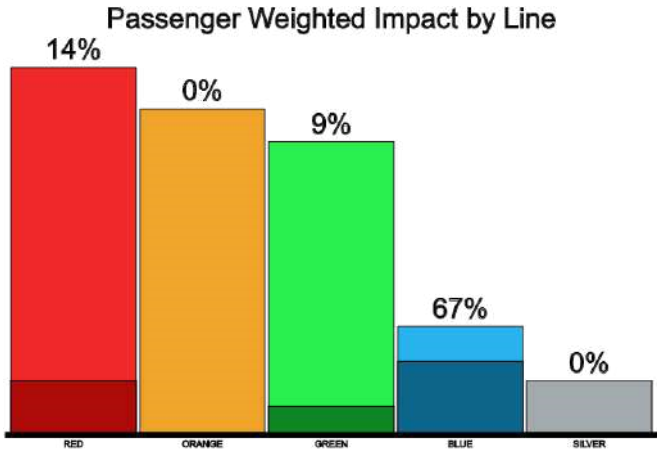

This analysis was performed using CRaVAT transit. The systemwide impacts shown assume that a large volume of water enters the rapid transit system at the relevant lowest critical elevations within the bounds of the coastal flood extents shown. Removal of links is determined by average track elevations, locations of track switches, and train/bus dispatch locations. The analysis assumes no flood mitigation efforts are undertaken and therefore represents a worst-case systemwide impact.

Vulnerable Locations For Selected Coastal Flood Scenario

Red Line - JFK/UMass-North Quincy

Blue Line - Aquarium Station Emergency Egress

Blue Line - Suffolk Downs - Beachmont

This analysis was performed using CRaVAT transit. The systemwide impacts shown assume that a large volume of water enters the rapid transit system at the relevant lowest critical elevations within the bounds of the coastal flood extents shown. Removal of links is determined by average track elevations, locations of track switches, and train/bus dispatch locations. The analysis assumes no flood mitigation efforts are undertaken and therefore represents a worst-case systemwide impact.

+0 m SLR (2013): 50 year Return Period

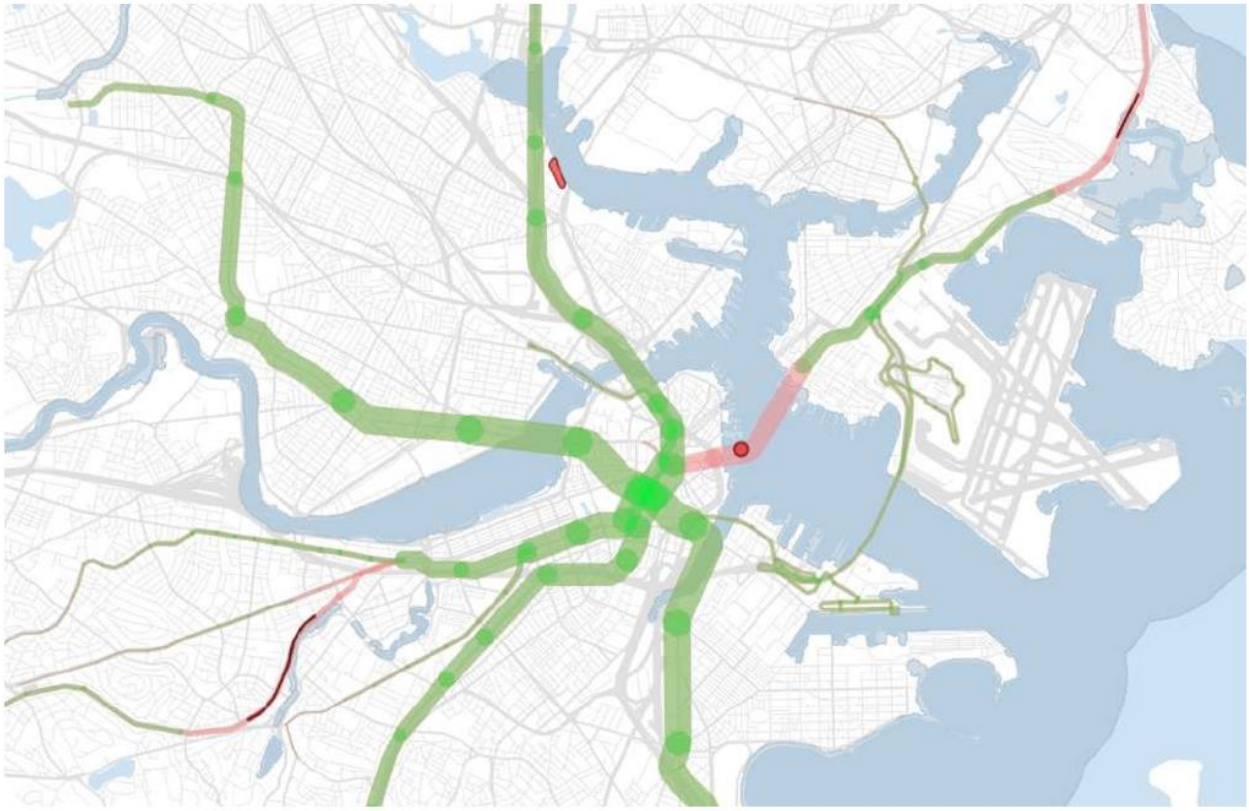

In this scenario, system resilience = 81%.

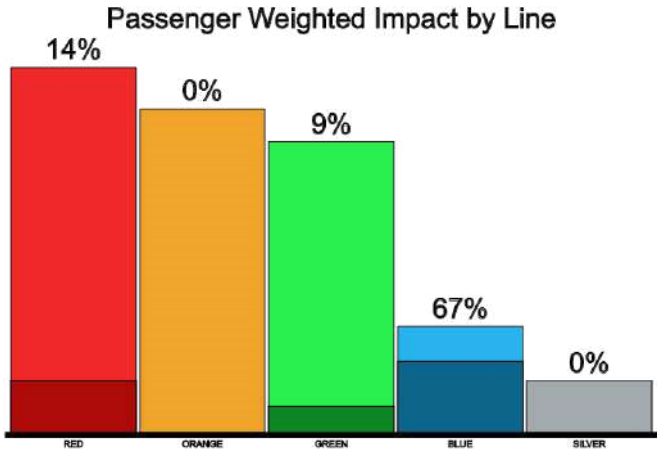

This analysis was performed using CRaVAT transit. The systemwide impacts shown assume that a large volume of water enters the rapid transit system at the relevant lowest critical elevations within the bounds of the coastal flood extents shown. Removal of links is determined by average track elevations, locations of track switches, and train/bus dispatch locations. The analysis assumes no flood mitigation efforts are undertaken and therefore represents a worst-case systemwide impact.

Vulnerable Locations For Selected Coastal Flood Scenario

Red Line - JFK/UMass-North Quincy

Orange Line - Wellington abutment

Blue Line - Aquarium Station Emergency Egress

Blue Line - Suffolk Downs - Beachmont

This analysis was performed using CRaVAT transit. The systemwide impacts shown assume that a large volume of water enters the rapid transit system at the relevant lowest critical elevations within the bounds of the coastal flood extents shown. Removal of links is determined by average track elevations, locations of track switches, and train/bus dispatch locations. The analysis assumes no flood mitigation efforts are undertaken and therefore represents a worst-case systemwide impact.

+0 m SLR (2013): 100 year Return Period

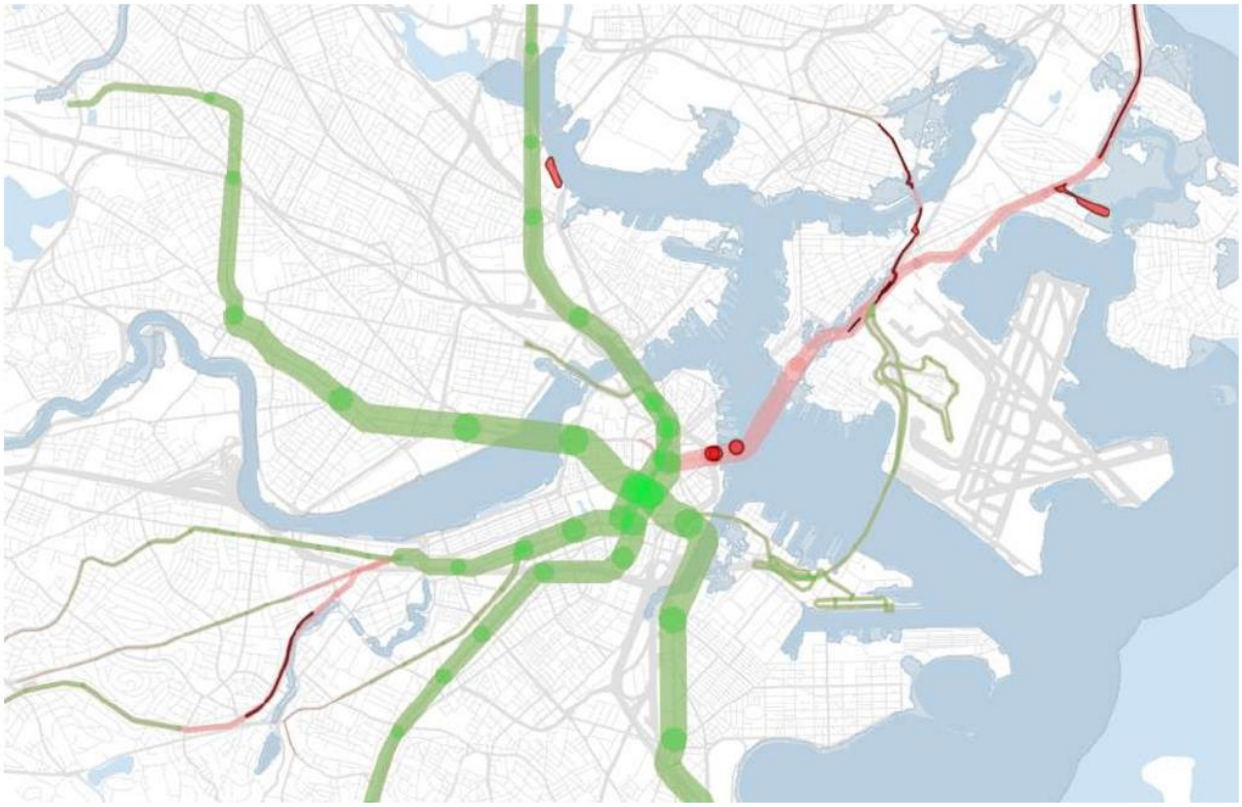

In this scenario, system resilience = 78%.

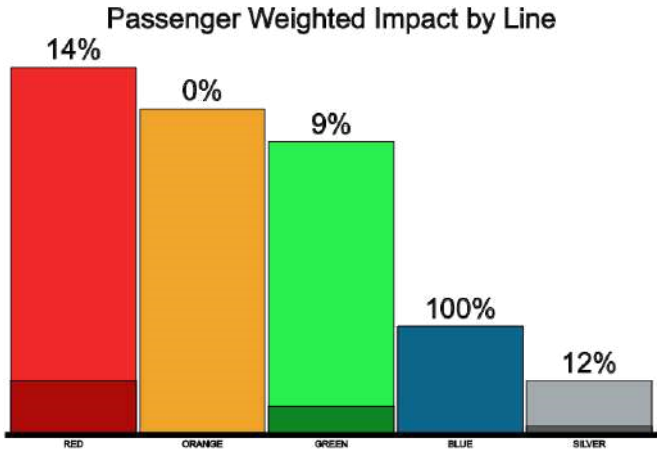

This analysis was performed using CRaVAT transit. The systemwide impacts shown assume that a large volume of water enters the rapid transit system at the relevant lowest critical elevations within the bounds of the coastal flood extents shown. Removal of links is determined by average track elevations, locations of track switches, and train/bus dispatch locations. The analysis assumes no flood mitigation efforts are undertaken and therefore represents a worst-case systemwide impact.

Vulnerable Locations For Selected Coastal Flood Scenario

Red Line - JFK/UMass - North Quincy

Orange Line - Wellington abutment

Blue Line - Aquarium Station Emergency Egress

Blue Line - Aquarium Station

Blue Line - Maverick Portal

Blue Line - Airport Station

Blue Line - Suffolk Downs - Wonderland

Silver Line - Airport - Chelsea

Silver Line - Silver Line Way - Design Center

Green Line - Fenway - Longwood

This analysis was performed using CRaVAT transit. The systemwide impacts shown assume that a large volume of water enters the rapid transit system at the relevant lowest critical elevations within the bounds of the coastal flood extents shown. Removal of links is determined by average track elevations, locations of track switches, and train/bus dispatch locations. The analysis assumes no flood mitigation efforts are undertaken and therefore represents a worst-case systemwide impact.

+0 m SLR (2013): 500 year Return Period

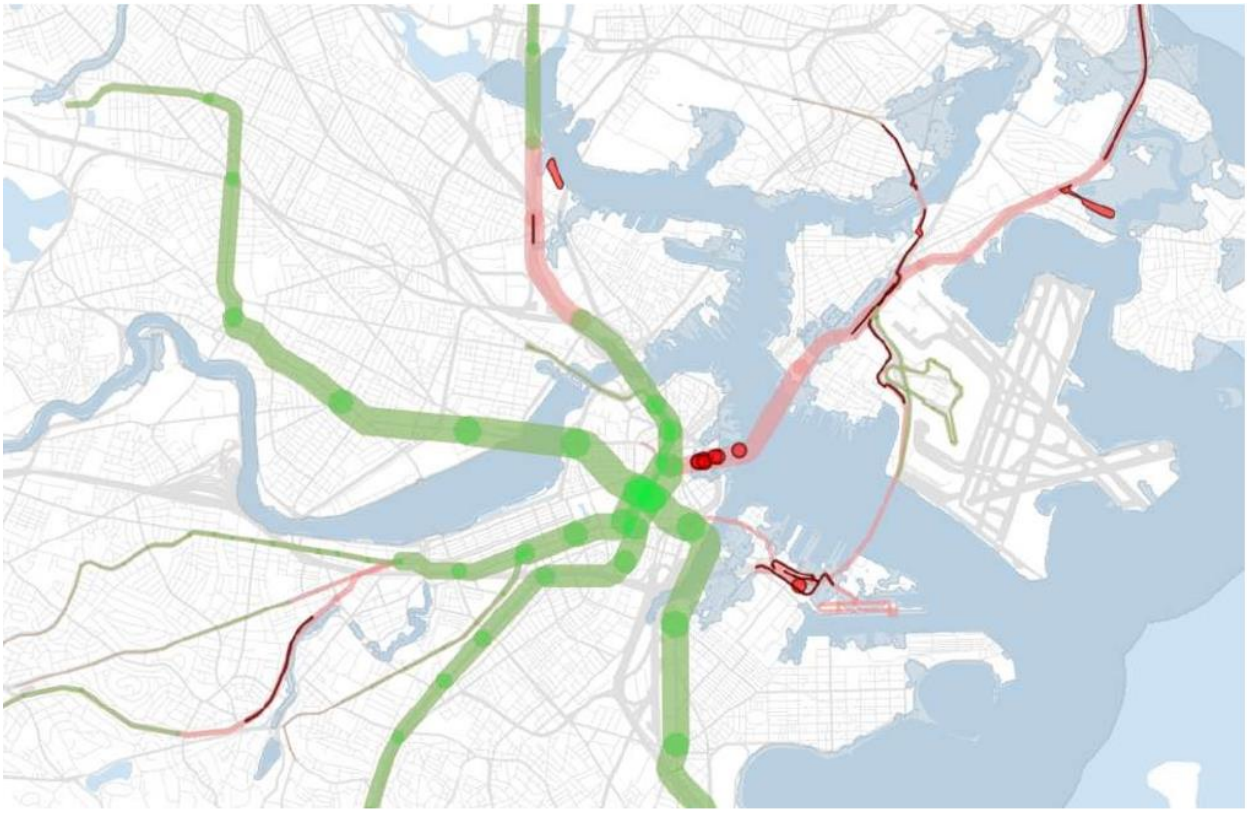

In this scenario, system resilience = 72%.

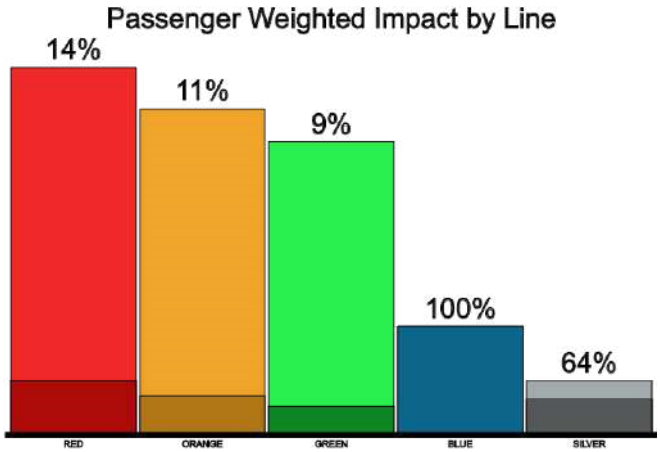

This analysis was performed using CRaVAT transit. The systemwide impacts shown assume that a large volume of water enters the rapid transit system at the relevant lowest critical elevations within the bounds of the coastal flood extents shown. Removal of links is determined by average track elevations, locations of track switches, and train/bus dispatch locations. The analysis assumes no flood mitigation efforts are undertaken and therefore represents a worst-case systemwide impact.

Vulnerable Locations For Selected Coastal Flood Scenario

Red Line - JFK/UMass-North Quincy

Orange Line - Wellington abutment

Blue Line - Aquarium Station Emergency Egress

Blue Line - Aquarium Station

Blue Line - Maverick Portal

Blue Line - Airport Station

Blue Line - Suffolk Downs - Wonderland

Silver Line - Airport - Chelsea

Silver Line - Ted Williams Tunnel

Silver Line - Silver Line Way - Design Center

Green Line - Fenway - Longwood

This analysis was performed using CRaVAT transit. The systemwide impacts shown assume that a large volume of water enters the rapid transit system at the relevant lowest critical elevations within the bounds of the coastal flood extents shown. Removal of links is determined by average track elevations, locations of track switches, and train/bus dispatch locations. The analysis assumes no flood mitigation efforts are undertaken and therefore represents a worst-case systemwide impact.

+0 m SLR (2013): 1,000 year Return Period

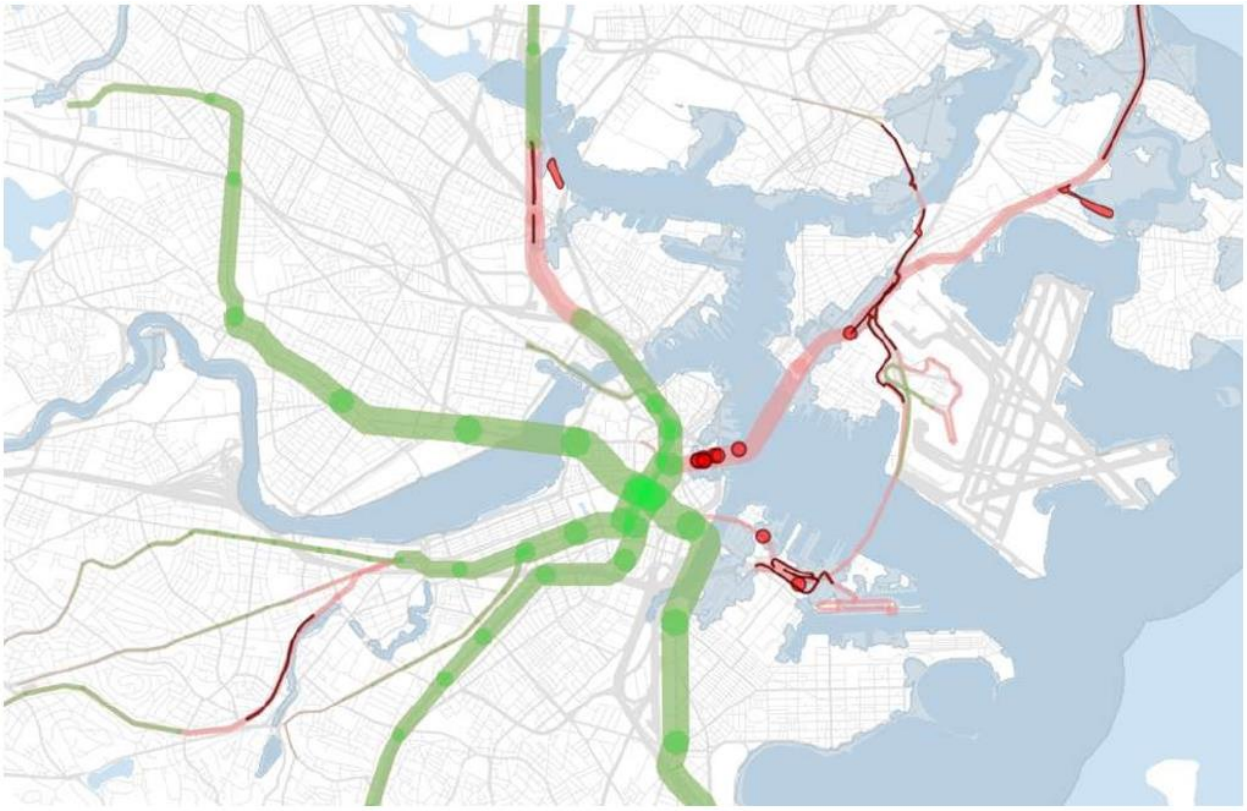

In this scenario, system resilience = 72%.

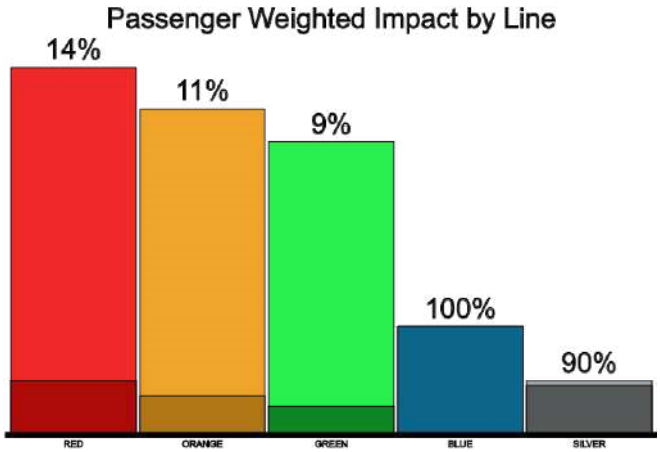

This analysis was performed using CRaVAT transit. The systemwide impacts shown assume that a large volume of water enters the rapid transit system at the relevant lowest critical elevations within the bounds of the coastal flood extents shown. Removal of links is determined by average track elevations, locations of track switches, and train/bus dispatch locations. The analysis assumes no flood mitigation efforts are undertaken and therefore represents a worst-case systemwide impact.

Vulnerable Locations For Selected Coastal Flood Scenario

Red Line - JFK/UMass - North Quincy

Orange Line - Sullivan Square - Community College

Orange Line - Wellington abutment

Blue Line - Aquarium Station Emergency Egress

Blue Line - Aquarium Station

Blue Line - Maverick Portal

Blue Line - Airport Station

Blue Line - Suffolk Downs - Wonderland

Silver Line - Airport - Chelsea

Silver Line - Ted Williams Tunnel

Silver Line - Silver Line Way - Design Center

Silver Line - Courthouse Station

Green Line - Fenway - Longwood

This analysis was performed using CRaVAT transit. The systemwide impacts shown assume that a large volume of water enters the rapid transit system at the relevant lowest critical elevations within the bounds of the coastal flood extents shown. Removal of links is determined by average track elevations, locations of track switches, and train/bus dispatch locations. The analysis assumes no flood mitigation efforts are undertaken and therefore represents a worst-case systemwide impact.

+0.21 m SLR (2030): 1 year Return Period

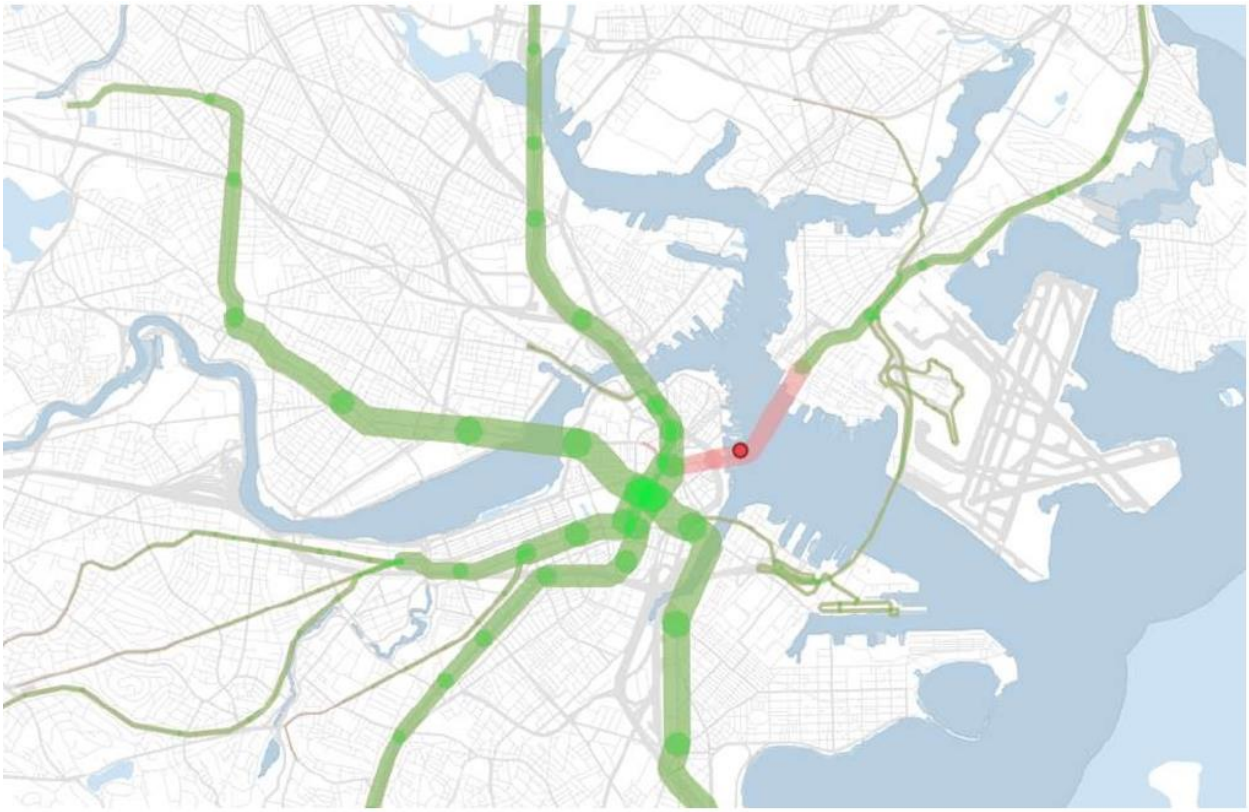

In this scenario, system resilience = 94%.

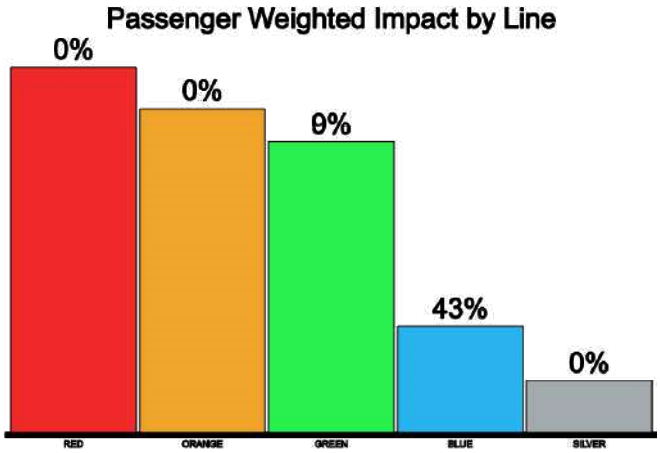

This analysis was performed using CRaVAT transit. The systemwide impacts shown assume that a large volume of water enters the rapid transit system at the relevant lowest critical elevations within the bounds of the coastal flood extents shown. Removal of links is determined by average track elevations, locations of track switches, and train/bus dispatch locations. The analysis assumes no flood mitigation efforts are undertaken and therefore represents a worst-case systemwide impact.

Vulnerable Locations For Selected Coastal Flood Scenario

Blue Line - Aquarium Station Emergency Egress

This analysis was performed using CRaVAT transit. The systemwide impacts shown assume that a large volume of water enters the rapid transit system at the relevant lowest critical elevations within the bounds of the coastal flood extents shown. Removal of links is determined by average track elevations, locations of track switches, and train/bus dispatch locations. The analysis assumes no flood mitigation efforts are undertaken and therefore represents a worst-case systemwide impact.

+0.21 m SLR (2030): 2 year Return Period

In this scenario, system resilience = 88%.

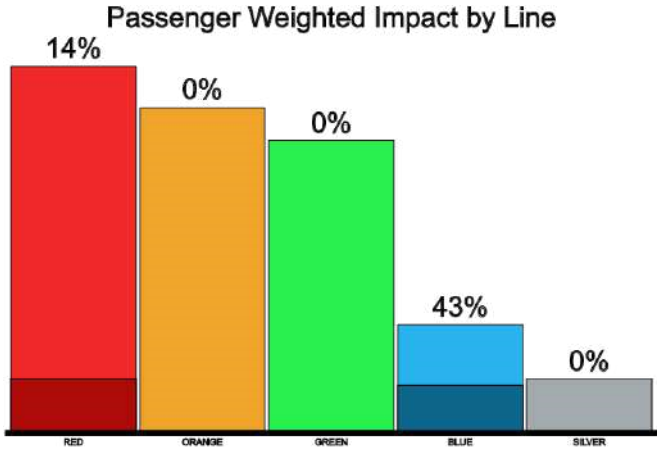

This analysis was performed using CRaVAT transit. The systemwide impacts shown assume that a large volume of water enters the rapid transit system at the relevant lowest critical elevations within the bounds of the coastal flood extents shown. Removal of links is determined by average track elevations, locations of track switches, and train/bus dispatch locations. The analysis assumes no flood mitigation efforts are undertaken and therefore represents a worst-case systemwide impact.

Vulnerable Locations For Selected Coastal Flood Scenario

Orange Line - Wellington abutment

Blue Line - Aquarium Station Emergency Egress

This analysis was performed using CRaVAT transit. The systemwide impacts shown assume that a large volume of water enters the rapid transit system at the relevant lowest critical elevations within the bounds of the coastal flood extents shown. Removal of links is determined by average track elevations, locations of track switches, and train/bus dispatch locations. The analysis assumes no flood mitigation efforts are undertaken and therefore represents a worst-case systemwide impact.

+0.21 m SLR (2030): 4 year Return Period

In this scenario, system resilience = 88%.

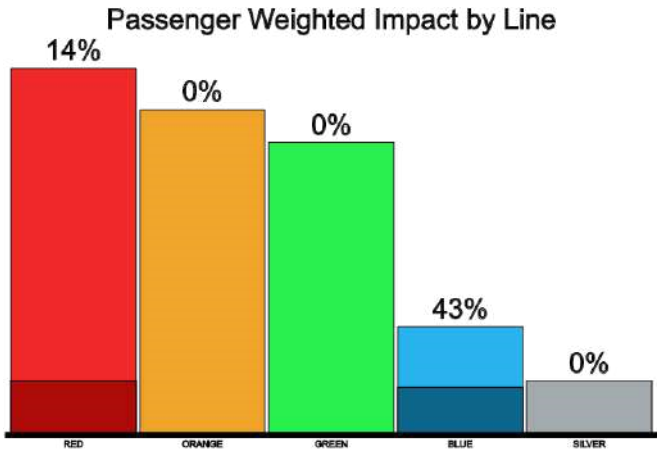

This analysis was performed using CRaVAT transit. The systemwide impacts shown assume that a large volume of water enters the rapid transit system at the relevant lowest critical elevations within the bounds of the coastal flood extents shown. Removal of links is determined by average track elevations, locations of track switches, and train/bus dispatch locations. The analysis assumes no flood mitigation efforts are undertaken and therefore represents a worst-case systemwide impact.

Vulnerable Locations For Selected Coastal Flood Scenario

Red Line - JFK/UMass - North Quincy

Orange Line - Wellington abutment

Blue Line - Aquarium Station Emergency Egress

This analysis was performed using CRaVAT transit. The systemwide impacts shown assume that a large volume of water enters the rapid transit system at the relevant lowest critical elevations within the bounds of the coastal flood extents shown. Removal of links is determined by average track elevations, locations of track switches, and train/bus dispatch locations. The analysis assumes no flood mitigation efforts are undertaken and therefore represents a worst-case systemwide impact.

+0.21 m SLR (2030): 10 year Return Period

In this scenario, system resilience = 81%.

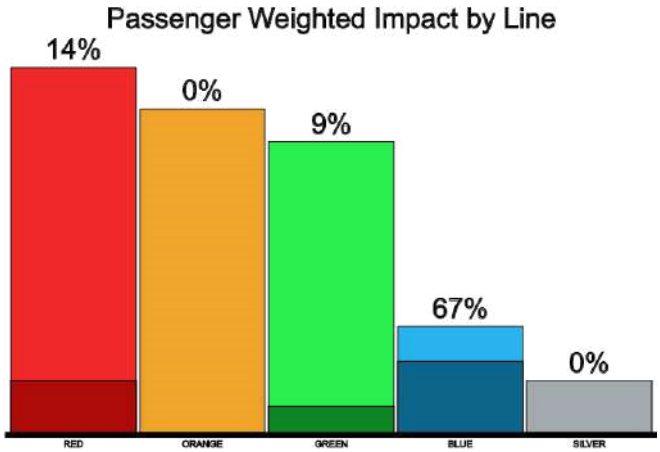

This analysis was performed using CRaVAT transit. The systemwide impacts shown assume that a large volume of water enters the rapid transit system at the relevant lowest critical elevations within the bounds of the coastal flood extents shown. Removal of links is determined by average track elevations, locations of track switches, and train/bus dispatch locations. The analysis assumes no flood mitigation efforts are undertaken and therefore represents a worst-case systemwide impact.

Vulnerable Locations For Selected Coastal Flood Scenario

Red Line – JFK/Umass – North Quincy

Orange Line – Wellington abutment

Blue Line – Aquarium Station Emergency Egress

Blue Line – Aquarium Station

Blue Line – Suffolk Downs – Beachmont

This analysis was performed using CRaVAT transit. The systemwide impacts shown assume that a large volume of water enters the rapid transit system at the relevant lowest critical elevations within the bounds of the coastal flood extents shown. Removal of links is determined by average track elevations, locations of track switches, and train/bus dispatch locations. The analysis assumes no flood mitigation efforts are undertaken and therefore represents a worst-case systemwide impact.

+0.21 m SLR (2030): 20 year Return Period

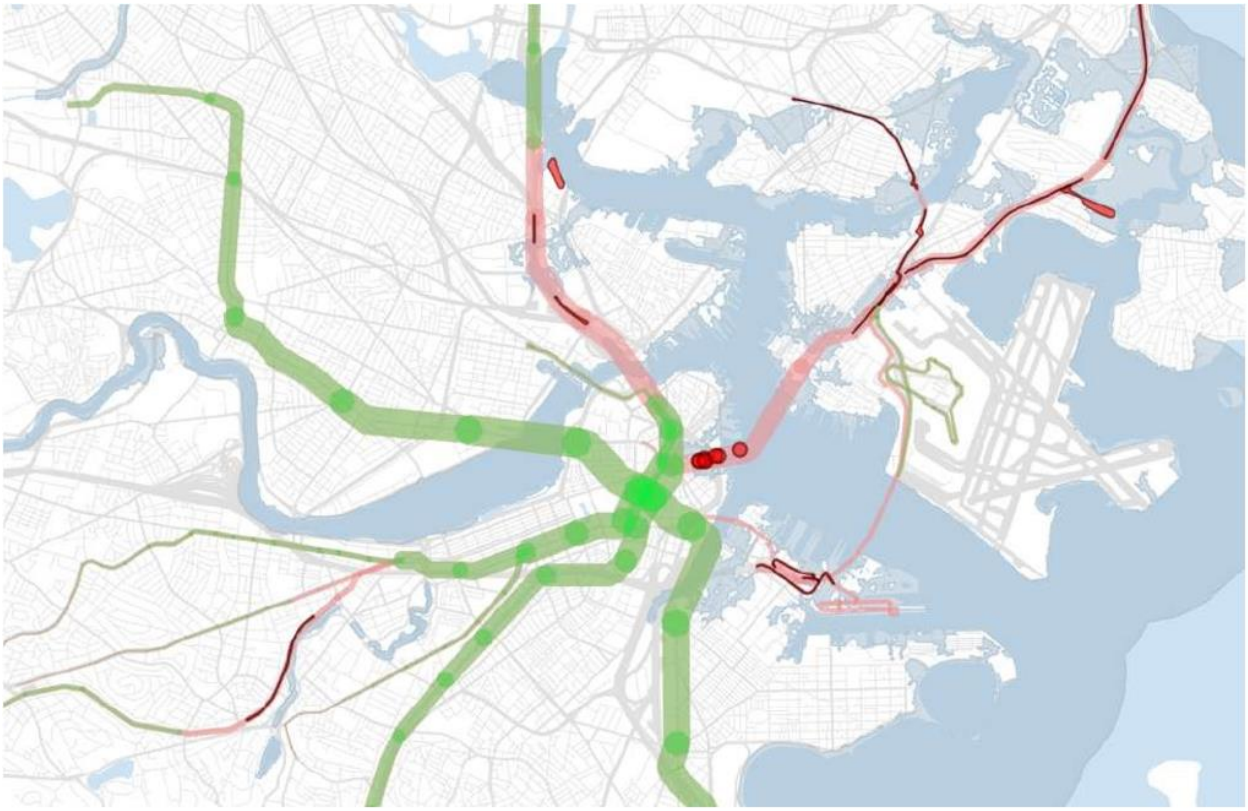

In this scenario, system resilience = 72%.

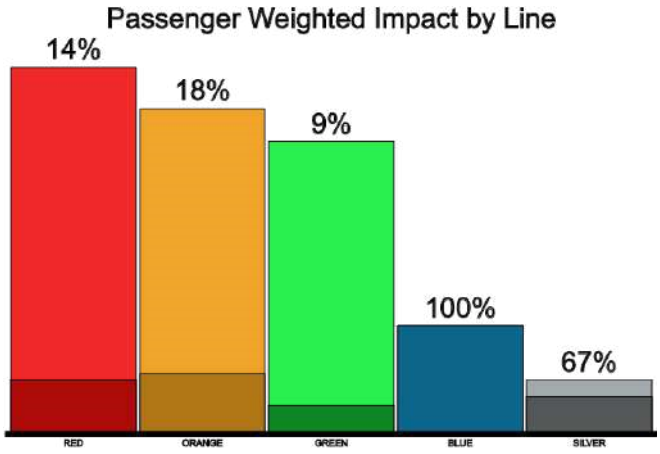

This analysis was performed using CRaVAT transit. The systemwide impacts shown assume that a large volume of water enters the rapid transit system at the relevant lowest critical elevations within the bounds of the coastal flood extents shown. Removal of links is determined by average track elevations, locations of track switches, and train/bus dispatch locations. The analysis assumes no flood mitigation efforts are undertaken and therefore represents a worst-case systemwide impact.

Vulnerable Locations For Selected Coastal Flood Scenario

Red Line – JFK/Umass – North Quincy

Orange Line – Wellington abutment

Blue Line – Aquarium Station Emergency Egress

Blue Line – Aquarium Station

Blue Line – Maverick Portal

Blue Line – Airport Station

Blue Line – Suffolk Downs – Wonderland

Silver Line – Airport – Chelsea

Silver Line – Silver Line Way – Design Center

Green Line – Fenway – Longwood

This analysis was performed using CRaVAT transit. The systemwide impacts shown assume that a large volume of water enters the rapid transit system at the relevant lowest critical elevations within the bounds of the coastal flood extents shown. Removal of links is determined by average track elevations, locations of track switches, and train/bus dispatch locations. The analysis assumes no flood mitigation efforts are undertaken and therefore represents a worst-case systemwide impact.

+0.21 m SLR (2030): 50 year Return Period

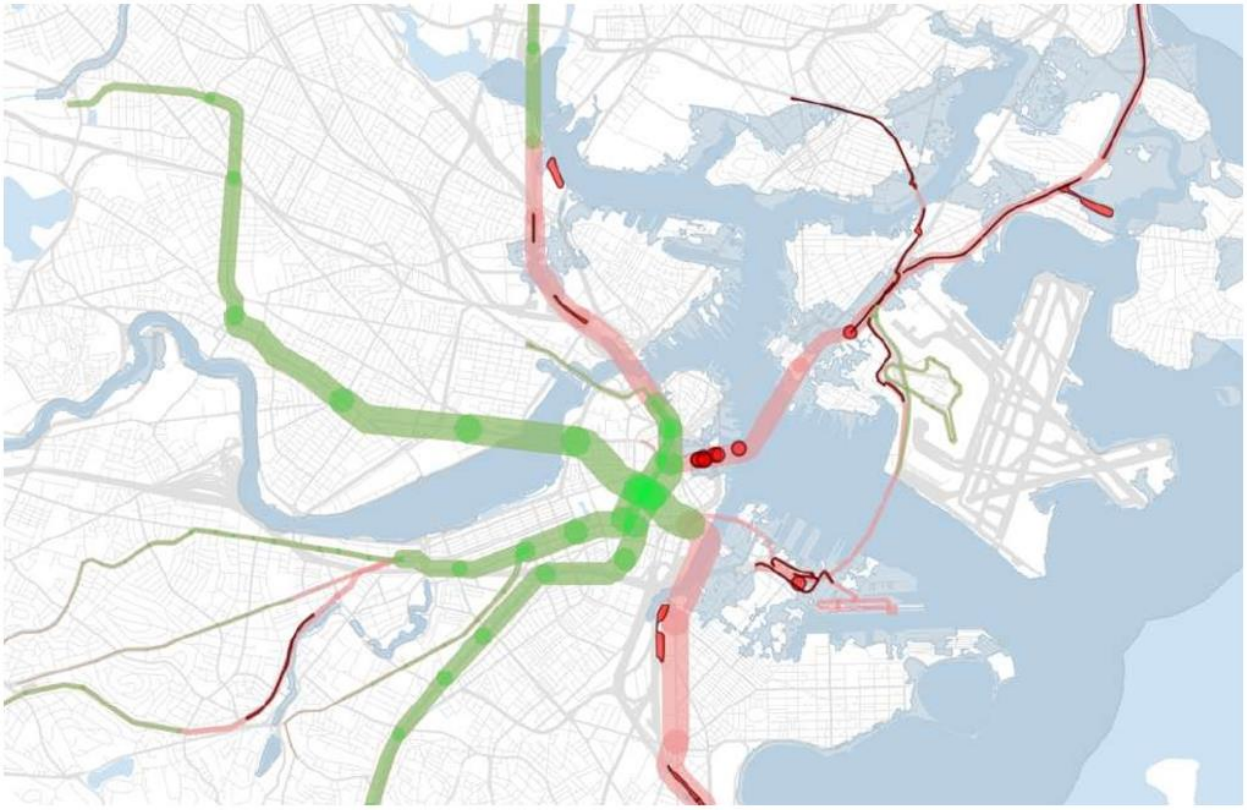

In this scenario, system resilience = 69%.

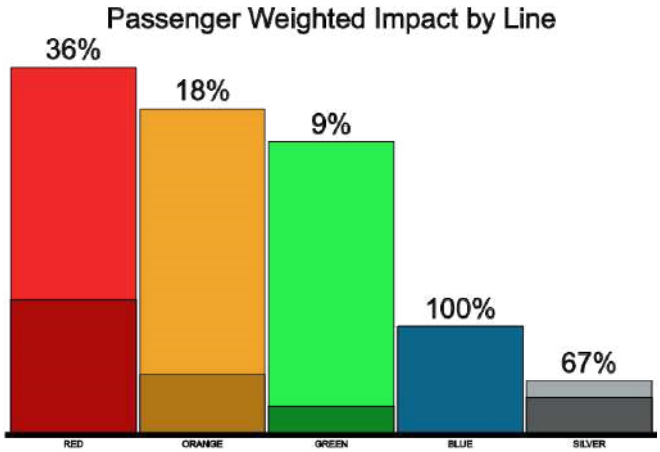

This analysis was performed using CRaVAT transit. The systemwide impacts shown assume that a large volume of water enters the rapid transit system at the relevant lowest critical elevations within the bounds of the coastal flood extents shown. Removal of links is determined by average track elevations, locations of track switches, and train/bus dispatch locations. The analysis assumes no flood mitigation efforts are undertaken and therefore represents a worst-case systemwide impact.

Vulnerable Locations For Selected Coastal Flood Scenario

Red Line – JFK/Umass Station

Red Line – JFK/Umass – North Quincy

Red Line – Cabot Yard

Orange Line – Sullivan Square

Orange Line – Community College Portal

Orange Line – Wellington abutment

Blue Line – Aquarium Station Emergency Egress

Blue Line – Aquarium Station

Blue Line – Maverick Portal

Blue Line – Orient Heights

Blue Line – Airport Station

Blue Line – Suffolk Downs – Wonderland

Silver Line – Airport – Chelsea

Silver Line – Ted Williams Tunnel

Silver Line – Silver Line Way – Design Center

Green Line – Fenway – Longwood

This analysis was performed using CRaVAT transit. The systemwide impacts shown assume that a large volume of water enters the rapid transit system at the relevant lowest critical elevations within the bounds of the coastal flood extents shown. Removal of links is determined by average track elevations, locations of track switches, and train/bus dispatch locations. The analysis assumes no flood mitigation efforts are undertaken and therefore represents a worst-case systemwide impact.

+0.21 m SLR (2030): 100 year Return Period

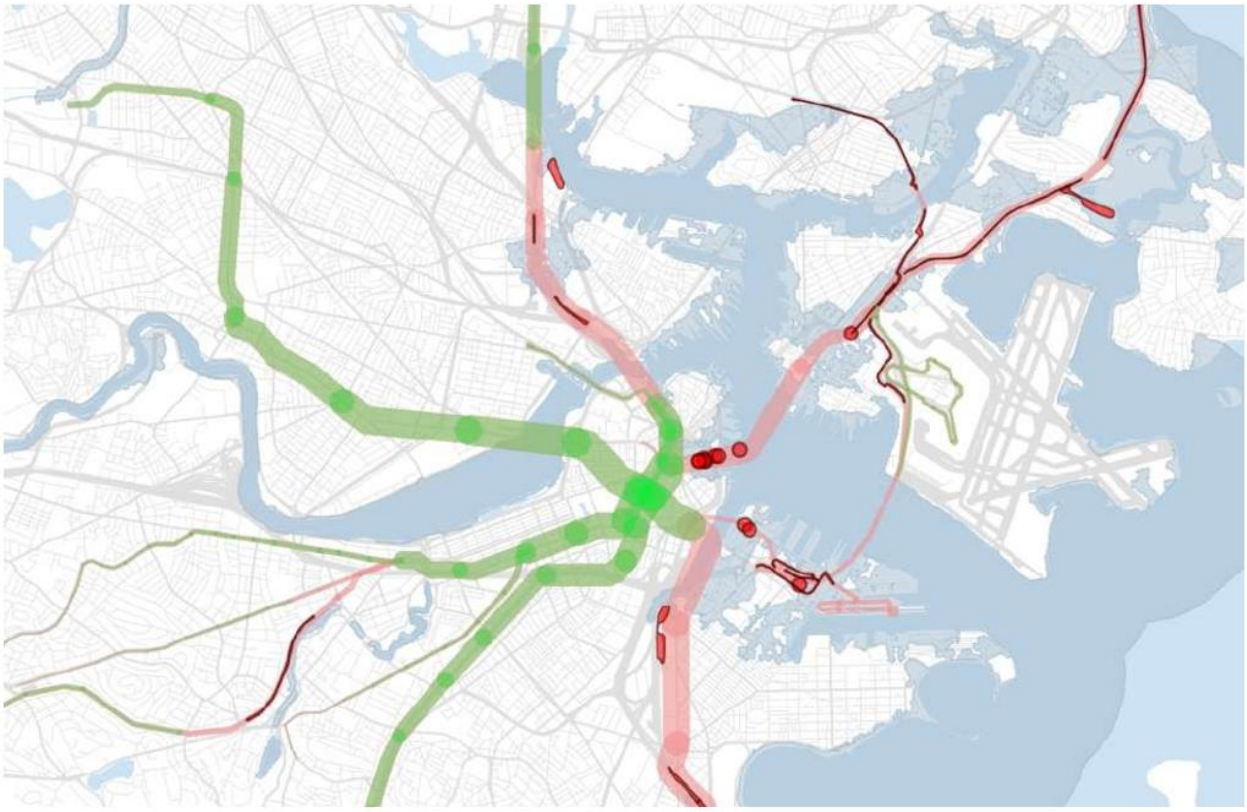

In this scenario, system resilience = 69%.

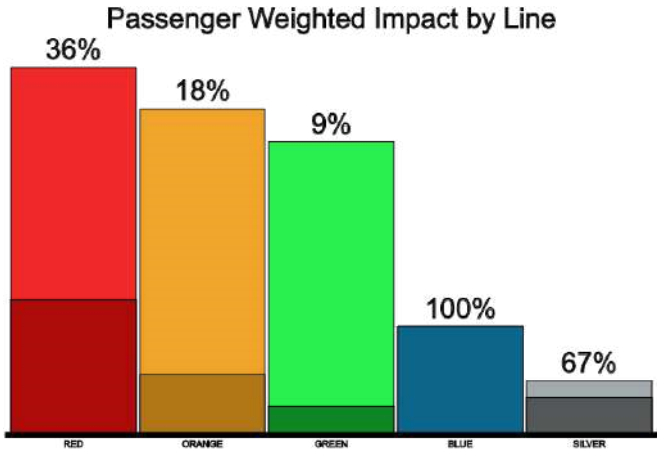

This analysis was performed using CRaVAT transit. The systemwide impacts shown assume that a large volume of water enters the rapid transit system at the relevant lowest critical elevations within the bounds of the coastal flood extents shown. Removal of links is determined by average track elevations, locations of track switches, and train/bus dispatch locations. The analysis assumes no flood mitigation efforts are undertaken and therefore represents a worst-case systemwide impact.

Vulnerable Locations For Selected Coastal Flood Scenario

Red Line - JFK/UMass Station

Red Line - JFK/UMass - North Quincy

Red Line - Cabot Yard

Orange Line - Sullivan Square

Orange Line - Community College Portal

Orange Line - Wellington abutment

Blue Line - Aquarium Station Emergency Egress

Blue Line - Aquarium Station

Blue Line - Maverick Portal

Blue Line - Orient Heights

Blue Line - Airport Station

Blue Line - Suffolk Downs - Wonderland

Silver Line - Courthouse Station

Silver Line - Airport - Chelsea

Silver Line - Ted Williams Tunnel

Silver Line - Silver Line Way - Design Center

Green Line - Fenway - Longwood

This analysis was performed using CRaVAT transit. The systemwide impacts shown assume that a large volume of water enters the rapid transit system at the relevant lowest critical elevations within the bounds of the coastal flood extents shown. Removal of links is determined by average track elevations, locations of track switches, and train/bus dispatch locations. The analysis assumes no flood mitigation efforts are undertaken and therefore represents a worst-case systemwide impact.

+0.21 m SLR (2030): 500 year Return Period

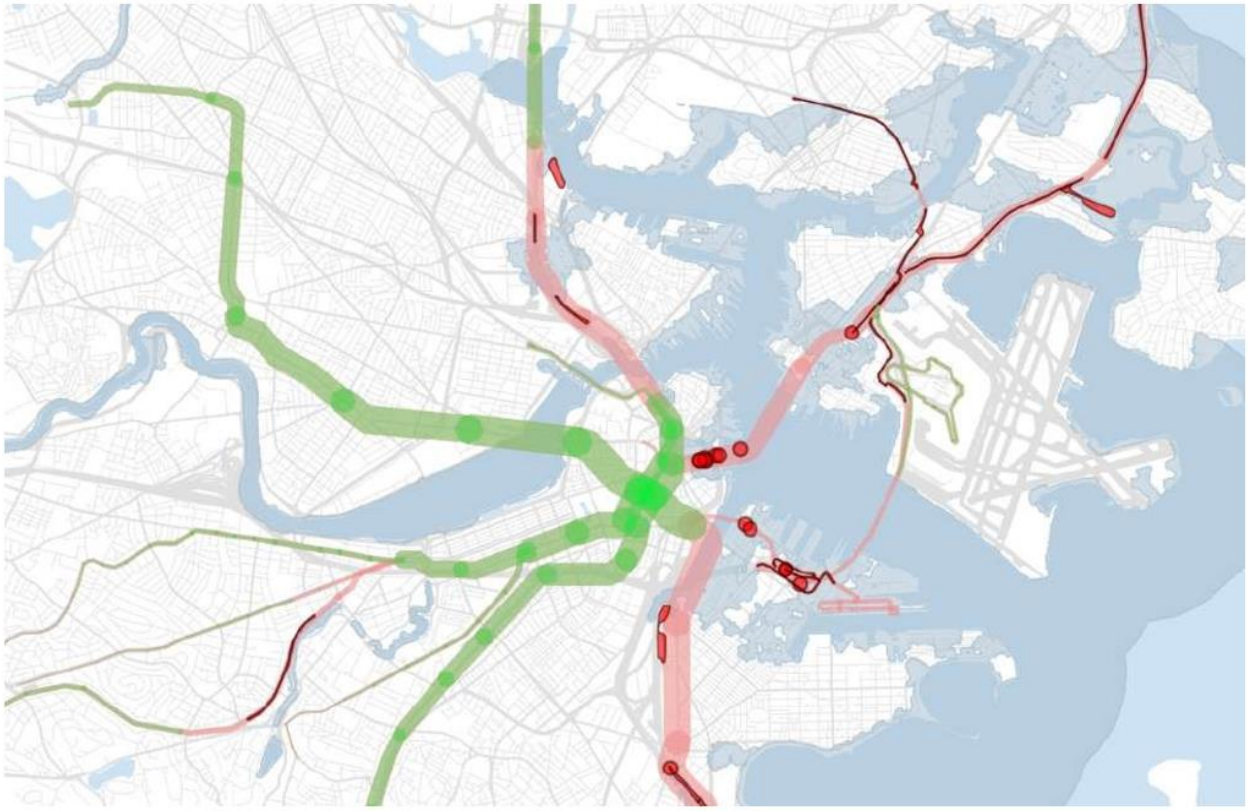

In this scenario, system resilience = 69%.

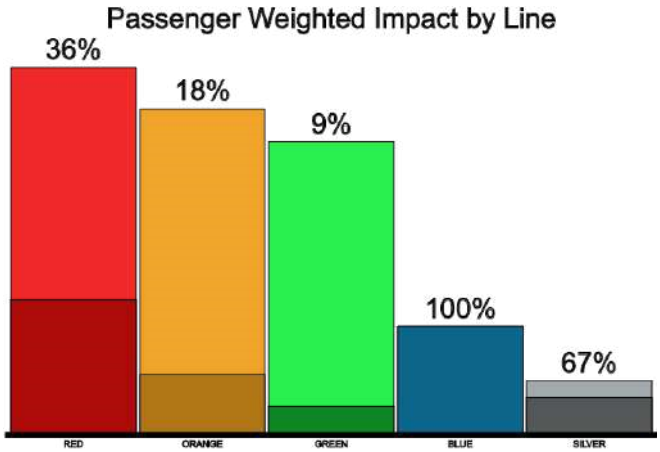

This analysis was performed using CRaVAT transit. The systemwide impacts shown assume that a large volume of water enters the rapid transit system at the relevant lowest critical elevations within the bounds of the coastal flood extents shown. Removal of links is determined by average track elevations, locations of track switches, and train/bus dispatch locations. The analysis assumes no flood mitigation efforts are undertaken and therefore represents a worst-case systemwide impact.

Vulnerable Locations For Selected Coastal Flood Scenario

Red Line - JFK/UMass - Andrew

Red Line - JFK/UMass Station

Red Line - JFK/UMass - North Quincy

Red Line - Cabot Yard

Orange Line - Sullivan Square - Community College

Orange Line - Community College Portal

Orange Line - Wellington abutment

Blue Line - Aquarium Station Emergency Egress

Blue Line - Aquarium Station

Blue Line - Maverick Portal

Blue Line - Orient Heights

Blue Line - Airport Station

Blue Line - Suffolk Downs - Wonderland

Silver Line - Courthouse Station

Silver Line - Airport - Chelsea

Silver Line - Ted Williams Tunnel

Silver Line - Silver Line Way - Design Center

Green Line - Fenway-Longwood

This analysis was performed using CRaVAT transit. The systemwide impacts shown assume that a large volume of water enters the rapid transit system at the relevant lowest critical elevations within the bounds of the coastal flood extents shown. Removal of links is determined by average track elevations, locations of track switches, and train/bus dispatch locations. The analysis assumes no flood mitigation efforts are undertaken and therefore represents a worst-case systemwide impact.

+0.21 m SLR (2030): 1,000 year Return Period

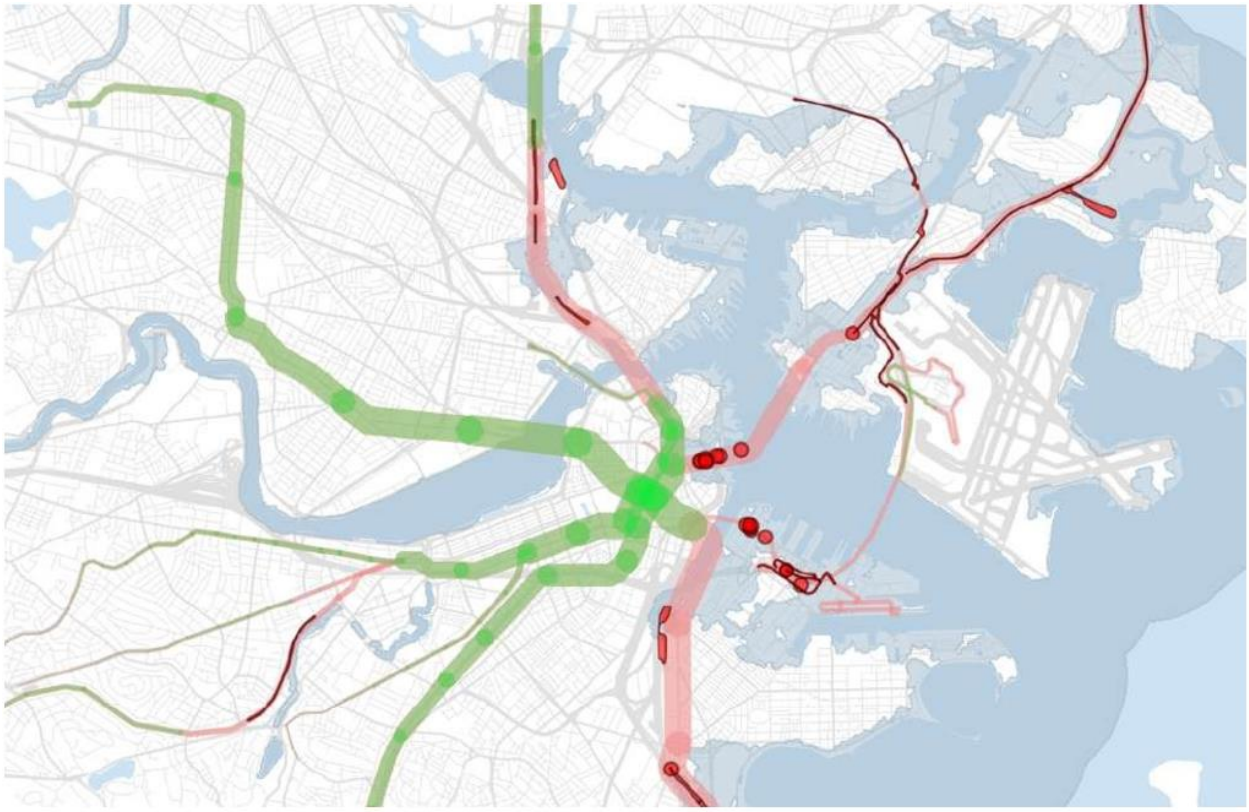

In this scenario, system resilience = 68%.

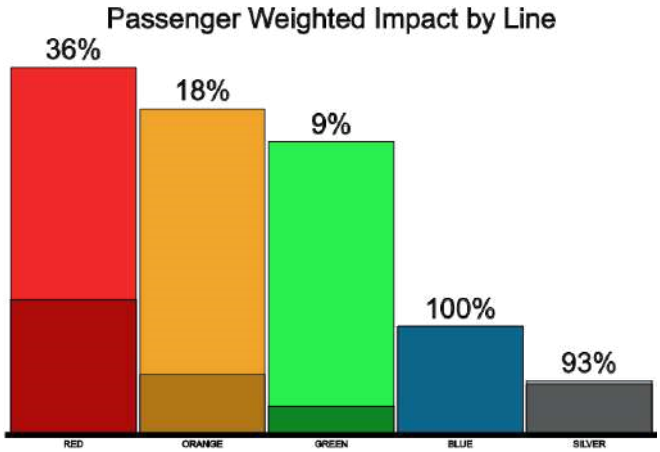

This analysis was performed using CRaVAT transit. The systemwide impacts shown assume that a large volume of water enters the rapid transit system at the relevant lowest critical elevations within the bounds of the coastal flood extents shown. Removal of links is determined by average track elevations, locations of track switches, and train/bus dispatch locations. The analysis assumes no flood mitigation efforts are undertaken and therefore represents a worst-case systemwide impact.

Vulnerable Locations For Selected Coastal Flood Scenario

Red Line - JFK/UMass - Andrew

Red Line - JFK/UMass Station

Red Line - JFK/UMass - North Quincy

Red Line - Cabot Yard

Orange Line - Sullivan Square - Community College

Orange Line - Community College Portal

Orange Line - Wellington abutment

Blue Line - Aquarium Station Emergency Egress

Blue Line - Aquarium Station

Blue Line - Maverick Portal

Blue Line - Orient Heights

Blue Line - Airport Station

Blue Line - Suffolk Downs - Wonderland

Silver Line - Courthouse Station

Silver Line - Airport - Chelsea

Silver Line - Ted Williams Tunnel

Silver Line - Silver Line Way - Design Center

Green Line - Fenway-Longwood

This analysis was performed using CRaVAT transit. The systemwide impacts shown assume that a large volume of water enters the rapid transit system at the relevant lowest critical elevations within the bounds of the coastal flood extents shown. Removal of links is determined by average track elevations, locations of track switches, and train/bus dispatch locations. The analysis assumes no flood mitigation efforts are undertaken and therefore represents a worst-case systemwide impact.

+1.04 m SLR (2070): 1 year Return Period

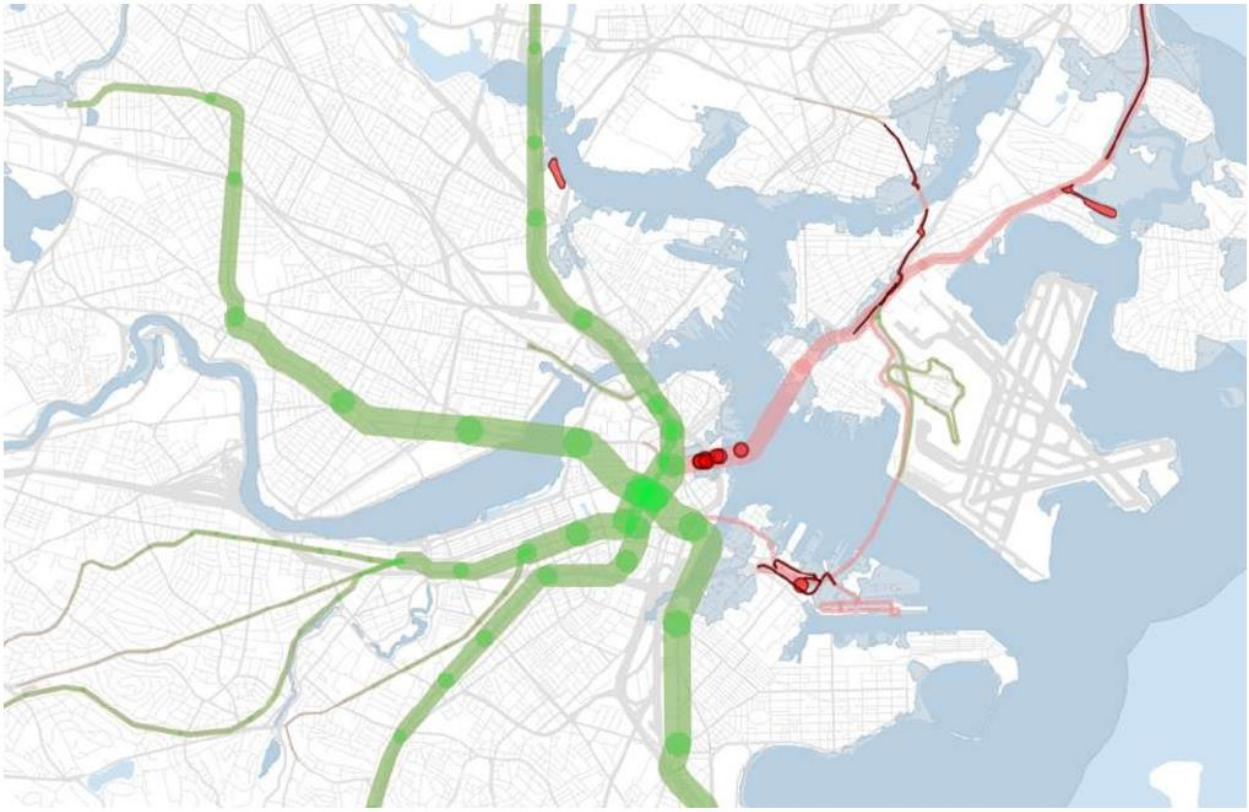

In this scenario, system resilience = 58%.

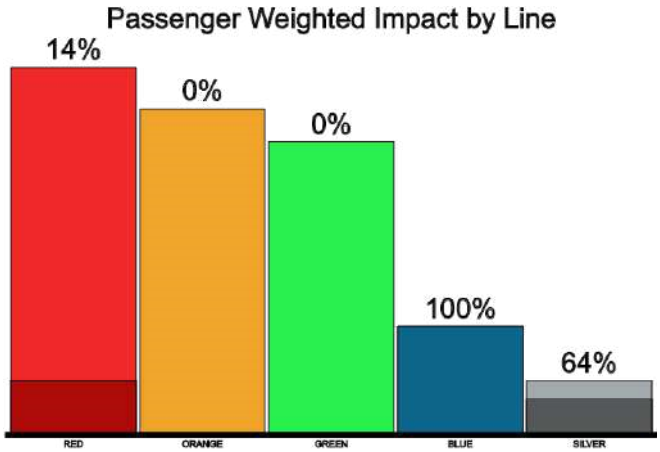

This analysis was performed using CRaVAT transit. The systemwide impacts shown assume that a large volume of water enters the rapid transit system at the relevant lowest critical elevations within the bounds of the coastal flood extents shown. Removal of links is determined by average track elevations, locations of track switches, and train/bus dispatch locations. The analysis assumes no flood mitigation efforts are undertaken and therefore represents a worst-case systemwide impact.

Vulnerable Locations For Selected Coastal Flood Scenario

Orange Line - Wellington abutment

Blue Line - Aquarium Station Emergency Egress

Blue Line - Aquarium Station

Blue Line - Maverick Portal

Blue Line - Airport Station

Blue Line - Suffolk Downs - Wonderland

Silver Line - Airport - Chelsea

Silver Line - Ted Williams Tunnel

Silver Line - Silver Line Way - Design Center

Green Line - Fenway - Longwood

This analysis was performed using CRaVAT transit. The systemwide impacts shown assume that a large volume of water enters the rapid transit system at the relevant lowest critical elevations within the bounds of the coastal flood extents shown. Removal of links is determined by average track elevations, locations of track switches, and train/bus dispatch locations. The analysis assumes no flood mitigation efforts are undertaken and therefore represents a worst-case systemwide impact.

+1.04 m SLR (2070): 2 year Return Period

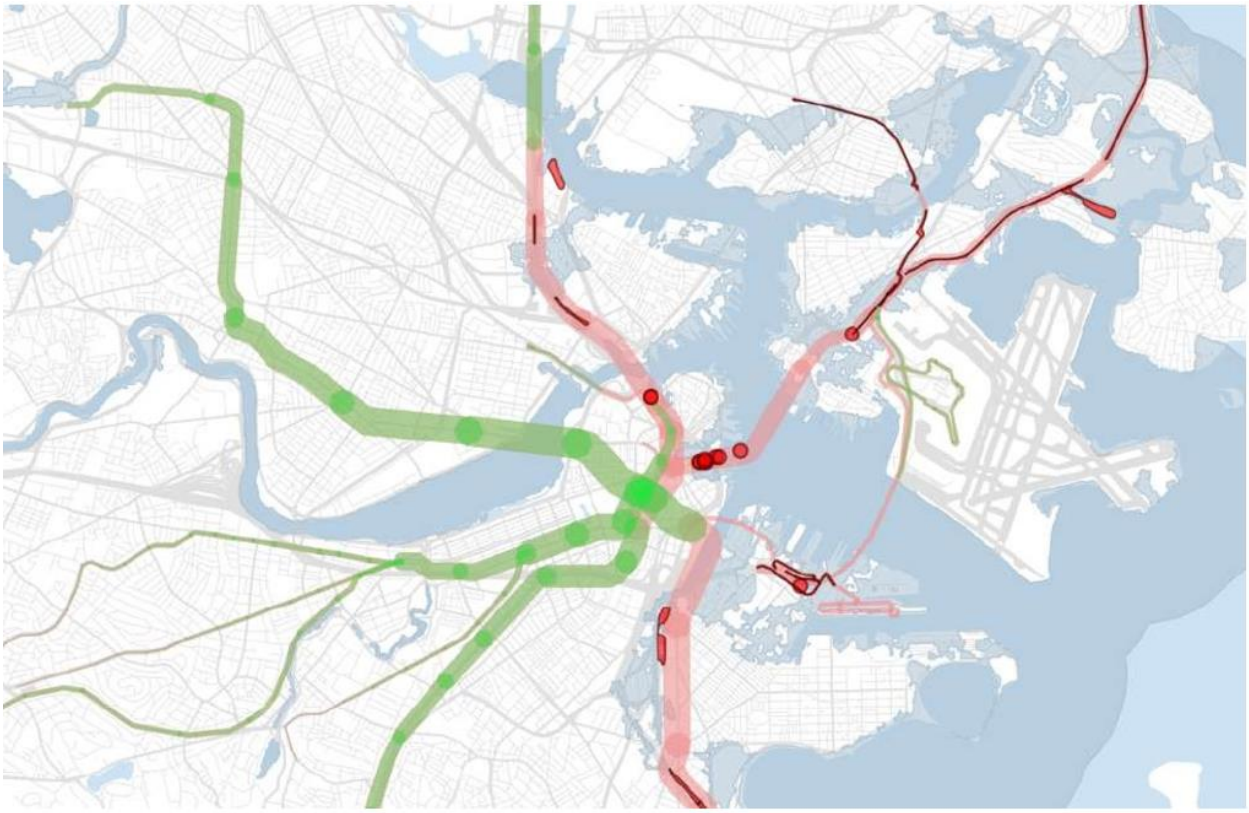

In this scenario, system resilience = 45%.

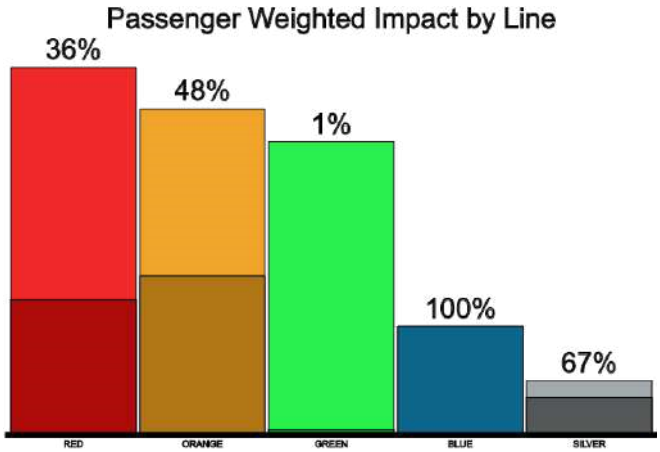

This analysis was performed using CRaVAT transit. The systemwide impacts shown assume that a large volume of water enters the rapid transit system at the relevant lowest critical elevations within the bounds of the coastal flood extents shown. Removal of links is determined by average track elevations, locations of track switches, and train/bus dispatch locations. The analysis assumes no flood mitigation efforts are undertaken and therefore represents a worst-case systemwide impact.

Vulnerable Locations For Selected Coastal Flood Scenario

Red Line - JFK/UMass - Andrew

Red Line - JFK/UMass Station

Red Line - North Quincy Station

Red Line - JFK/UMass - North Quincy

Red Line - Cabot Yard

Orange Line - Sullivan Square - Community College

Orange Line - Community College Portal

Orange Line - North Station

Orange Line - Wellington abutment

Orange Line - Wellington abutment

Blue Line - Aquarium Station Emergency Egress

Blue Line - Aquarium Station

Blue Line - Oreint Heights

Blue Line - Maverick Portal

Blue Line - Airport Station

Blue Line - Maverick - Wonderland

Silver Line - Airport - Chelsea

Silver Line - Ted Williams Tunnel

Silver Line - Silver Line Way - Design Center

Green Line - North Station

Green Line - Fenway - Longwood

This analysis was performed using CRaVAT transit. The systemwide impacts shown assume that a large volume of water enters the rapid transit system at the relevant lowest critical elevations within the bounds of the coastal flood extents shown. Removal of links is determined by average track elevations, locations of track switches, and train/bus dispatch locations. The analysis assumes no flood mitigation efforts are undertaken and therefore represents a worst-case systemwide impact.

+1.04 m SLR (2070): 4 year Return Period

In this scenario, system resilience = 45%.

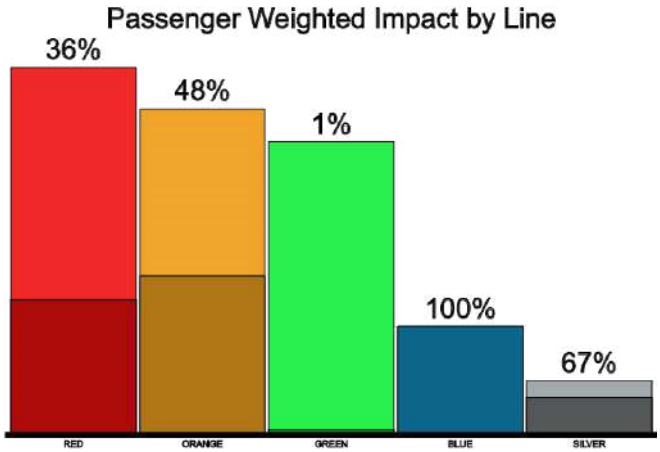

This analysis was performed using CRaVAT transit. The systemwide impacts shown assume that a large volume of water enters the rapid transit system at the relevant lowest critical elevations within the bounds of the coastal flood extents shown. Removal of links is determined by average track elevations, locations of track switches, and train/bus dispatch locations. The analysis assumes no flood mitigation efforts are undertaken and therefore represents a worst-case systemwide impact.

Vulnerable Locations For Selected Coastal Flood Scenario

Red Line - Andrew Portal

Red Line - JFK/UMass - Andrew

Red Line - JFK/UMass Station

Red Line - North Quincy Station

Red Line - JFK/UMass - North Quincy

Red Line - Cabot Yard

Orange Line - Sullivan Square - Community College

Orange Line - Community College Portal

Orange Line - North Station

Orange Line - Wellington abutment

Orange Line - Wellington abutment

Blue Line - Aquarium Station Emergency Egress

Blue Line - Aquarium Station

Blue Line - Oreint Heights

Blue Line - Maverick Portal

Blue Line - Airport Station

Blue Line - Maverick - Wonderland

Silver Line - Courthouse Station

Silver Line - Airport - Chelsea

Silver Line - Ted Williams Tunnel

Silver Line - Silver Line Way - Design Center

Green Line - North Station

Green Line - Fenway – Longwood

+1.04 m SLR (2070): 10 year Return Period

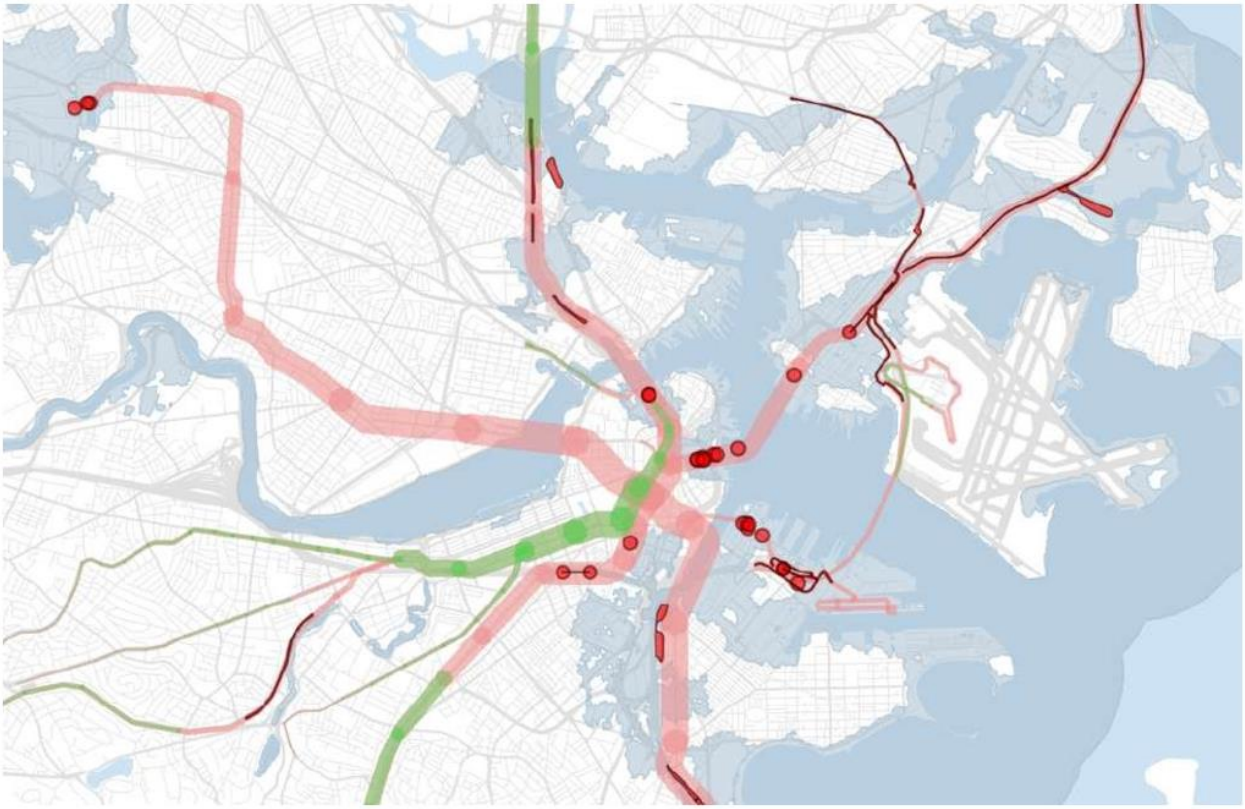

In this scenario, system resilience = 35%.

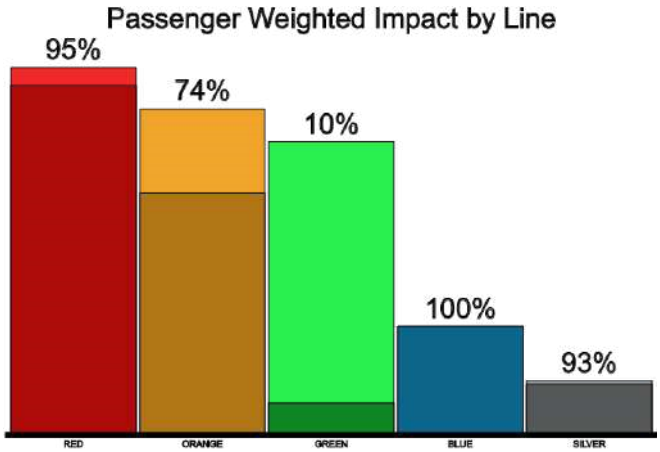

This analysis was performed using CRaVAT transit. The systemwide impacts shown assume that a large volume of water enters the rapid transit system at the relevant lowest critical elevations within the bounds of the coastal flood extents shown. Removal of links is determined by average track elevations, locations of track switches, and train/bus dispatch locations. The analysis assumes no flood mitigation efforts are undertaken and therefore represents a worst-case systemwide impact.

Vulnerable Locations For Selected Coastal Flood Scenario

Red Line - Andrew Portal

Red Line - Alewife Station

Red Line - JFK/UMass - Andrew Red Line - JFK/UMass Station

Red Line - North Quincy Station

Red Line - JFK/UMass - North Quincy

Red Line - Cabot Yard

Orange Line - Tufts-Back Bay Portals

Orange Line - Assembly - Community College

Orange Line - Community College Portal

Orange Line - North Station

Orange Line - Chinatown Station

Orange Line - Wellington abutment

Orange Line - Wellington abutment

Blue Line - Aquarium Station Emergency Egress

Blue Line - Aquarium Station

Blue Line - Oreint Heights

Blue Line - Maverick Portal

Blue Line - Airport Station

Blue Line - Maverick - Wonderland

Silver Line - Courthouse Station

Silver Line - Airport - Chelsea

Silver Line - Ted Williams Tunnel

Silver Line - Silver Line Way - Design Center

Green Line - North Station

Green Line - Fenway – Longwood

This analysis was performed using CRaVAT transit. The systemwide impacts shown assume that a large volume of water enters the rapid transit system at the relevant lowest critical elevations within the bounds of the coastal flood extents shown. Removal of links is determined by average track elevations, locations of track switches, and train/bus dispatch locations. The analysis assumes no flood mitigation efforts are undertaken and therefore represents a worst-case systemwide impact.

+1.04 m SLR (2070): 20 year Return Period

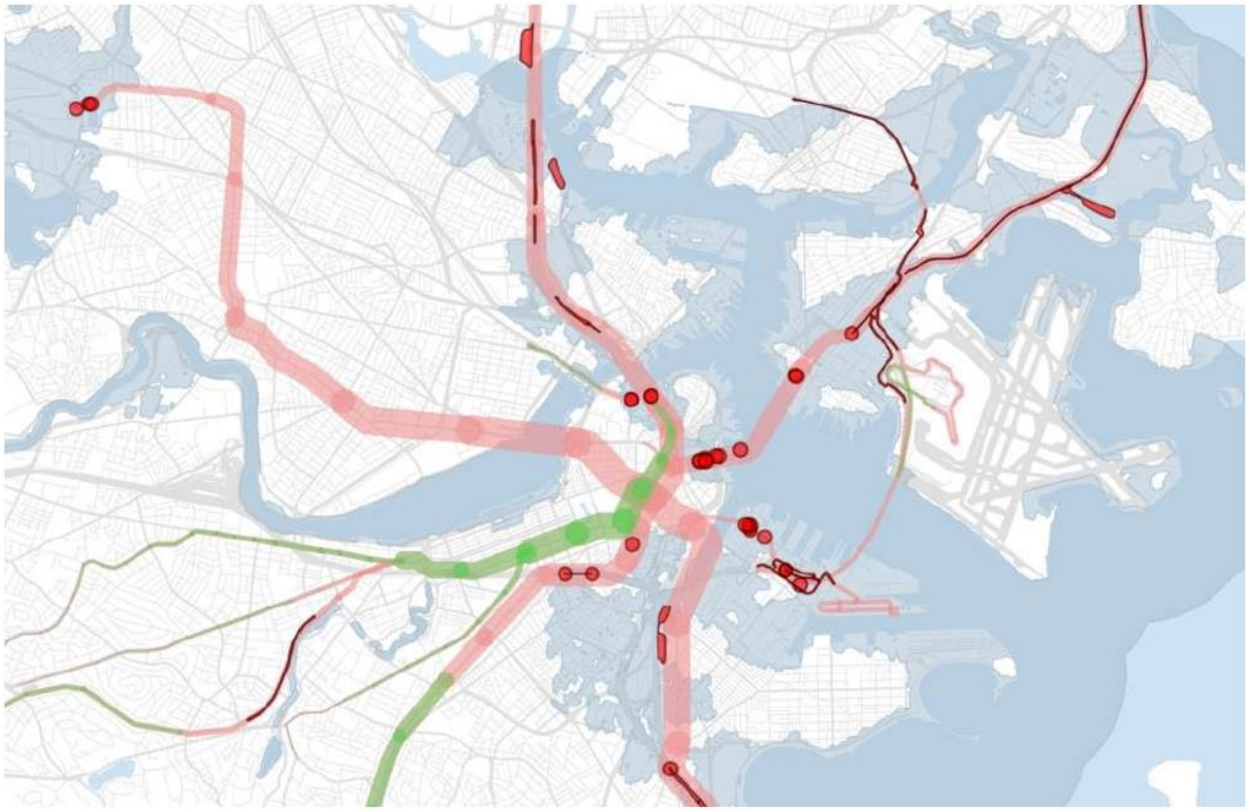

In this scenario, system resilience = 34%.

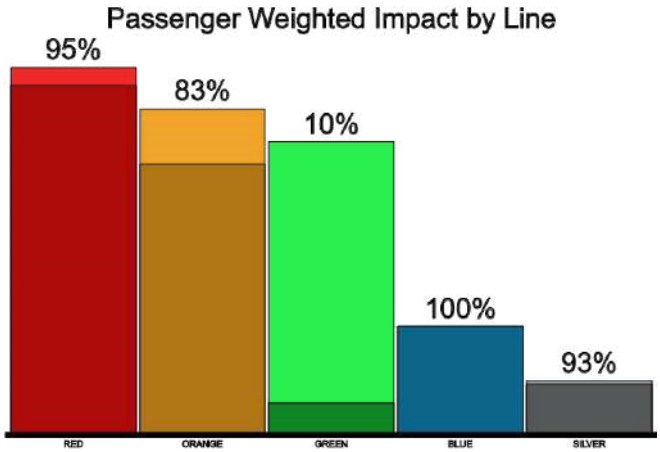

This analysis was performed using CRaVAT transit. The systemwide impacts shown assume that a large volume of water enters the rapid transit system at the relevant lowest critical elevations within the bounds of the coastal flood extents shown. Removal of links is determined by average track elevations, locations of track switches, and train/bus dispatch locations. The analysis assumes no flood mitigation efforts are undertaken and therefore represents a worst-case systemwide impact.

Vulnerable Locations For Selected Coastal Flood Scenario

Red Line - Andrew Portal

Red Line - Alewife Station

Red Line - JFK/UMass - Andrew

Red Line - JFK/UMass Station

Red Line - North Quincy Station

Red Line - JFK/UMass - North Quincy

Red Line - Cabot Yard

Orange Line - Wellington Yard

Orange Line - Tufts-Back Bay Portals

Orange Line - Assembly - Community College

Orange Line - Community College Portal

Orange Line - North Station

Orange Line - Chinatown Station

Orange Line - Wellington abutment

Orange Line - Wellington abutment

Blue Line - Aquarium Station Emergency Egress

Blue Line - Aquarium Station

Blue Line - Oreint Heights

Blue Line - Maverick Station

Blue Line - Maverick Portal

Blue Line - Airport Station

Blue Line - Maverick - Wonderland

Silver Line - Courthouse Station

Silver Line - Airport - Chelsea

Silver Line - Ted Williams Tunnel

Silver Line - Silver Line Way - Design Center

Green Line - North Station

Green Line - Fenway – Longwood

This analysis was performed using CRaVAT transit. The systemwide impacts shown assume that a large volume of water enters the rapid transit system at the relevant lowest critical elevations within the bounds of the coastal flood extents shown. Removal of links is determined by average track elevations, locations of track switches, and train/bus dispatch locations. The analysis assumes no flood mitigation efforts are undertaken and therefore represents a worst-case systemwide impact.

+1.04 m SLR (2070): 50 year Return Period

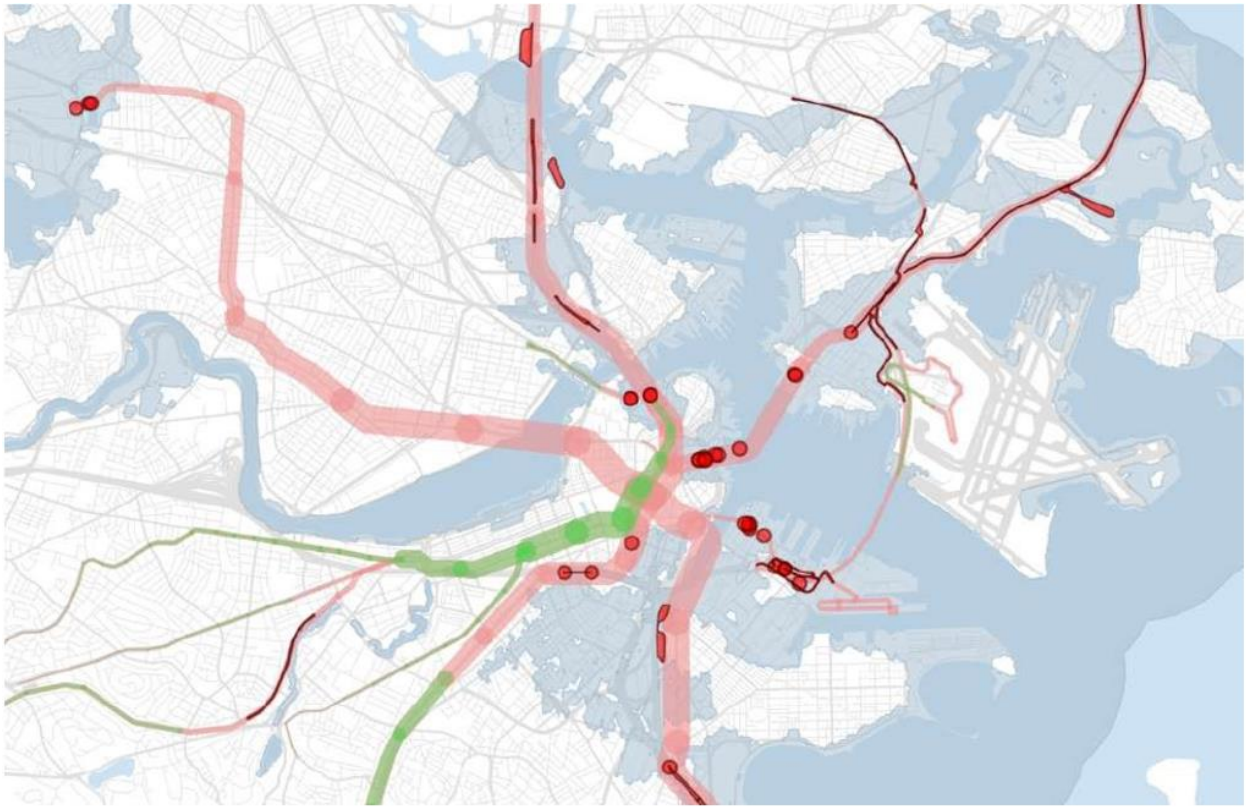

In this scenario, system resilience = 34%.

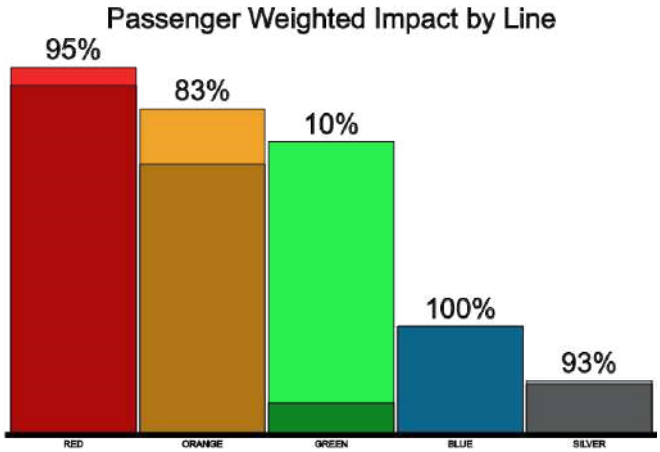

This analysis was performed using CRaVAT transit. The systemwide impacts shown assume that a large volume of water enters the rapid transit system at the relevant lowest critical elevations within the bounds of the coastal flood extents shown. Removal of links is determined by average track elevations, locations of track switches, and train/bus dispatch locations. The analysis assumes no flood mitigation efforts are undertaken and therefore represents a worst-case systemwide impact.

Vulnerable Locations For Selected Coastal Flood Scenario

Red Line - Andrew Portal

Red Line - Alewife Station

Red Line - JFK/UMass - Andrew

Red Line - JFK/UMass Station

Red Line - North Quincy Station

Red Line - JFK/UMass - North Quincy

Red Line - Cabot Yard

Orange Line - Wellington Yard

Orange Line - Tufts-Back Bay Portals

Orange Line - Assembly - Community College

Orange Line - Community College Portal

Orange Line - North Station

Orange Line - Chinatown Station

Orange Line - Wellington abutment

Orange Line - Wellington abutment

Blue Line - Aquarium Station Emergency Egress

Blue Line - Aquarium Station

Blue Line - Oreint Heights

Blue Line - Maverick Station

Blue Line - Maverick Portal

Blue Line - Airport Station

Blue Line - Maverick - Wonderland

Silver Line - Courthouse Station

Silver Line - Airport - Chelsea

Silver Line - Ted Williams Tunnel

Silver Line - Silver Line Way - Design Center

Green Line - North Station

Green Line - Fenway – Longwood

This analysis was performed using CRaVAT transit. The systemwide impacts shown assume that a large volume of water enters the rapid transit system at the relevant lowest critical elevations within the bounds of the coastal flood extents shown. Removal of links is determined by average track elevations, locations of track switches, and train/bus dispatch locations. The analysis assumes no flood mitigation efforts are undertaken and therefore represents a worst-case systemwide impact.

+1.04 m SLR (2070): 100 year Return Period

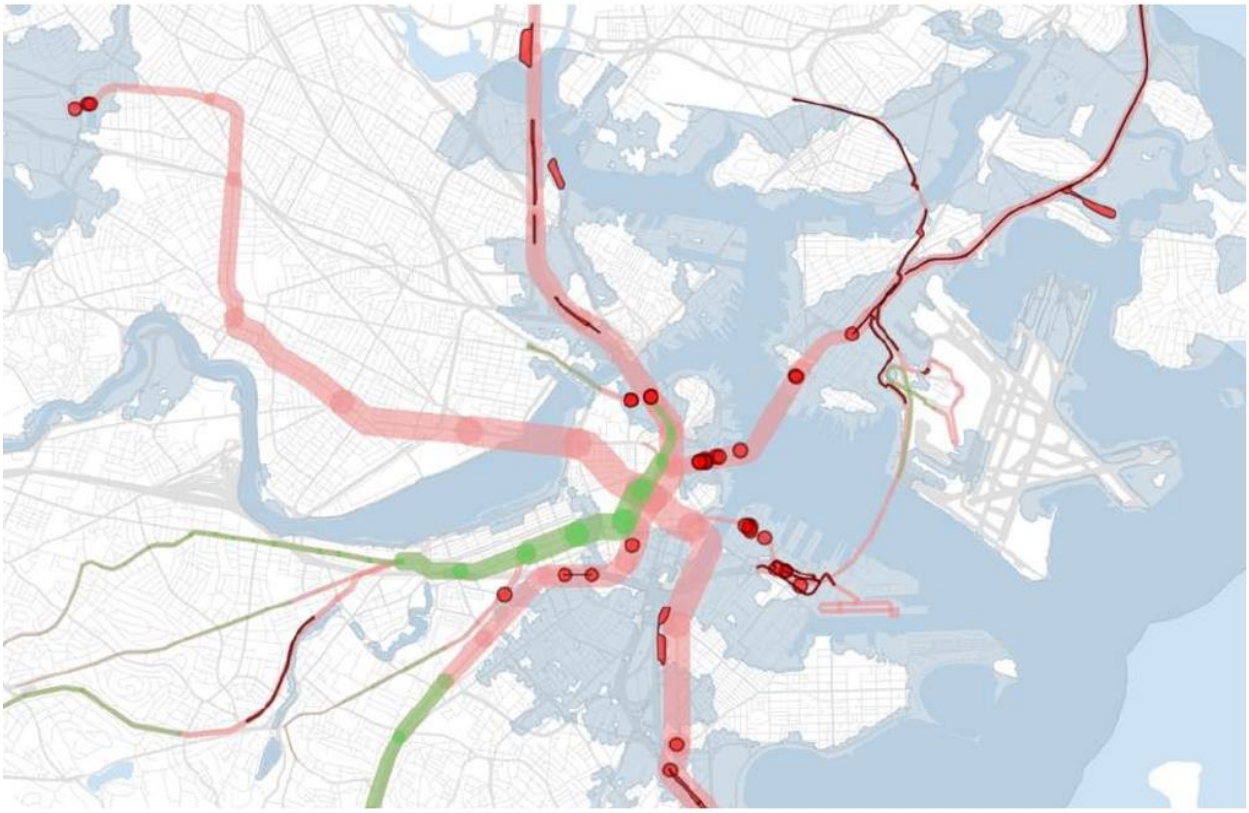

In this scenario, system resilience = 33%.

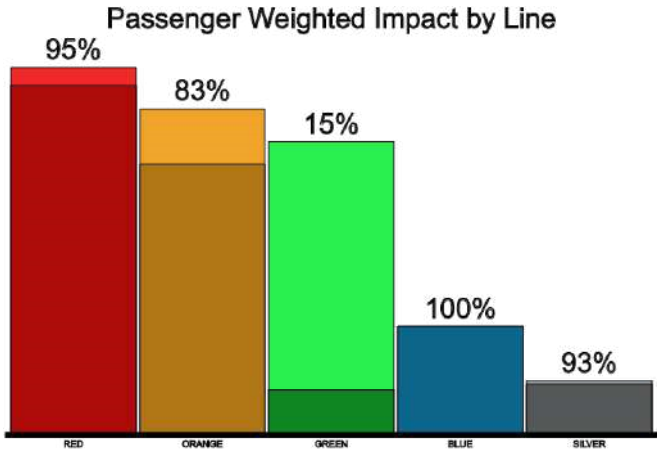

This analysis was performed using CRaVAT transit. The systemwide impacts shown assume that a large volume of water enters the rapid transit system at the relevant lowest critical elevations within the bounds of the coastal flood extents shown. Removal of links is determined by average track elevations, locations of track switches, and train/bus dispatch locations. The analysis assumes no flood mitigation efforts are undertaken and therefore represents a worst-case systemwide impact.

Vulnerable Locations For Selected Coastal Flood Scenario

Red Line - Andrew Portal

Red Line - Andrew Station

Red Line - Alewife Station

Red Line - JFK/UMass - Andrew

Red Line - JFK/UMass Station

Red Line - North Quincy Station

Red Line - JFK/UMass - North Quincy

Red Line - Cabot Yard

Orange Line - Wellington Yard

Orange Line - Tufts-Back Bay Portals

Orange Line - Assembly - Community College

Orange Line - Community College Portal

Orange Line - North Station

Orange Line - Chinatown Station

Orange Line - Wellington abutment

Orange Line - Wellington abutment

Blue Line - Aquarium Station Emergency Egress

Blue Line - Aquarium Station

Blue Line - Oreint Heights

Blue Line - Maverick Station

Blue Line - Maverick Portal

Blue Line - Airport Station

Blue Line - Maverick - Wonderland

Silver Line - Courthouse Station

Silver Line - Airport - Chelsea

Silver Line - Ted Williams Tunnel

Silver Line - Silver Line Way - Design Center

Green Line - North Station

Green Line - Prudential Center Station

Green Line - Fenway – Longwood

+1.04 m SLR (2070): 500 year Return Period

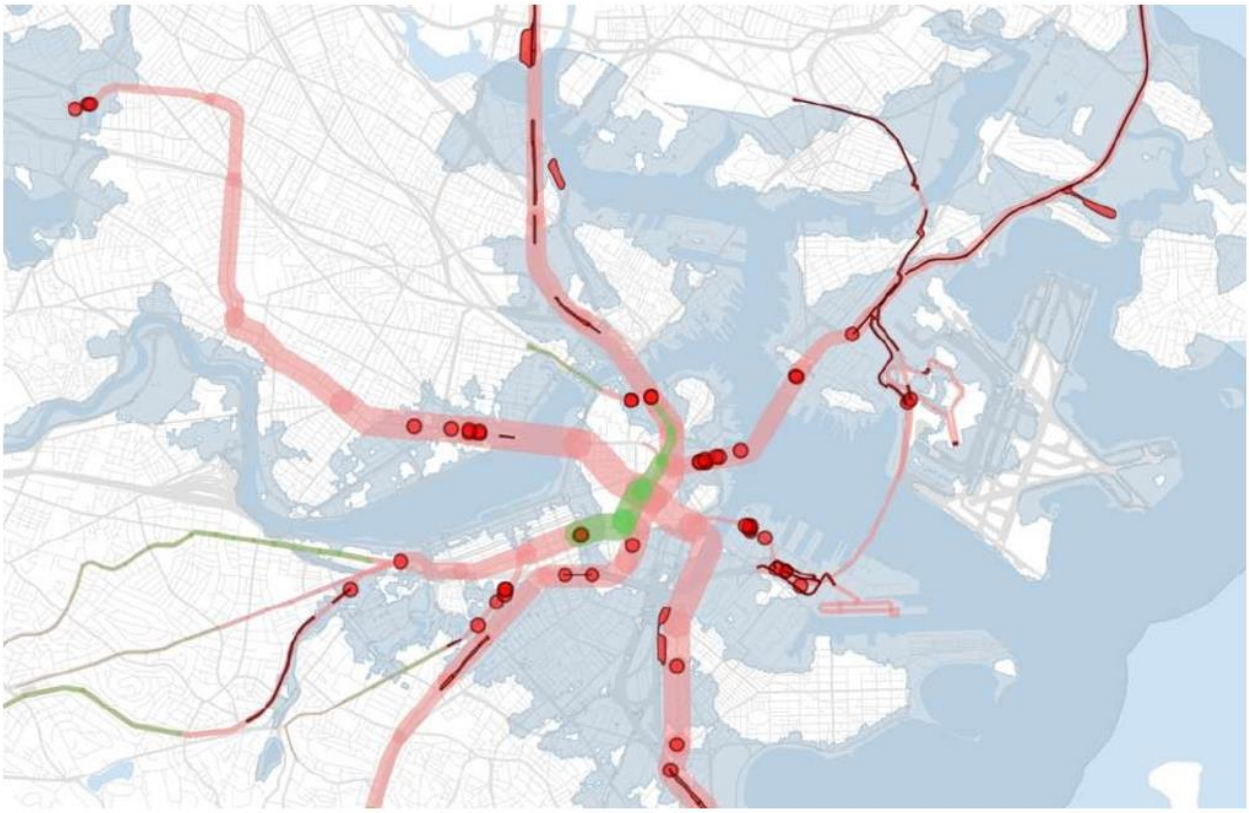

In this scenario, system resilience = 31%.

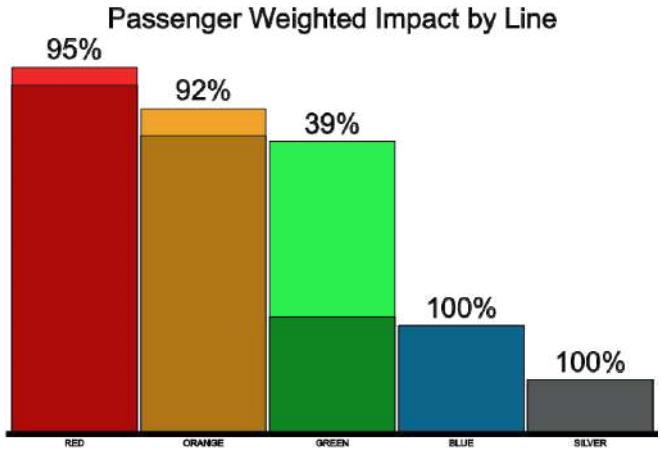

This analysis was performed using CRaVAT transit. The systemwide impacts shown assume that a large volume of water enters the rapid transit system at the relevant lowest critical elevations within the bounds of the coastal flood extents shown. Removal of links is determined by average track elevations, locations of track switches, and train/bus dispatch locations. The analysis assumes no flood mitigation efforts are undertaken and therefore represents a worst-case systemwide impact.

Vulnerable Locations For Selected Coastal Flood Scenario

Red Line - Kendall/MIT Station

Red Line - Andrew Portal

Red Line - Andrew Station

Red Line - Alewife Station

Red Line - JFK/UMass - Andrew

Red Line - JFK/UMass Station

Red Line - North Quincy Station

Red Line - JFK/UMass - North Quincy

Red Line - Cabot Yard

Orange Line - Massachusetts Ave Station

Orange Line - Wellington Yard

Orange Line - Tufts-Back Bay Portals

Orange Line - Assembly - Community College

Orange Line - Community College Portal

Orange Line - North Station

Orange Line - Chinatown Station

Orange Line - Wellington abutment

Orange Line - Wellington abutment

Blue Line - Aquarium Station Emergency Egress

Blue Line - Aquarium Station

Blue Line - Oreint Heights

Blue Line - Maverick Station

Blue Line - Maverick Portal

Blue Line - Airport Station

Blue Line - Maverick - Wonderland

Silver Line - Courthouse Station

Silver Line - Airport - Chelsea

Silver Line - Ted Williams Tunnel

Silver Line - Silver Line Way - Design Center

Green Line - North Station

Green Line - Arlington Station

Green Line - Prudential Center Station

Green Line - Symphony Station

Green Line - Symphony Station - Northeastern University

Green Line - Kenmore Station

Green Line - Fenway Portal

Green Line - Fenway – Longwood

This analysis was performed using CRaVAT transit. The systemwide impacts shown assume that a large volume of water enters the rapid transit system at the relevant lowest critical elevations within the bounds of the coastal flood extents shown. Removal of links is determined by average track elevations, locations of track switches, and train/bus dispatch locations. The analysis assumes no flood mitigation efforts are undertaken and therefore represents a worst-case systemwide impact.

+1.04 m SLR (2070): 1,000 year Return Period

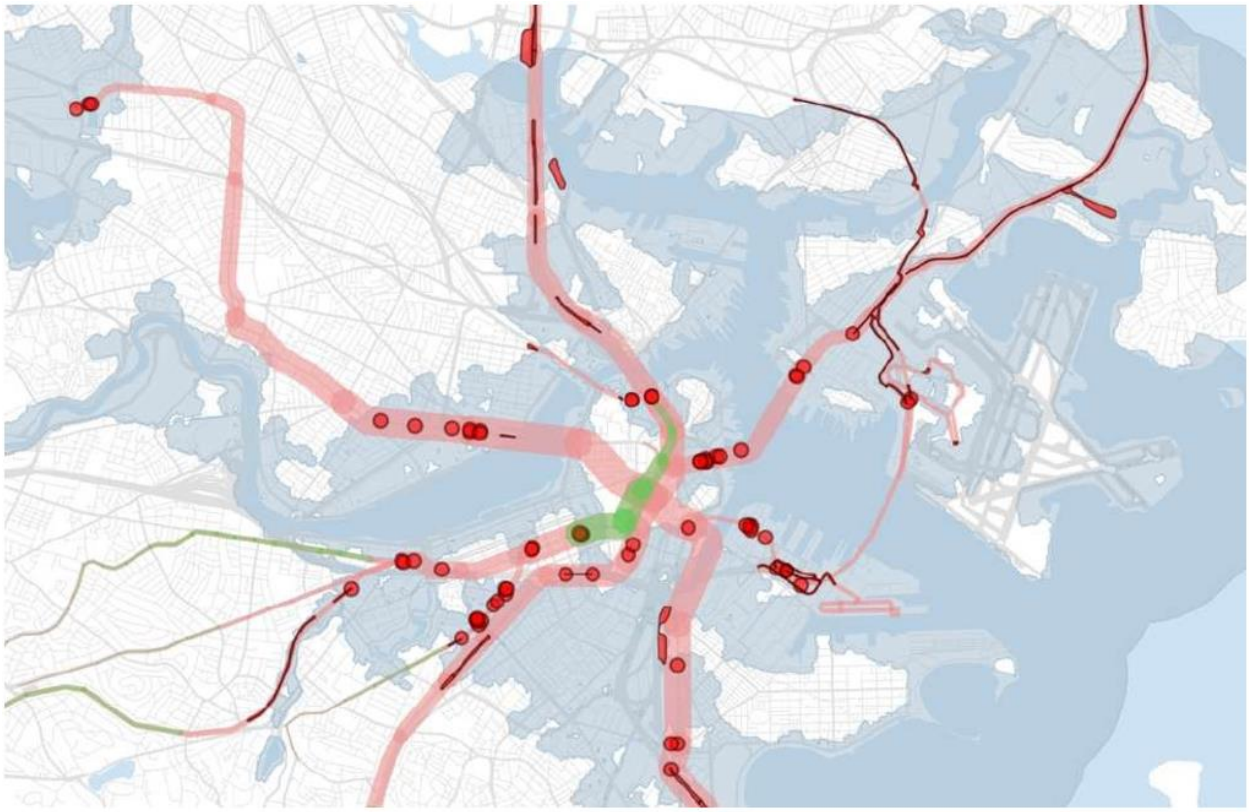

In this scenario, system resilience = 31%.

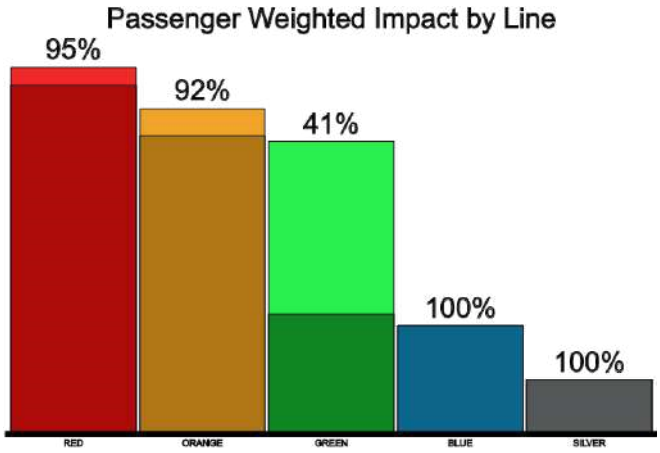

This analysis was performed using CRaVAT transit. The systemwide impacts shown assume that a large volume of water enters the rapid transit system at the relevant lowest critical elevations within the bounds of the coastal flood extents shown. Removal of links is determined by average track elevations, locations of track switches, and train/bus dispatch locations. The analysis assumes no flood mitigation efforts are undertaken and therefore represents a worst-case systemwide impact.

Vulnerable Locations For Selected Coastal Flood Scenario

Red Line - Kendall/MIT Station

Red Line - Andrew Portal

Red Line - Andrew Station

Red Line - Alewife Station

Red Line - JFK/UMass - Andrew

Red Line - JFK/UMass Station

Red Line - North Quincy Station

Red Line - JFK/UMass - North Quincy

Red Line - Cabot Yard

Orange Line - Massachusetts Ave Station

Orange Line - Wellington Yard

Orange Line - Tufts-Back Bay Portals

Orange Line - Assembly - Community College

Orange Line - Community College Portal

Orange Line - North Station

Orange Line - Chinatown Station

Orange Line - Wellington abutment

Orange Line - Wellington abutment

Blue Line - Aquarium Station Emergency Egress

Blue Line - Aquarium Station

Blue Line - Oreint Heights

Blue Line - Maverick Station

Blue Line - Maverick Portal

Blue Line - Airport Station

Blue Line - Maverick - Wonderland

Silver Line - Courthouse Station

Silver Line - Airport - Chelsea

Silver Line - Ted Williams Tunnel

Silver Line - Silver Line Way - Design Center

Green Line - Lechmere Station

Green Line - North Station

Green Line - Arlington Station

Green Line - Copley Station

Green Line - Prudential Center Station

Green Line - Symphony Station

Green Line - Symphony Station - Northeastern Station

Green Line - Kenmore Station

Green Line - Fenway Portal

Green Line - Fenway – Longwood

This analysis was performed using CRaVAT transit. The systemwide impacts shown assume that a large volume of water enters the rapid transit system at the relevant lowest critical elevations within the bounds of the coastal flood extents shown. Removal of links is determined by average track elevations, locations of track switches, and train/bus dispatch locations. The analysis assumes no flood mitigation efforts are undertaken and therefore represents a worst-case systemwide impact.

Appendix C: MBTA Rapid Transit System: Lowest Critical Elevations

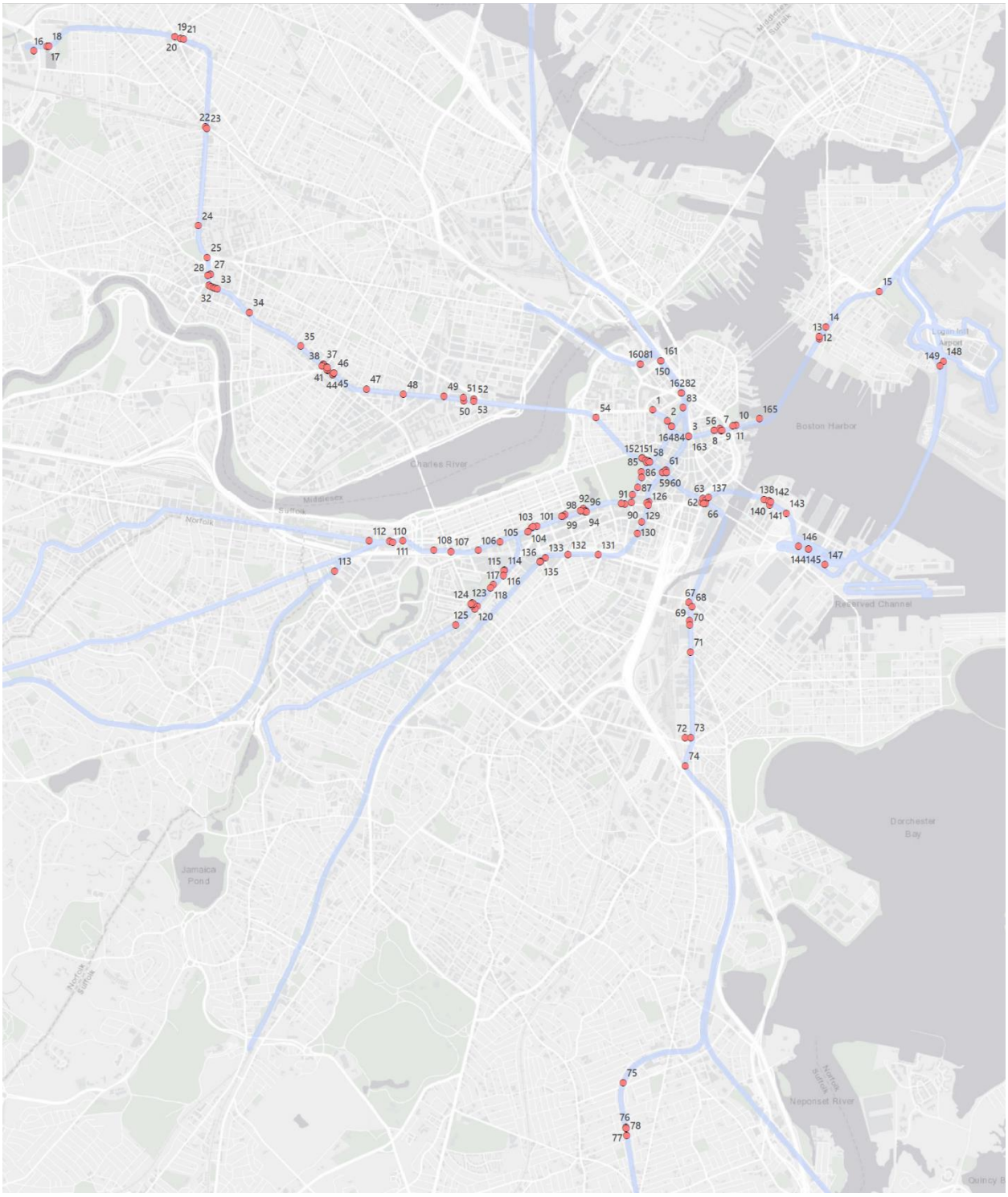

Figure 55: Lowest *critical elevation (LCE) points identitifed in the MBTA rapid transit system. These locations were identified as potential flood ingress points.*

Table 10*: Details of the lowest critical elevation (LCE) points identified in the MBTA rapid transit system.*

ID	Line	Station 1	Station 2	Ghost Link ID
1	Blue	Bowdoin	Bowdoin	317
2	Blue	State Street	Bowdoin	316
3	Blue	State Street	State Street	315
5	Blue	State Street	Aquarium	314
6	Blue	Aquarium	Aquarium	314
7	Blue	Aquarium	Aquarium	314
8	Blue	Aquarium	Aquarium	314
9	Blue	Aquarium	Aquarium	314
10	Blue	Aquarium	Aquarium	314
11	Blue	Aquarium	Aquarium	314
12	Blue	Maverick	Maverick	314
13	Blue	Maverick	Maverick	314
14	Blue	Maverick	Maverick	313
15	Blue	Maverick	Maverick	312
16	Red	Alewife	Alewife	1
17	Red	Alewife	Alewife	1
18	Red	Alewife	Alewife	1
19	Red	Davis	Davis	2
20	Red	Davis	Davis	2
21	Red	Davis	Davis	3
22	Red	Porter	Porter	3
23	Red	Porter	Porter	3
24	Red	Porter	Harvard	3
25	Red	Harvard	Harvard	3

ID	Line	Station 1	Station 2	Ghost Link ID
26	Red	Harvard	Harvard	3
27	Red	Harvard	Harvard	3
28	Red	Harvard	Harvard	3
29	Red	Harvard	Harvard	3
30	Red	Harvard	Harvard	3
31	Red	Harvard	Harvard	3
32	Red	Harvard	Harvard	3
33	Red	Harvard	Harvard	4
34	Red	Harvard	Central	4
35	Red	Harvard	Central	5
36	Red	Harvard	Central	5
37	Red	Harvard	Central	5
38	Red	Central	Central	5
39	Red	Central	Central	5
40	Red	Central	Central	5
41	Red	Central	Central	5
42	Red	Central	Central	5
43	Red	Central	Central	5
44	Red	Central	Central	5
45	Red	Central	Central	5
46	Red	Central	Central	5
47	Red	Central	Kendall	5
48	Red	Central	Kendall	5
49	Red	Central	Kendall	6
50	Red	Kendall	Kendall	6
51	Red	Kendall	Kendall	6
52	Red	Kendall	Kendall	7

ID	Line	Station 1	Station 2	Ghost Link ID
53	Red	Kendall	Kendall	7
54	Red	MGH	Park St	7
152	Green	Park St	Park St	207
55	Red	MGH	Park St	8
56	Red	Park St	Park St	8
57	Red	Park St	Park St	8
58	Red	Park St	Park St	8
59	Red	DTX	DTX	9
60	Red	DTX	DTX	9
61	Red	DTX	DTX	9
62	Red	South STA	South STA	10
63	Red	South STA	South STA	10
64	Red	South STA	South STA	10
65	Red	South STA	South STA	10
66	Red	South STA	South STA	10
67	Red	Broadway	Broadway	12
68	Red	Broadway	Broadway	12
69	Red	Broadway	Andrew	12
70	Red	Broadway	Andrew	12
71	Red	Broadway	Andrew	13
72	Red	Andrew	Andrew	14
73	Red	Andrew	Andrew	14
74	Red	Andrew	JFK/UMass	14
75	Red	Fields Corner	Shawmut	35
76	Red	Shawmut	Shawmut	19
77	Red	Shawmut	Shawmut	19
78	Red	Shawmut	Ashmont	36

ID	Line	Station 1	Station 2	Ghost Link ID
79	Red	Ashmont	Ashmont	48
80	Red	Ashmont	Ashmont	15
81	Green	North Station	North Station	202
82	Green	Haymarket	Haymarket	205
83	Green	Haymarket	Govt Ctr	205
84	Green	Govt Ctr	Govt Ctr	206
85	Green	Park St	Park St	207
86	Green	Park St	Boylston	208
87	Green	Park St	Boylston	208
88	Green	Boylston	Boylston	208
89	Green	Boylston	Boylston	208
90	Green	Boylston	Boylston	209
91	Green	Boylston	Arlington	209
92	Green	Arlington	Arlington	210
93	Green	Arlington	Arlington	210
94	Green	Arlington	Arlington	210
95	Green	Arlington	Arlington	210
96	Green	Arlington	Arlington	210
97	Green	Arlington	Arlington	210
98	Green	Arlington	Copley	210
99	Green	Arlington	Copley	210
100	Green	Arlington	Copley	210
101	Green	Arlington	Copley	211
102	Green	Copley	Copley	211
103	Green	Copley	Copley	211
104	Green	Copley	Copley	211
105	Green	Copley	Hynes	212

ID	Line	Station 1	Station 2	Ghost Link ID
106	Green	Copley	Hynes	213
107	Green	Hynes	Hynes	213
108	Green	Hynes	Kenmore	213
109	Green	Hynes	Kenmore	213
110	Green	Hynes	Kenmore	214
111	Green	Kenmore	Kenmore	214
112	Green	Kenmore	Blanford	215
113	Green	Kenmore	Fenway	240
114	Green	Copley	Prudential	271
115	Green	Copley	Prudential	271
116	Green	Prudential	Prudential	271
117	Green	Prudential	Symphony	271
118	Green	Prudential	Symphony	271
119	Green	Symphony	Symphony	272
120	Green	Symphony	Symphony	272
121	Green	Symphony	Symphony	272
122	Green	Symphony	Symphony	272
123	Green	Symphony	Symphony	272
124	Green	Symphony	Symphony	272
125	Green	Symphony	Northeastern	272
126	Orange	Chinatown	Chinatown	112
127	Orange	Chinatown	Chinatown	111
128	Orange	Chinatown	Chinatown	113
129	Orange	Chinatown	Tufts	113
130	Orange	Tufts	Tufts	114
131	Orange	Tufts	Back Bay	115
132	Orange	Back Bay	Back Bay	115

ID	Line	Station 1	Station 2	Ghost Link ID
133	Orange	Back Bay	Back Bay	116
134	Orange	Back Bay	Mass Ave	116
135	Orange	Back Bay	Mass Ave	116
136	Orange	Back Bay	Mass Ave	116
137	Silver	South Station	Courthouse	401
138	Silver	Courthouse	Courthouse	401
139	Silver	Courthouse	Courthouse	401
140	Silver	Courthouse	Courthouse	401
141	Silver	Courthouse	Courthouse	401
142	Silver	Courthouse	Courthouse	401
143	Silver	Courthouse	WTC	401
144	Silver	WTC	WTC	402
145	Silver	WTC	WTC	402
146	Silver	Terminal E	SL Way	405
147	Silver	SL Way	Terminal A	405
148	Silver	SL Way	Terminal A	406
149	Silver	Airport	SL Way	420
150	Green	North Station	North Station	203
151	Green	Park St	Park St	207
153	Green	Park St	Park St	207
154	Green	Park St	Park St	207
155	Green	Park St	Park St	207
156	Green	Park St	Park St	207
157	Orange	DTX	DTX	112
158	Orange	DTX	DTX	112
159	Orange	DTX	DTX	112
160	Orange	North Station	North Station	108

ID	Line	Station 1	Station 2	Ghost Link ID
161	Orange	North Station	North Station	109
162	Orange	Haymarket	Haymarket	110
163	Orange	State Street	State Street	110
164	Blue	Govt Ctr	Govt Ctr	316
165	Blue	Aquarium	Aquarium	314

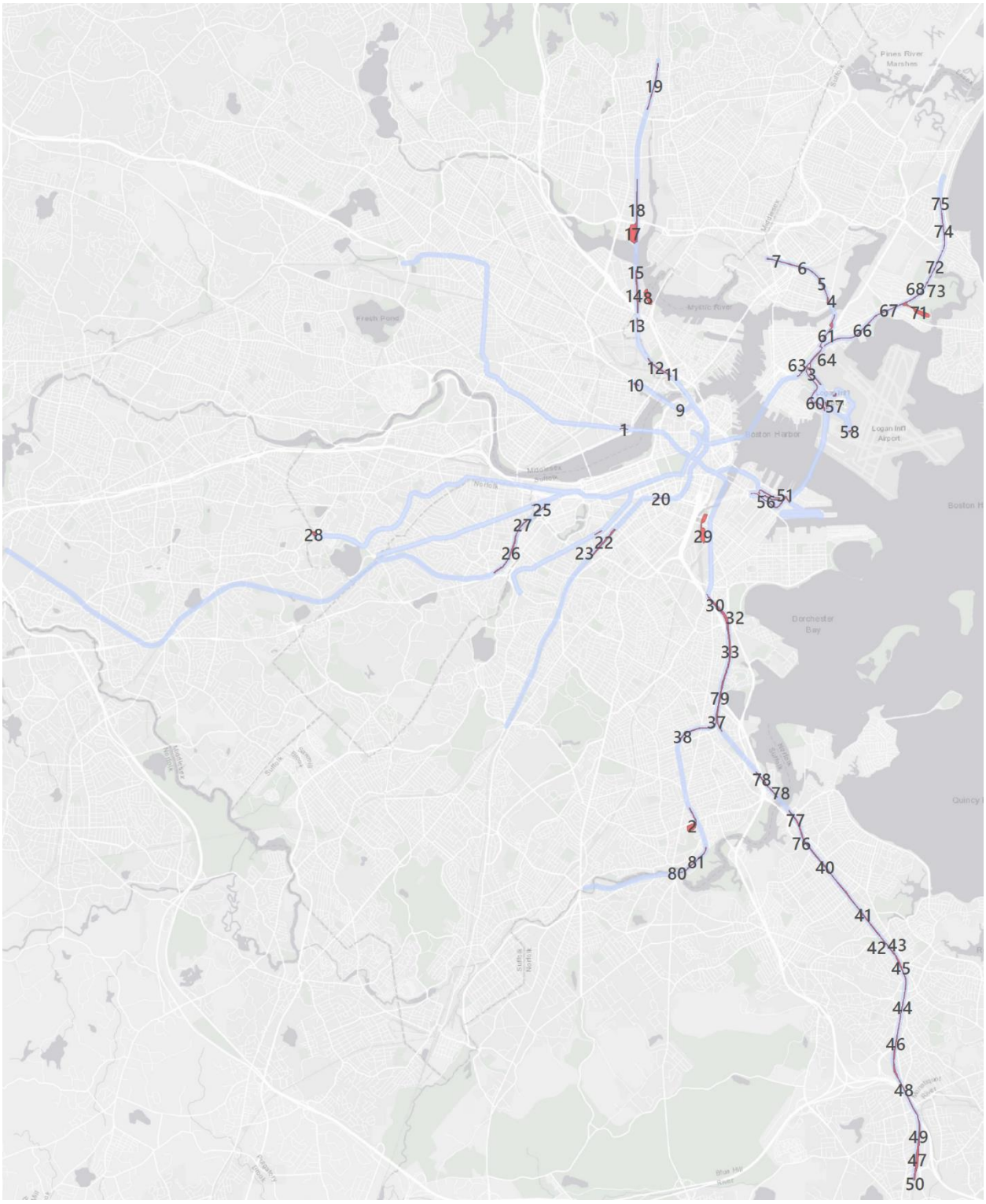

Figure 56: Lowest critical elevation (LCE) points identified in the MBTA rapid transit system. These locations were identified as potential flood ingress points.

Table 11*: Details of the lowest critical elevation (LCE) points identified in the MBTA rapid transit system.*

ID	Line	Station 1	Station 2	Ghost Link ID
1	Red	Kendall	MGH	7
2	Red	Codman YARD	Codman YARD	38
3	Silver	Terminal E	Airport	410
4	Silver	Airport	Eastern Ave	411
5	Silver	Eastern Ave	Box District	412
6	Silver	Box District	Bellingham Square	413
7	Silver	Bellingham Square	Chelsea	414
8	Bus	Alford St	Alford St	0
9	Green	Science Park	North Station	201
10	Green	Lechmere	Lechmere	201
11	Orange	Community College	North Station	107
12	Orange	Sullivan	Community College	107
13	Orange	Sullivan	Community College	106
14	Orange	Assembly	Sullivan	106
15	Orange	Wellington	Assembly	106
16	Orange	Wellington	Assembly	104
17	Orange	Wellington YARD	Wellington YARD	104
18	Orange	Malden	Wellington	103
19	Orange	Oak Grove	Malden	101
20	Orange	Tufts	Back Bay	115
21	Orange	Mass Ave	Mass Ave	116
22	Orange	Mass Ave	Ruggles	117
23	Orange	Ruggles	Ruggles	118
24	Green	Symphony	Northeastern	272

ID	Line	Station 1	Station 2	Ghost Link ID
25	Green	Fenway	Fenway	232
26	Green	Longwood	Brookline Village	242
27	Green	Fenway	Longwood	242
28	Green	Bos Col YARD	Bos Col YARD	224
29	Red	Andrew	JFK/UMass	15
30	Red	Andrew	JFK/UMass	15
31	Red	Andrew	JFK/UMass	17
32	Red	Andrew	JFK/UMass	16
33	Red	JFK/UMass	Savin Hill	18
34	Red	JFK/UMass	Savin Hill	32
35	Red	JFK/UMass	Savin Hill	33
36	Red	JFK/UMass	Savin Hill	17
37	Red	Savin Hill	Fields Corner	33
38	Red	Fields Corner	Shawmut	35
39	Red	Fields Corner	Shawmut	34
40	Red	North Quincy	Wollaston	22
41	Red	Wollaston	Quincy Center	22
42	Red	Wollaston	Quincy Center	23
43	Red	Wollaston	Quincy Center	24
44	Red	Quincy Center	Quincy Adams	26
45	Red	Quincy Center	Quincy Adams	25
46	Red	Quincy Center	Quincy Adams	27
47	Red	Quincy Adams	Braintree	30
48	Red	Quincy Adams	Braintree	28
49	Red	Quincy Adams	Braintree	29
50	Red	Quincy Adams	Braintree	31
51	Silver	Terminal E	SL Way	403
52	Silver	WTC	SL Way	402

ID	Line	Station 1	Station 2	Ghost Link ID
53	Silver	WTC	SL Way	402
54	Silver	WTC	SL Way	403
55	Silver	SL Way	Harbor St	450
56	Silver	SL Way	Terminal A	405
57	Silver	SL Way	Terminal A	406
58	Silver	Terminal A	Terminal B	407
59	Silver	Terminal E	Airport	410
60	Silver	Airport	SL Way	420
61	Silver	Airport	Eastern Ave	411
62	Blue	Maverick	Airport	312
63	Blue	Airport	Airport	311
64	Blue	Airport	Wood Island	310
65	Blue	Airport	Wood Island	310
66	Blue	Wood Island	Orient Heights	310
67	Blue	Wood Island	Orient Heights	309
68	Blue	Orient Heights	Suffolk Downs	306
69	Blue	Orient Heights	Suffolk Downs	307
70	Blue	Orient Heights	Suffolk Downs	308
71	Blue	Orient YARD	Orient YARD	307
72	Blue	Suffolk Downs	Beachmont	304
73	Blue	Suffolk Downs	Beachmont	305
74	Blue	Beachmont	Revere Beach	303
75	Blue	Beachmont	Revere Beach	302
76	Red	JFK/UMass	North Quincy	21
77	Red	JFK/UMass	North Quincy	20
78	Red	JFK/UMass	North Quincy	19
78	Red	JFK/UMass	North Quincy	20
79	Red	JFK/UMass	North Quincy	18

ID	Line	Station 1	Station 2	Ghost Link ID
80	Red	Mattapan Trolley	Mattapan Trolley	39
81	Red	Mattapan Trolley	Mattapan Trolley	39
82	Green	St. Marys Street	Kenmore	231

Appendix D: MBTA Critical Coastal Flood Vulnerabilities Memorandum

Urgent Locations (Exposure under 1-100 year storms today)

The following locations (apart from Orient Heights Yard) have been shown to lie within the current 1-100 year floodplain, based on the BH-FRM 2013 model. Locations within this section are currently inadequately protected against 1-100 year coastal flood events. It is recommended that projects at locations identified in this section be designed for at least the current FEMA 1-500 year floodplain, as it is roughly coincident with the BH-FRM 2030 1-100 year projections. For projects with a useful life span anticipated to be greater than 20 years, it is recommended that 2070 1-100 year projections be consulted instead.

These locations have been ranked by frequency of flooding and severity of system-wide impact, should each location be removed from service:

Figure 57: Blue Line - Aquarium Station

Figure 58: Blue Line - Orient Heights

Figure 59: Blue Line - Maverick Station and Portal

Figure 60: Blue Line - Airport Station

Figure 61: Blue Line - Wood Island to Orient Heights

Figure 62: Blue Line - Suffolk Downs to Beachmont

Figure 63: Blue Line - Beachmont to Wonderland

Figure 63: Red Line – Mattapan Trolley

Figure 57: Blue Line - Aquarium Station, comparison of 1-100 year flood events projected for:

a) 2030

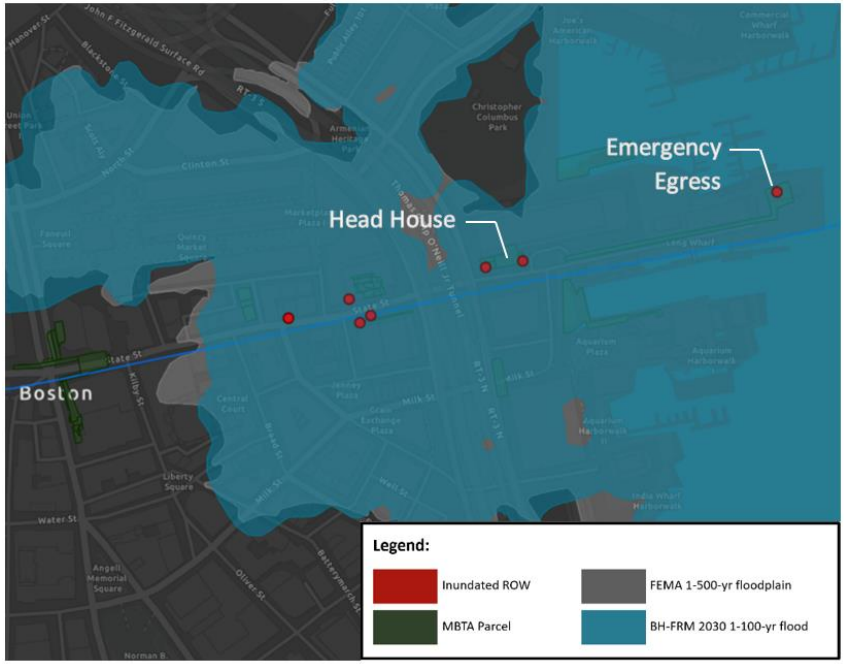

b) 2070

Aquarium Station, particularly the head house on Long Wharf experienced significant inundation during a record-setting Nor'easter in January 2018, and later on the same year on March 2nd, 2018 (Weston & Sampson, 2019). Seen in Figure 57a above, surface flooding is projected to be extensive around Aquarium Station, reaching a projected depth of 1.5 feet in a 1-100 year flood event at the station's head house (Bosma et al., 2015). Under projected 2070 conditions, shown in Figure 57b, a larger area of inundation is shown, reaching a projected depth of 4.5 feet at the station's head house in a 1-100 year flood event (Bosma et al., 2015). Should Aquarium Station be inundated, the resulting service disruption would prove detrimental to the populations of East Boston and Revere, as 72% of Blue Line trips in 2010 were work-home trips, wherein a majority of riders also reported a complete dependence on the Blue Line for these trips (MBTA, 2018). Adjusting for ridership, the flooding of Aquarium Station would result in an 11% loss of system-wide functionality. The 2030 scenario shown above considers +8.2 inches of SLR, while the 2070 scenario considers +41 inches of SLR (Bosma et al. 2015).

Figure 58: Blue Line - Orient Heights Yard, comparison of 1-100 year flood events projected for:

a) 2030

b) 2070

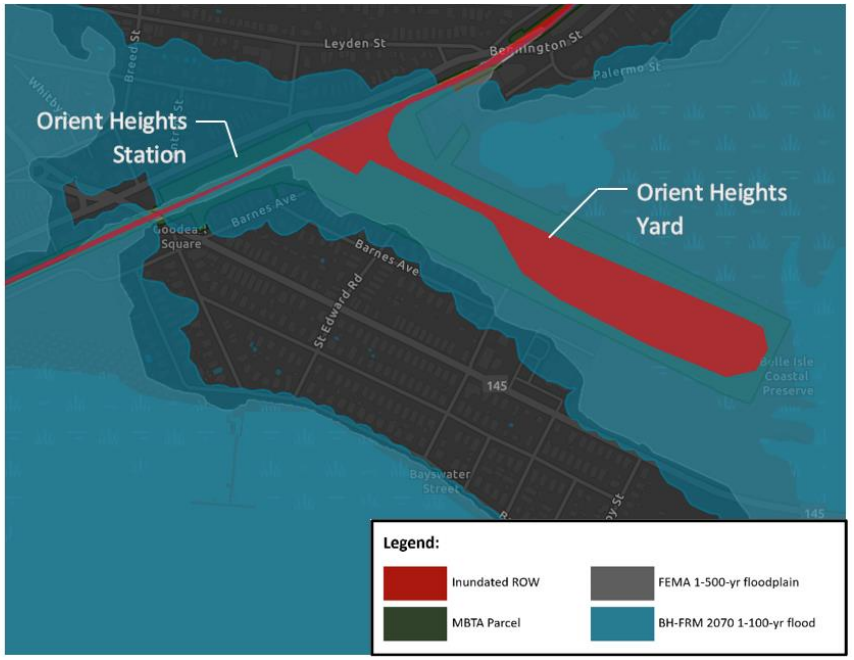

Orient Heights Yard, the main rail yard for the Blue Line, houses the line's only wheel truing machine, which is both crucial for maintenance and highly vulnerable to flood risks (AECOM 2018). Shown in Figure 58a, both the Orient Heights station and yard are exposed to flooding by 2030, with a projected inundation depth of 1 foot in the Orient Heights Yard in a 1-100 year flood event (Bosma et al., 2015). Figure 58b shows that more extensive flooding is projected in 2070, reaching a depth of 3.5 feet in a 1-100 year flood event (Bosma et al., 2015). In addition to housing rolling stock, spare parts, notably traction motors, would also be vulnerable to flood damage with current storage practices (AECOM 2018). In a worst-case scenario, inundation at Orient Heights would eliminate service for the entirety of the Blue Line for a two-week period, with estimated service impacts lasting a year or more (Botros et al. 2019). Such a service disruption would prove detrimental to the populations of East Boston and Revere, as 72% of Blue Line trips in 2010 were work-home trips, wherein a majority of riders also reported a complete dependence on the Blue Line for these trips (MBTA 2018). Adjusting for ridership, the flooding of Orient Heights (and corresponding loss of the Blue Line) results in an 18% loss of system-wide functionality. The 2030 scenario shown above considers +8.2 inches of SLR, while the 2070 scenario considers +41 inches of SLR (Bosma et al. 2015).

Figure 59: Blue Line - Maverick Station and portal, comparison of 1-100 year flood events projected for:

a) 2030

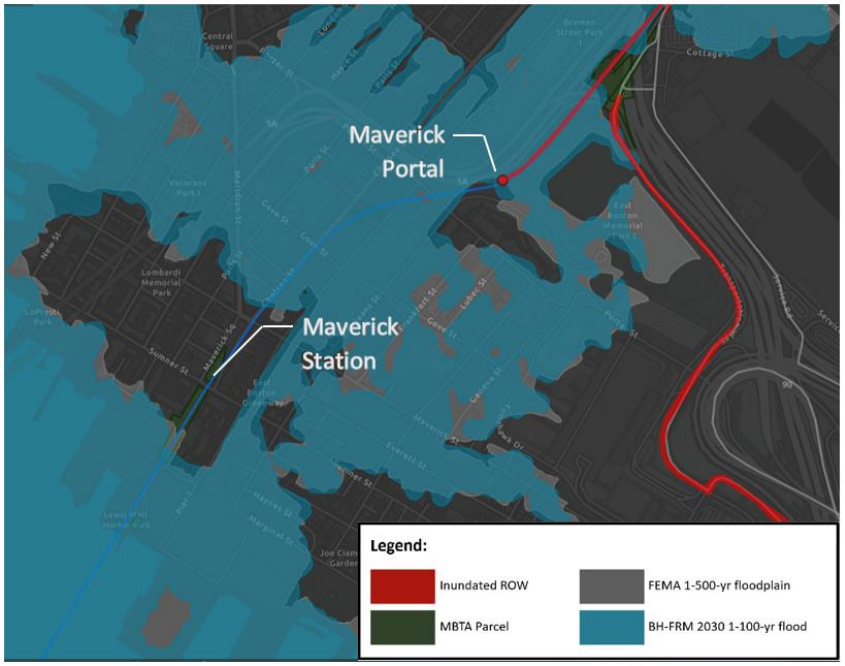

b) 2070

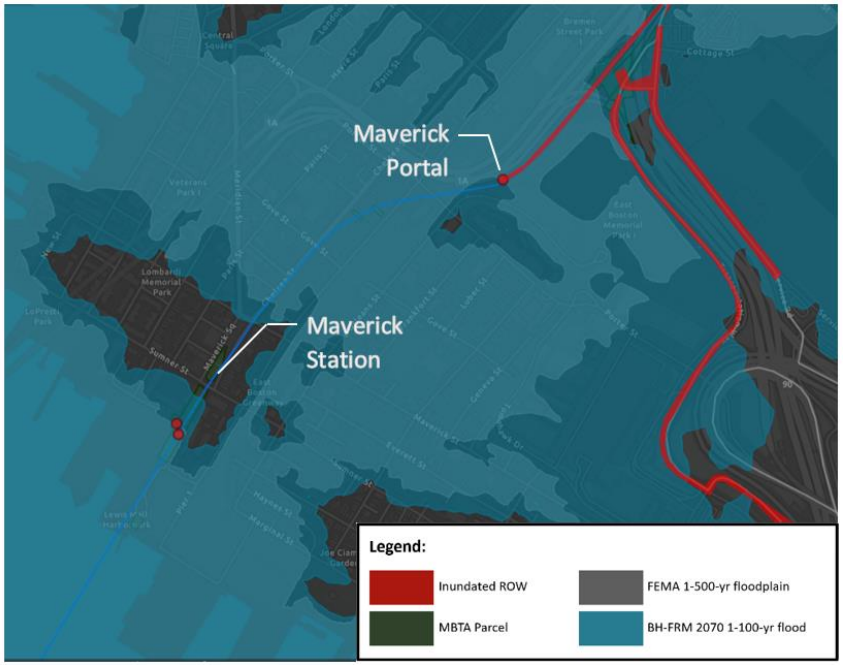

Maverick Portal currently lies within the 1-100 year flood plain, with a projected inundation depth of 1.5 feet (Bosma et al., 2015), As shown in Figure 59a, Maverick Portal is prone to flooding under 2030 projections, with a projected inundation of 2.5 feet in a 1-100 year flood event (Bosma et al., 2015). By 2070, shown in Figure 59b, flooding is projected to be more extensive, reaching a projected depth of 10 feet at Maverick Portal in a 1-100 year flood event, whilst also exposing Maverick Station to flooding. Track elevation at the Maverick Portal is 7.5 ft (NAVD88). Should this portal flood, it is likely that the East Boston Tunnel, which dates from 1904, would flood beyond Aquarium Station. A similar tunnel, the East River Tunnel in New York City, completed in 1910, was flooded during Hurricane Sandy and sustained an estimated $334 million in damages when assessed in 2014 (HNTB, 2014). Adjusting for ridership, the flooding of Maverick Station or the Maverick Portal would result in an 12% loss of system-wide functionality. The 2030 scenario shown above considers +8.2 inches of SLR, while the 2070 scenario considers +41 inches of SLR (Bosma et al., 2015).

Figure 60: Blue Line - Airport Station, comparison of 1-100 year flood events projected for:

a) 2030

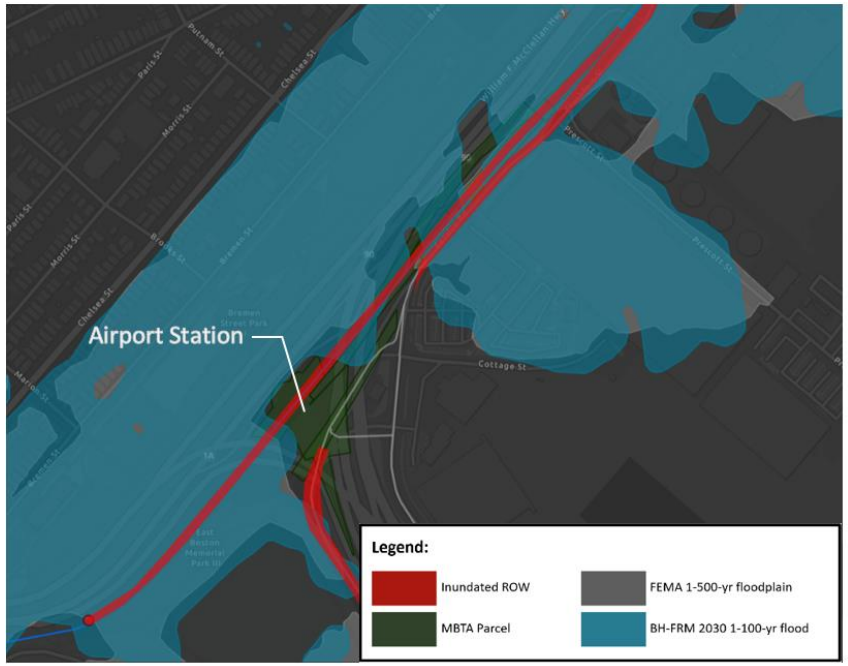

b) 2070

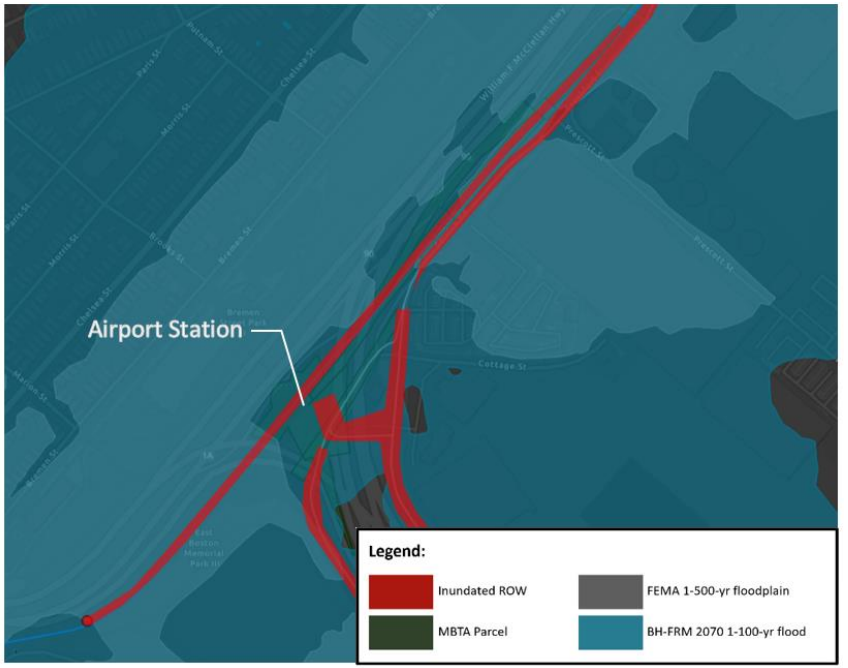

Track elevation at Airport Station is approximately 11 ft (NAVD88) and lies within the current 1-100 year flood plain. As shown in Figure 60a, Airport Station is prone to flooding under 2030 1-100 year flood event projections, with a projected inundation of 2.0 feet (Bosma et al., 2015). By 2070, shown in Figure 60b, flooding is projected to be more extensive, reaching a projected depth of 5.0 feet in a 1-100 year flood event (Bosma et al., 2015). Should this station flood, access from Downtown Boston to Logan Airport would become severely limited. However, the Blue Line represents a relatively small percentage of mode share for passengers traveling to Logan Airport; just 1.5% of trips to or from Logan relied on the Blue Line according to 2019 data (Morrison, 2019). Adjusting for ridership, the flooding of Airport Station would result in an 11% loss of system-wide functionality. The 2030 scenario shown above considers +8.2 inches of SLR, while the 2070 scenario considers +41 inches of SLR (Bosma et al., 2015).

Figure 61: Blue Line - Wood Island Station to Orient Heights Station, comparison of 1-100 year flood events projected for:

a) 2030

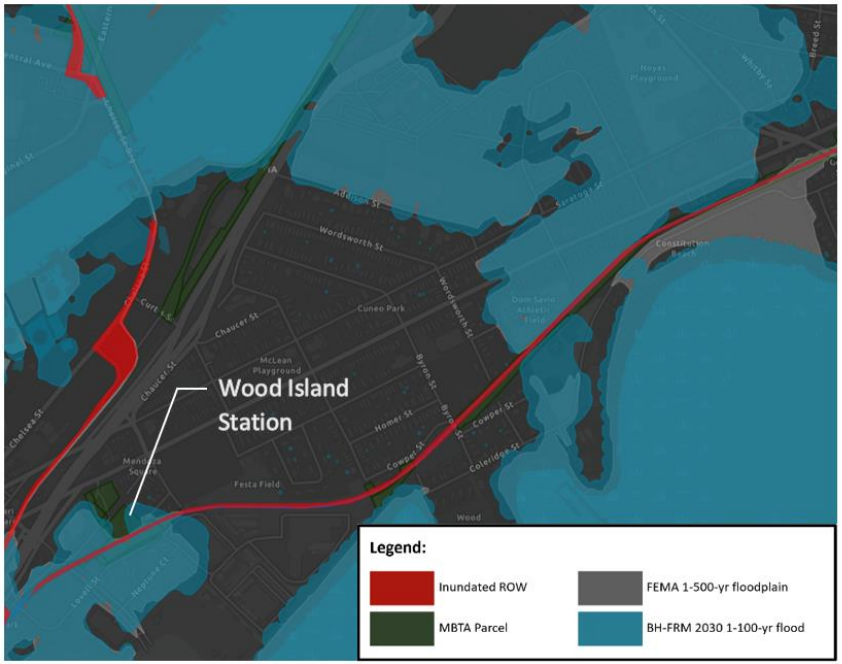

b) 2070

Shown in Figure 61a, Wood Island Station is projected to be vulnerable under 2030 conditions, whilst the tracks from Wood Island to Orient Heights would also be vulnerable under 2070 conditions, as shown in Figure 61b. Flooding at Wood Island Station is projected to reach a depth of 1 foot under 2030 conditions in a 1-100 year flood event and 4.0 feet in a 1-100 year flood event under 2070 conditions (Bosma et al., 2015). Adjusting for ridership, the flooding of Wood Island Station or the tracks connecting it to Orient Heights Station, would result in an 8% loss of system-wide functionality, assuming that service remains in place between Bowdoin and Airport Stations. The 2030 scenario shown above considers +8.2 inches of SLR, while the 2070 scenario considers +41 inches of SLR (Bosma et al., 2015).

Figure 62: Blue Line - Suffolk Downs to Beachmont, comparison of 1-100 year flood events projected for:

a) 2030

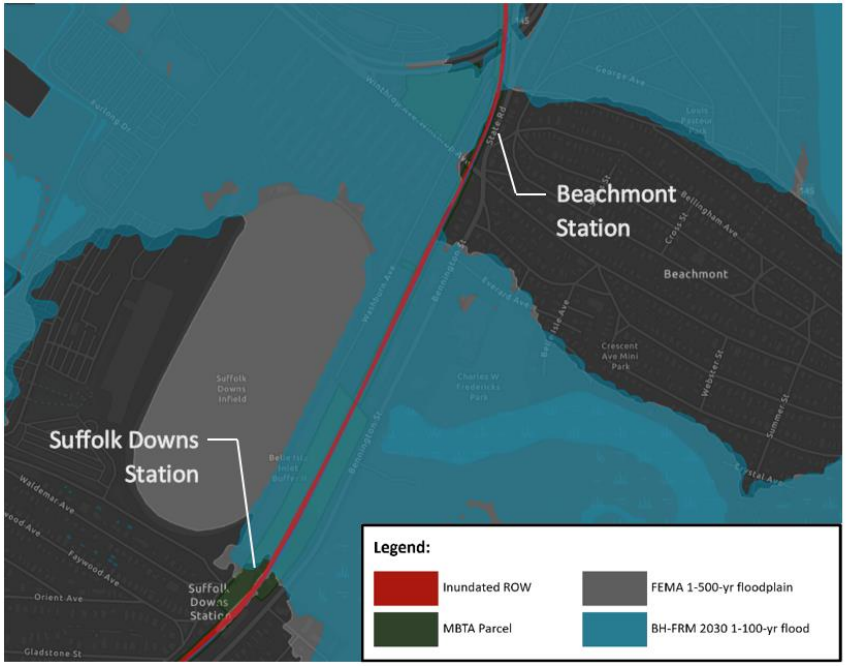

b) 2070

Shown in Figure 62a, Suffolk Downs Station and the tracks approaching Beachmont Station are projected to be vulnerable under 2030 conditions, as well as under 2070 conditions, as shown in Figure 62b. Flooding at Suffolk Downs Station and the tracks to Beachmont Station are projected to reach a depth of 1.5 feet under 2030 conditions in a 1-100 year flood event and 10.0 feet in a 1-100 year flood event under 2070 conditions (Bosma et al., 2015). Adjusting for ridership, the flooding of Suffolk Downs Station and the tracks connecting it to Beachmont would result in a 5% loss of system-wide functionality. The 2030 scenario shown above considers +8.2 inches of SLR, while the 2070 scenario considers +41 inches of SLR (Bosma et al., 2015).

Figure 63: Blue Line – Beachmont to Wonderland, comparison of 1-100 year flood events projected for:

a) 2030

b) 2070

Shown in Figure 63a, the tracks from Beachmont Station to Revere Beach Station, as well as Revere Beach Station is projected to be vulnerable under 2030 conditions, as well as under 2070 conditions, as shown in Figure 63b. Flooding at this location is projected to reach a depth of 1.5 feet under 2030 conditions in a 1-100 year flood event and 4.5 feet in a 1-100 year flood event under 2070 conditions (Bosma et al., 2015). As shown in the figure above, the extent of the BH-FRM approximately coincides with the location of the Revere Beach Station; however, it is clear based on the FEMA 1-500 year flood map that the remaining portions of the Blue Line shown would also be subject to flooding. It should be noted that a small section of the Blue Line, the elevated portion that includes Beachmont Station, remains above the projected floodplains. Adjusting for ridership, the flooding of the tracks from Beachmont to Wonderland would result in a 3% loss of system-wide functionality. The 2030 scenario shown above considers +8.2 inches of SLR, while the 2070 scenario considers +41 inches of SLR (Bosma et al., 2015).

Figure 64: Red Line – Mattapan Trolley, comparison of 1-100 year flood events projected for:

a) 2030

b) 2070

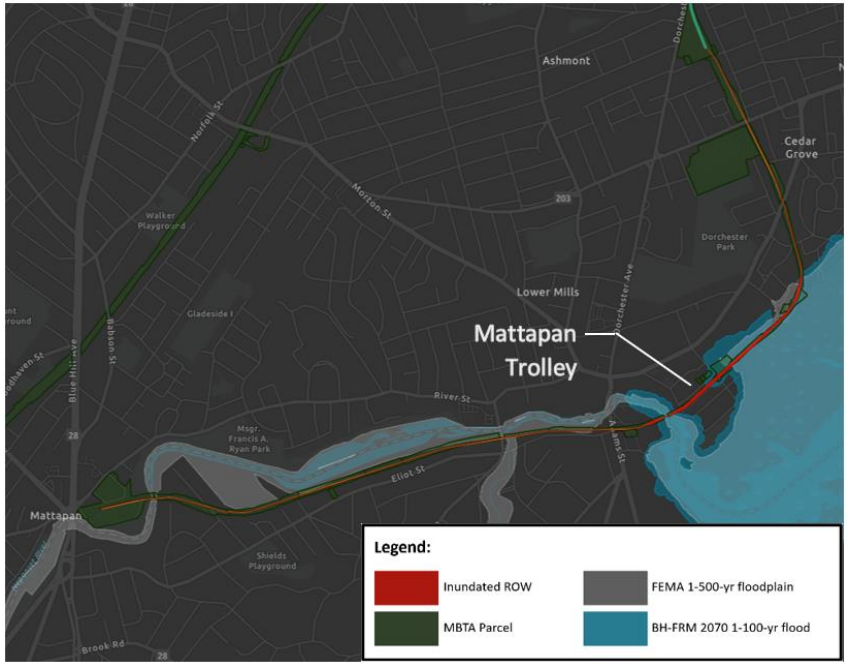

Shown in *Figure 64*a, the Mattapan Trolley line is projected to be vulnerable under 2030 conditions, as well as under 2070 conditions, as shown in *Figure 64*b. As shown in the figure above, the extent of the BH-FRM approximately coincides with the midpoint of the trolley line; however, it is clear based on the FEMA 1-500 year flood map that the remaining portions of the Mattapan Line shown would also be subject to flooding. Adjusting for ridership, the flooding of the Mattapan Trolley line would result in less than a 1% loss of system-wide functionality, due to its currently low ridership. The 2030 scenario shown above considers +8.2 inches of SLR, while the 2070 scenario considers +41 inches of SLR (Bosma et al., 2015).

High Priority (Exposure under 2030 1-100 year projections)

The following locations have been shown to lie within the projected 1-100 year floodplain, based on the BH-FRM 2030 model, with 8.2 inches of SLR. Locations within this section are anticipated to be inadequately protected against 1-100 year coastal flood risks in 10 years. It should be noted that locations within this section will be subject to flooding more severe than shown under scenarios with higher SLR. For projects at locations in this section and a useful life span anticipated to be greater than 20 years, it is recommended that 2070 flood projections be consulted for these locations instead of the current FEMA 1-500 year floodplain.

These locations have been ranked by severity of system-wide impact, should each location be removed from service:

Figure 65: Red Line - Cabot Yard

Figure 66: Silver Line - Courthouse Station

Figure 67: Red Line - JFK/UMass Station to Andrew Station

Figure 68: Red Line - North Quincy Station

Figure 68: Orange Line - Sullivan Square Station to Community College Station

Figure 69: Red Line - Alewife Station

Figure 71: Silver Line - Ted Williams Tunnel and Silver Line Way to Design Center

Figure 71: Silver Line - Airport Station to Chelsea Station

Figure 65: Red Line – Cabot Yard, comparison of 1-100 year flood events projected for:

a) 2030 b) 2070

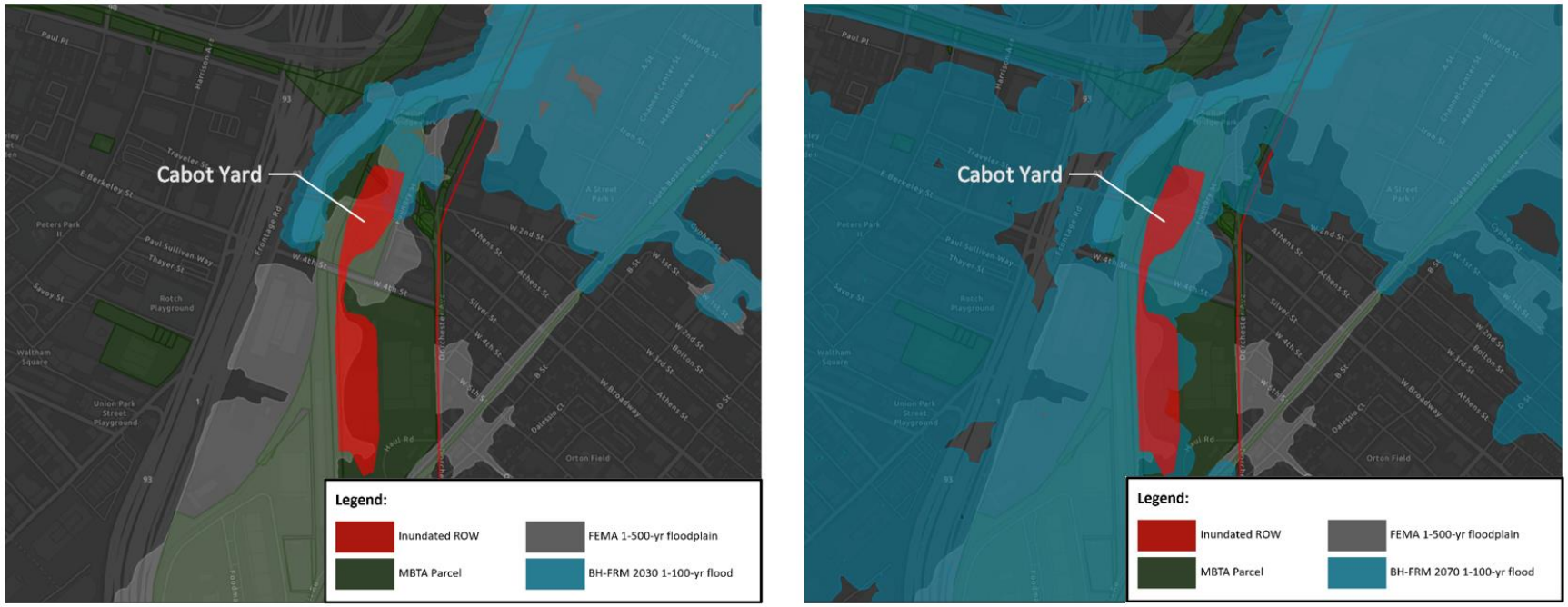

Shown in Figure 651a, Cabot Yard is projected to be vulnerable under 2030 conditions, as well as under 2070 conditions, as shown in Figure 65b. Flooding at Cabot Yard is initially projected to be marginal, reaching a depth of 0.5 feet under 2030 conditions in a 1-100 year flood event, but reaches a depth of 4.0 feet in a 1-100 year flood event under 2070 conditions (Bosma et al., 2015). While portions of Cabot Yard are vulnerable to flooding under 2030 BH-FRM projections, the extent of flooding is likely nonconservative, when considering the inundation extents presented in the FEMA 1-500 year flood map. Should Cabot Yard flood, and rolling stock be damaged, it is possible that service to the majority or entirety of the Red Line would be suspended. Adjusting for ridership, the flooding of Cabot Yard and damage to rolling stock could result in a 21%-45% loss of system-wide functionality under worst-case scenarios. The 2030 scenario shown above considers +8.2 inches of SLR, while the 2070 scenario considers +41 inches of SLR (Bosma et al., 2015).

Figure 66: Silver Line – Courthouse Station, comparison of 1-100 year flood events projected for:

a) 2030 b) 2070

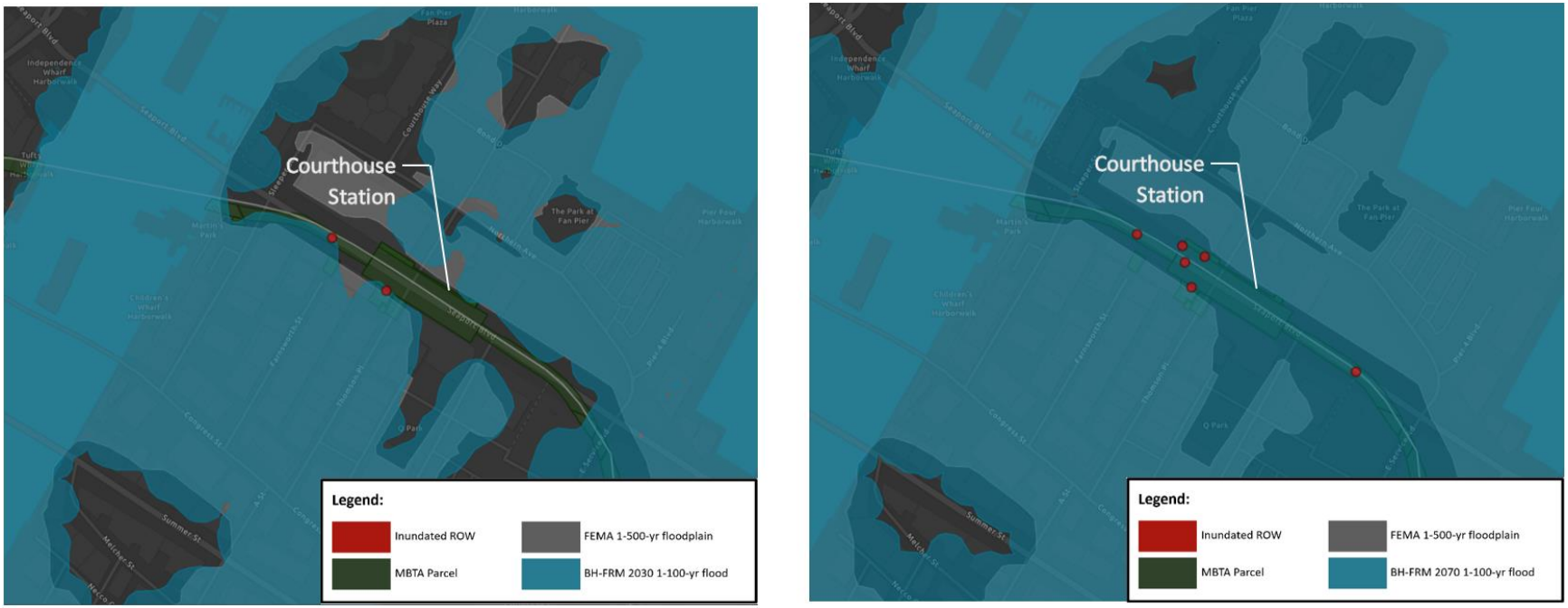

Shown in Figure 66a, Courthouse Station is projected to be vulnerable under 2030 conditions, as well as under 2070 conditions, as shown in Figure 66b. Flooding at Courthouse Station is projected to reach a depth of 0.5 feet under 2030 conditions in a 1-100 year flood event, and reaches a depth of 3.0 feet in a 1-100 year flood event under projected 2070 conditions (Bosma et al., 2015). Should Courthouse Station flood, it is possible that the Red Line at South Station would also flood and therefore be impacted. Connecting to Logan Airport, the Silver Line also provided service to 2.5% of airport passengers in 2019 (Morrison, 2019). Adjusting for ridership, the flooding of Courthouse Station and the potential flooding of the Red Line could result in a 30% loss of system-wide functionality under worst-case scenarios. The 2030 scenario shown above considers +8.2 inches of SLR, while the 2070 scenario considers +41 inches of SLR (Bosma et al., 2015).

Figure 67: Red Line – Andrew Station to JFK/UMass Station, comparison of 1-100 year flood events projected for:

a) 2030 b) 2070

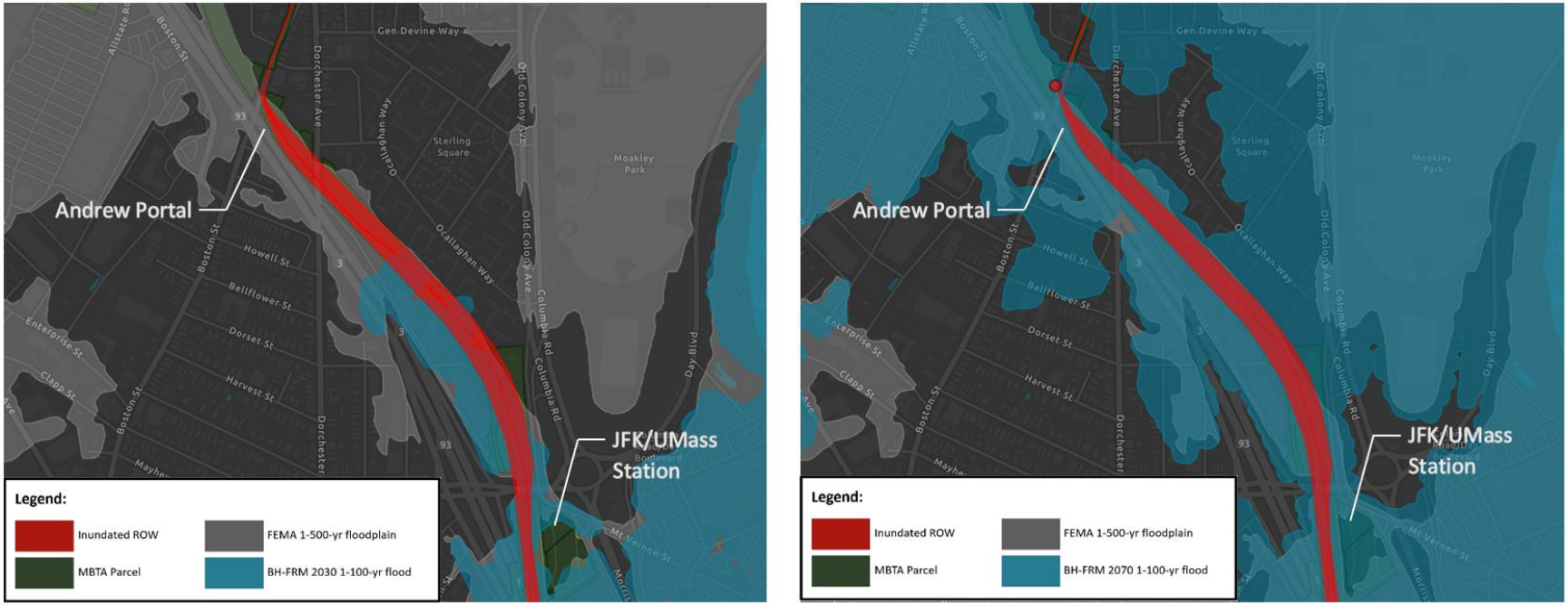

Shown in Figure 67a, JFK/UMass Station, as well as the right of way (ROW) leading to Andrew Station, which notably includes both Columbia Junction (the connection to Cabot Yard), as well as Andrew Portal, are projected to be vulnerable under 2030 conditions, as well as under 2070 conditions, as shown in Figure 67b. Flooding at this critical section of track is projected to be reach a depth of 0.5 feet under 2030 conditions in a 1-100 year flood event, and reaches a depth of 3.0 feet in a 1-100 year flood event under 2070 conditions (Bosma et al., 2015). It should be noted that the BH-FRM 2030 1-100 year flood projections are likely nonconservative, as this entire section of the Red Line falls within the FEMA 1-500 year flood map. Should this section of track flood, it is possible that Cabot Yard would become inaccessible. Adjusting for ridership, the flooding of JFK/UMass Station and the tracks connecting it to Andrew Station would result in a 21% loss of system-wide functionality under worst-case scenarios. The 2030 scenario shown above considers +8.2 inches of SLR, while the 2070 scenario considers +41 inches of SLR (Bosma et al., 2015).

Figure 68: Red Line – North Quincy Station, comparison of 1-100 year flood events projected for:

a) 2030

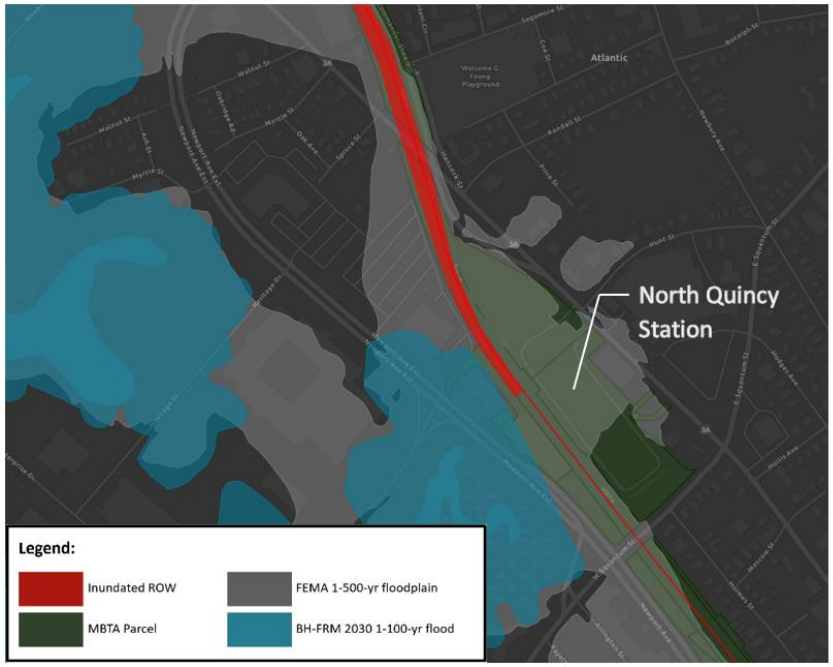

b) 2070

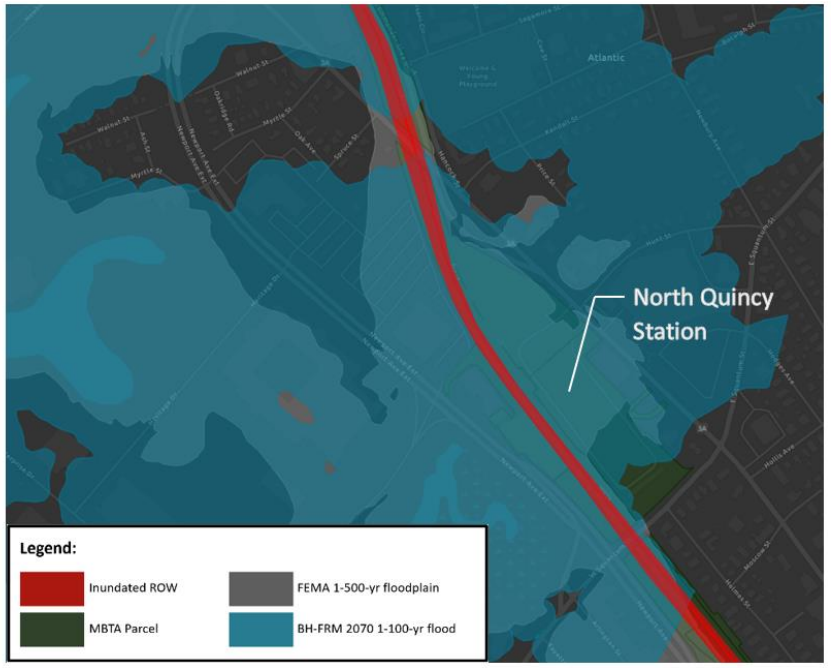

Shown in Figure 68a, North Quincy Station, as well as the right of way (ROW) leading to JFK/UMass Station, are projected to be vulnerable under the FEMA 1-500 year storm, and not likely vulnerable according to 2030 projections, but are expected to be vulnerable under 2070 conditions, as shown in Figure 68b. Flooding at North Quincy Station is projected to reach a depth of 4.0 feet in a 1-100 year flood event under 2070 conditions (Bosma et al., 2015). It should be noted that the BH-FRM 2030 1-100 year flood projections are likely nonconservative, as this section of the Red Line falls within the FEMA 1-500 year flood map. Adjusting for ridership, the flooding of JFK/UMass Station and the tracks connecting it to Andrew Station would result in an 11% loss of system-wide functionality. The 2030 scenario shown above considers +8.2 inches of SLR, while the 2070 scenario considers +41 inches of SLR (Bosma et al., 2015).

Figure 69: Orange Line – Sullivan Square Station to Community College Station, comparison of 1-100 year flood events projected for:

a) 2030 b) 2070

Shown in Figure 69a, Sullivan Square and Community College Stations, as well as the right of way (ROW) between them, are projected to be vulnerable under 2030 projections, as well as under 2070 conditions, as shown in Figure 69b. Flooding just south of Sullivan Square Station is projected to reach a depth of 1 foot in a 1-100 year flood event under 2030 conditions, and is projected to reach a depth of 3.5 feet under 2070 conditions (Bosma et al., 2015). This section of track is vulnerable via the Ryan Playground flood pathway, at which adaptation projects have been proposed (City of Boston, 2017). Adjusting for ridership, the flooding of this section of the Orange Line would result in an 10% loss of system-wide functionality. The 2030 scenario shown above considers +8.2 inches of SLR, while the 2070 scenario considers +41 inches of SLR (Bosma et al., 2015).

Figure 70: Red Line - Alewife Station, comparison of 1-100 year flood events projected for:

a) 2030

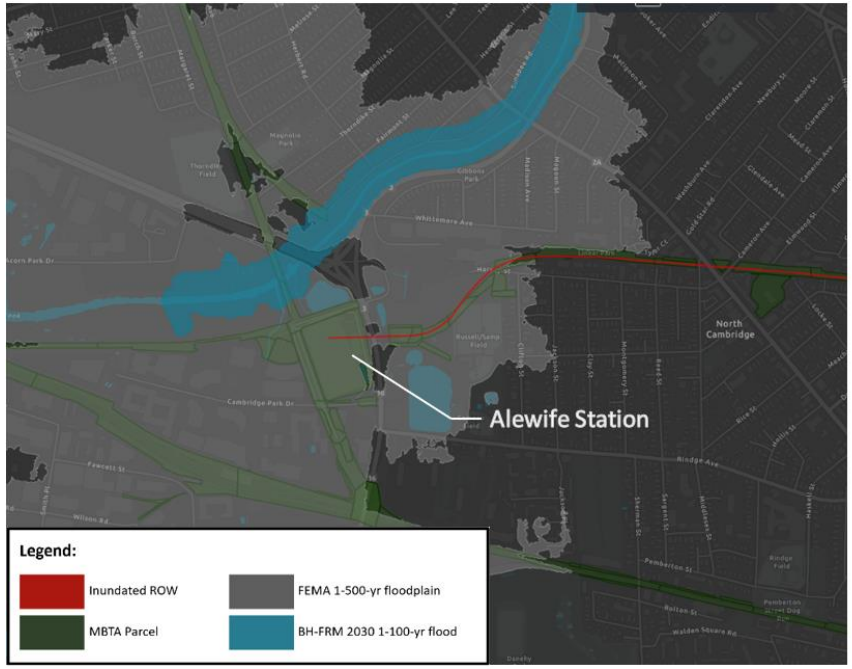

b) 2070

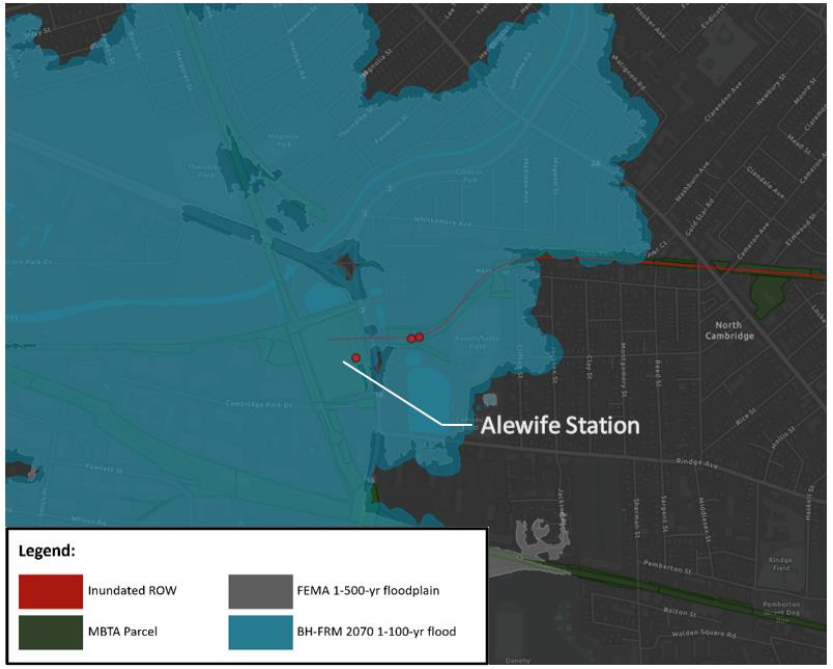

Shown in Figure 70a, Alewife Station is projected to be vulnerable under the FEMA 1-500 year flood map, but is not projected to be vulnerable under the BH-FRM 2030 projections. However, Alewife Station is projected to be vulnerable under 2070 conditions, as shown in Figure 70b due to the flanking and overtopping of the Amelia Earhart Dam. Flooding is projected to reach a depth of 10 feet under 2070 conditions (Bosma et al., 2015). Adjusting for ridership, the flooding of Alewife Station would result in a 6% loss of system-wide functionality. The 2030 scenario shown above considers +8.2 inches of SLR, while the 2070 scenario considers +41 inches of SLR (Bosma et al., 2015).

Figure 71: Silver Line - Ted Williams Tunnel and Silver Line Way to Design Center, comparison of 1-100 year flood events projected for:

a) 2030 b) 2070

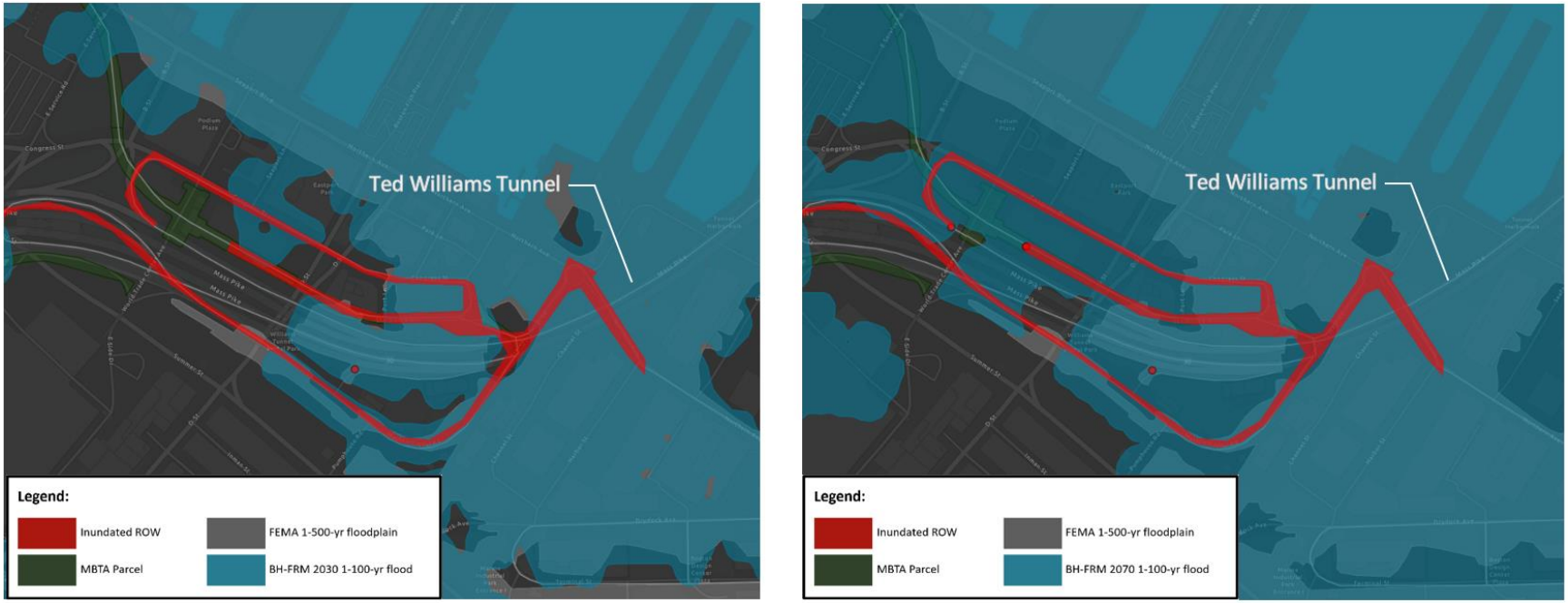

Shown in Figure 71a, the Ted Williams Tunnel and the Silver Line from Silver Line Way to Design Center is projected to be vulnerable under 2030 projections, as well as under 2070 conditions, as shown in Figure 71b. Flooding at the portal of the Ted Williams Tunnel is projected to reach a depth of at least 1 foot in a 1-100 year flood event under 2030 conditions, and is projected to reach a depth of at least 4.5 feet under 2070 conditions (Bosma et al., 2015). The Ted Williams Tunnel connects to Logan Airport, with the Silver Line providing service to 2.5% of airport passengers in 2019 (Morrison, 2019). Adjusting for ridership, the flooding of this portion of the Silver Line would result in a 3% loss of system-wide functionality. The 2030 scenario shown above considers +8.2 inches of SLR, while the 2070 scenario considers +41 inches of SLR (Bosma et al., 2015).

Figure 72: Silver Line - Airport Station to Chelsea Station, comparison of 1-100 year flood events projected for:

a) 2030

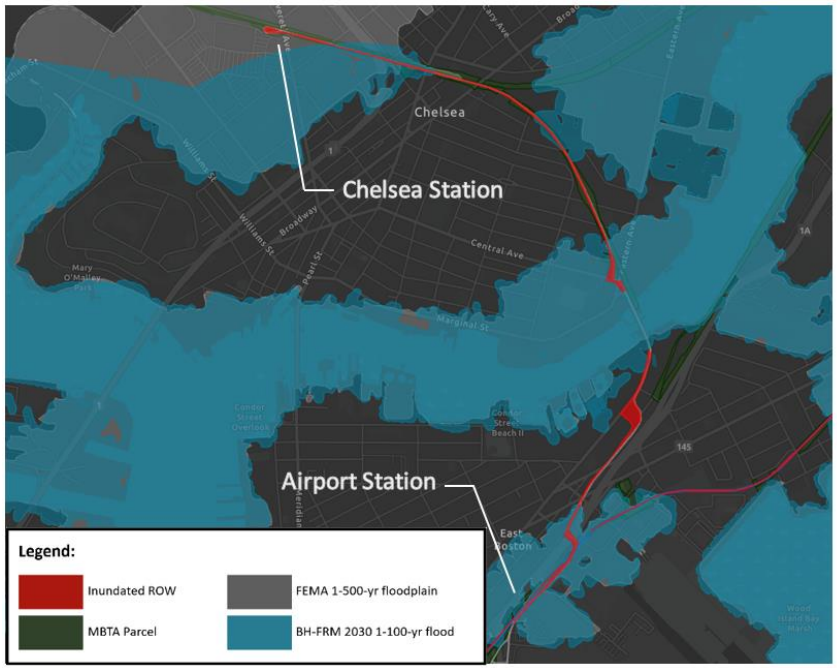

b) 2070

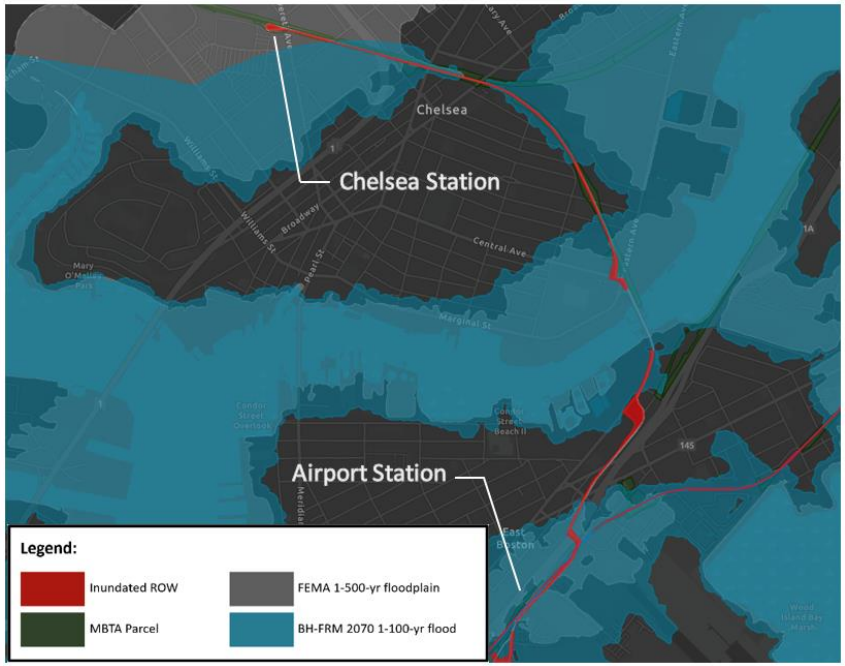

Shown in Figure 71a, the current route of the Silver Line, from Airport Station to Chelsea Station is projected to be vulnerable under 2030 projections, as well as under 2070 conditions, as shown in Figure 71b. Flooding just north of Airport Station is projected to reach a depth of 2.5 feet in a 1-100 year flood event under 2030 conditions, and is projected to reach a depth of 5.0 feet under 2070 conditions (Bosma et al., 2015). Adjusting for ridership, the flooding of this portion of the Silver Line would result in an 3% loss of system-wide functionality. The 2030 scenario shown above considers +8.2 inches of SLR, while the 2070 scenario considers +41 inches of SLR (Bosma et al., 2015).

Priority Locations:

The following locations have been shown to lie within the projected 1-20 year and 1-100 year floodplains, based on the BH-FRM 2070 model, with 41 inches of SLR. Locations within this section are anticipated to be inadequately protected in less than 50 years. It should be noted that locations within this section will be subject to flooding more severe than shown under more infrequent flooding scenarios. For projects at locations in this section and a useful life span anticipated to be greater than 30 years, it is recommended that 2070 1-100 year flood projections be consulted for these locations instead of the FEMA 500 year floodplain.

These locations have been ranked by severity of system-wide impact, should each location be removed from service:

Figure 73: Orange and Green Lines - North Station, comparison of 1-100 year flood events projected for:

a) 2030 b) 2070

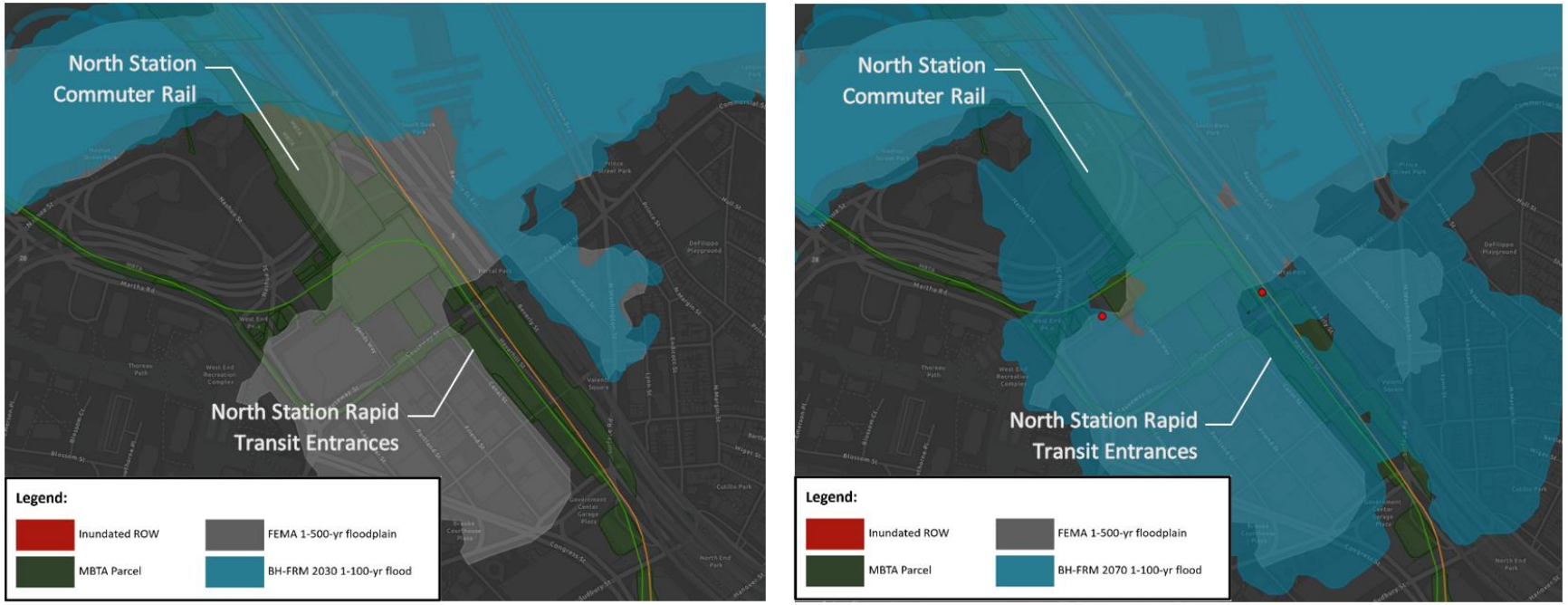

Shown in Figure 73a, North Station is not projected to be vulnerable under 2030 projections, but is projected to be flooded according to the FEMA 1-500 year map. Under 2070 conditions, as shown in Figure 73b, North Station is expected to be vulnerable. Flooding is projected to reach a depth of 2.5 feet under 2070 conditions (Bosma et al., 2015). Adjusting for ridership, if the flooding of North Station affects rapid transit service, it would result in a 33% loss of system-wide functionality. The 2030 scenario shown above considers +8.2 inches of SLR, while the 2070 scenario considers +41 inches of SLR (Bosma et al., 2015).

Figure 74: Orange Line - Wellington Yard, comparison of 1-100 year flood events projected for:

a) 2030 b) 2070

Shown in Figure 74a, Wellington Yard is not projected to be vulnerable under 2030 projections, but is projected to be vulnerable under 2070 conditions, as shown in Figure 74b. Flooding is projected to reach a depth of 1 foot under 2070 conditions (Bosma et al., 2015). However, the extents of the BH-FRM coincides with a portion of Wellington Yard; the vulnerability of the remaining portion of the yard is unclear. Adjusting for ridership, the loss of Wellington Yard could result in an 8%-33% loss of system-wide functionality, in worst case scenarios. The 2030 scenario shown above considers +8.2 inches of SLR, while the 2070 scenario considers +41 inches of SLR (Bosma et al., 2015).

Figure 75: Orange Line - Tufts Medical Center Station, comparison of 1-100 year flood events projected for:

a) 2030 b) 2070

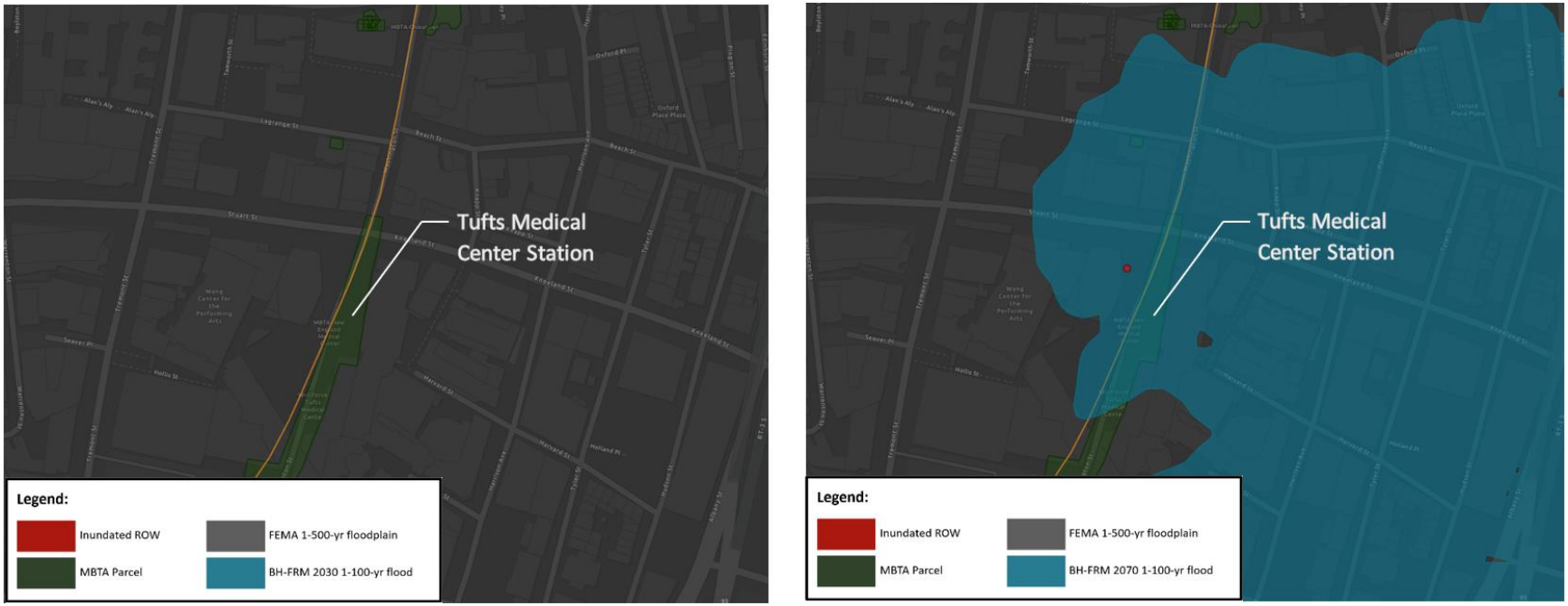

Shown in Figure 75a, Tufts Medical Center Station is not projected to be vulnerable under 2030 projections, but is projected to be vulnerable under 2070 conditions, as shown in Figure 75b. Flooding is projected to reach a depth of 2.5 feet under 2070 conditions (Bosma et al., 2015). Adjusting for ridership, the flooding of Tufts Medical Center Station would result in a 25% loss of system-wide functionality. The 2030 scenario shown above considers +8.2 inches of SLR, while the 2070 scenario considers +41 inches of SLR (Bosma et al., 2015).

Figure 76: Red Line – Andrew Station, comparison of 1-100 year flood events projected for:

a) 2030 b) 2070

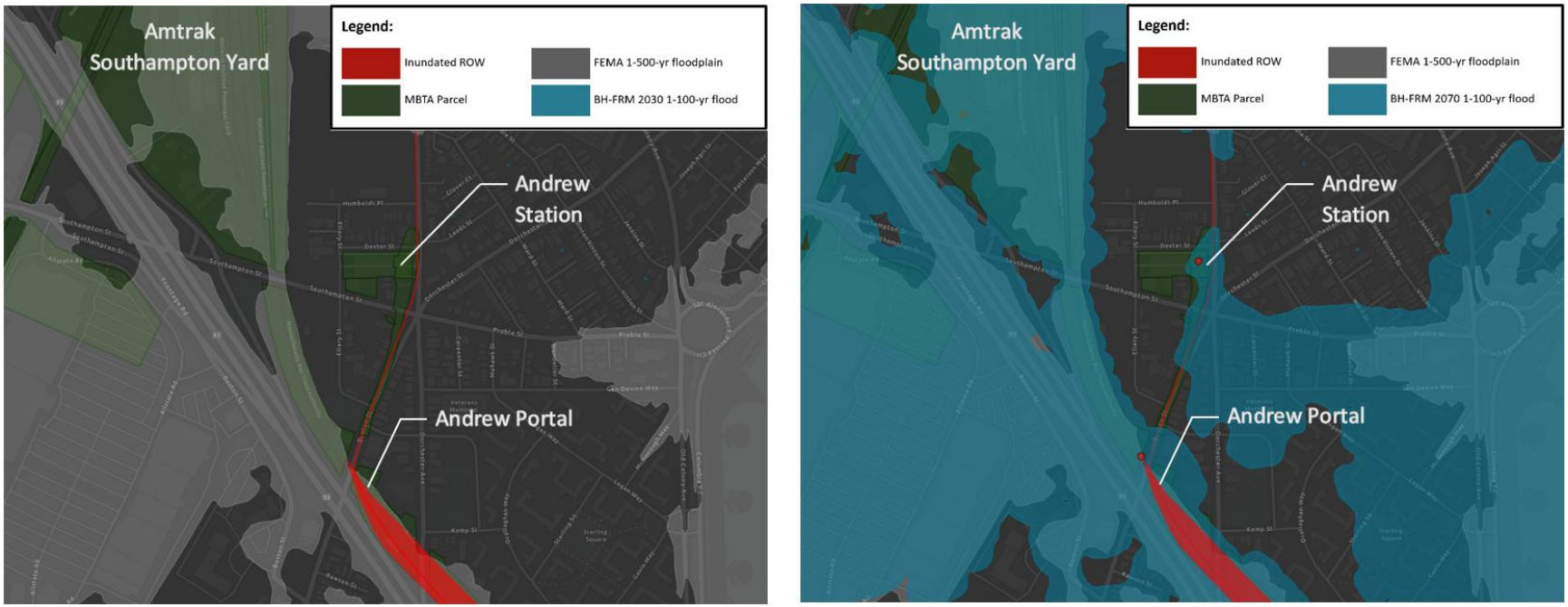

Shown in Figure 76a, Andrew Station is not projected to be vulnerable under 2030 conditions, but is projected to be vulnerable under 2070 conditions, as shown in Figure 76b. Flooding at Andrew Station is projected to be reach a depth of 1.0 foot under 2070 conditions in a 1-100 year flood event (Bosma et al., 2015). Adjusting for ridership, the flooding of Andrew Station would result in a 20% loss of system-wide functionality under worst-case scenarios. The 2030 scenario shown above considers +8.2 inches of SLR, while the 2070 scenario considers +41 inches of SLR (Bosma et al., 2015).

Figure 77: Orange Line - Tufts Medical Center and Back Bay Station Portals, comparison of 1-100 year flood events projected for:

a) 2030 b) 2070

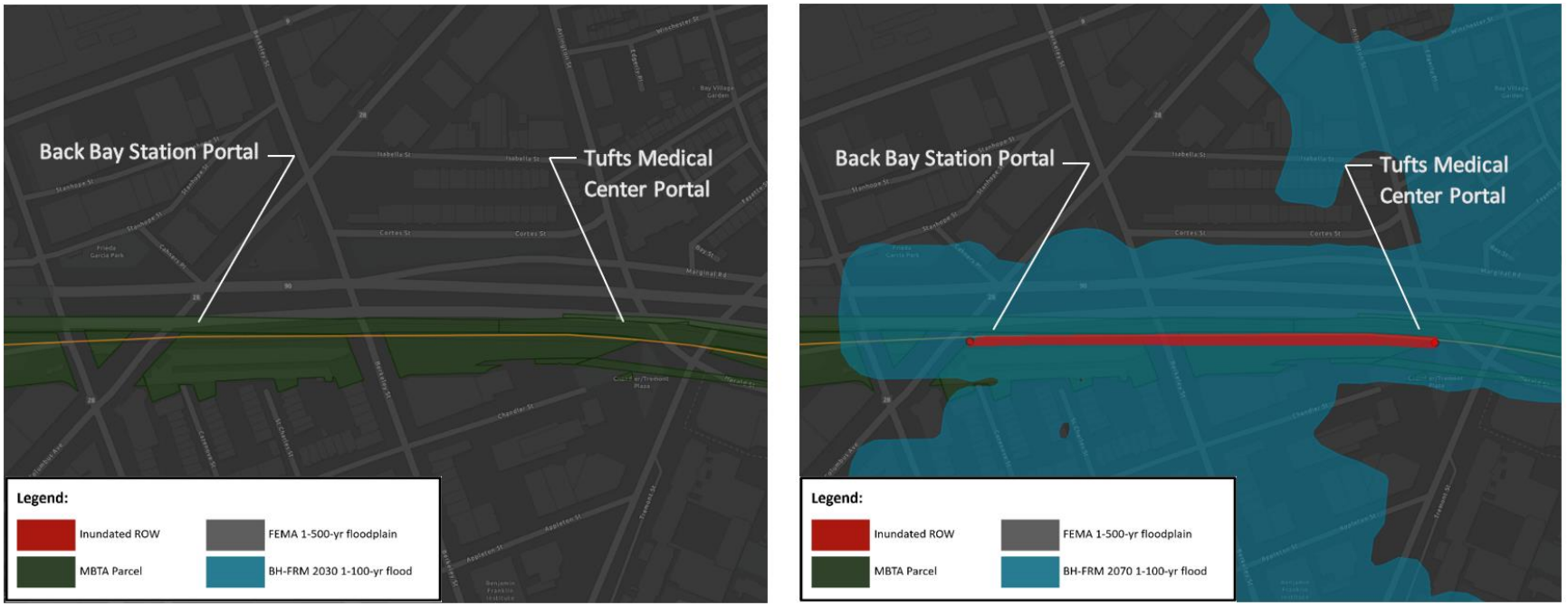

Shown in Figure 77a, the Tufts Medical Center and Back Bay Station portals are not projected to be vulnerable under 2030 projections, but are projected to be vulnerable under 2070 conditions, as shown in Figure 77b. Flooding is projected to reach a depth 1.0 foot under 2070 conditions (Bosma et al., 2015). Adjusting for ridership, the flooding of this portion of the Orange Line would result in a 17% loss of system-wide functionality. The 2030 scenario shown above considers +8.2 inches of SLR, while the 2070 scenario considers +41 inches of SLR (Bosma et al., 2015).

Figure 78: Red Line - Tenean Yard, comparison of 1-100 year flood events projected for:

a) 2030 b) 2070

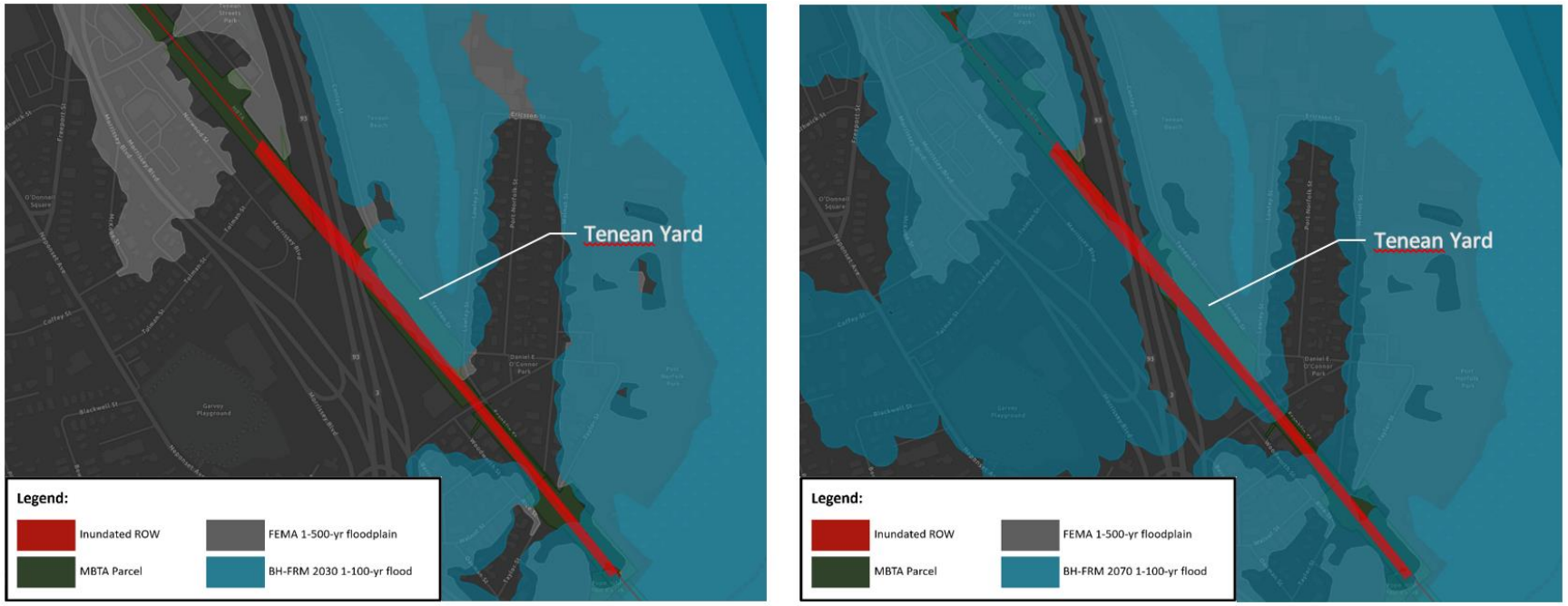

Shown in Figure 78a, Tenean Yard is projected to be vulnerable under 2030 projections, as well as under 2070 conditions, as shown in Figure 78b. Flooding is projected to reach a depth of 1.5 feet in a 1-100 year flood event under 2030 conditions, and is projected to reach a depth of 3.5 feet under 2070 conditions (Bosma et al., 2015). Adjusting for ridership, the flooding of the Red Line track adjacent to Tenean Yard under the 2070 scenario would result in a 13% loss of system-wide functionality. The 2030 scenario shown above considers +8.2 inches of SLR, while the 2070 scenario considers +41 inches of SLR (Bosma et al., 2015).

Figure 79: Orange Line - Community College Portal, comparison of 1-100 year flood events projected for:

a) 2030 b) 2070

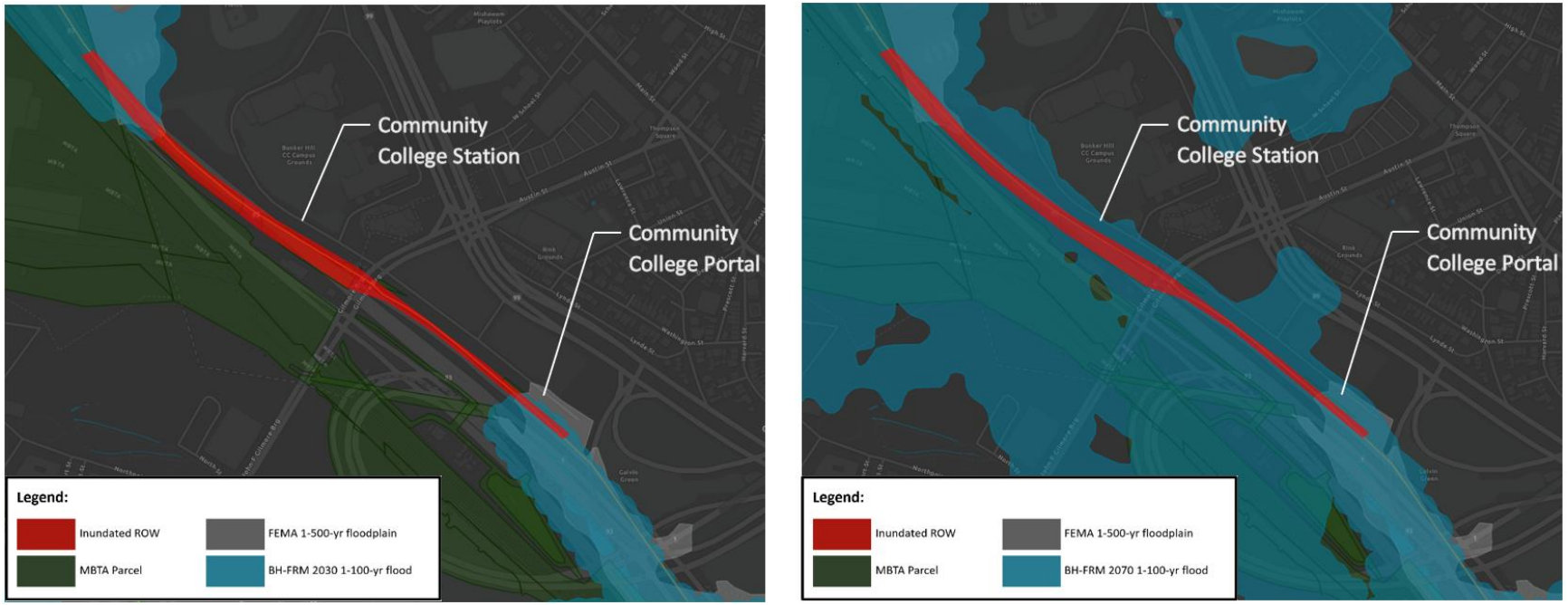

Shown in Figure 79a, the Community College Portal is projected to be vulnerable under 2030 projections, as well as under 2070 conditions, as shown in Figure 79b. While it is unclear if the portal would actually flood under the 1-100 year flood event under 2030 conditions, flooding is projected to reach a depth of 10 feet under 2070 conditions (Bosma et al., 2015). Adjusting for ridership, the flooding of this portion of the Orange Line would result in a 10% loss of system-wide functionality. The 2030 scenario shown above considers +8.2 inches of SLR, while the 2070 scenario considers +41 inches of SLR (Bosma et al., 2015).

Recognized Locations:

The following locations have been shown to lie within the projected 1-100 year floodplain, based on the BH-FRM 2070 model, with 41 inches of SLR. Locations within this section are anticipated to be inadequately protected in 50 years. For projects at locations in this section and a useful life span anticipated to be greater than 50 years, it is recommended that 2070 1-100 year flood projections be consulted for these locations instead of the FEMA 500 year floodplain.

These locations have been ranked by severity of system-wide impact, should each location be removed from service:

Figure 79: Green Line - Prudential Center Station

Figure 80: Green Line - Fenway Portal and Longwood Station

Figure 80: Green Line - Prudential Center Station, comparison of 1-100 year flood events projected for:

a) 2030 b) 2070

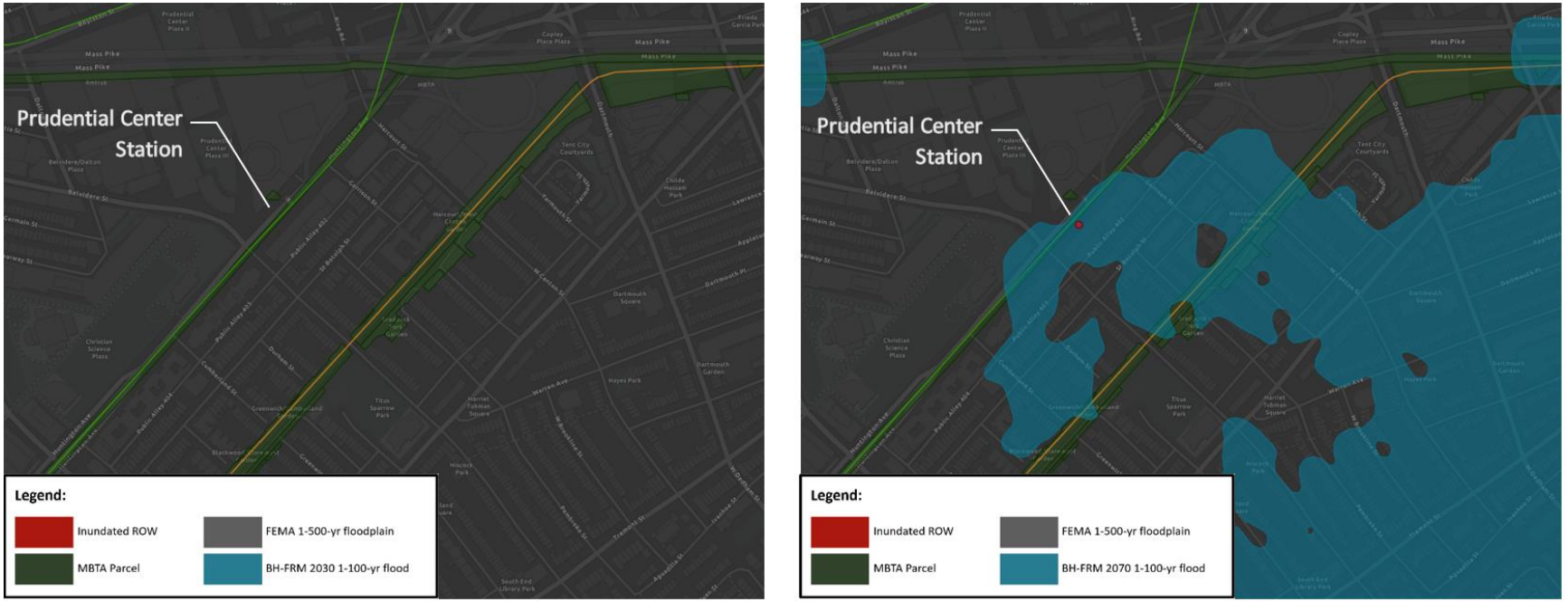

Shown in Figure 80a, Prudential Center Station is not projected to be vulnerable under 2030 projections, but is projected to be vulnerable under 2070 conditions, as shown in Figure 80b. Flooding is projected to reach a depth 0.5 feet under 2070 conditions (Bosma et al., 2015). Adjusting for ridership, the flooding of this portion of the Green Line would result in a 7% loss of system-wide functionality. The 2030 scenario shown above considers +8.2 inches of SLR, while the 2070 scenario considers +41 inches of SLR (Bosma et al., 2015).

Figure 81: Green Line - Fenway Portal and Longwood Station, comparison of 1-100 year flood events projected for:

a) 2030 b) 2070

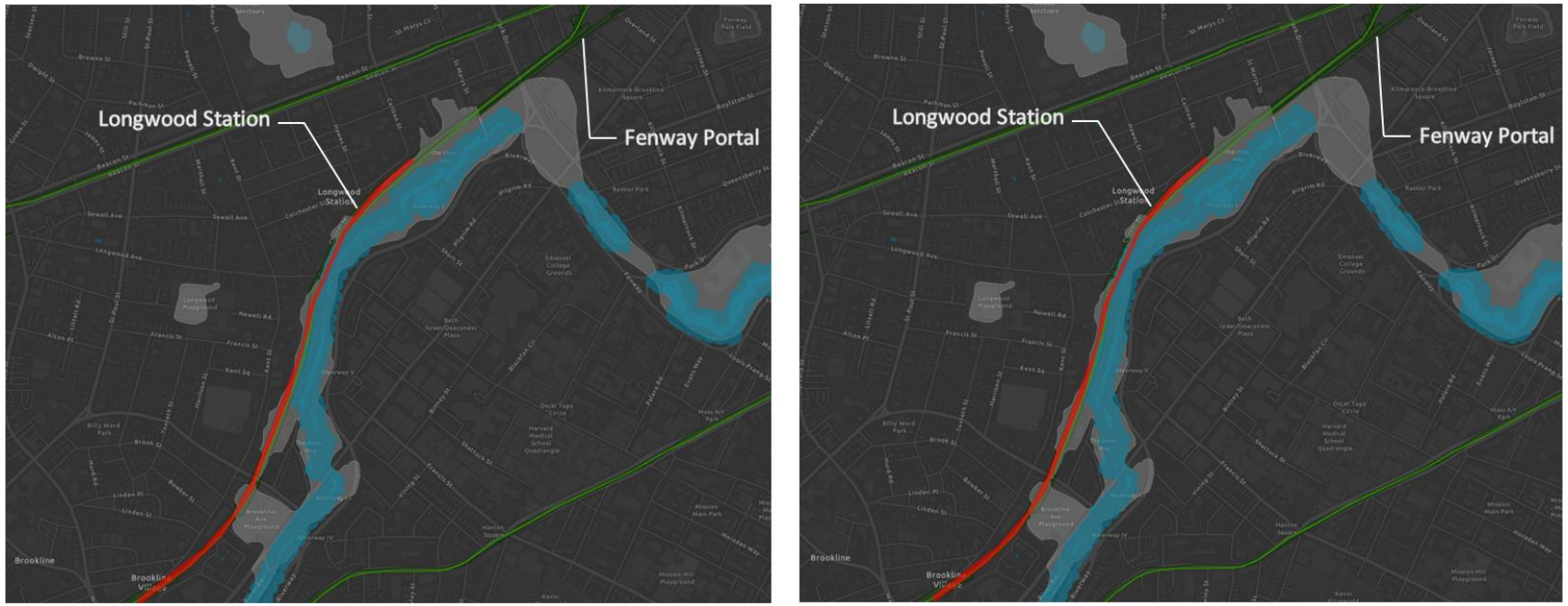

Shown in Figure 81a, Fenway Portal, Longwood Station, and the tracks in the proximity of the Muddy River on the D branch, are projected to be vulnerable under 2030 projections, as well as under 2070 conditions, as shown in Figure 81b. Flooding is projected to reach a depth of 2.5 feet in a 1-100 year flood event under 2030 conditions, and is projected to reach a depth of 2.5 feet under 2070 conditions (Bosma et al., 2015). While it is likely that these flood vulnerabilities are an artifact of the BH-FRM projections, it is clear from the FEMA 1-500 year flood map and historic events, notably the Green Line flooding in October, 1996, that this area is vulnerable to flooding. Adjusting for ridership, the flooding of this portion of the Green Line would result in an 14-33% loss of system-wide functionality. An FTA sponsored resiliency project is currently underway at this location to address this vulnerability (Riley-Gilbert, 2018). The 2030 scenario shown above considers +8.2 inches of SLR, while the 2070 scenario considers +41 inches of SLR (Bosma et al., 2015).

References:

AECOM. (2018). *Massachusetts Bay Transportation Authority: Orient Heights Maintenance and Storage Facilities Current and Future Vulnerabilities to Climate Stressors.* Boston, MA.

Bosma, K., Douglas, E., Kirshen, P., McArthur, K., Miller, S., Watson, C. (June, 2015). *MassDOT-FHWA Pilot Project Report: Climate Change and Extreme Weather Vulnerability Assessments and Adaptation Options for the Central Artery.* MassDOT.

Botros, R., Diaz, N., Rambert, R., and Shah, A. (2019). *Final Memorandum: MBTA Climate Resilience Decision-Making Tool.*

City of Boston, MA Office of Coastal Zone Management, Barr Foundation, Green Ribbon Commission (2017). *Coastal Resilience Solutions for East Boston and Charlestown*. Boston, MA: City of Boston.

HNTB. (2014, September). *Structural Assessment of the Amtrak Under River Tunnels in NYC Inundated by Super Storm Sandy.* New York, NY.

Massachusetts Bay Transportation Authority (MBTA). (2018). *Blue Line Vulnerability Assessment Report*. Boston, MA: Massachusetts Department of Transportation.

Morrison, H. (2019, October). *Advancing Sustainable Mobility: Transportation Policy & Planning for the 21st Century*. Presentation at the Massachusetts Institute of Technology Department of Urban Studies and Planning, Cambridge, MA.

Riley-Gilbert, M. (2018, January). *Weather and Climate Resiliency at the MBTA*. Presentation at NCSE 2018 Conference: The Science, Business, and Education of Sustainable Infrastructure, Washington, DC.

Weston & Sampson. (2019). *Flood Resilience Recommendations for Aquarium Station through the Maverick Portal*. Peabody, MA.

Appendix E: Empirical Case Studies

In addition to the Winter 2018 Nor'easter in Boston, rapid transit resilience was briefly investigated for other events on record, both in Boston and New York City. This appendix outlines these scenarios, providing relevant commentary for each.

The NYC MTA and Hurricane Irene

Using data available from the New York City MTA, Chan & Schofer (2016) investigated the system response and resilience of the MTA rail rapid transit system under several perturbation scenarios. For each scenario, system performance was tracked over time throughout a period of disruption. Within this study, system performance was quantified as the percentage of revenue vehicle miles (RVM) travelled compared to RVM scheduled. Usage of this metric as a measure of system performance is problematic for several reasons. First, the relative importance of the lost RVM is not considered by the metric. Second, the topology of the perturbed system is neither described nor characterized by this metric. Third, this performance metric captures demand signals, as system performance artificially increases on weekends, as less service is demanded and by extension scheduled. Defining resilience in this manner is especially problematic for spatially isolated communities that are reliant on public transit, such as the Far Rockaways community, whose transit service was not restored for more than 200 days after Hurricane Sandy made landfall (Chan & Schofer, 2016, Graham et al., 2016). Despite the limitations of this system performance metric, the case studies presented can still provide insight into the response and resilience of rapid transit systems to climate-related exposures.

Minor Perturbations

The results presented by Chan & Schofer (2016) appear to indicate that under perturbations of smaller magnitudes, the assumption of linear system recovery is reasonable. Shown in , the MTA rail rapid transit system was closed for only 1 full day in response to Hurricane Irene. Afterwards, the system recovered rapidly, exhibiting a nearly linear recovery behavior.

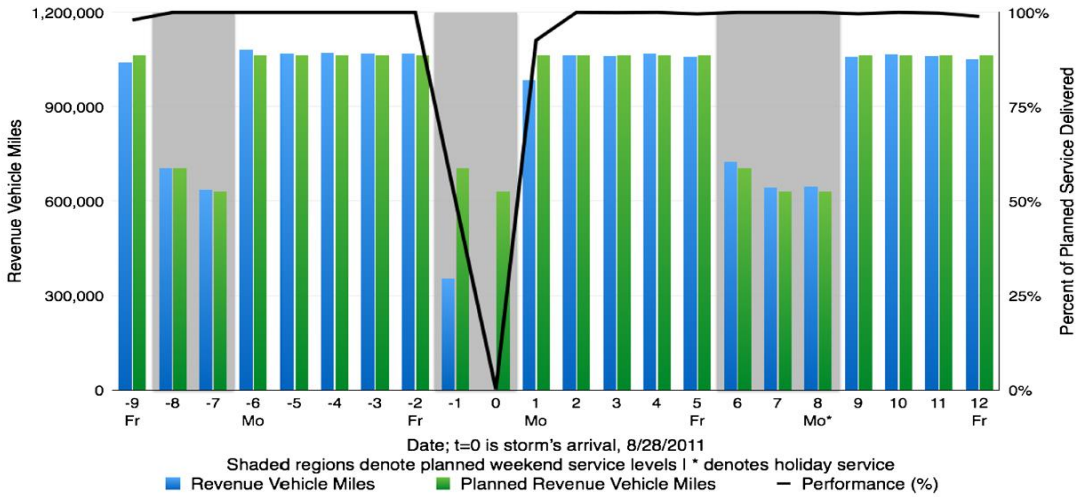

Figure 82*: System performance of the New York City MTA rail rapid transit network during Hurricane Irene (Chan & Schofer, 2016).*

Similarly, under a smaller perturbation, a blizzard in 2010 shown in Figure 83, system recovery took several days, though was also approximately linear. While a miniscule sample size, the results presented by Chan & Schofer (2016) appear to suggest that under small perturbations, in which damage is minimal, a linear system recovery is a reasonable approximation.

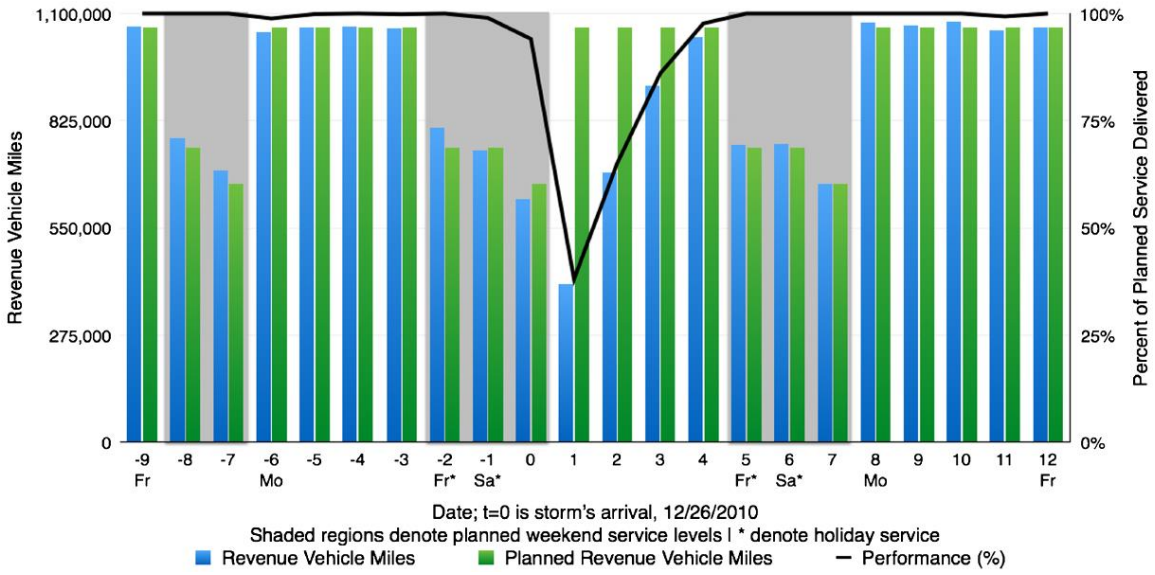

Figure 83: System performance of the New York City MTA rail rapid transit network during a winter 2010 blizzard (Chan & Schofer, 2016).

Major Perturbations

In contrast, Hurricane Sandy had a much more substantial impact on MTA rail rapid transit service, as shown in *Figure 84* below. The entire system was shut down for two full days as a result of the storm, due to extensive inundation and damage. System response also exhibits nonlinear behavior, with full restoration of system performance occurring more than 200 days later. System resilience, when considering performance until 12 days after landfall, was 56%. Rates of recovery are largely influenced by the resourcefulness of the transit agency and the rapidity of restoration actions undertaken, yet this exact relationship remains unclear.

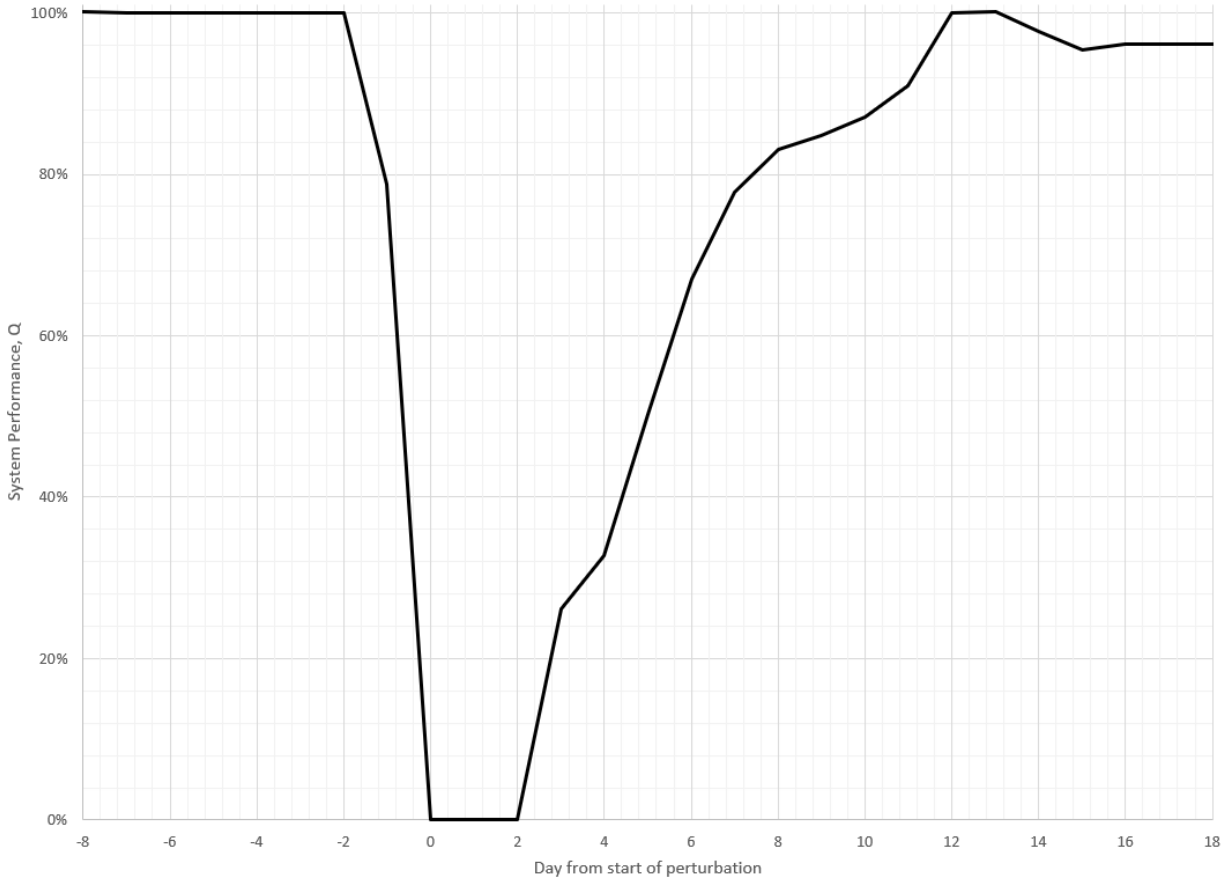

Figure 84: System performance of the New York City MTA rail rapid transit network during Hurricane Sandy (after Chan & Schofer, 2016). System resilience, up to 12 days after landfall was 56%.

The MBTA and the Winter of 2015

In an attempt to further interrogate the relation between recovery actions and system recovery, the impacts of the 2015 winter storms on the MBTA's rail rapid transit system was investigated. The data presented in this section is courtesy of a report produced by the Volpe Center (2015). The winter of 2015 was the snowiest on record in greater Boston, with 91.4 inches of snow falling between January 25th, 2015 and February 28th, 2015. Within the report, the percentage of rail cars in service for each line in the during the AM and PM peak periods was reported for every day in the aforementioned period. While this is an operations-centric measure of system performance that also neglects topological and passenger-based aspects of system performance, it still provides a reasonable estimation of the degree to which the system was impacted by winter snow events. This measure of system performance over time is shown in *Figure 85*. Each winter storm that occurred during this interval is shown in red, with the depth of snowfall noted above. The reduction of fleet size was attributed to damage of rolling stock caused by over-voltage, snow in motors, as well as snow piles blocking access to portions of the system. Measuring the area under the system performance curve for the duration of the study period, system resilience was 77%. While this value is not intrinsically useful on its own, it can inform decision makers of the degree to which recovery actions during the entire perturbation period were successful.

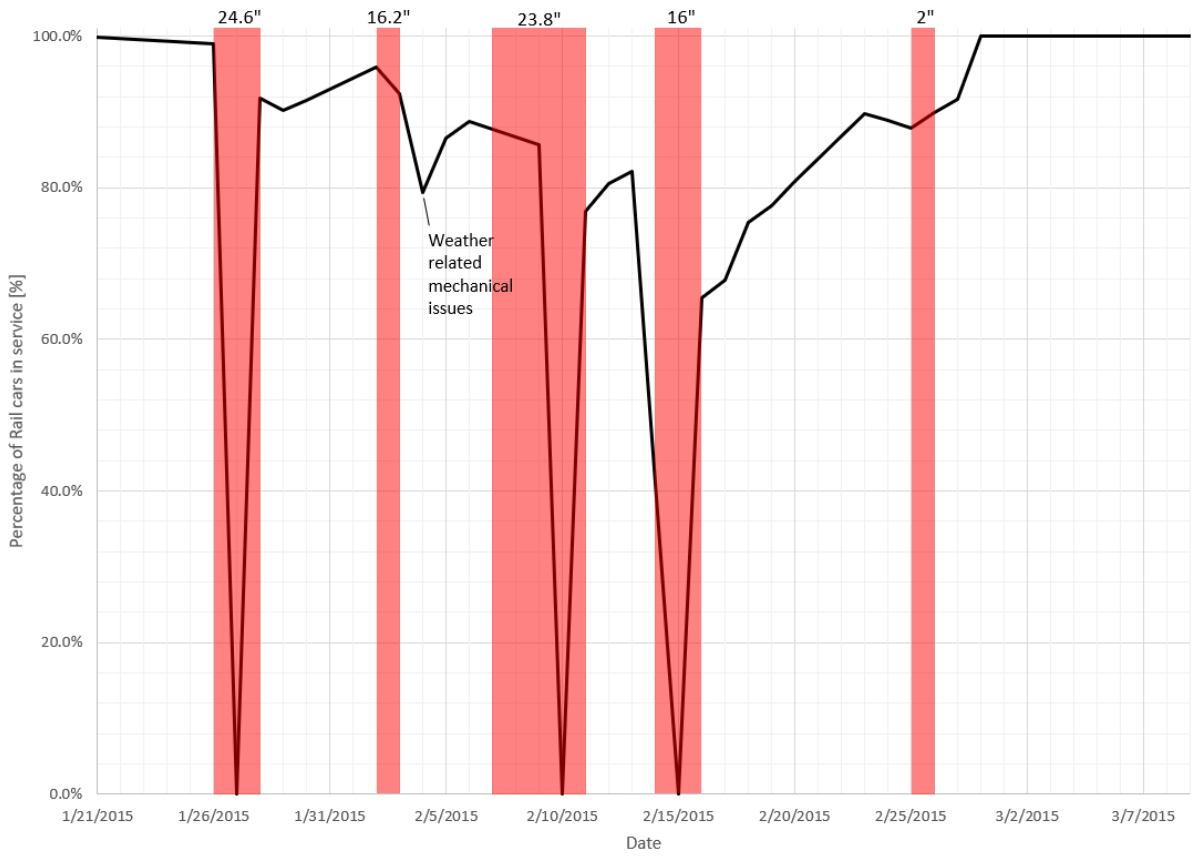

Figure 85: System performance of the MBTA rail rapid transit network during winter 2015. Snowfall is shown in red, with depth of snow noted. Note that the performance decrease shown on 2/4/2015 was due to weather related mechanical issues on the Orange Line. Data courtesy of the Volpe Center (2015).

Additional data was also provided on the recovery efforts undertaken for each day during the study period and is shown in *Figure 86*. For nearly the entirety of the perturbation period, from January 27th, 2015 to February 28th, 2015, the MBTA snow plan was in effect. This snow plan specifies operating procedures that personnel should follow to minimize snow buildup on the tracks, freezing of rolling stock and catenary lines, and snow plowing procedures. Additionally, 3rd rail heaters are activated every hour where installed. Observing the period from February 2nd to February 11th, it is clear that these procedures were inadequate,

even before the third snowfall of the study period, as system performance was declining prior to the arrival of the third storm.

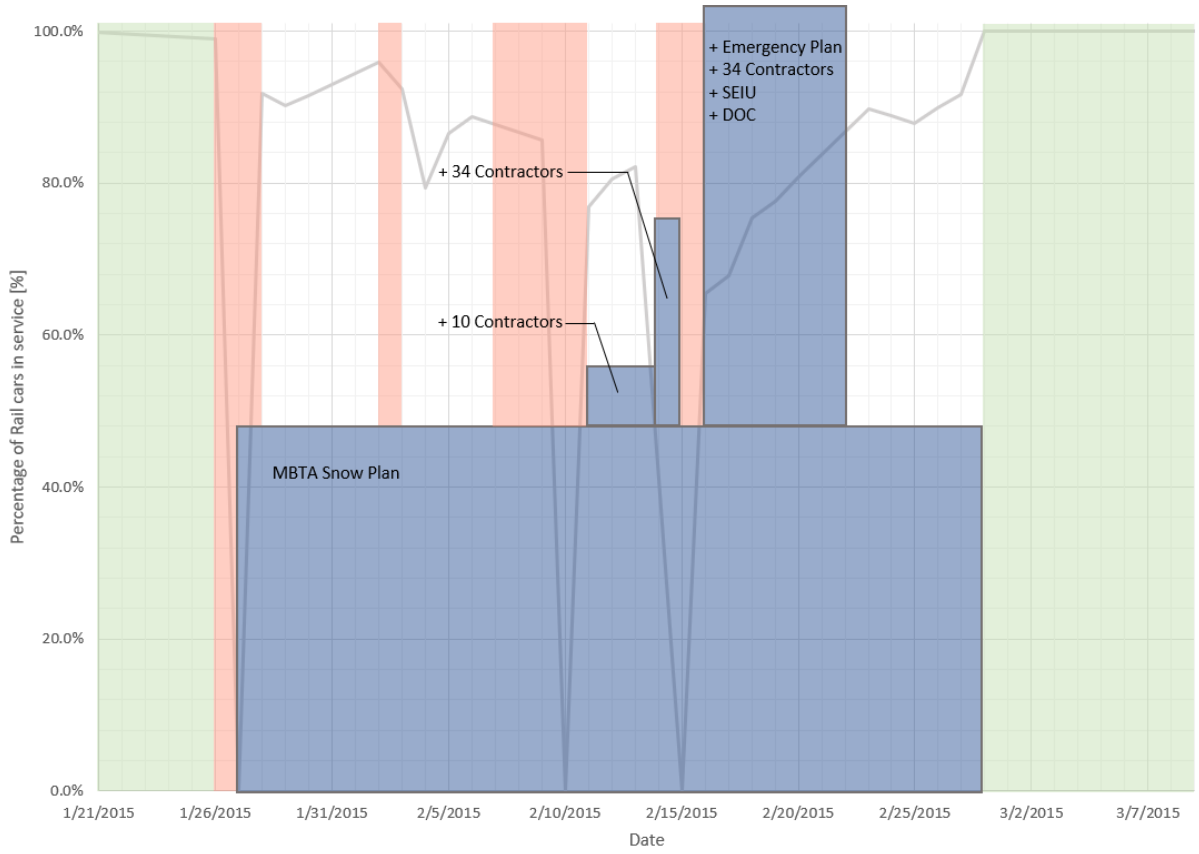

Figure 86: System performance and response of the MBTA rail rapid transit network during winter 2015. Snowfall is shown in red, green indicates time periods beyond the perturbation period, and blue indicates recovery actions taken by the MBTA. Data courtesy of the Volpe Center (2015).

In response to both the declining system performance and the third storm, the MBTA enlisted the aid of 10 additional contractors to remove snow from rights of way, yards, and maintenance facilities. In anticipation of the fourth storm of the perturbation period, an additional 24 contractors, making a total of 34 contractors were hired to clear snow in support of the MBTA system. This fourth storm, coupled with the cumulative snow buildup from the prior three, which had not melted due to unusually cold temperatures,

further degraded system performance, with only 63% of rolling stock available for service the day after the storm. In response, the MBTA also enacted its Emergency Plan, employed the labor of 100 Service Employees International Union (SEIU) members, as well as 80 department of corrections inmates to dig out the Red Line from JFK/UMass Station to Braintree Station by hand. The relation between these recovery action and system recovery is unclear, partially due to the close spacing of perturbation events, as well as the complex and compounding nature of snow-based impacts.

The response of the MBTA to the winter storms of 2015 provides a unique case study, from which the relation between system performance and adaptive capacity can begin to be observed. This case study underscores the organizational and socio-technical nature of adaptive capacity efforts, which rely on the effective coordination and management of people, equipment, and time. Further investigation into the allocation of resources under perturbation events is needed to better understand the adaptive capacity of transit systems.

References:

Chan, R., & Schofer, J. L. (2016). Measuring transportation system resilience: response of rail transit to weather disruptions. *Natural Hazards Review, 17*(1), 05015004.

Volpe Center. (March, 2015). *MBTA 2015 Winter Event Timeline.* Boston, MA: Massachusetts Bay Transportation Authority.